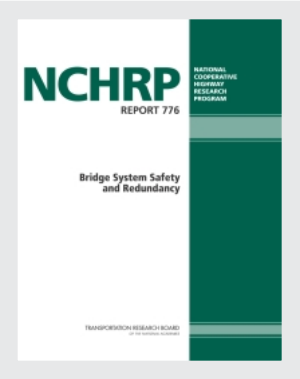

Bridge System Safety and Redundancy

DETAILS

126 pages | 8.5 x 11 | PAPERBACK
ISBN 978-0-309-40170-8 | DOI 10.17226/22365

AUTHORS

Ghosn, Michel; Yang, Jian; Beal, David; and Sivakumar, Bala

NATIONAL COOPERATIVE HIGHWAY RESEARCH PROGRAM

NCHRP REPORT 776

Bridge System Safety and Redundancy

Michel Ghosn
Jian Yang
Department of Civil Engineering
City College
City University of New York
New York, NY

WITH CONTRIBUTIONS FROM

David Beal
Hingham, MA

Bala Sivakumar
HNTB Corporation
New York, NY

Subscriber Categories
Bridges and Other Structures

Research sponsored by the American Association of State Highway and Transportation Officials
in cooperation with the Federal Highway Administration

TRANSPORTATION RESEARCH BOARD

WASHINGTON, D.C.
2014
www.TRB.org

NATIONAL COOPERATIVE HIGHWAY RESEARCH PROGRAM

Systematic, well-designed research provides the most effective approach to the solution of many problems facing highway administrators and engineers. Often, highway problems are of local interest and can best be studied by highway departments individually or in cooperation with their state universities and others. However, the accelerating growth of highway transportation develops increasingly complex problems of wide interest to highway authorities. These problems are best studied through a coordinated program of cooperative research.

In recognition of these needs, the highway administrators of the American Association of State Highway and Transportation Officials initiated in 1962 an objective national highway research program employing modern scientific techniques. This program is supported on a continuing basis by funds from participating member states of the Association and it receives the full cooperation and support of the Federal Highway Administration, United States Department of Transportation.

The Transportation Research Board of the National Academies was requested by the Association to administer the research program because of the Board's recognized objectivity and understanding of modern research practices. The Board is uniquely suited for this purpose as it maintains an extensive committee structure from which authorities on any highway transportation subject may be drawn; it possesses avenues of communications and cooperation with federal, state and local governmental agencies, universities, and industry; its relationship to the National Research Council is an insurance of objectivity; it maintains a full-time research correlation staff of specialists in highway transportation matters to bring the findings of research directly to those who are in a position to use them.

The program is developed on the basis of research needs identified by chief administrators of the highway and transportation departments and by committees of AASHTO. Each year, specific areas of research needs to be included in the program are proposed to the National Research Council and the Board by the American Association of State Highway and Transportation Officials. Research projects to fulfill these needs are defined by the Board, and qualified research agencies are selected from those that have submitted proposals. Administration and surveillance of research contracts are the responsibilities of the National Research Council and the Transportation Research Board.

The needs for highway research are many, and the National Cooperative Highway Research Program can make significant contributions to the solution of highway transportation problems of mutual concern to many responsible groups. The program, however, is intended to complement rather than to substitute for or duplicate other highway research programs.

NCHRP REPORT 776

Project 12-86
ISSN 0077-5614
ISBN 978-0-309-28408-0
Library of Congress Control Number 2014940562

COPYRIGHT INFORMATION

NOTICE

The project that is the subject of this report was a part of the National Cooperative Highway Research Program, conducted by the Transportation Research Board with the approval of the Governing Board of the National Research Council.

The members of the technical panel selected to monitor this project and to review this report were chosen for their special competencies and with regard for appropriate balance. The report was reviewed by the technical panel and accepted for publication according to procedures established and overseen by the Transportation Research Board and approved by the Governing Board of the National Research Council.

The opinions and conclusions expressed or implied in this report are those of the researchers who performed the research and are not necessarily those of the Transportation Research Board, the National Research Council, or the program sponsors.

The Transportation Research Board of the National Academies, the National Research Council, and the sponsors of the National Cooperative Highway Research Program do not endorse products or manufacturers. Trade or manufacturers' names appear herein solely because they are considered essential to the object of the report.

Published reports of the

NATIONAL COOPERATIVE HIGHWAY RESEARCH PROGRAM

are available from:

Transportation Research Board
Business Office
500 Fifth Street, NW
Washington, DC 20001

and can be ordered through the Internet at:

http://www.national-academies.org/trb/bookstore

Printed in the United States of America

THE NATIONAL ACADEMIES

Advisers to the Nation on Science, Engineering, and Medicine

The **National Academy of Sciences** is a private, nonprofit, self-perpetuating society of distinguished scholars engaged in scientific and engineering research, dedicated to the furtherance of science and technology and to their use for the general welfare. On the authority of the charter granted to it by the Congress in 1863, the Academy has a mandate that requires it to advise the federal government on scientific and technical matters. Dr. Ralph J. Cicerone is president of the National Academy of Sciences.

The **National Academy of Engineering** was established in 1964, under the charter of the National Academy of Sciences, as a parallel organization of outstanding engineers. It is autonomous in its administration and in the selection of its members, sharing with the National Academy of Sciences the responsibility for advising the federal government. The National Academy of Engineering also sponsors engineering programs aimed at meeting national needs, encourages education and research, and recognizes the superior achievements of engineers. Dr. C. D. Mote, Jr., is president of the National Academy of Engineering.

The **Institute of Medicine** was established in 1970 by the National Academy of Sciences to secure the services of eminent members of appropriate professions in the examination of policy matters pertaining to the health of the public. The Institute acts under the responsibility given to the National Academy of Sciences by its congressional charter to be an adviser to the federal government and, on its own initiative, to identify issues of medical care, research, and education. Dr. Harvey V. Fineberg is president of the Institute of Medicine.

The **National Research Council** was organized by the National Academy of Sciences in 1916 to associate the broad community of science and technology with the Academy's purposes of furthering knowledge and advising the federal government. Functioning in accordance with general policies determined by the Academy, the Council has become the principal operating agency of both the National Academy of Sciences and the National Academy of Engineering in providing services to the government, the public, and the scientific and engineering communities. The Council is administered jointly by both Academies and the Institute of Medicine. Dr. Ralph J. Cicerone and Dr. C. D. Mote, Jr., are chair and vice chair, respectively, of the National Research Council.

The **Transportation Research Board** is one of six major divisions of the National Research Council. The mission of the Transportation Research Board is to provide leadership in transportation innovation and progress through research and information exchange, conducted within a setting that is objective, interdisciplinary, and multimodal. The Board's varied activities annually engage about 7,000 engineers, scientists, and other transportation researchers and practitioners from the public and private sectors and academia, all of whom contribute their expertise in the public interest. The program is supported by state transportation departments, federal agencies including the component administrations of the U.S. Department of Transportation, and other organizations and individuals interested in the development of transportation. **www.TRB.org**

www.national-academies.org

COOPERATIVE RESEARCH PROGRAMS

CRP STAFF FOR NCHRP REPORT 776

Christopher W. Jenks, *Director, Cooperative Research Programs*
Christopher Hedges, *Manager, National Cooperative Highway Research Program*
Waseem Dekelbab, *Senior Program Officer*
Danna Powell, *Senior Program Assistant*
Eileen P. Delaney, *Director of Publications*
Hilary Freer, *Senior Editor*

NCHRP PROJECT 12-86 PANEL
Field of Design—Area of Bridges

Bijan Khaleghi, *Washington State DOT, Tumwater, WA* (Chair)
Hussam Z. "Sam" Fallaha, *Florida DOT, Tallahassee, FL*
Jeffrey Ger, *Federal Highway Administration, Tallahassee, FL*
John S. Hastings, *Tennessee DOT, Nashville, TN*
Susan E. Hida, *California DOT, Sacramento, CA*
David J. Kiekbusch, *Wisconsin DOT, Madison, WI*
Norman L. McDonald, *Iowa DOT, Ames, IA*
Sheila Rimal Duwadi, *FHWA Liaison*
Stephen F. Maher, *TRB Liaison*

FOREWORD

By Waseem Dekelbab
Staff Officer
Transportation Research Board

This report provides proposed revisions to Section 1.3—Design Philosophy of the *AASHTO LRFD Bridge Design Specifications* with detailed examples of the application of the proposed revisions. The proposed revisions include system factors that can be used during the design and safety assessment of bridges subjected to distributed lateral load being evaluated using the displacement-based approach specified in the *AASHTO Guide Specifications for LRFD Seismic Bridge Design* or the traditional force-based approach. Also, the report presents system factors calibrated for application with bridge systems subjected to vertical vehicular loads. The material in this report will be of immediate interest to highway design engineers.

Quantification of redundancy is not fully formulated for bridge engineers. Redundancy can be considered during design by using load modifiers (i.e., design factors on the load side of the LRFD equation that reflect the ductility, redundancy, and operational importance of the structure) from the *AASHTO Load and Resistance Factor Design (LRFD) Bridge Design Specifications*. However, the value of load modifiers is determined by judgment rather than through a calibration process. To ensure uniform system performance for different bridge configurations, geometrical arrangements, and material and structure types, system factors were proposed in *NCHRP Report 406: Redundancy in Highway Bridge Superstructures* and *NCHRP Report 458: Redundancy in Highway Bridge Substructures*. These past efforts developed superstructure and substructure redundancy independently. A new approach was needed to focus on a combined system including superstructure and substructure interaction.

Research was performed under NCHRP Project 12-86 by the City College of the City University of New York to (1) develop a methodology to quantify bridge system reliability for redundancy; (2) recommend revisions to the *AASHTO LRFD Bridge Design Specifications*; and (3) provide illustrative applications based on the recommended revisions.

A number of deliverables are provided as appendices. These are not published herein but are available on the TRB website by searching for *NCHRP Report 776*. These appendices are titled as follows:

- APPENDIX A.1—Specifications
- APPENDIX A.2—Commentary
- APPENDIX A.3—Implementation examples
- APPENDIX B.1—Redundancy Analysis of Truss Bridge Example
- APPENDIX B.2—Redundancy Analysis of Steel Tub Bridge
- APPENDIX B.3—Redundancy Analysis of Prestressed Multi-cell Prestressed Concrete Bridge
- APPENDIX C—Review of the States of the Art and Practice

CONTENTS

Note: Many of the photographs, figures, and tables in this report have been converted from color to grayscale for printing. The electronic version of the report (posted on the Web at www.trb.org) retains the color versions.

AUTHOR ACKNOWLEDGMENTS

A project of this scope required the input of many colleagues who contributed in various ways to the success of this study. The project's principal investigator, Professor Michel Ghosn, is especially grateful for the selfless dedication of the graduate students who spent long hours helping move this project forward and specifically acknowledges the following contributions:

Research team:

- David Beal for his reviews, helpful comments, and suggestions.
- Bala Sivakumar from HNTB, for his reviews, advice, and valuable comments and for leading the HNTB team including O. Murat Hamutcuoglu and Feng Miao who performed the analysis of example bridges.
- Professor Dan Frangopol from Lehigh University for performing the sensitivity analysis for reliability index calculations.
- Professor Gongkang Fu from Illinois Institute of Technology for providing models for bridge foundations.

Research assistants:

- Jian Yang, research assistant at the City College of New York/City University of New York (CUNY).
- Feng Miao, research assistant at CUNY.
- Giorgio Anitori, research assistant at the Technical University of Catalonia, Spain.
- Graziano Fiorillo, research assistant at the City College of New York/CUNY.
- Alexandre Beregeon, exchange student at the City College of New York/CUNY.
- Tuna Yelkikanat, research assistant at the City College of New York/CUNY.

Special contributors:

- Professor Joan Ramon Casas, Technical University of Catalonia (UPC), Barcelona, Spain, who provided financial support during the PI's fellowship stay at UPC in 2010, and for providing additional support through the help of a research assistant. Professor Casas also provided technical expertise, assistance, and advice.
- Professor Yongming Tu from Southeast University (SEU), Nanjing, China, and Lennart Elfgren, professor emeritus of the Department of Civil, Environmental, and Natural Resources Engineering, Luleå University of Technology, Sweden, for developing and providing the model for the Åby bridge truss bridge example.

SUMMARY

Bridge System Safety and Redundancy

This report develops a method to calibrate system factors that can be applied during the design and load capacity evaluation of highway bridges to account for bridge redundancy and system safety. The proposed system factors can be used during the design and safety assessment of bridges subjected to distributed lateral load being evaluated using the displacement-based approach specified in the AASHTO Guide Specifications for LRFD Seismic Bridge Design or the traditional force-based approach. Also, the report presents system factors calibrated for application with bridge systems subjected to vertical vehicular loads. The proposed system factor tables are presented for each load case as described below. More details are provided in the body of this report.

The proposed system factors are used to modify the design/safety-check equation so that the required member capacity is evaluated using the following equation:

$$\phi_s \phi R_n^N = \sum \gamma_i Q_i \tag{S1}$$

where R_n^N is the required member capacity accounting for bridge redundancy, ϕ_s is the system factor specified in this Summary, ϕ is the member resistance factor as specified in the current AASHTO LRFD Bridge Design Specifications, γ_i is the load factor for load i, Q_i is the load effect of load i. The recommended values for the system factors are provided in the tables and equations below.

Bridge Systems under Distributed Lateral Load Evaluated Using the Displacement-Based Method

The displacement-based approach was found to explicitly consider the system effects of the entire bridge system. Accordingly, there is no measurable reserve system capacity that could be used to take advantage of bridge system redundancy. Therefore, the recommended system factor should serve to improve the reliability of the system and it takes the form

$$\phi_s = \exp^{-0.60(\Delta\beta_{u\ target})} \tag{S2}$$

where the 0.60 value in the exponential equation is used to account for the uncertainties associated with estimating the system capacity and the seismic demand. $\Delta\beta_{u\ target}$ is the target reliability index margin that should be specified by the code writers. $\Delta\beta_{u\ target}$ is the additional reliability that a system should provide beyond the reliability index that is used for the design of individual members. The AASHTO LRFD Bridge Design Specifications were calibrated so that bridge members under vertical gravity load generally produce a reliability index $\beta_{member} = 3.5$. However, it is generally expected that bridge systems provide additional reserve strengths so that system collapse does not take place should one member reach its limit capacity.

A $\Delta\beta_{u\ target}$ provides a reliability measure of that reserve strength. The reliability index for members of bridge systems subjected to seismic load or other lateral loads has not been determined. Nevertheless, it is herein proposed that a $\Delta\beta_{u\ target}$ on the order of 0.50 be used for bridges evaluated when subjected to lateral load. Because the displacement-based approach does not provide any additional system reserve strength, Equation S2 is proposed in order to obtain a reliability index for the system similar to that observed when using the traditional force-based method.

Bridge Systems under Distributed Lateral Load Evaluated Using the Force-Based Method

When the evaluation of bridge systems under lateral load is undertaken using the force-based method, the proposed system factor takes the form

$$\phi_s = \exp^{-\xi \times \Delta\beta_{u\ target}} \left[F_{mc} + C_\phi \frac{\gamma_\varphi \varphi_u - \varphi_{tunc}}{\varphi_{tconf} - \varphi_{tunc}} \right] \tag{S3}$$

where ξ in the exponential equation is the dispersion coefficient used to account for the uncertainties associated with estimating the system capacity and the hazard demand. $\Delta\beta_{u\ target}$ is the target reliability index margin that should be specified by code writers. It is herein proposed that a $\Delta\beta_{u\ target}$ equal to 0.50 be used in order to obtain a reliability index of the bridge system similar to that observed in *NCHRP Report 458* for unconfined multi-column bridge bents when subjected to other than seismic load. F_{mc} is a multi-column factor, C_φ is a curvature factor, φ_u is the ultimate curvature of the weakest column in the bent, γ_φ is the curvature correction factor for cases with weak connecting elements and weak details, φ_{tunc} is the average curvature for a typical unconfined column, φ_{tconf} is the average curvature for a typical confined column. The values recommended for each of the parameters in Equation S3 are provided in Table S1. The value for the ultimate curvature at failure φ_u is calculated from the ultimate plastic analysis of the column's cross section.

The values for F_{mc}, C_φ, φ_{tunc} and φ_{tconf} provided in Table S1 were extracted from the analysis of a large number of bridges with two-, three-, and four-column piers and bents. The piers and bents covered a range of column sizes, vertical reinforcement ratios, and confinement ratios. The analyses also considered the effect of different foundation stiffnesses. The values for φ_{tunc} and φ_{tconf} are the average curvatures obtained from the analysis of the column sizes used in *NCHRP Report 458.* The columns analyzed in *NCHRP Report 458* represent typical column sizes and reinforcement ratios collected from a national survey conducted as part of that study. The values for φ_{tunc} and φ_{tconf} are used in Equation S3 to compare the confinement ratio of the column being evaluated to the average confinement ratios observed in typical confined and unconfined columns.

A correction factor is applied in Equation S3 to reduce the ultimate column curvature for the cases where the shear capacity or the detailing of the columns or the capacity of the cap beams and pile caps are not sufficient to allow the columns to reach their full ultimate capacities, but the bridge columns do reach their plastic moment capacities. The correction factor is given as

$$\gamma_\varphi = \frac{M_{available} - M_{p\ column}}{M_{u\ column} - M_{p\ column}} \qquad \text{if } M_{u\ column} \geq M_{available} \geq M_{p\ column}$$

$$\gamma_\varphi = \frac{\varphi_{u\ connection}}{\varphi_u} \qquad \text{if } M_{available} \geq M_{u\ column} \text{ and } \varphi_{u\ connection} < \varphi_u \tag{S4}$$

$$\gamma_\varphi = 1.0 \qquad \text{if } M_{available} \geq M_{u\ column} \text{ and } \varphi_{u\ connection} \geq \varphi_u$$

system is non-redundant (see Table S1) $\qquad$ if $M_{available} < M_{p\ column}$

Table S1. Recommended values for redundancy parameters for straight bridges with one-column and multi-column bents of equal height under horizontal load.

Variable	Applicability	Recommended Value
$\Delta\beta_{u\ target}$, target reliability index margin	All systems	0.50
ξ, dispersion coefficient	Seismic loads	0.60
	All other lateral loads	0.35
ϕ_s, system factor for • One-column bents • Longitudinal loading of systems with bearing connections between superstructures and substructures • Systems where failure is controlled by shear or where failure is in the connections or where the detailing is not sufficient to allow plastic moment capacity of the members to be reached • Systems evaluated using the displacement-based approach		$\phi_s = \exp^{-\xi\Delta\beta_{u\ target}}$
F_{mc}, multi-column factor based on number of columns in each bent when the bridge is loaded laterally for both integral and bearing superstructure-substructure connections; also F_{mc} is a multi-bent factor based on the number of bents between expansion joints when a bridge with integral column/superstructure connections is loaded longitudinally	Two-column subsystems	1.10
	Three-column subsystems	1.16
	Multi-column subsystems	1.18
C_{φ}, curvature factor	All systems	0.24
φ_{tunc}, typical unconfined column ultimate curvature	All systems	3.64×10^{-4} (1/in)
φ_{tconf}, typical confined column ultimate curvature	All systems	1.55×10^{-3} (1/in)

where $M_{available}$ = moment capacity of the connecting elements such as cap beams and pile caps or the reduced moment that can be supported by the column based on the available shear reinforcement, development length, splice, or connection detailing.

Details on how to calculate the available moment capacity for a member with weak detailing are available in the FHWA Seismic Retrofitting Manual for Highway Structures, Part 1, Bridges, as $M_{p\ column}$ = plastic moment capacity of column, $M_{u\ column}$ = ultimate overstrength moment capacity of column calculated using nonlinear sectional capacity analysis programs or conservatively estimated to be 1.15 $M_{p\ column}$, φ_u = ultimate curvature of the weakest column in the bent, and $\varphi_{u\ connection}$ = minimum ultimate curvature of the connecting elements.

Bridge Systems under Concentrated Lateral Load

The analysis of systems subjected to statically applied concentrated lateral loads to a girder or column have demonstrated that they primarily cause local effects with little contribution from the remaining members of the system. Therefore, the system factor for evaluating the effect of concentrated lateral forces is

$$\phi_s = \exp^{-0.35(\Delta\beta_{u\ target})} \tag{S5}$$

where the 0.35 value in the exponential equation is used to account for the uncertainties associated with estimating the capacity of the member and the force applied.

Bridge Systems under Vertical Vehicular Load

System factors for multi-beam I-girder and box-girder bridges are proposed for evaluating the redundancy of originally intact systems subjected to vehicular overloads and for damaged bridges that have been previously exposed to local member damage.

Redundancy of Originally Intact Systems under Overloads

The system factors for I-girder bridges and spread box-girder bridges are provided in Tables S2 and S3 in function of the capacity of the bridge to resist first member failure represented by the variable, LF_1, the dead load to resistance ratio of the members and based on the material and geometric properties of the bridge. The proposed systems factors were calibrated so that the system provides a reliability index margin $\Delta\beta_u = 0.85$ as recommended in *NCHRP Report 406*. This $\Delta\beta_u$ target value was obtained based on the reliability evaluation of bridge systems that have traditionally shown good system performance. The reliability index margin $\Delta\beta_u$ reflects the required reliability of the system beyond the reliability of the first member to fail.

D/R is the dead load to resistance ratio for the bridge beams. LF_1 is a factor related to the capacity of the system to resist the failure of its most critical bridge member calculated from a linear structural analysis of the bridge up until the first member fails. LF_1 gives the number of HS-20 trucks that the bridge member can carry in addition to the dead load. It can be expressed as

$$LF_1 = LF_1^+ = \frac{R^+ - D^+}{L_1^+} \quad \text{when} \quad \frac{LF_1^-}{LF_1^+} \geq 1.0$$
$$LF_1 = LF_1^- = \frac{R^- - D^-}{L_1^-} \quad \text{when} \quad \frac{LF_1^-}{LF_1^+} < 1.0 \qquad \text{(S6)}$$

That is, LF_1 in Tables S2 and S3 represents the load carrying capacity of the weakest section of the beam that can be either the positive bending section or the negative bending section depending on the moment capacity in each region (R), the dead load moment in each region (D), and the effect of the applied live load moment on the most critical beam (L_1) where the live load represents two side-by-side HS-20 trucks applied at the middle of the span or two trucks in one lane applied in each of two contiguous spans. The positive superscript in LF_1, R, D, and L_1 is for the positive bending region, the negative superscript is for the negative bending regions.

Table S2. System factors for overloads on I-girder bridges.

Bridge Cross-Section Type	System Factor
Simple-span 4 I-beams at 4 ft	$\phi_s = 0.80 + 0.16 D/R$
Simple-span 4 I-beams at 6 ft	$\phi_s = 0.90 + 0.09 D/R$
Simple-span 6 I-beams at 4 ft	$\phi_s = 0.95 + 0.05 D/R$
Continuous span 4 I-beams at 4 ft with compact members	$\phi_s = 0.93 + 0.07 D/R$
Continuous steel I-girder bridges with noncompact negative bending sections and $LF_1^- \leq 1.16 LF_1^+ + 0.75$	$\phi_s = 0.80 + 0.16 D/R$
All other simple-span and continuous I-beam bridges	$\phi_s = 1 + \frac{1 - 1.5(D/R)^2}{1 + LF_1^2}$

Table S3. System factors for overloads on spread box-girder bridges.

Bridge Cross-Section Type	System Factor
Narrow simple-span box-girder bridges less than 24-ft wide	$\phi_s = 0.83 + 0.14\,D/R$
All other simple-span box-girder bridges	$\phi_s = 1 + \dfrac{1 - 1.5(D/R)^2}{1 + LF_1^2}$
Narrow continuous box-girder bridges less than 24-ft wide	$\phi_s = 1 + \dfrac{1 - 1.5(D/R)^2}{1 + LF_1^2}$
Continuous steel box-girder bridges with noncompact negative bending sections and $LF_1^- \le 1.75 LF_1^+$	$\phi_s = 1 + \dfrac{1 - 1.5(D/R)^2}{1 + LF_1^2}$
All other continuous box-girder bridges	$\phi_s = 1 + 4 \times \dfrac{1 - 1.5(D/R)^2}{1 + LF_1^2}$

The parameter L_1 gives the live load applied on the most critical member, which is defined as the member that fails first. It can be calculated as

$$L_1 = D.F. \times LL \tag{S7}$$

where D.F. is the load distribution factor and LL is the effect of the HL-93 truck load with no impact factor and no lane load.

Redundancy of Damaged Systems under Vertical Loads

The system factors for damaged I-girder and spread box-girder bridges are provided in Tables S4 and S5 as a function of the redundancy ratio $R_d = \dfrac{LF_d}{LF_1}$ which gives the capacity of a damaged bridge system that has previously lost the load carrying capacity of a main member given as LF_d and the ability of the originally intact bridge to resist first member failure which

Table S4. System factors for damaged I-girder bridges under vertical loads.

Bridge Cross-Section Type	Redundancy Ratio $R_d = \dfrac{LF_d}{LF_1}$	System Factor
Simple-span and continuous prestressed concrete I-girder bridges with four beams at 4 ft	$R_d = 0.56\gamma_{transverse}\gamma_{weight}$	$\phi_s = \dfrac{R_d}{0.47 - (0.47 - R_d)\dfrac{D}{R}}$
Simple-span and continuous compact steel I-girder bridges with four beams at 4 ft	$R_d = 0.64\gamma_{transverse}\gamma_{weight}$	
All other simple-span I-girder bridges	$R_d = (1 - 0.056\,S)\gamma_{transverse}\gamma_{weight}$	
Continuous noncompact steel I-girder bridges with four beams at 4 ft	$R_d = 0.58\gamma_{transverse}$	
All other continuous noncompact steel I-girder bridges	$R_d = (1.00 - 0.08\,S)\gamma_{transverse}$	
All other continuous compact steel and prestressed concrete I-girder bridges	$R_d = (1.35 - 0.08\,S)\gamma_{transverse}$	

where S = beam spacing in feet.

Table S5. System factors for damaged spread box-girder bridges under vertical loads.

Bridge Cross-Section Type	Redundancy Ratio $R_d = \frac{LF_d}{LF_1}$	System Factor
Fractured simple-span steel box-girder bridges less than 24-ft wide	Non-redundant	ϕ_s=0.80
Narrow simple-span steel box-girder bridges less than 24 ft with no torsional rigidity	$R_d = 0.46\gamma_{transverse}$	$\phi_s = \frac{R_d}{0.47 - (0.47 - R_d)\frac{D}{R}}$
All other simple-span box-girder bridges	$R_d = 0.72\gamma_{transverse}$	
Continuous steel box-girder bridges with noncompact negative bending sections and $LF_1^- \le 1.75LF_1^+$	$R_d = 0.72\gamma_{transverse}$	
All other continuous box-girder bridges	$R_d = \left(0.59 + \frac{4.50}{LF_1}\right)\gamma_{transverse}$	

is represented by the variable, LF_1, defined in Equation S6. For the spread box-girder bridges, three different damage scenarios are considered. In the first scenario, one box is assumed to have been exposed to a fatigue-type fracture that sliced through the entire bottom flange and two webs. The second scenario assumed major damage to one web while maintaining the torsional capacity of the box. The third scenario considered that the failure of the web also led to the loss of the torsional rigidity of the box.

Tables S4 and S5 list the expressions for R_d as a function of beam spacing, slab strength, and the dead weight applied on the damaged member for the bridge types analyzed in this study and the corresponding system factor. The proposed systems factors were calibrated so that a damaged system provides a reliability index margin $\Delta\beta_d = -2.70$ as recommended in *NCHRP Report 406.* This $\Delta\beta_d$ target value was obtained based on the reliability evaluation of damaged bridge systems that have traditionally shown good system performance. The reliability index margin $\Delta\beta_d$ reflects the required reliability of the damaged system compared to the reliability of the first member to fail in an originally intact system.

The effect of the weight of the damaged beam that must be carried by the remaining system is considered using

$$\gamma_{weight} = 1.23 - 0.23\omega_{beam}\,(kip/ft) \tag{S8}$$

ω_{beam} = total dead weight on the damaged beam in kip per unit length.

The effect of the slab, bracings, and diaphragms is considered using

$$\gamma_{transverse} = 0.50\frac{M_{transverse}}{13.5\ kip.ft/ft} + 0.50 \tag{S9}$$

$$M_{transverse} = M_{slab} + M_{br/L} \tag{S10}$$

where $M_{transverse}$ = combined moment capacity for lateral load transverse expressed in kip-ft per unit slab width, M_{slab} = moment capacity of slab per unit width, and $M_{br/L}$ = contribution

of the bracing and diaphragms to transverse moment capacity calculated using Equations S11 or S12.

The equivalent transverse moment capacity for cross bracing as defined in the *FHWA Steel Bridge Design Handbook: Bracing System Design* (2012) can be obtained as

$$M_{br/L} = \frac{F_{br} h_b}{L_b} \tag{S11}$$

The equivalent transverse moment capacity for diaphragms is given by

$$M_{br/L} = \frac{M_{br}}{L_b} \tag{S12}$$

where M_{br} = moment capacity of diaphragms contributing to lateral transverse distribution of vertical load between adjacent main bridge girders; F_{br} = bracing chord force determined from the applicable limit state for the bolts (see AISC Steel Construction Manual, Part 7), welds (see AISC, Part 8), and connecting elements (see AISC, Part 9); L_b = spacing of the cross frames or diaphragms; and h_b = distance between the bracing top and bottom chords.

The range of applicability of $\gamma_{transverse}$ has been verified for I-girder bridges and showed an upper limit value in the range of $\gamma_{transverse}$ = 1.10 to 1.20 with 1.10 being a conservative value.

Multi-cell box-girder bridges have been found to be sufficiently redundant for the ultimate system reserve strength condition and the ability of the originally intact system to resist collapse if member strength is exceeded with a recommended system factor $\phi_s = 1.0$. Multi-cell box-girder bridges are highly redundant for system strength of damaged bridge condition with a recommended system factor $\phi_s = 1.2$ for systems that may have sustained damage to one of the webs. Single-cell box-girder bridges are not redundant and the recommended system factor for both the ultimate condition and the damaged state condition is $\phi_s = 0.80$.

Recommended system factors for typical straight superstructures are specified in Table S6 for single-cell and multi-cell boxes for resistance to collapse of the originally intact system and Table S7 for single-cell and multi-cell boxes in damaged state condition.

Table S6. System factors for single-cell and multi-cell box-girder superstructures for resistance to collapse conditions under vertical loading.

Bridge Cross-Section Type	System Factor
Single-cell box-girder bridges	$\phi_s = 0.80$
Multi-cell box-girder bridges	$\phi_s = 1.00$

Table S7. System factors for single-cell and multi-cell box-girder superstructures in damaged state condition under vertical loads.

Bridge Cross-Section Type	System Factor
Single-cell box-girder bridges	$\phi_s = 0.80$
Multi-cell box-girder bridges	$\phi_s = 1.20$

General Comment

The analyses in *NCHRP Report 406* and *NCHRP Report 458* concentrated on bridges that closely met the member strength design requirements. The analyses performed in this study considered the redundancy of deficient bridges as well as overdesigned bridges that expand the applicability of the proposed system factors. The proposed system factors are expressed in terms of a limited number of parameters related to the relevant geometric properties of the system and the strength and material properties of the primary bridge members.

CHAPTER 1

Introduction

1.1 Background

Structural redundancy is defined as the ability of a structural system to continue to carry load after the failure of one or several structural components. Although this concept is well understood, no consensus is currently available on non-subjective measures engineers should use to quantify structural redundancy and how to apply such measures to design adequately redundant bridges. In an attempt to overcome this gap, the AASHTO Load and Resistance Factor Design (LRFD) Bridge Design Specifications (2012) propose to consider redundancy during bridge design by using load modifiers that reflect the ductility, redundancy, and operational importance of the structure (Frangopol and Nakib, 1991). However, the values of the load modifiers provided in the AASHTO LRFD were determined by judgment rather than through a calibration process. Furthermore, the LRFD specifications do not provide clear guidance on how to select the ductility or the redundancy modifiers.

Following several years of research, *NCHRP Report 406: Redundancy in Highway Bridge Superstructures* by Ghosn and Moses (1998) and *NCHRP Report 458: Redundancy in Highway Bridge Substructures* by Liu, Neuenhoffer, Ghosn, and Moses (2001) proposed non-subjective and quantifiable measures of redundancy after studying the behavior of typical bridge superstructure and substructure systems beyond the failure of their first components. Accordingly, a quantitative measure of redundancy was defined in terms of the capacity of the system as compared to the capacity of the weakest component. Three different limit states for the system were proposed: (1) collapse of overloaded originally intact systems, (2) exceeding the functionality limit of overloaded intact systems, (3) collapse of damaged bridges. An intact system is a bridge that was not damaged prior to the initiation of a loading process. Damaged bridges are those that may have been exposed to a damaging event that resulted in the loss or the reduction in the load carrying capacity of a major component. The recent literature often has referred to this limit state as structural robustness.

NCHRP Report 406 and *NCHRP Report 458* then proceeded to calibrate sets of system factor tables using reliability methods to ensure uniform system performance for different typical bridge configurations, geometrical arrangements, and material and structure types. In *NCHRP Report 406*, superstructure system factors are applied on the resistance side of the LRFD equation for slab on girder type bridges based on the girder spacing and number of girders in the system. System factor charts were provided for simple-span and continuous steel and pretensioned I-beam superstructures subjected to traffic loads. However, the report did not address box-girder superstructures with sufficient detail to make specific recommendations.

As presented in *NCHRP Report 406*, the system factor tables are intended for use when analyzing the redundancy of the most typical bridge configurations and dimensions. Recognizing that it will not be possible to develop system factor tables to cover all possible bridge configurations or damage scenarios and in order to provide the engineers with a method to analyze the redundancy of bridge types and conditions not covered in the available tables, *NCHRP Report 406* provides a direct redundancy analysis procedure to generate the system factors using nonlinear analysis and incrementally increasing the design load.

In *NCHRP Report 458*, substructure system factors were provided for confined and unconfined 2- and 4-column piers founded on spread footings, drilled shafts, or piles in various soil types. A direct redundancy analysis procedure also was provided to cover other substructure configurations. The ability of the superstructure to enhance the substructure's redundancy was recognized as poor for typical systems where the interaction between the superstructure and substructure relied on support bearings. Specifically, the report did not study integral construction systems.

The system factor tables provided in *NCHRP Report 406* were subsequently simplified and included in the Load and

Resistance Factor Rating (LRFR) method in the AASHTO Manual for Bridge Evaluation (MBE) (2011), which also recommended the use of the direct redundancy analysis method for special cases. Since then, several consulting firms (with the cooperation of the Wisconsin Department of Transportation) have applied the recommendations of *NCHRP Report 406* for the safety assessment of existing bridges (Hubbard, Shkurti, and Price, 2004; Milwaukee Transportation Partners, 2005). More recently, Hunley and Harik (2012) performed detailed analyses of box-girder bridges with different configurations to study the effect of external bracing on straight and curved steel box-girder bridges using the methods and criteria proposed in *NCHRP Report 406.* These studies and other similar investigations have applied variations of the *NCHRP Report 406* method to analyze different bridge damage scenarios. The influence of different diaphragm configurations on improving the redundancy of box-girder bridges under various bridge geometric and damage conditions was analyzed on a case-by-case basis as was the intent of *NCHRP Report 406.*

Hunley and Harik (2007) state that "the approach proposed in NCHRP Report 406 has gained acceptance from agencies and bridge designers on several projects." The work of *NCHRP Report 406* also has been well received in Europe where it was included in a set of recommended guidelines for evaluating the safety of existing railway bridges (Guideline for Load and Resistance Assessment of Existing European Railway Bridges, 2007). The method proposed in *NCHRP Report 406* and *NCHRP Report 458* or variations on the method also have been adopted by several research studies throughout the world to analyze the redundancy of bridge structural systems (Hunley and Harik, 2012; Mohammadkhani-Shali, 2007; Imhof, 2004; Casas and Wisniewski, 2005).

As part of *NCHRP Report 458*, the authors presented the recommendations of *NCHRP Report 406* and *NCHRP Report 458* in a format that would be implementable in the AASHTO LRFD and LRFR. The format addressed redundancy in a comprehensive compatible set of specifications that covered bridge superstructures and substructures independently. However, the format has not been implemented in the LRFD specifications pending more investigation to simplify the format, increase the range of applicability of the system factors, and further confirm the validity and practicality of the approach.

1.2 Research Objectives

In summary, the framework and methods of *NCHRP Report 406* have led to the development of non-subjective and quantifiable measures of bridge redundancy that have been successfully applied to provide system factor tables for a range of bridge superstructure and substructure configurations. A variation of the *NCHRP Report 406* recommendations also has been adopted as part of the AASHTO LRFR for the safety evaluation of highway bridges. The direct redundancy analysis method proposed in *NCHRP Report 406* to analyze configurations and damage scenarios not considered in the report has been successfully applied by engineering firms, bridge agencies, and researchers to analyze the redundancy of different types of bridges subjected to various types of damage scenarios. However, *NCHRP Report 406* and *NCHRP Report 458* did not provide system factors for some bridge system and subsystem configurations that have become more popular in recent years. Also, the report did not verify the applicability of the factors for analyzing the combined system, including the interaction between the superstructure and substructure. Hence, the objectives of this research study are to

1. Review the state of the art as well as the state of practice on the subject of structural redundancy to assess the method proposed in *NCHRP Report 406* and compare it to alternative approaches for quantifying structural redundancy and considering redundancy during the design of new bridges and the evaluation of existing bridges.
2. Verify the applicability of the *NCHRP Report 406* method and investigate the validity of the results in *NCHRP Reports 406* and *458* for analyzing the redundancy of complete bridge systems combining superstructure and substructure interaction.
3. Extend the system factors to cover common bridge configurations including those not addressed in *NCHRP Report 406* and *NCHRP Report 458.*
4. Consolidate the recommendations made in *NCHRP Reports 406* and *458* into a format that can be incorporated into the AASHTO LRFD and LRFR specifications.
5. Illustrate how the recommended approach and system factors can be applied in bridge engineering practice.

This report summarizes the findings of the study and verifies and complements the results presented in *NCHRP Report 406* and *NCHRP Report 458.* The summaries serve to develop a set of specifications that would be implementable in the AASHTO LRFD and LRFR specifications.

1.3 Report Outline

This report presents the findings of the NCHRP Project 12-86 research and uses the results of new analyses to verify and complement the results presented in *NCHRP Reports 406* and *458.* This report is divided into the following six chapters.

- Chapter 1 provides the background for this study and summarizes its objectives.
- Chapter 2 presents a review of the general concepts of bridge redundancy and the method adopted to quantify the redundancy of bridge systems and subsystems.

- Chapter 3 addresses the redundancy of bridge systems subjected to lateral loads when bridge safety is evaluated using displacement-based criteria.
- Chapter 4 addresses the redundancy of bridge systems subjected to lateral loads when bridge safety is evaluated using the traditional force-based method.
- Chapter 5 addresses the redundancy of bridge systems subjected to vertical loads.
- Chapter 6 gives the conclusions of this study.
- Appendices are not included herein but are available on the TRB website and can be found by searching for *NCHRP Report 776*. Appendix A gives a proposed set of specifications to design bridge members based on the level of bridge redundancy. Appendix B provides examples illustrating the application of the system factors and the direct analysis method for evaluating the redundancy of bridges. Appendix C gives a review of the literature and state of practice. Appendix D gives the summary of the models and the results for the analysis of different types of bridge superstructures.

References

AASHTO (2012) *LRFD Bridge Design Specifications.* 6th ed, Washington, D.C.

AASHTO MBE-2-M (2011) *Manual for Bridge Evaluation*, 2nd ed, Washington, D.C.

Casas, J. R. and Wisniewski, D. F. (2005) Safety Formats and Required Safety Levels—Background document, WP4-G-R-01, Sustainable Bridges—VI Framework Program. Brussels, Belgium.

Frangopol, D. M. and Nakib, R. (1991), "Redundancy in Highway Bridges," *Engineering Journal*, American Institute of Steel Construction, 28(1), 45–50.

Ghosn, M. and Moses, F. (1998) *NCHRP Report 406: Redundancy in Highway Bridge Superstructures*, Transportation Research Board, National Research Council, Washington, D.C.

Guideline for Load and Resistance Assessment of Existing European Railway Bridges (2007) http://www.sustainablebridges.net/main.php/SB4.2_Guideline_LRA.pdf?fileitem=28868626

Hubbard, F., Shkurti, T., and Price, K. D. (2004) "Marquette Interchange Reconstruction: HPS Twin Box Girder Ramps," International Bridge Conference, Pittsburgh, PA.

Hunley, T. and Harik, I. (2007) "Redundancy of Twin Steel Box Girder Bridges," World Steel Bridge Symposium, National Steel Bridge Alliance, New Orleans, LA.

Hunley, T. C. and Harik, I. E. (2012) "Structural Redundancy Evaluation of Steel Tub Girder Bridges," *Journal of Bridge Engineering*, 17(3), May 1, 2012.

Imhof, D. (2004) "Risk Assessment of Existing Bridge Structures," Ph.D. diss., King's College, Cambridge University, England.

Liu, D., et al. (2001) *NCHRP Report 458: Redundancy in Highway Bridge Substructures*, Transportation Research Board, National Research Council, Washington, D.C.

Milwaukee Transportation Partners (2005) "Redundancy of Box Girder Steel Bridges—A Study for the Marquette Interchange HPS Twin Box Girder Structures," Project ID 1060-05-1222.

Mohammadkhani-Shali, Soheil (2007) "Study of System Redundancy in Bridges: Failure Mechanism Analysis Using Response Surface Methods," PhD thesis, Ecole National des Ponts et Chausses, ENPC, Paris, France.

CHAPTER 2

General Concepts of Bridge Redundancy

2.1 Introduction

Redundancy is defined as the capability of a bridge system to continue to carry load after the failure of one of its members. This means that the system has additional reserve strength such that the failure of one member does not result in the collapse of the entire structure or a significant portion of it. The initial member failure can be either brittle or ductile. It can be caused by the application of large overloads, extreme loads, or the loss in the load carrying capacity of one element due to damaging events such as fatigue, brittle fracture, member deterioration, or an accident such as a collision by a truck, ship, or debris.

For the case of damaged bridges that may have lost an initial member, the object of this project is not to perform a dynamic progressive collapse analysis to check whether the bridge will be able to survive the hazard that causes an initial sudden failure of the element. Instead, the object of the redundancy analysis performed in this study is to investigate whether a damaged bridge system that has survived a damaging event will be able to continue to carry some traffic load for a limited period of time that would allow the traffic to clear the bridge and maintain the bridge's ability to continue to carry some load until the damage is noticed and reported to the proper authorities so corrective actions (i.e., bridge closure, repair, or replacement) are undertaken.

Traditionally, bridges have been designed on a member-by-member basis, and the interaction of the members and their ability to provide different levels of redundancy following the damage to, or the failure of, one or several members have not been directly considered. A convenient method to take into consideration the redundancy of bridge systems would consist of developing a set of system factors that can be included as specifications in bridge design and evaluation manuals. The system factors would be applicable for routinely checking the safety of typical bridge configurations so that the members of bridges with low levels of redundancy are required to have higher safety levels than bridges with high levels of redundancy. Alternatively, for a more precise evaluation of a bridge's redundancy, a direct analysis approach should be used. The direct analysis would consist of using a structural model and a finite element analysis program that consider the elastic and inelastic behavior of the bridge system. This program would be used to evaluate the load carrying capacity of an initially intact bridge, as well as the behavior of the bridge under different damage scenarios. The program would check the structure to verify whether its behavior is acceptable, with sufficiently high levels of safety and functionality during the application of expected large loads.

Many safety-related decisions must be made in order to develop the system factors or to use the direct analysis approach. These include (1) the limit states that should be checked, (2) the level of loads that must be carried by the structure before the limit states are reached, (3) the type of damage conditions that must be borne by the structure, and (4) the inclusion of uncertainties in the analysis model.

This report reviews the results of the analyses of bridge systems including superstructures and substructures, as well as combined systems conducted during this current project and during *NCHRP Report 406* and *NCHRP Report 458*. The goal is to develop a set of system factors that can be included in bridge specifications to evaluate the safety of existing bridges and to design new bridges taking into consideration their levels of redundancy.

This chapter gives a general overview of the concepts of bridge safety and redundancy and describes the procedure adopted to develop a set of system factors that can be incorporated into the design and safety-check equations in order to account for bridge system redundancy during the design of new bridges and the evaluation of existing bridges. Specifically, Section 2.2 of this chapter gives a general overview of bridge performance under externally applied actions and the general concept of bridge safety. Section 2.3 proposes deterministic measures of redundancy. Section 2.4 gives a review

of reliability theory and its application for calibrating bridge design and safety assessment codes. Section 2.5 develops the reliability model used in this study for the probabilistic evaluation of bridge redundancy and the calibration of system factors. The concepts presented in this chapter are adapted in Chapter 3 for calibrating system factors that account for the redundancy of bridge systems subjected to lateral actions when bridge system safety is checked using the displacement-based method. Chapter 4 uses the concepts presented in this chapter to develop system factors that account for the redundancy of bridge systems subjected to lateral loads when their safety is checked using force-based analysis methods. Chapter 5 uses the concepts presented in this chapter to develop system factors that account for the redundancy of bridge systems subjected to vertical loads.

2.2 Bridge System Behavior

Current bridge design and evaluation techniques deal with individual members and use procedures that do not fully account for the effect of the complete structural system. As currently performed, the safety check verifies that the strength of each member is greater than the effects of applied forces by a "comfortable" safety margin. Member forces are calculated using an elastic analysis while member capacity (when appropriate) is calculated using inelastic member behavior. In current and previous bridge design and evaluation specifications, the safety margin for strength is provided through the application of safety factors (load and/or resistance factors) that are calibrated on the basis of experience and engineering judgment (ASD and LFD) or on a combination of experience and structural reliability methods (LRFD).

Although this traditional member-oriented approach has been used successfully for years, it does not provide an adequate representation of the safety of the complete bridge system. In many instances, the failure of an individual member does not lead to the collapse of the complete bridge system. Current specifications do not directly differentiate between bridges that would collapse when one member fails and those that will be able to continue to carry loads after the failure of one member. Because of this difference in the consequences of a member's failure, it is reasonable for the specifications to require that members of non-redundant bridges be designed to higher standards than members of redundant bridges. This goal can be achieved by applying system factors in the safety-check equations or as currently stipulated in the AASHTO LRFD Bridge Design Specifications by applying load modifiers. Because the load modifiers specified in the current LRFD were based on the judgment of the code writers rather than an evaluation of bridge redundancy, the object of this NCHRP 12-86 project is to propose an approach to account for bridge system redundancy based on measurable criteria.

A first step in the process of evaluating bridge redundancy is to have a good understanding of the behavior of bridge systems under applied loads. The performance of a bridge system can be represented as shown in Figure 2.1, which gives a conceptual representation of the response of a structure to different levels of applied loads and the different criteria that should be considered when evaluating member safety or system safety as well as system redundancy. The model is valid for representing the behavior of systems under vertical loads or for systems under lateral loads.

The green line in Figure 2.1 labeled "Intact system" may represent the applied load versus maximum displacement of a ductile bridge system when subjected to different levels of load. In this case, a load capacity evaluation is performed to study the behavior of an intact system that was not previously subjected to any damaging load or event.

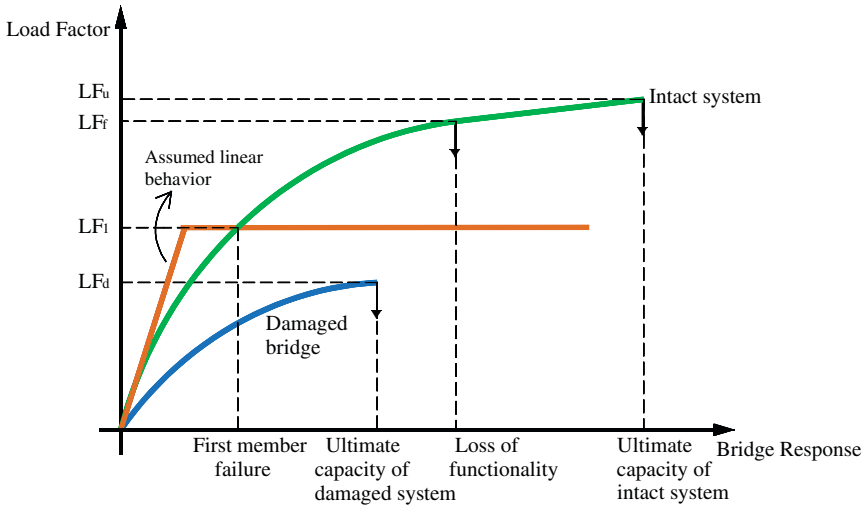

Figure 2.1. Representation of typical behavior of bridge systems.

To perform the load capacity analysis, the bridge is first loaded by the dead load and then the transient load is incrementally applied. The first structural member will fail when the transient load reaches LF_1. LF_1 would then be related to member safety. LF_1 may represent the actual load or the multiple of a basic load such as the number of design trucks that the system can carry before the first member reaches its limit capacity. Although LF_1 should be evaluated using the actual response of the bridge accounting for material nonlinearity, it has been common in structural design practice to assume linear-elastic response while evaluating the ability of the system to resist the failure of the most critical member as indicated using the bilinear brown curve in Figure 2.1.

Generally, the system will be able to carry additional load after LF_1 is reached and the ultimate capacity of the entire bridge is not reached until the transient load reaches LF_u. LF_u would give an evaluation of system safety. Large deformations rendering the bridge unfit for use are reached when the transient load reaches LF_f. LF_f gives a measure of system functionality. A bridge that has been loaded up to this point is said to have lost its functionality.

Damage to bridge members leading to the loss in member and system capacity is also a concern. Bridge members are often subjected to fatigue stresses that may lead to the fracture and loss of the load carrying capacity of a main member. In addition, deterioration and corrosion, fire, or an accident, such as a collision by a truck, ship, or debris, could cause the reduction in the load carrying capacity of one or several main members. To ensure the safety of the public, bridges should be able to sustain these damages and still operate at a sufficient level of capacity. Although a damaged bridge cannot be expected to have the same capacity of an intact system, an adequately redundant system should still be able to carry its own weight and some level of transient load to allow for clearing the bridge before closure and the undertaking of necessary repairs. Therefore, in addition to verifying the safety of the intact structure, the evaluation of a bridge's safety and redundancy should consider the consequences of the failure of a critical bridge member.

If the bridge has sustained major damage due to the brittle failure of one or more of its members, its behavior can be represented by the blue curve labeled "Damaged bridge" in Figure 2.1. The ultimate capacity of the damaged bridge is reached when the transient load applied after the application of the dead load reaches LF_d. LF_d would give a measure of the remaining safety of a damaged system.

In summary, based on the bridge performance curve presented in Figure 2.1, a bridge can be considered safe if it

- Provides a reasonable safety level against first member failure,
- Provides an adequate level of safety before it reaches its ultimate system capacity under extreme loading conditions,
- Does not produce large deformations under expected heavy transient loads, and
- Is able to carry a sufficient level of traffic load after damage to or the loss of a component.

Although the explanations provided in this section are presented in terms of the loads or load factors, labeled "LF" on the vertical axis of the graph, the same criteria can be expressed in terms of the response of the bridge or the horizontal axis of the graph. Most typically, the response of the bridge is represented by the maximum displacement at a critical section.

The load factor values that a system can support before a limit state is reached represent the system safety of the bridge. Redundancy is a measure of the relationship between the overall system performance and that of its most critical member as will be explained next.

2.3 Measures of Bridge Redundancy

Traditionally, bridge engineers have defined redundancy of bridges in terms of the availability of alternate load paths that can redistribute the load should one of the main members fail. Commonly, the availability of alternate load paths has been associated with the number of supporting elements. Thus, according to current practice a multi-girder bridge superstructure would be considered redundant if it is formed by four or more parallel elements (although some engineers have defined bridges with three parallel girders as redundant). Variations in bridge cross-section configurations including the type of girders, beam spacing, and boundary conditions are not usually considered. Furthermore, a system is currently classified as either redundant or non-redundant and no consideration is given to the degree of redundancy. Accordingly, a system formed by two spread box-girders is usually considered to be similar to a system formed by two I-girders in terms of their redundancies independent of the spacing between the I-girders or the webs of the boxes or whether the spans are continuous or simply supported. The current approach ignores the additional torsional rigidity of the boxes that may improve the load distribution and would change the redundancy level of the system when compared to that of I-girder bridges.

In a first attempt at providing a method to explicitly incorporate redundancy criteria during the bridge design process, the AASHTO LRFD Bridge Design Specifications apply load modifiers in the design-check equations to account for redundancy during the design of new bridges. The method is based on the recommendation of Frangopol and Nakib (1991). Specifically, the AASHTO LRFD recommends using a load modifier, η_R, depending on the level of bridge redundancy with η_R taking values equal to 0.95, 1.0, or 1.05. Two other load modifiers η_D and η_I also are used to account for member ductility and the importance of the structure in

terms of defense/security considerations. However, the LRFD specifications do not explain how to identify which bridges have low and high redundancy or how to define low and high ductility. As explained in the LRFD Commentary, the recommended values for η_R have been subjectively assigned based on judgment pending additional research.

The Canadian Code CAN/CSA-S6-06 (2006) directs bridge engineers to use different load factors for different target reliability index values that are selected based on the redundancy of the bridge system and the ductility of the member being evaluated. However, like the LRFD, this approach relies on the judgment of the engineer in deciding which bridges are redundant and in judging the consequence of a member's failure.

Perhaps the most specific approach for evaluating bridge redundancy is provided in the Pennsylvania (PennDOT) bridge design specifications. According to PennDOT, three-girder bridges without floorbeams and stringers are considered as non-redundant and should be avoided if possible. A 3-D redundancy analysis is required for the evaluation of all non-redundant structures to check whether the failure of any tension component or other critical component will not cause collapse. To that effect, two new Extreme Event Limit States labeled as III and IV are added to the LRFD specifications. Extreme event III is meant to check that the failure of one element of a component will not lead to the failure of the component. Extreme event IV is meant to check that the failure of one component will not lead to the failure of the structure. These limit states require the analysis of a damaged bridge with the HL-93 design load along with a reduced dead load factor equal to 1.05 and live load factors of 1.30 and 1.15, for extreme events III and IV respectively, when using the HL-93 live load in all of the lanes. When a permit load is used in the governing lane and the HL-93 in other lanes, the live load factors on the permit load are 1.10 and 1.05 for extreme events III and IV, respectively. The analysis of the damaged bridge is performed with these load combinations, which the structure should be able to carry even if they cause large deformations as long as they do not lead to collapse. No justification is provided for the selection of the live load factors for the new Extreme Event Limit States.

From the above three examples and other studies reported in the review of the literature undertaken during the course of this project and summarized in Appendix C (available on the TRB website by searching for *NCHRP Report 776*), it is clear that accounting for bridge redundancy during the safety analysis of new or existing bridges is of primary importance. However, the mechanisms and the criteria that should be used to quantify bridge redundancy and consider it during the evaluation of bridge safety still have not been fully established. The aim of this project is to develop methods to quantify bridge redundancy and propose a set of non-subjective criteria that are implementable in bridge design and safety analysis processes.

Because redundancy is defined as the capability of a structure to continue to carry loads after the failure of one main member, a comparison between the overall capacity of originally intact and damaged bridge systems as represented by LF_u, LF_f, LF_d, in Figure 2.1, compared to the capacity of the most critical member represented by LF_1, would provide a measure of the level of bridge redundancy. In this context, the researchers define a "system reserve ratio" or "redundancy ratio" for the ultimate limit state as R_u. For the serviceability limit state, the redundancy ratio is defined as R_f. For the damaged bridge condition, the redundancy ratio is defined as R_d, where

$$R_u = \frac{LF_u}{LF_1}$$

$$R_f = \frac{LF_f}{LF_1} \qquad (2.1)$$

$$R_d = \frac{LF_d}{LF_1}$$

The redundancy ratios, R_u, R_f, and R_d, provide non-subjective deterministic measures of bridge redundancy. For example, when the ratio R_u is equal to 1.0 ($LF_u = LF_1$), the ultimate capacity of the bridge system is equal to the capacity of the bridge to resist failure of its most critical member; such a bridge is non-redundant. As R_u increases, the level of bridge redundancy increases. Similar observations can be made about R_f and R_d.

Although the redundancy ratio R_u cannot fall below 1.0, the two ratios R_f and R_d may, under certain circumstances, have values less than 1.0. A value of R_f less than 1.0 means that the bridge will exhibit large deformations at a load level smaller than the load that will cause the first member failure. This situation might occur in certain bridges because LF_1 is calculated with a linear-elastic model, whereas LF_f accounts for the nonlinear behavior of the bridge. A value for R_d less than 1.0 means that a damaged bridge may fail at a lower live load than the load that will cause the first member failure in the originally intact linear-elastic system. Thus, the minimum value that R_u can take is normally 1.0, indicating that some bridge systems may collapse when only one member reaches its load carrying capacity. However, R_d can be as low as 0.0, indicating that a bridge system may collapse under its own dead weight if a certain damage scenario takes place. The measures given in Equation 2.1 indicate that structural systems are associated with different levels of redundancy. This is different than current convention that stipulates that a system is either redundant or non-redundant.

The measures of redundancy set in Equation 2.1 are normalized, which makes them independent of the bridge specifications being followed and whether the bridge system is

overdesigned or under designed. This makes the proposed measures valid for the evaluation of existing bridges as well as new designs. The measures also are valid whether the bridge is deficient or up to standards.

To check whether a bridge system has adequate levels of redundancy, it is sufficient to use a nonlinear structural analysis program to calculate LF_u, LF_f, LF_d, and LF_1, and to verify that R_u, R_f, and R_d are adequate. If the system configuration does not provide sufficient levels of redundancy, the bridge configuration may need to be changed. Note that even if the levels of redundancy R_u, R_f, and R_d are lower than expected, the bridge may still have high overall levels of member and system safety with high values for LF_u, LF_f, LF_d, and LF_1. Alternatively, a redundant system with high R_u, R_f, and R_d values may have low overall system safety levels. Thus, a bridge with adequate redundancy levels may still be unsafe for certain applications if its member safety level LF_1 is too low. Therefore, the goal of any bridge design specifications should not be limited to providing adequate redundancy levels but to assure adequate system safety levels. Thus, if a bridge system does not provide an adequate level of redundancy, the bridge members could be conservatively designed to increase LF_1 as well as LF_u, LF_f, and LF_d, and reduce the probability of member failures and, more importantly, reduce the probability of system collapse.

The evaluation of member and system safety can be performed using a direct nonlinear analysis of the system to obtain LF_1, LF_u, LF_f, and LF_d and verifying that they are adequate. However, executing a direct analysis of system safety and redundancy involves advanced analysis tools and expertise that may not be readily available for day-to-day evaluation of common types of bridges. For this reason, it has been proposed that the evaluation of the redundancy of common-type bridges be simplified by developing system factors that can be applied during the design and safety evaluation process to strengthen the members of bridges that are not sufficiently redundant.

As part of this and previous NCHRP projects, hundreds of bridge superstructure and substructure configurations have been evaluated to study the relationship between LF_u, LF_f, LF_d, and LF_1 and the redundancy ratios R_u, R_f, and R_d defined in Equation 2.1. The results of these analyses are used in this study to calibrate system factors that account for bridge redundancy during the design and safety evaluation of bridge systems. The calibration of load and resistance factors in modern structural design and evaluation codes and specifications has been based on probabilistic methods to ensure that the codes provide consistent levels of safety considering the uncertainties associated with estimating the strength of structural members and systems, those associated with predicting the maximum loads that the structure will be subjected to within its service life, and the response of the bridge structure to these applied loads. Therefore, the calibration of system factors that should be implemented in the next generation of structural codes to account for structural redundancy also should be based on the same probabilistic principles. The theory of structural reliability as developed over the past decades provides the basic tools necessary for performing such calibrations, as will be explained in Section 2.4.

2.4 Overview of Structural Reliability

Theoretical Background

The aim of structural reliability theory is to account for the uncertainties encountered while evaluating the safety of structural members and systems or during the calibration of load and resistance factors for structural design and evaluation codes. To account for the uncertainties associated with predicting the load carrying capacity of a structure, the intensities of the expected loads, the effects of these loads, as well as the capacity of structural members may be represented by random variables.

The value that a random variable can take is described by a probability density function (PDF). That is, a random variable may take a specific value with a certain probability and the ensemble of these values and their probabilities are described by the PDF. The most important statistical characteristics of a random variable are its mean value or average, and the standard deviation that gives a measure of dispersion or a measure of the uncertainty in estimating the variable. The standard deviation of a random variable R with a mean $\overline{R}$ is represented by σ_R. A dimensionless measure of the uncertainty is the coefficient of variation (COV), which is the ratio of the standard deviation divided by the mean value. For example, the COV of the random variable R is represented by V_R such that

$$V_R = \frac{\sigma_R}{\overline{R}} \tag{2.2}$$

Structural codes and specifications often specify nominal or characteristic values for the variables used in design or load rating equations. These nominal values are related to the means through bias values. The bias is defined as the ratio of the mean to the nominal value used during the design or evaluation process. For example, if R is the member resistance, the mean of R, namely, $\overline{R}$ can be related to the nominal or design value, R_n, through a bias factor, b_r, such that

$$\overline{R} = b_r R_n \tag{2.3}$$

where b_r is the resistance bias, and R_n is the nominal value as specified by the design code. For example, A50 steel has a nominal design yield stress of 50 ksi but coupon tests show an actual average value close to 56 ksi. Hence, the bias of the yield stress is 56/50 or 1.12.

In structural analysis, safety may be described as the situation where capacity (member strength or resistance, the maximum strain that a structural material can take before rupturing or crushing, ductility capacity) exceeds demand (applied load, applied moment, applied stresses, applied strains, or ductility demand). Probability of limit state exceedance (i.e., probability that capacity is less than applied load effects which is often referred to as probability of failure) may be formally calculated; however, its accuracy depends upon detailed data on the probability distributions of the variables that represent the capacity and the demand. Since such data often are not available, approximate models are used for calculation.

In the application of structural reliability theory for the evaluation of the safety of a structural member or system, the reserve margin of safety of a bridge component is often defined as, Z, such that

$$Z = R - S \tag{2.4}$$

where R is the resistance or member capacity and S is the total load effect. Probability of limit state exceedance, P_f, is the probability that the resistance R is less than or equal to the total applied load effect S or the probability that Z is less than or equal to zero. This is symbolized by the following equation:

$$P_f = \Pr[Z \le 0] = \Pr[R \le S] \tag{2.5}$$

where Pr is used to denote the term probability.

The calibration of the AASHTO LRFD and LRFR specifications was based on evaluating the member resistance and the effects of the applied loads on the member. However, the same approach can be followed if the safety check consists of comparing the capacity of the entire system.

If the strength capacity R and the load demand S follow independent normal (Gaussian) distributions, then the probability of limit state exceedance can be obtained based on the mean of Z and its standard deviation, which can be calculated from the mean of R and S and their standard deviations as

$$P_f = \Phi\left(\frac{0-\overline{Z}}{\sigma_z}\right) = \Phi\left(-\frac{\overline{R}-\overline{S}}{\sqrt{\sigma_R^2+\sigma_S^2}}\right) \tag{2.6}$$

where Φ is the normal probability function that gives the probability that the normalized random variable is below a given value, $\overline{Z}$ is the mean safety margin, and σ_Z is the standard deviation of the safety margin. Thus, Equation 2.6 gives the probability that Z is less than 0 (or R less than S). The reliability index, β, is defined such that

$$P_f = \Phi(-\beta) \tag{2.7}$$

For example, if the reliability index is $\beta = 3.5$, then the implied probability of limit state exceedance is obtained from the normal distribution tables given in most books on statistics as $P_f = 2.326\text{x}10^{-4}$. If $\beta = 2.5$ then $P_f = 6.21\text{x}10^{-3}$. A $\beta = 2.0$ implies that $P_f = 2.23\text{x}10^{-2}$. One should note that these P_f values are only notional measures of risk that are used to compare different structural design and load capacity evaluation methodologies but are not actuarial values related to the collapse of the structure because of the different meaning that failure can take. For example, if the strain at one critical point of the structure exceeds the ultimate strain for this material, the failure is only localized and will not necessarily entail an actual failure in the sense that the structure will necessarily collapse. Furthermore, because of the many assumptions used in assembling the statistics of the applied load effects and in the definition of the capacity of a member or system, the calculated probabilities can only be treated as notional probabilistic measures of safety. Therefore, and in order to avoid referring to P_f as the probability of failure, it is most common to use the reliability index, β, as a measure of safety in structural applications.

If both the capacity and the demand that are represented by the resistance R and the load S can be modeled by normal distributions, the reliability index is obtained from

$$\beta = \frac{\overline{Z}}{\sigma_Z} = \frac{\overline{R}-\overline{S}}{\sqrt{\sigma_R^2+\sigma_S^2}} \tag{2.8}$$

where R and S are assumed statistically independent.

Thus, the reliability index, β, which is often used as a measure of structural safety, gives in this case the number of standard deviations that the mean margin of safety falls on the safe side as represented in Figure 2.2. Because it gives a measure of safety in terms of a number of standard deviations, it is more practical to use the reliability index β which may range between 0.0 to 6.0 to assess the safety of structures rather than using probability values which may range from

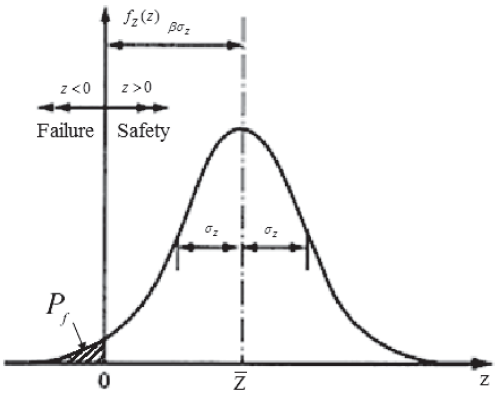

Figure 2.2. Graphical representation of reliability index.

values as high as 50% to values as low as 10^{-9} or lower without giving an intuitive understanding of the corresponding level of safety.

The reliability index, β, defined in Equations 2.7 and 2.8 provides an exact evaluation of the probability of exceedance if R and S follow normal distributions. Although β was originally developed for normal distributions, similar calculations can be made if R and S are lognormally distributed (i.e., when the logarithms of the basic variables follow normal distributions). In this case, the reliability index can be calculated as

$$\beta = \frac{\ln\left(\frac{\overline{R}}{\overline{S}}\frac{\sqrt{1+V_S^2}}{\sqrt{1+V_R^2}}\right)}{\sqrt{\ln[(1+V_R^2)(1+V_S^2)]}} \tag{2.9}$$

which, for values of V_R and V_S on the order of 20% or less can be approximated as

$$\beta = \frac{\ln\left(\frac{\overline{R}}{\overline{S}}\right)}{\sqrt{V_R^2+V_S^2}} \tag{2.10}$$

Experience shows that Equation 2.10 provides a good approximation to the reliability index in many practical applications. For example, when evaluating the reliability levels implied in current and proposed load rating procedures during their work on NCHRP Project 20-07 Task 285, Ghosn et al. (2012) found that Equation 2.10 gives a very good approximation to the reliability index β even when the load effect, S, did not exactly follow a lognormal distribution.

Approximate iterative methods have been developed to obtain the reliability index for the cases when the basic variables are neither normal nor lognormal. A commonly used approach that has been shown to provide good approximations for the reliability index, β, for common structural reliability problems is the First Order Reliability Method (FORM). FORM uses an iterative calculation to obtain an estimate of the probability of limit state exceedance. This is accomplished by approximating the failure equation (i.e., when Z = 0) by a tangent multi-dimensional plane at the point on the failure surface closest to the mean value and mapping non-normal probability distribution functions into equivalent normal functions. For example, during the calibration of the AASHTO LRFD Bridge Design Specifications, Nowak (1999) used the FORM algorithm developed by Rackwitz and Fiessler (1978) to calculate the reliability index for the case when R is assumed to follow a lognormal distribution and S is a normal random variable. More advanced techniques including SORM (Second Order Reliability Methods) also have been developed.

However, Monte Carlo simulations can be used to provide estimates of the probability of exceeding a structure's limit state. Monte Carlo simulations are suitable for any random variable distribution type and limit state equation. In essence, a Monte Carlo simulation creates a large number of "experiments" through the random generation of sets of resistance and load variables. Estimates of the probability of exceedance are obtained by comparing the number of experiments where the load exceeds the resistance to the total number of generated experiments. Given values of the probability of exceedance, P_f, the reliability index, β, is calculated from Equation 2.7 and used as a measure of structural safety even for non-normal distributions. Kulicki et al. (2007) used the Monte Carlo simulation while reviewing the code calibration effort reported by Nowak (1999) and verified that the results of the FORM method with the Rackwitz-Fiessler algorithm, and those of the Monte Carlo simulation are essentially similar. More detailed explanations of the principles discussed in this section can be found in published texts on structural reliability (e.g., Thoft-Christensen and Baker, 1982; Melchers, 1999).

The member reliability index has been used by many code writing groups throughout the world as a measure of structural safety. Reliability index values in the range of β = 2 to 4 are usually specified for individual members depending on the type of member and the structural application. For example, the calibration of the Strength I limit state in the AASHTO LRFD Bridge Design Specifications aimed to achieve a uniform target reliability index $\beta_{target} = 3.5$ for a range of typical bridge span lengths, beam spacing, and materials (Nowak, 1999). A reliability index $\beta_{target} = 2.5$ was used by Moses (2001) for the calibration of the legal load rating in the AASHTO LRFR. These values usually correspond to the failure of a single component. If there is adequate redundancy, overall system reliability indices will be higher.

Although the AASHTO LRFD and LRFR bridge specifications were calibrated based on satisfying member reliability criteria, the same concepts can be used to assess the reliability of a complete bridge system. Difficulties arise in system reliability evaluations because the system resistance R is a function of the resistances of the individual members of the system and their interaction. When an explicit closed-form formulation of this relationship is not possible, evaluations of the system capacity can be performed for specific samples of the member resistances using advanced finite element analysis (FEA) programs. The system reliability can then be evaluated using analytically derived margin of safety equations, Z, obtained by fitting approximate functions through the results of the finite element analysis. Using an iterative approach, the approximate function is fitted to the samples that lie very close to the actual failure surface. This method is known as the Response Surface Method (RSM) (Melchers, 1999).

An important consideration during the reliability analysis process is the type of probability density function that each random variable follows and the accuracy of the simplified

equations in determining the reliability index β. Saydam and Frangopol (2013) compared the results that would be obtained when Equation 2.10 is used instead of the more exact Equation 2.9, assuming that R and S follow lognormal distributions. They also compared the results from both Equations 2.9 and 2.10 to those of the FORM if the probability distribution of the live load in actuality follows an extreme value type I Gumbel distribution rather than the assumed lognormal distribution. They found that the percent error introduced by using the simple expressions in system reliability analysis depends not only on the COV of the resistance and load effect but also on the ratio between the mean values of resistance and load effect. While the percent error is high when the reliability index is small and the ratio of R/S is close to 1.0, the differences in the reliability indices remain relatively close when the COV is within the 20% to 30% range. However, when the reliability index is on the high side, above 4.5, the effect of the probability distribution of the load becomes important.

Reliability-Based Code Calibration Approach

The reliability index β is seldom used in practice for making decisions related to ensuring structural safety during the design of a new bridge or the evaluation of an existing structure, but it is mostly used by code writing groups for recommending appropriate load and resistance factors for use during the structural design process or when evaluating specifications. One commonly used calibration approach is based on the principle that the members of all types of structures should have uniform or consistent reliability levels over the full range of applications. For example, load and resistance factors should be chosen to produce similar member reliability index β values for steel and concrete bridges of different span lengths, number of lanes, number of beams and beam spacing, simple or continuous spans, and roadway categories. Thus, in a traditional code, a single target β must be achieved for all applications. More recently, researchers and code groups have been suggesting that higher values of β should be used for members of more important structures such as bridges with longer spans, bridges that carry more traffic, or bridges that, according to AASHTO, are classified as critical for "social/survival or security/defense requirements" and for non-redundant configurations. This is based on concepts that structures should provide uniform risk rather than uniform member reliabilities where risk takes into consideration the consequences of failure should a bridge member exceed its limit state. Since higher β levels would require higher construction costs, the justification should be based on a cost-benefit analysis whereby target β values are chosen to provide a balance between cost and risk (Aktas, Moses, and Ghosn, 2001). This type of reasoning has been informally used to justify the adoption of a member reliability index $\beta = 2.5$ for the 5-year service life during the load rating of existing bridges as compared to a reliability index $\beta = 3.5$ for a 75-year design life when designing the members of new bridges or to apply a load modifier to increase the reliability level of non-ductile members and members of non-redundant bridge configurations.

Because it is difficult to estimate the lifecycle costs and assess the consequences of failure including the direct, indirect, and user costs that ensue when a bridge member exceeds its limit, a formal risk analysis or cost-benefit analysis is seldom used in practice. Instead, recent codes have adopted informal methods based on the perception of risk. This informal risk-inspired process is currently complementing the approach taken by previous codes that generally used the reliability index of previous safe designs to decide on the reliability criteria that new codes should achieve. In most cases, appropriate target β values are deduced based on the reliability levels of a sample population of satisfactorily performing existing designs. That is, if the safety performance of bridges designed (or rated) according to current standards has generally been found satisfactory, then the average reliability index obtained from current designs is used as the target that the new code should satisfy. The aim of the calibration procedure is to minimize designs that deviate from the target reliability index.

The calibration based on past performance has been found to be robust in the sense that it minimizes the effects of any inadequacies in the database as reported by Ghosn and Moses (1986). Ghosn and Moses (1986) found that the load and resistance factors obtained following a calibration based on "safe existing designs" are relatively insensitive to errors in the statistical database as long as the same statistical data and criteria used to find the target reliability index also are used to calculate the load and resistance factors for the new code. In fact, a change in the load and resistance statistical properties (e.g., in the COV) would affect the computed β values for all the bridges in the selected sample population of existing bridges and consequently their average β value. Assuming that the performance history of these bridges is satisfactory, then the target reliability index would be changed to the new "average" and the calibrated load and resistance factors that would be used for new designs would remain approximately the same.

The calibration of resistance and live load factors for a new bridge code is usually executed by code writing groups as follows:

- A representative sample of bridges that have been designed to efficiently satisfy existing codes and that have shown good safety record is assembled.
- Reliability indices are calculated for each bridge of the representative sample set. The calculation is based on statistical information about the randomness of the strength of members, the statistics of load intensities, and their effects on the structures.

- In general, there will be considerable scatter in such computed reliability indices. A target β is selected to correspond to the average reliability index of the representative bridge sample set.
- For the development of the new code, load and resistance factors as well as nominal loads are selected by an iterative optimization process to satisfy the target β as closely as possible for the whole range of applications.

The above approach was followed by Nowak (1999) and Moses (2001) to calibrate the appropriate live load factors for the AASHTO LRFD and LRFR Legal Load Ratings in order to meet a target member reliability index $\beta = 3.50$ for the 75-year service life of new bridge design and a member reliability index $\beta = 2.5$ for the 5-year rating period of existing bridges. The reliability calibration of the LRFD and LRFR was based on maintaining the same reliability level on the individual main beam members in shear and bending.

No direct consideration was made during the calibration of the AASHTO LRFD and LRFR for system redundancy or system reliability. Load modifiers, η, have been included in the LRFD design-check equations to account for bridge redundancy, member ductility, and importance of the structure. However, as stated in the commentary, the assigned values were based on judgment and were not calibrated to meet specific reliability index targets. The concept of applying a load modifier is based on the perception of risk in terms of considering the consequence of the failure of a non-ductile member of a non-redundant bridge, or the failure of a member of an important structure. However, the specifications do not provide clear guidelines to help engineers decide when a bridge can be defined to have low levels of redundancy requiring the use of a load modifier greater than 1.0. In a similar vein, the AASHTO LRFR recommends the application of system factors less than 1.0 placed on the resistance side of members of bridges that are known to have low levels of redundancy based on the number of beams and beam spacing, or for some connection types that are known to have low levels of ductility.

Using a more directly risk-inspired approach, the Canadian Code (CAN/CSA-S6-06) recommends different target reliability index β values depending on the failure mode, the system behavior, as well as the element behavior, and the inspectability of bridges. The recommended target reliabilities vary between $\beta = 2.50$ and 4.0 as shown in Table 2.1 and the member resistance factor is changed based on the target reliability level. It is also noted that it is not clear how the target reliability levels in Table 2.1 were determined and how an engineer can evaluate whether one element failure leads to total collapse or will only lead to local failure, and how to determine whether the failure will be sudden or gradual if no direct nonlinear analysis is performed.

Table 2.1. Target reliability index for normal traffic in Canadian Code.

System Behavior	Element Behavior	Inspection Level		
		INSP1	INSP2	INSP3
S1	E1	4.00	3.75	3.75
	E2	3.75	3.50	3.25
	E3	3.50	3.25	3.00
S2	E1	3.75	3.50	3.50
	E2	3.50	3.25	3.00
	E3	3.25	3.00	2.75
S3	E1	3.50	3.25	3.25
	E2	3.25	3.00	2.75
	E3	3.00	2.75	2.50

Notes:
- S1 - element failure leads to total collapse; S2 - element failure does not cause total collapse; S3 - local failure only;
- E1 - sudden loss of capacity with no warning; E2 – sudden failure with no warning but with some post-failure capacity; E3 – gradual failure;
- INSP1 – component not inspectable; INSP2 – inspection records available to the evaluator; INSP3 – inspections of the critical and substandard members directed by the evaluator.

Summary

This section reviewed reliability analysis methods and how current codes are calibrated to satisfy target reliability criteria. The review also explains how current recommendations for including redundancy in bridge design and evaluation are mostly based on the judgment of the code writers and the perception of risk rather than on non-subjective, reliability-based criteria. To meet the objectives of this study, and following the format adopted in the AASHTO LRFD Bridge Design Specifications and the Canadian bridge code, it is recommended that different design criteria be established for bridges based on their levels of redundancy. This project proposes that the said objectives be achieved by applying a system factor in the safety-check equation such that bridges with low levels of redundancy be required to have higher member resistances than those of bridges with high levels of redundancy. Although requiring a higher capacity for the members of non-redundant bridges will not make them redundant, it will increase the overall system reliability so that non-redundant bridge systems would have similar system reliability levels as those of redundant systems. This can be done by using a member safety-check equation of the form

$$\phi_s \phi R^N = \gamma_d D_n + \gamma_l L_n (1 + I) \tag{2.11}$$

where ϕ_s is the system factor which is defined as a statistically based multiplier relating to the safety and redundancy of the complete system. The system factor is applied to the factored nominal member resistance. The proposed system factor replaces the load modifier η used in Section 1.3.2 of the LRFD specifications. The system factor is placed on the left side of the equation because the system factor is related

to the capacity of the system and should be placed on the resistance side of the equation as is the norm in reliability-based LRFD codes. ϕ is the member resistance factor, R^N is the required resistance capacity of the member accounting for the redundancy of the system, γ_d is the dead load factor, D_n is the dead load effect, γ_l is the live load factor, L_n is the live load effect on an individual member, and I is the dynamic amplification factor.

When a system factor ϕ_s equal to 1.0 is used, Equation 2.11 becomes the same as the current design equation. If ϕ_s is greater than 1.0, this indicates that the system's configuration provides a sufficient level of redundancy and that a redundant bridge could have lower member capacities than those of a non-redundant bridge and yet have a sufficiently high level of system safety. When ϕ_s is less than 1.0, then the level of redundancy is not sufficient and the bridge members will have to be designed to produce higher member capacities to account for the consequence of a member failure on the system's safety.

The next section describes an approach that builds on the method originally proposed in *NCHRP Report 406* to calibrate system factors for typical bridge configurations based on reliability criteria.

2.5 Reliability Calibration of System Factors

This section describes the approach used in this study to calibrate the system factors that can be used in the design-check equation to account for bridge redundancy during the design of new bridges and the safety evaluation of existing bridges. The calibration is executed using reliability principles in keeping with modern code calibration practice. The general procedure presented in this section is formulated for bridges subjected to vertical traffic loads. Chapters 3, 4, and 5 extend the procedure and provide specific details that are applied to calibrate the system factors for systems under lateral, as well as vertical, loads.

As observed in Section 2.4, the reliability analysis of a bridge member or system requires as input statistical data on the member or system capacity as well as the loads that will be applied on the bridge structure and how the effect of these loads is distributed throughout the structure. As explained in Section 2.3, the evaluation of a bridge's safety should verify that the bridge (1) will provide a reasonable safety level against first member failure, (2) will not reach its ultimate system capacity under extreme loading conditions, (3) will not undergo excessive deformations under expected traffic load conditions, and (4) will be able to carry some traffic loads after damage to, or the loss of, a component.

As explained in Section 2.3, a bridge member's capacity can be evaluated using the parameter LF_1 while the originally intact system capacity can be evaluated using the parameters

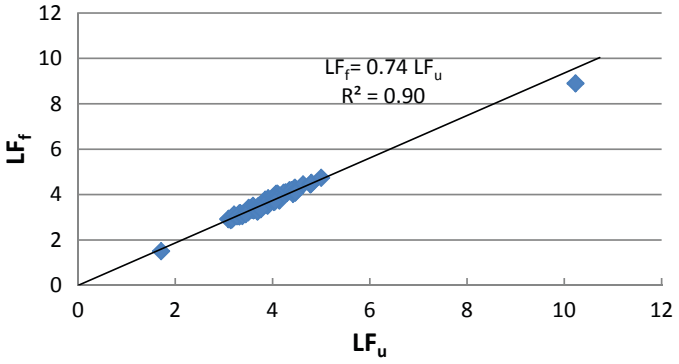

Figure 2.3. LF_f versus LF_u for steel I-girder bridges.

LF_u and LF_f, which assess the ultimate capacity and the functionality of the originally intact system. A damaged bridge's capacity can be evaluated using the parameter LF_d. Although *NCHRP Report 406* and *NCHRP Report 458* considered the redundancy analysis for the functionality limit state separately, a review of the *NCHRP Report 406* data shows that LF_f and LF_u are highly correlated, which leads to similar system factors for both limit states. As an example, Figures 2.3 and 2.4 show the relation between LF_f and LF_u for simple-span steel I-girder and prestressed I-girder bridges where LF_f is selected to be the load factor at which the bridge under vertical load reaches a maximum vertical displacement equal to span length/100. The fact that the trend lines in both figures pass through the origin, and the slope is exactly the same, indicate that the correlation between the two variables is very strong, which implies that there is no need to analyze a bridge's ultimate limit state and its functionality limit state separately. For this reason, in this report the evaluation of the capacity of intact bridges will be based solely on the ultimate limit as represented by LF_u.

The criteria for evaluating the safety and redundancy of bridge structures as explained in Section 2.3 are based on the

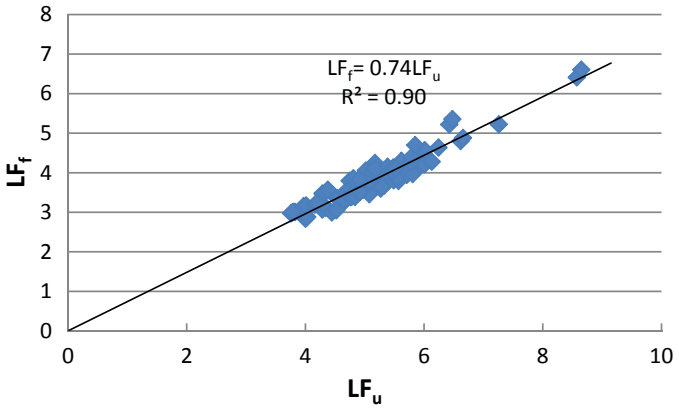

Figure 2.4. LF_f versus LF_u for prestressed I-girder bridges.

deterministic measures defined in Equation 2.1 that do not take into consideration the uncertainties in evaluating the system capacity and the loading. As explained in Section 2.4, the safety of a bridge member, that of the originally intact entire system, or that of a damaged system, should be assessed using reliability criteria. In addition to the probabilistic models for member and system capacities, the reliability analysis requires as input information on the expected live loads. The member and system capacities of an originally intact system should be able to sustain the maximum load expected over the bridge's entire design life. The maximum load is herein defined as the extreme loading condition. However, a major damage to a bridge is not expected to remain unnoticed for a long period after damage given that all bridges are inspected on a 2-year cycle. Therefore, it is suggested that the vertical vehicular load that a damaged bridge should be able to sustain should correspond to the maximum load over the 2-year inspection cycle. This load is herein defined as regular loading. The reliability formulation of the problem is presented next.

Safety Margin Equations for Bridges under Vertical Loads

The first necessary step for performing the reliability analysis of a bridge under the effect of vertical vehicular load consists of setting up the safety margin equations that compare the resistance of the member or the system to the applied loads. These safety margin equations would be used in Equations 2.5 through 2.8 to find the probability of limit state exceedance and the reliability index. Using the results of an incremental analysis that traces the performance curve shown in Figure 2.1, and ignoring the functionality limit state that, as explained earlier, is highly correlated to the ultimate limit state, the following safety margin equations are obtained:

$$\begin{aligned} &\text{For first member failure:} && Z_1 = LF_1 - LL_{75} \\ &\text{For the ultimate capacity of an originally intact system:} && Z_u = LF_u - LL_{75} \\ &\text{For the capacity of a damaged system:} && Z_d = LF_d - LL_2 \end{aligned} \quad (2.12)$$

where LL_{75} gives the maximum load expected in a 75-year design life expressed in terms of the number of AASHTO HS-20 trucks. The 75-year load is used in Equation 2.12 for the member and ultimate limit states because the AASHTO LRFD specifies that bridges should be designed for a 75-yr design life. LL_2 gives the maximum load expected in a 2-year inspection cycle expressed in terms of the number of AASHTO HS-20 trucks. The 2-year load is used for the damaged bridge because the damage should be detected during or before the 2-year inspection. LF_1, LF_u, and LF_d give the multiples of the HS-20 trucks needed to cause the failure of the first member, reach the ultimate capacity of the originally intact system, and cause the collapse of a damaged system. The HS-20 truck is used to express the maximum load in order to keep the same basis as that used for finding LF_1, LF_u, LF_f, and LF_d. LL_{75} and LL_2 must include the total live load on the bridge including the dynamic amplification factor. Additional discussions on these random variables are provided next.

Loading Models

Extreme Live Loading Conditions

In addition to carrying its dead load, a bridge should be able to carry the maximum truck load expected to be applied on it during its design life without reaching its ultimate capacity. This maximum expected live load is a statistical variable that depends on the number of trucks that simultaneously cross the bridge, the positions of the trucks on the bridge deck, the weights of the trucks, the distribution of the weights to the individual axles, and the trucks' axle configurations. In addition, the load is a function of the dynamic amplification caused by the interaction between the moving loads and the structure. According to the AASHTO LRFD Bridge Design Specifications, the design life of a bridge is normally equal to 75 years. For longer, expected bridge lifespans, there is a higher probability of having heavier trucks simultaneously on the bridge. The 75-year lifespan, however, seems to provide an asymptotic limit beyond which the increase in the maximum expected load is practically negligible (Nowak, 1999). The 75-year exposure period was used in the LRFD to calibrate the live load factors for the reliability analysis of bridge members and the calibration of the resistance and load factors. In this study, the same expected live load is used for the ultimate limit state of the system as well as the first member failure limit state. In the latter case, the 75-year exposure period is consistent with the basis for the AASHTO LRFD specifications (Nowak, 1999).

As indicated by Nowak (1999), the maximum expected lifetime load can be expressed in terms of equivalent AASHTO HS-20 loads. For example, the maximum live load effect in a 75-year period, labeled LL_{75}, is defined as the multiple of the HS-20 loads needed to produce the same load effect as the maximum expected 75-year load. Table 2.2 gives the expected LL_{75} values for simple-span bridges of different span lengths for two-lane loadings as well as one-lane loading as provided by Nowak (1999). In the two-lane case, the values are lower than for the one-lane case because they multiply two HS-20 loads. In this study, the two-lane loading is used as the reference load configuration. The LL_{75} values in Table 2.2 are the same values used by Nowak (1999) in the calibration of AASHTO's LRFD Bridge Design Specifications and include an average dynamic amplification factor equal to 1.10. Table 2.2 also shows the COV of the LL_{75} values. The

Table 2.2. Mean and COV of applied live loads as function of HS-20 trucks.

Span Length (ft)	Two-Lane Loading		One-Lane Loading		COV	Distribution Type
	LL_{75}	LL_2	LL_{75}	LL_2	V_{LL}	
45	1.67	1.53	1.97	1.81	19%	
60	1.72	1.6	2.02	1.86	19%	
80	1.81	1.67	2.14	1.98	19%	lognormal
100	1.89	1.75	2.26	2.08	19%	
120	1.98	1.84	2.35	2.17	19%	
150	2.01	1.87	2.37	2.19	19%	
	Includes 1.10 Dynamic Amplification		Includes 1.13 Dynamic Amplification			

COV is the ratio of the standard deviation of LL_{75} divided by the mean value. The COV values in Table 2.2 also are taken from Nowak (1999). These COV values are used in this study to be consistent with the values used during the calibration of the AASHTO LRFD specifications. Specific information on the probability distribution of the static live load or the dynamic amplification factor was not provided by Nowak (1999), who assumed that the combined effect of the dead loads plus live load follows a normal probability distribution. Ghosn et al. (2012), however, observed that the maximum live load may be approximated by a lognormal distribution because it is obtained from the product of several random variables. The Central Limit Theorem states that the product of a large number of random variables should approach a lognormal distribution.

Regular Live Load Conditions

A damaged bridge system should still be able to continue to carry some load after the occurrence of a damaging event that reduces the load carrying capacity of a main member. This would allow (1) for clearing the traffic that is on the bridge, (2) the safe crossing of regular traffic if the damage goes unnoticed for a limited period of time, and (3) the passage of emergency vehicles during disaster recovery. It is herein proposed that in addition to carrying its dead load, a damaged bridge should be able to carry the maximum live loads expected during a 2-year exposure period. The maximum live load expected over the 2-year exposure period is defined as "regular traffic load." The 2-year exposure period is chosen because it corresponds to the biennial mandatory bridge inspection cycle. Thus, the 2-year exposure period is selected based on the premise that even if damage such as a fatigue fracture goes unnoticed for a short period of time, it is bound to be discovered during inspection. LL_2 is defined as the multiple of the HS-20 loads needed to produce the same load effect as that expected under regular truck traffic conditions.

Table 2.2 gives the expected 2-year loads expressed as multipliers of the effect of two AASHTO HS-20 trucks for two-lane loadings and the expected 2-year loads expressed as multipliers of the effect of one AASHTO HS-20 for one-lane loadings. The LL_2 values in Table 2.2 are adopted from the work of Nowak (1999). They include the mean dynamic amplification factor of 1.13. Because no statistical data on the COV of LL_2 are available, the same COVs are assumed to be valid for both LL_{75} and LL_2, although it is generally known that the shorter period is normally associated with slightly higher COVs. The same COV values are used because a breakdown of the sources of uncertainty in the load model was not provided by Nowak (1999). Using the same COV follows the approximation made by Moses (2001) who assumed that the COV for the 5-year and 75-year live loads are the same. This assumption should not alter the final results because the reliability calibration process is known to be a robust process in the sense that errors in the database do not influence the final results as long as the new design or evaluation procedures are calibrated to match current acceptable practice (Ghosn and Moses, 1986). Following the same logic discussed for the 75-year loading, it may be reasonable to assume that the 2-year loading approaches a lognormal distribution.

Resistance Model

According to Nowak (1999), the load carrying capacities or resistances R of structural members may be modeled as lognormal variables. For prestressed concrete members, the mean moment capacity is about 1.05 times the nominal value obtained from typical code-specified methods with a COV of 7.5%. For composite steel members, the bias between the mean moment capacity and that obtained using code-specified methods is estimated at 1.12 with a COV of 10%. Nowak (1999) also gives bias and COV values for the dead load effect that are on the order of 1.05 and a COV of about 10% for cast-in-place members with slightly lower bias and COV for factory-made members and higher COV for pavement.

The load factors LF_1, LF_u, and LF_d are related to the bridge members' resistances, dead weights, and the effect of the applied live loads. Specifically, the calculation of the load

factor for first member failure LF_1 can be calculated from the capacity of the most critical member of the bridge, R, the dead load effect on that member, D, and L_1, which is the load effect on the member calculated due to the HS-20 trucks. Specifically, LF_1 can be obtained from

$$LF_1 = \frac{R-D}{L_1} = \frac{R-D}{D.F. \times LL_{HS-20}} \tag{2.13}$$

where L_1 is expressed in terms of the fraction of the HS-20 truck that is carried by the most critical member, which is obtained by multiplying the load effect of the HS-20 by the distribution factor, D.F. Although L_1 is calculated in this study using a structural model of the entire bridge, an approximation for L_1 can be obtained using an accurate estimation of the distribution factors such as those of the LRFD specifications.

Equation 2.13 is identical to the rating factor equation used when evaluating the load carrying capacity of existing bridges without the load and resistance factors or the impact factor. Equation 2.13 serves the same purpose as the rating factor in that it provides a measure of the load carrying capacity of the system up to first member failure but on the basis of the nominal unfactored resistances and loads.

In the analyses performed in this study, the capacity of a bridge system also is expressed in terms of the load factors LF_u and LF_d, which represent the differences between the overall capacities of the originally intact system and that of the damaged system minus the effect of the dead load as demonstrated in Equation 2.13 for LF_1. Using the statistical models of resistance and dead load from Nowak (1999) along with the resistance and dead loads of the simple-span I-girder bridges analyzed in this study and in *NCHRP Report 406*, the biases and COV for the load factor LF_1 are obtained as shown in Table 2.3. Wang et al. (2011) performed a reliability analysis of several bridge systems using a push down analysis similar to the one used in this study. They observed that the load capacity evaluation will lead to capacities that approach lognormal probability distributions with an overall COV on the same order of that provided by Nowak (1999) for individual members. Based on this observation, the biases and COVs obtained in Table 2.3 will be used for the member capacities expressed in terms of LF_1 as well as the system capacities of the intact and damaged systems expressed in terms of LF_u and LF_d.

Simplified Reliability Evaluation

As explained in Section 2.3, bridge safety should be assessed in terms of the three limit states identified as (1) member failure, (2) ultimate limit state, and (3) damaged condition limit state. These three limit states should be checked to ensure the satisfactory and safe performance of any bridge system under extreme or regular loading conditions. "Adequate" safety margins also should be provided to account for the uncertainties associated with determining bridge system capacity as well as the uncertainties associated with determining the live load levels that will be applied on the bridge. Following current state-of-the-art practice in bridge code calibration, adequate safety margins should be established based on structural reliability criteria similar to those used in the development of AASHTO's LRFD and LRFR specifications, as well as the Canadian Codes (Nowak, 1999; Moses, 2001; and CAN/CSA-S6-06).

The measure of safety used in the development of structural design and evaluation codes is the reliability index β (Nowak, 1999). The reliability index can be used as a measure of the reliability of structural members as well as structural systems. The reliability index accounts for both the margin of safety implied by the design procedure and the uncertainties in estimating member strengths and applied loads. The reliability index can be related to the probability of a limit state exceedance as shown in Equations 2.5 and 2.7.

Assuming that the member resistance of a bridge under vertical load represented by the load factor LF_1, and the applied maximum lifetime live load represented by the factor LL_{75} are random variables that follow lognormal distributions, then the reliability index β_{member} for the failure of the first member can be expressed based on the safety margin Equation 2.12 using the simplified lognormal format of Equation 2.10, which is reasonable for the cases when the COVs are less than 20%. Accordingly

$$\beta_{member} = \frac{\ln\left(\frac{\overline{R}}{\overline{S}}\right)}{\sqrt{V_R^2 + V_S^2}} = \frac{\ln\left(\frac{\overline{LF_1}HS20}{\overline{LL_{75}}HS20}\right)}{\sqrt{V_{LF}^2 + V_{LL}^2}} = \frac{\ln\left(\frac{\overline{LF_1}}{\overline{LL_{75}}}\right)}{\sqrt{V_{LF}^2 + V_{LL}^2}} \tag{2.14}$$

where $\overline{LF_1}$ is the mean value of the load factor that will cause the first member failure in the bridge, assuming elastic analysis. As explained through Equation 2.13, LF_1 is related to the unfactored live load margin (R-D). Thus, $\overline{LF_1}$, which is

Table 2.3. Mean and COV of load capacity as function of HS-20 trucks.

Bridge Type	Bias for Member Resistance	COV for Member Resistance	Bias for LF	COV for LF	Distribution Type
Prestressed concrete	1.05	7.5%	1.05	13.7%	Lognormal
Composite steel	1.12	10%	1.14	13%	

the mean value of LF_1, relates to the strength capacity of the member represented by the resistance R and the dead load D. $\overline{LL_{75}}$ is the mean value of the maximum expected 75-year live load, including dynamic load allowance effect. V_{LF} is the COV of LF_1, while V_{LL} is the COV of the maximum expected live load LL_{75}. The denominator in Equation 2.14 gives an overall measure of the uncertainty in estimating the resistance, the dead load, and the live load including dynamic amplification.

Using equations similar to Equation 2.14 has been common during the reliability analysis of bridge members. However, the reliability analysis of an entire bridge system involves a much more complicated process than the one normally used for the analysis of individual members. This is because the analysis must take into consideration the interaction of all the bridge members throughout the entire loading process from the initiation of loading until collapse during which each member may undergo different levels of deformations including linear-elastic and nonlinear strains. The most effective approach to account for all the random factors that control a system's behavior, including the uncertainties in the linear and nonlinear material modeling, is through simulations. System reliability simulation programs require extensive computational effort, which cannot be accommodated within the constraints of this project. For this reason, a simplified reliability formulation is adopted in this study, which uses a lognormal model for the system capacity analogous to the model used for individual members. A few comparisons have been performed as part of this study to verify that the proposed simplified approach gives results that fall within a reasonably acceptable range as those from advanced simulation techniques. The analyses of Wang et al. (2011) also suggest that the simplified reliability model should be applicable.

The proposed simplified approach to find the reliability index for the ultimate capacity of a bridge system assuming that the load factor LF_u and the live load factor LL_{75} follow lognormal distributions will lead to a reliability index of the system for the ultimate limit state that can be defined as

$$\beta_{ultimate} = \frac{\ln\left(\frac{\overline{R}}{\overline{S}}\right)}{\sqrt{V_R^2 + V_S^2}} = \frac{\ln\left(\frac{\overline{LF_u}HS20}{\overline{LL_{75}}HS20}\right)}{\sqrt{V_{LF}^2 + V_{LL}^2}} = \frac{\ln\left(\frac{\overline{LF_u}}{\overline{LL_{75}}}\right)}{\sqrt{V_{LF}^2 + V_{LL}^2}} \quad (2.15)$$

where $\overline{LF_u}$ is the mean value of the load factor corresponding to the ultimate limit state. $\overline{LF_u}$ relates to the strength capacity of the system and the dead load. $\overline{LL_{75}}$ and V_{LL} are the mean of the 75-year live load and its COV and are the same values used to calculate β_{member}. The limited data on the COV of bridge systems suggest that LF_u and LF_d have COV V_{LF} similar to those used for LF_1. The theory of reliability of structural systems demonstrates that, in general, the COV of a system is smaller than the COV of the individual members. However, this observation is based on the assumption that the structural model used during the nonlinear analysis is exact. In this study, the COVs of the intact and damaged system capacity (LF_u and LF_d) are assumed to be equal to the COV of the member capacity (LF_1) to account for the modeling uncertainties. As done for the evaluation of the reliability of the individual members, Equation 2.15 also assumes that the live load (LL_{75}) follows a lognormal distribution.

Following the same logic, the system's ability to sustain loads after damage can be expressed as a system reliability index for damaged conditions, $\beta_{damaged}$, defined as

$$\beta_{damaged} = \frac{\ln\left(\frac{\overline{R}}{\overline{S}}\right)}{\sqrt{V_R^2 + V_S^2}} = \frac{\ln\left(\frac{\overline{LF_D}HS20}{\overline{LL_2}HS20}\right)}{\sqrt{V_{LF}^2 + V_{LL}^2}} = \frac{\ln\left(\frac{\overline{LF_d}}{\overline{LL_{75}}} \times \frac{\overline{LF_{75}}}{\overline{LL_2}}\right)}{\sqrt{V_{LF}^2 + V_{LL}^2}} \quad (2.16)$$

where $\overline{LF_d}$ is the mean load factor to reach the ultimate capacity of the damaged system. $\overline{LF_d}$ is the capacity of the system to carry live load after one member is damaged. A 2-year exposure period is used for the damaged condition. The mean live load for the 2-year period is expressed as $\overline{LL_2}$, which is a multiplier of the effects of two HS-20 vehicles. Equation 2.16 assumes that the capacity of the damaged bridge system, as well as the load, follow lognormal distributions.

The reliability index formulations of Equations 2.15 and 2.16 are conservative as they assume that the bridge members' strengths are fully correlated.

Probabilistic Measures of Bridge Redundancy

Equations 2.14, 2.15, and 2.16 provide reliability measures that evaluate the safety of bridge members and systems. However, as explained in Section 2.3, bridge redundancy is not a direct measure of the overall system capacity or overall system safety, but a measure of the additional safety provided by the system relative to that of a member. Equation 2.1 provides a set of redundancy measures based on a deterministic evaluation of the additional safety that the system can provide beyond its capacity to resist the failure of a critical member. Alternatively, and in order to take into consideration the uncertainties in estimating the system and member capacities as well as the applied loads, probabilistic measures of redundancy can be defined. In this context, a probabilistic evaluation of system redundancy would entail an examination of the differences between the reliability of the intact and damaged system expressed in terms of $\beta_{ultimate}$ and $\beta_{damaged}$ and the reliability of the most critical member, β_{member}, using different methods (Frangopol and Curley, 1987; Frangopol and Nakib, 1991; Hendawi and Frangopol, 1994). Specifically, Ghosn and Moses (1998) defined a set of "reliability index margins" $\Delta\beta_u$,

$\Delta\beta_d$ that compare the reliability indices for the ultimate and damaged limit states to that of the most critical member. The reliability index margins $\Delta\beta_u$, $\Delta\beta_d$ are defined as

$$\Delta\beta_u = \beta_{ultimate} - \beta_{member}$$
$$\Delta\beta_d = \beta_{damaged} - \beta_{member} \tag{2.17}$$

Using the simplified lognormal reliability model of Equations 2.14 through 2.16 for a superstructure under the effect of vertical live loading and assuming that the COV of LF_u, LF_d, and LF_1 are all equal to the same value, V_{LF}, the probabilistic and deterministic measures of redundancy are found to be directly related to each other as shown in the following:

$$\Delta\beta_u = \beta_{ultimate} - \beta_{member} = \frac{\ln\left(\frac{\overline{LF_u}}{\overline{LL_{75}}}\right) - \ln\left(\frac{\overline{LF_1}}{\overline{LL_{75}}}\right)}{\sqrt{V_{LF}^2 + V_{LL}^2}}$$
$$= \frac{\ln\left(\frac{\overline{LF_u}}{\overline{LF_1}}\right)}{\sqrt{V_{LF}^2 + V_{LL}^2}} = \frac{\ln(R_u)}{\sqrt{V_{LF}^2 + V_{LL}^2}} \tag{2.18}$$
$$\Delta\beta_d = \beta_{damaged} - \beta_{member} = \frac{\ln\left(\frac{\overline{LF_d}}{\overline{LL_2}}\right) - \ln\left(\frac{\overline{LF_1}}{\overline{LL_{75}}}\right)}{\sqrt{V_{LF}^2 + V_{LL}^2}}$$
$$= \frac{\ln\left(\frac{\overline{LF_f}}{\overline{LF_1}}\frac{\overline{LL_{75}}}{\overline{LL_2}}\right)}{\sqrt{V_{LF}^2 + V_{LL}^2}} = \frac{\ln\left(R_d\frac{\overline{LL_{75}}}{\overline{LL_2}}\right)}{\sqrt{V_{LF}^2 + V_{LL}^2}}$$

The relationships in Equation 2.18 show that for a lognormal model, and assuming that the bias in the load factor is the same, the reliability index margins are directly related to the redundancy ratios $R_u = LF_u/LF_1$ and $R_d = LF_d/LF_1$, as defined in Equation 2.1. Accordingly, a bridge system will provide adequate levels of system redundancy if the reliability index margins defined in Equation 2.18 are adequate.

Establishing Reliability-Based Redundancy Criteria

Modern-day structural design codes are calibrated to provide uniform levels of member reliability indices. The AASHTO LRFD specifications were calibrated to provide a member reliability index, $\beta = 3.5$, assuming that the system provides sufficient levels of redundancy. Bridges that are not sufficiently redundant are "penalized" by requiring that their members be more "conservatively designed" so that their member reliability indices are higher than $\beta = 3.5$. This is effectively executed by applying the load modifiers η specified in the AASHTO LRFD Bridge Design Specifications. Mertz (2008) explains that applying a load modifier $\eta = 1.10$ will effectively raise the member reliability index to a value $\beta = 4.0$. This is essentially done to compensate for the lower system reliability level that a non-redundant bridge with $\beta_{member} = 3.5$ has compared to the system reliability level of a redundant bridge with the same member reliability index. However, the member reliability index is reduced to a value $\beta = 3.0$ for bridges that are redundant when they are assigned the load modifier $\eta = 0.95$. This essentially "rewards" the members of redundant bridges by allowing a lower member reliability index. This is essentially done because redundant bridges with $\beta = 3.0$ will provide sufficiently high system reliability levels comparable to those of non-redundant bridges with $\beta_{member} = 4.0$. One can observe from this interpretation, that although not explicitly stated in the AASHTO LRFD, the rationale behind the application of the load modifiers is consistent with the concept of providing adequate spread between the reliability indices of the system and that of the members. Systems where the spread is large can be allowed lower values of member reliability levels; those where the spread is small will have to be assigned higher member reliability levels.

By using target reliability indices ranging between $\beta = 2.5$ and 4.0 as shown in Table 2.1, the Canadian CAN/CSA-S6-06 code achieves the same goals by explicitly changing the target member reliability index rather than using the preset load modifier values of the AASHTO LRFD.

The rationale behind the AASHTO LRFD and the Canadian CAN/CSA-S6-06 code methods for accounting for bridge redundancy is consistent with the concept proposed in this project to evaluate the system redundancy based on the reliability index margins of Equation 2.18. However, the final decision on what values should be assigned to the AASHTO load modifiers or what member reliability indices should be used in the Canadian Code, are left up to the bridge engineer who should use his/her judgment to decide how to classify a bridge in terms of its level of redundancy and to assess the consequences of a member's failure. Furthermore, the proposed AASHTO LRFD load modifier values were arbitrarily assigned by the code writers and the target reliability values in CAN/CSA-S6-06 were selected arbitrarily in a manner that is not consistent with modern-day code calibration methods.

Following the procedures proposed in the AASHTO LRFD and the Canadian bridge code, it is recommended that different design criteria be established for bridges based on their levels of redundancy. This can be achieved by applying a system factor in the safety-check equation such that bridges with low levels of redundancy be required to have higher member resistances than those of bridges with high levels of redundancy. For bridges under vertical live loads, this goal can be achieved by using a member safety-check equation of the form provided in Equation 2.11, which is repeated below.

$$\phi_s\phi R^N = \gamma_d D_n + \gamma_l L_n(1+I) \tag{2.11}$$

The system factors to be applied in conjunction with Equation 2.11 should be calibrated using a reliability model such

that a system factor equal to 1.0 indicates that the bridge is sufficiently redundant and that the reliability index of the system is higher than that of the member by an amount equal to a target value. Following common reliability-based code calibration processes, the target values can be established by studying the reliability of bridge systems that have historically shown adequate levels of redundancy in the sense that one of their critical members has failed, and the system did not undergo collapse.

Determination of Reliability-Based Redundancy Criteria

Equation 2.18 provides non-subjective reliability-based measures to evaluate the redundancy of bridge systems. Bridges whose reliability index margins are adequate should be considered to be redundant. In Section 2.4, it was explained that the determination of the reliability criteria that bridge members should satisfy was established based on matching a target reliability index equal to the average reliability index of bridges that have historically been known to have performed well. To remain consistent with modern code calibration methods, it is herein proposed that bridges that have reliability index margins $\Delta\beta_u$ and $\Delta\beta_d$ equal to or above target values be classified as redundant. The determination of the minimum target $\Delta\beta_{u\ target}$ and $\Delta\beta_{d\ target}$ values that a bridge should satisfy must be established based on a review of the performance of existing redundant designs. This section describes how this selection process is performed for a system under vertical loads.

To establish the target reliabilities, a large number of common-type simple-span prestressed I-girder and steel I-girder bridges having span lengths varying between 45 ft and 150 ft were analyzed in *NCHRP Report 406.* The bridges have 4 to 10 beams with spacing varying between 4 ft and 12 ft. The results of these analyses are given in Appendixes B and C of *NCHRP Report 406.* For each bridge configuration, the load multipliers, LF_1, LF_u, and LF_d, were calculated using a nonlinear incremental bridge analysis program. A grillage model is used for the incremental analysis of the superstructure assuming two side-by-side HS-20 trucks as the base live load model. The validity of the grillage model for this type of analysis was extensively tested as part of *NCHRP Report 406* and further verified during the course of this current project.

Given the load factors LF_1, LF_u, and LF_d, the reliability indices β_{member}, $\beta_{ultimate}$, and $\beta_{damaged}$ were calculated for each bridge configuration using Equations 2.14, 2.15, and 2.16. Several comparisons were performed with results of FORM algorithms to verify that the application of the simplified lognormal equations gives reasonably accurate results for the purposes of this study. The results of the reliability index calculations are then used to establish the reliability-based redundancy criteria and the target reliability index margins necessary for calibrating the system factors.

Ultimate Limit State Criteria

In current practice, all two-girder bridges, and according to several opinions, even three-girder bridges, are defined as non-redundant. On the other hand, all bridges with four or more beams are always classified as redundant and experimental investigations have demonstrated that when one girder of four-girder bridges has been overloaded, the bridge has been able to sustain considerable traffic load without collapsing. Therefore, it is recommended to use the average $\Delta\beta_u$ value obtained from four-girder bridges as the target reliability index margin that all bridges should satisfy to be considered as adequately redundant. The calculations performed in *NCHRP Report 406* show that typical two-lane, simple-span, steel and prestressed concrete I-beam bridges with four beams at spacings equal to or greater than 4 ft have $\Delta\beta_u$ average value of 0.85. The range of $\Delta\beta_u$ is between 0.04 and 1.23 for steel bridges and between 0.02 and 1.53 for prestressed concrete bridges. Generally, it is observed that for the same span length and beam spacing, the prestressed concrete bridges have higher dead weight, which results in lower values of LF_1, leading to slightly higher $R_u = LF_u/LF_1$ ratios and $\Delta\beta_u$ values. To account for all possible differences in the four-beam bridges, *NCHRP Report 406* proposed to use a $\Delta\beta_{u\ target} = 0.85$ as the target reliability index margin that bridges deemed to be adequately redundant should satisfy for the ultimate limit state.

Damaged Condition

Damaged bridges are assumed to have lost the load carrying capacity of an external girder. *NCHRP Report 406* also analyzed the large set of simple-span steel and prestressed concrete I-girder bridge configurations that it assembled assuming that the external girder is no longer capable of carrying any load while its dead load as well as the total live load must be carried by the remaining members. Damaged two-lane bridges with four beams analyzed in *NCHRP Report 406* gave an average value for $\Delta\beta_d$ equal to −2.70. Based on these results, it is recommended to use a target $\Delta\beta_{d\ target} = -2.70$ as the target relative reliability index for the damaged condition.

Calibration of System Factors

The calibration of the system factor ϕ_s that should be applied in Equation 2.11 can be executed using the reliability formulation presented above so that the reliability index of the members and of the systems for bridges that are not sufficiently redundant is increased. That is, when the available

reliability index margins $\Delta\beta_u$ and $\Delta\beta_d$ are lower than the target values $\Delta\beta_{u\,target} = 0.85$ and $\Delta\beta_{d\,target} = -2.70$, a system factor $\phi_s < 1.0$ should be used in Equation 2.11. However, ϕ_s should serve to lower the reliability index for the member and the system when the available $\Delta\beta_u$ and $\Delta\beta_d$ are higher than the target values.

The amount by which the reliability indexes of the systems $\beta_{ultimate}$ and β_{damage} should be increased should be equal to the deficit in the available $\Delta\beta_u$ and $\Delta\beta_d$ when compared to the target values. The goal is to ensure that non-redundant bridge configurations will still provide $\beta_{ultimate}$ and β_{damage} values similar to those of redundant bridges. Because the design process controls the member capacities, achieving higher $\beta_{ultimate}$ and β_{damage} values can be done by imposing higher β_{member} through the application of a system factor ϕ_s into the design and safety evaluation Equation 2.11.

The formulation can be summarized as described in this section for the ultimate limit state for bridges under vertical loads. The same exact procedure is also valid for finding the system factor for the damaged condition limit state and for calibrating system factors for systems under lateral loads, as will be explained in Chapters 3, 4, and 5. Some of the equations presented in earlier sections of this chapter are repeated for consolidating the derivation.

The reliability index for a bridge member is calculated using the equation

$$\beta_{member} = \frac{\ln\left(\dfrac{\overline{LF_1}}{\overline{LL_{75}}}\right)}{\sqrt{V_{LF}^2 + V_{LL}^2}} \tag{2.19}$$

where $\overline{LF_1}$ is the mean value of LF_1, which is calculated from the linear structural analysis of the bridge up until the first member fails. LF_1 gives the number of HS-20 trucks that the bridge member can carry in addition to the dead load. It can be expressed as

$$LF_1 = \frac{R - D}{L_1} \tag{2.20}$$

where R is the bridge member capacity, D is the dead load effect and L_1 is the load effect on that member due to the application of one set of HS-20 trucks on the bridge.

If LF_1 is found based on the nominal values of R and D, then the mean $\overline{LF_1}$ is related to the nominal value of LF_1 through a bias b_{LF} such that

$$b_{LF} = \frac{\overline{LF_1}}{LF_1} \tag{2.21}$$

The results of the nonlinear analysis of the entire system will serve to find the load factor LF_u, which also is used to find the reliability index for the ultimate limit state.

$$\beta_{ultimate} = \frac{\ln\left(\dfrac{\overline{LF_u}}{\overline{LL_{75}}}\right)}{\sqrt{V_{LF}^2 + V_{LL}^2}} \tag{2.22}$$

The reliability index margin is found from

$$\Delta\beta_u = \beta_{ultimate} - \beta_{member} \tag{2.23}$$

The calculated reliability index margin is compared to the target value and the deficit is found as

$$\Delta\beta_{u\,deficit} = \Delta\beta_{u\,target} - \Delta\beta_u = \Delta\beta_{u\,target} - (\beta_{ultimate} - \beta_{member}) \tag{2.24}$$

A negative $\Delta\beta_{u\,deficit}$ indicates that the redundancy level of the system is more than adequate, while a positive $\Delta\beta_{u\,deficit}$ indicates that the redundancy of the system is not sufficient. The system factor should serve to change the resistances of the bridge members so that a system that is adequately redundant could be allowed to have lower member resistances while the member resistances of a system that is not adequately redundant should be increased. The change in the member resistance should be sufficient to offset the deficit in the reliability index margin defined as $\Delta\beta_{u\,deficit}$, so that the modified bridge will produce a modified system reliability index $\beta^N_{ultimate}$ higher than the current reliability index for non-redundant systems or lower for redundant systems such that

$$\begin{aligned}\beta^N_{ultimate} &= \beta_{ultimate} + \Delta\beta_{u\,deficit} \\ &= \beta_{ultimate} + \Delta\beta_{u\,target} - (\beta_{ultimate} - \beta_{member}) \\ \beta^N_{ultimate} &= \Delta\beta_{u\,target} + \beta_{member}\end{aligned} \tag{2.25}$$

Thus, the new ultimate system capacity is related to the reliability index by

$$\beta^N_{ultimate} = \frac{\ln\left(\dfrac{\overline{LF_u^N}}{\overline{LL_{75}}}\right)}{\sqrt{V_{LF}^2 + V_{LL}^2}} \tag{2.26}$$

where $\overline{LF_u^N}$ is the mean value that the new system ultimate capacity should reach. Also,

$$\frac{\ln\left(\dfrac{\overline{LF_u^N}}{\overline{LL_{75}}}\right)}{\sqrt{V_{LF}^2 + V_{LL}^2}} = \Delta\beta_{u\,target} + \beta_{member} \tag{2.27}$$

and

$$\overline{LF_u^N} = \overline{LL_{75}} e^{(\Delta\beta_{u\,target} + \beta_{member})\sqrt{V_{LF}^2 + V_{LL}^2}} \tag{2.28}$$

and the nominal system capacity is obtained from

$$LF_u^N = \frac{\overline{LF_u^N}}{b_{LF}} \tag{2.29}$$

The required member capacity can be inferred from the relationship established between LF_u and LF_1 for the typical bridge configurations analyzed in this study. For example, in *NCHRP Report 406* it was observed that the ratio $R_u = LF_u/LF_1$ is approximately constant for I-girder bridges designed to exactly satisfy the AASHTO design specifications. Further analysis of the *NCHRP Report 406* data and additional analyses performed as part of this project show that a better approximation for the relationship between LF_u and LF_1 for deficient and overdesigned I-girder and box bridges is obtained from an equation of the form

$$LF_u = 1.16 \times LF_1 + 0.75 \tag{2.30}$$

Therefore, the required load factor for first member failure can be obtained from

$$LF_1^N = \frac{LF_u^N - 0.75}{1.16} \tag{2.31}$$

If the load factor for first member is related to the member resistance as shown in Equation 2.20 by $LF_1^N = \frac{R^N - D}{L_1}$, the required member resistance is

$$R^N = LF_1^N \times L_1 + D \tag{2.32}$$

and the system factor associated with this bridge system configuration is obtained as

$$\phi_s = \frac{R}{R^N} \tag{2.33}$$

so that if the original design equation based on the member reliability is given as

$$\phi R = \gamma_d D_n + \gamma_l L_N (1 + I) \tag{2.34}$$

then

$$\phi_s = \frac{R}{R^N} = \frac{\gamma_d D_n + \gamma_l L_N (1 + I)}{\phi R^N} \tag{2.35}$$

leading to Equation 2.11 given as

$$\phi_s \phi R^N = \gamma_d D_n + \gamma_l L_N (1 + I) \tag{2.36}$$

2.6 Summary

This chapter presents a method to consider redundancy during the design and load capacity evaluation of bridge systems. In keeping with the concept of *NCHRP Report 406*, which also is consistent with the AASHTO LRFD, AASHTO LRFR, and the Canadian Code, the method developed in this study consists of penalizing less redundant designs by requiring more conservative member capacities than required by current member-oriented specifications. However, bridges with redundant configurations can be rewarded by allowing a lower level of safety factors on their member strength capacities. This is achieved by applying a system factor in the design-check equation where a system factor $\phi_S > 1.0$ applied in combination with the resistance factor indicate that the bridge is redundant while a system factor $\phi_S < 1.0$ is used for less redundant configurations.

The chapter describes the reliability-based calibration procedure that should be followed to determine the appropriate system factors. The procedure is explained using bridges under vertical loads, but the same approach can be followed for bridges under lateral loads as will be explained in Chapters 3 and 4. The implementation of the procedure to calibrate systems factors for systems subjected to lateral or vertical loads is described in Chapters 3, 4, and 5.

References

AASHTO (2012) *LRFD Bridge Design Specifications*, 6th ed, Washington, D.C.

AASHTO MBE-2-M (2011) *Manual for Bridge Evaluation*, 2nd ed, Washington, D.C.

AASHTO (2002) *Standard Specifications for Highway Bridges*, 17th ed, Washington, D.C.

Aktas, E., Moses, F., and Ghosn, M. (2001) "Cost and Safety Optimization of Structural Design Specifications," *Journal of Reliability Engineering and System Safety* 73(3), Sept. 2001, 205–212.

CAN/CSA-S6-06 (2006) *Canadian Highway Bridge Design Code*, Canadian Standards Association, Canada.

Frangopol, D. M. and Curley, J. P. (1987) "Effects of Damage and Redundancy on Structural Reliability," *Journal of Structural Engineering* 113 (7) 1533–1549.

Frangopol, D. M. and Nakib, R. (1991) "Redundancy in Highway Bridges," *Engineering Journal*, American Institute of Steel Construction, 28(1), 45–50.

Ghosn, M. and Moses, F. (1986) "Reliability Calibration of a Bridge Design Code," *ASCE Journal of Structural Engineering*, April.

Ghosn, M., and Moses, F. (1998) *NCHRP Report 406: Redundancy in Highway Bridge Superstructures*, Transportation Research Board, National Research Council, Washington D.C.

Ghosn, M., Sivakumar, B., and Miao, F. (2012) "Development of State-Specific Load and Resistance Factor Rating Method," in press, *ASCE Journal of Bridge Engineering*, posted ahead of print February 1, 2012. doi:10.1061/(ASCE)BE.1943-5592.0000382.

Hendawi, S. and Frangopol, D. M. (1994) "System Reliability and Redundancy in Structural Design and Evaluation," *Structural Safety* 16 (1+2), 47–71.

Kulicki, J. M., Mertz, D. R., and Nowak, A. S. (2007) "Updating the Calibration Report for AASHTO LRFD Code," Final Report, NCHRP Project 20-7/186, Transportation Research Board, National Research Council, Washington, D.C.

Liu, D., et al. (2001) *NCHRP Report 458: Redundancy in Highway Bridge Substructures*, Transportation Research Board, National Research Council, Washington, D.C.

Melchers, R. E. (1999) *Structural Reliability Analysis and Prediction*, 2nd ed, New York: Wiley.

Mertz, D. R. (2008) "Load Modifier for Ductility, Redundancy, and Operational Importance," *Aspire Magazine*, Issue 08, fall.

Moses, F. and Ghosn, M. (1985) "A Comprehensive Study of Bridge Loads and Reliability," Final Report to Ohio DOT.

Moses, F. (2001) *NCHRP Report 454: Calibration of Load Factors for LRFR Bridge Evaluation*, Transportation Research Board, National Research Council, Washington, D.C.

Nowak, A. S. (1999) *NCHRP Report 368: Calibration of LRFD Bridge Design Code*, Transportation Research Board, National Research Council, Washington, D.C.

Rackwitz, R. and Fiessler, B. (1978) "Structural Reliability under Combined Random Load Sequences," *Computers and Structures* 9, 489–494.

Saydam, D. and Frangopol, D. M. (2013) "Applicability of Simple Expressions for Bridge System Reliability Assessment," *Computers & Structures*, Vol. 114–115, 59–71.

Thoft-Christensen, P. and Baker, M. J. (1982) *Structural Reliability and its Applications.* New York: Springer-Verlag.

Wang, N., Ellingwood, B. R., and Zureick, A. H. (2011) "Bridge Rating Using System Reliability Assessment II: Improvements to Bridge Rating Practices," *ASCE Journal of Bridge Engineering*, 16(6), Nov/Dec 863–871.

CHAPTER 3

Displacement-Based System Safety and Redundancy of Bridges

3.1 Behavior of Bridge Systems under Distributed Lateral Load

When a bridge system is subjected to an increasing distributed lateral load, its response is often represented in terms of the maximum lateral displacement at a critical point as a function of the applied lateral load's intensity. A typical bridge behavior can be represented using the green plot shown in Figure 3.1. This behavior is usually simulated using a pushover analysis whereby a load is applied laterally on the bridge system and an incremental load analysis is performed taking into consideration the nonlinear behavior of each bridge member. The load is continuously incremented until the bridge fails. The load that causes the bridge to fail is designated as P_u in Figure 3.1. This load defines the maximum load carrying capacity of the system. The displacement at bridge failure is designated as δ_{uc}, which represents the ultimate displacement capacity of the system.

Traditionally, to simplify the analysis process, especially in previous decades when computational tools to perform nonlinear incremental pushover analyses were not widely available, bridge engineers used the results of linear-elastic analyses to check the safety of bridge systems subjected to lateral loads. During the bridge design process, bridge members are proportioned based on their plastic member capacities even when a linear-elastic analysis is performed to find the load effects. This method, known as the force-based approach, has been the standard approach for checking the safety of bridges under all types of lateral loading conditions. The forced-based approach can be represented by the brown curve in Figure 3.1 where a linear-elastic analysis behavior is assumed until one member reaches its plastic capacity. The load that causes the one member to reach its plastic capacity is designated as P_{p1} in Figure 3.1. This load defines the "nominal" load carrying capacity of the system.

Because earthquakes impose displacements on structural systems rather than forces, the traditional force-based approach, which is sufficiently valid for other types of loadings, had to be modified in order to take into consideration the effect of member ductility on the seismic response of bridges. Accordingly, the results of a linear-elastic seismic analysis are adjusted by applying a response modification factor on the linear-elastic response of bridge members to reduce the calculated elastic forces and moments to "equivalent plastic" load effects. Bridge members are designed and detailed to meet these "equivalent plastic" load effects. In principle, the response modification factor would account for the plastic deformation that may be sustained until a theoretical failure point marked by "x" on the brown curve of Figure 3.1 is reached. The ratio of the plastic deformation limit to the linear-elastic limit represents the ductility of the member. The ductility of the system also is assumed to be represented by the maximum response of the most critical member.

Although this traditional force-based approach has been the standard method for years, it does not provide an adequate representation of the safety of the entire bridge system. This is because a linear-elastic analysis does not properly model the redistribution of the loads to the members of the bridge as the members undergo nonlinear deformations and because neither the bridge members and certainly nor the system exhibit pure elasto-plastic (bilinear) behaviors. For this reason, in recent years, the seismic assessment of bridge systems has shifted from the force-based approach to a response-based approach. Specifically, the recently implemented AASHTO Guide Specifications for LRFD Seismic Bridge Design (2011) are based on a displacement-based approach whereby the system capacity is defined in terms of the maximum displacement that can be sustained by the system before system collapse. This is represented by δ_{uc} in Figure 3.1. By ensuring that the displacement capacity is higher than the imposed seismic displacement demand, δ_d, the bridge system will be safe.

According to the AASHTO LRFD seismic guide provisions, the ultimate displacement capacity of a bridge system can be directly obtained using a pushover analysis of the entire bridge system. This will directly define the ultimate system

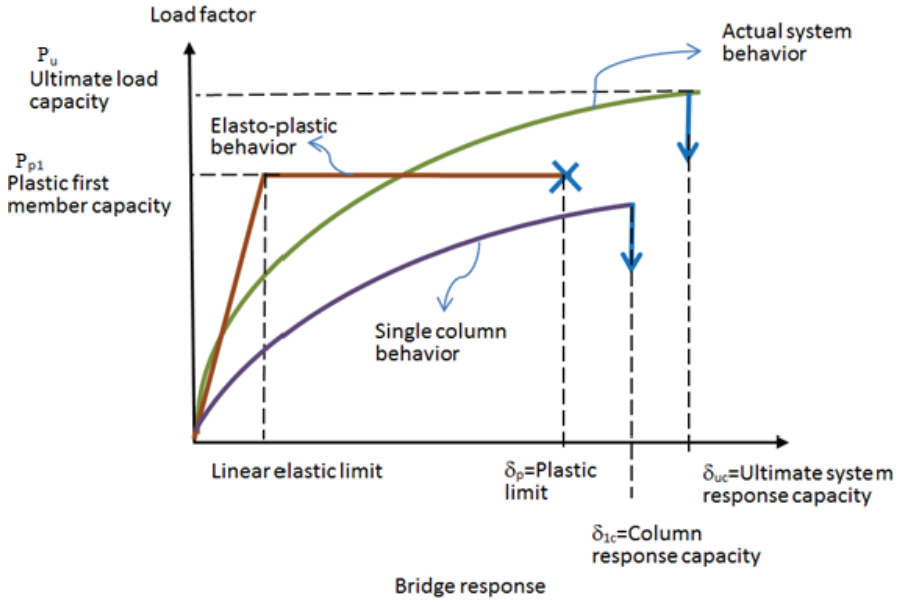

Figure 3.1. Representation of typical behavior of bridge systems under distributed lateral load.

response capacity δ_{uc}. Alternatively, for bridges in low seismic regions, the AASHTO seismic guide provides equations that give the maximum displacement capacity of bridge columns in function of the column height, cross-section size, end constraints, and lateral confinement reinforcement ratio. These equations were presumably derived to provide a conservative estimate of the maximum displacement that individual bridge columns can sustain, which also is assumed to be equivalent to the maximum displacement that the system can sustain. The response of an individual column can be modeled as shown by the purple curve in Figure 3.1 and the column response capacity is represented by δ_{1c}.

3.2 Redundancy of Bridge Systems under Lateral Load

Measures of Redundancy

Traditionally, structural design codes define a structure's capacity in terms of the ability of its individual members to sustain the applied loads using a linear-elastic analysis. Given that the failures of individual members do not necessarily lead to the collapse of the system, structural redundancy is defined as the ability of a structural system to continue to carry load after one critical member reaches its load carrying capacity. Based on the system behavior explained in Section 3.1 as described in Figure 3.1, and to remain consistent with the definition of bridge redundancy established for systems under vertical loads as explained in *NCHRP Report 406* and Chapter 2, quantifiable measures of system redundancy for bridges subjected to a distributed lateral load are proposed as follows:

For force-based designs:
$$R_{fu} = \frac{P_u}{P_{p1}} \tag{3.1}$$

For displacement-based designs:
$$R_{du} = \frac{\delta_{uc}}{\delta_{1c}} \tag{3.2}$$

Analysis of Typical Bridge Configurations

To obtain estimates of the force-based and displacement-based redundancy of typical bridge system configurations, this study performed the pushover analysis of several bridges and compared their system response capacities, δ_{uc}, to their individual column response capacities, δ_{1c}. Also, the study compared the systems' ultimate load capacities, P_u, to the first member plastic capacities, P_{p1}. The analyses were performed on continuous three-span I-girder steel bridges with two bents supported by three columns each, three-span bridges carrying a multi-cell prestressed concrete bridge superstructure where each bent consisted of two columns and three-span bridges carrying two prestressed concrete girder boxes where each bent consisted of two columns. The load transfer mechanism between the I-girder superstructure and the substructure was through bearings on a cap beam, although the possibility of having an integral connection between cap beam, I-girders, and columns was also analyzed. For the box-girder bridges, the response of bridges with integral connections between the

columns and the superstructure is compared to the effects of pinned connections. For all bridge configurations, the effect of changes in column height and size, lateral confinement and longitudinal reinforcement ratios, reduction in member curvatures due to deficiencies in column/connection detailing and changes in foundation stiffness are investigated.

Evaluation of Displacement-Based Redundancy

The results of the pushover analyses performed on the entire bridge system are compared to the results performed on one column for each of the bridge configurations and variations on the base case configurations analyzed in this study. The ultimate system response capacity, δ_{uc}, is compared to the column response capacity, δ_{1c}, for the I-girder bridges and the box-girder bridges.

The results for the I-girder bridges are presented in Figure 3.2, which plots δ_{uc} versus δ_{1c} for each column detailing and size analyzed. The values of the plotted displacements are provided in the last two columns of Table 4.7. The analysis included 27.5-ft, 32.5-ft, and 37.5-ft columns designed with lateral confinement reinforcement ratios ρ_s = 0.24%, 0.3% (detail category B) and 0.5% (detail category C) in addition to cases where the maximum curvature is reduced by 50% and 75% to account for deficiencies in design. Different foundation stiffnesses are used to represent pile foundations and spread footing foundations as well as rigid foundations and pinned foundations. The possibility of integral girder/cap-beam/column connections is compared to girder-bearings on cap beam designs. Figure 3.2 shows the plot of the displacement capacity of the system versus the displacement obtained when one isolated column is analyzed. The data points are clearly aligned along the equal displacement line indicating that δ_{uc} is very close to δ_{1c} or R_{du} = 1.0 for all of the cases analyzed. This demonstrates that the displacement capacity of one column reflects the displacement capacity of the entire bridge structural system very accurately and the redundancy of the system is directly accounted for when using the displacement-based approach for evaluating bridges under lateral loads. These results are expected due to the large stiffness of the deck under the effect of lateral load, which will ensure the compatibility of the displacements of all of the columns at the deck level.

The results for the multi-cell box-girder bridge are presented in Figure 3.3. The values of the displacements are provided on the last two columns of Table 4.6. The analysis included 20-ft, 25-ft, and 30-ft columns designed with lateral confinement reinforcement ratios ρ_s = 1%, 0.3% (detail category B) and 0.5% (detail category C) in addition to cases where the maximum curvature is reduced by 50% and 75% to account for deficiencies in design. The columns' diameters were varied between 6-ft, 7-ft and 8-ft. Different foundation stiffnesses are used to represent pile and spread footing foundations as well as rigid foundations. The possibility of integral column/superstructure connections is compared to the cases where the load is transferred between the superstructure and the

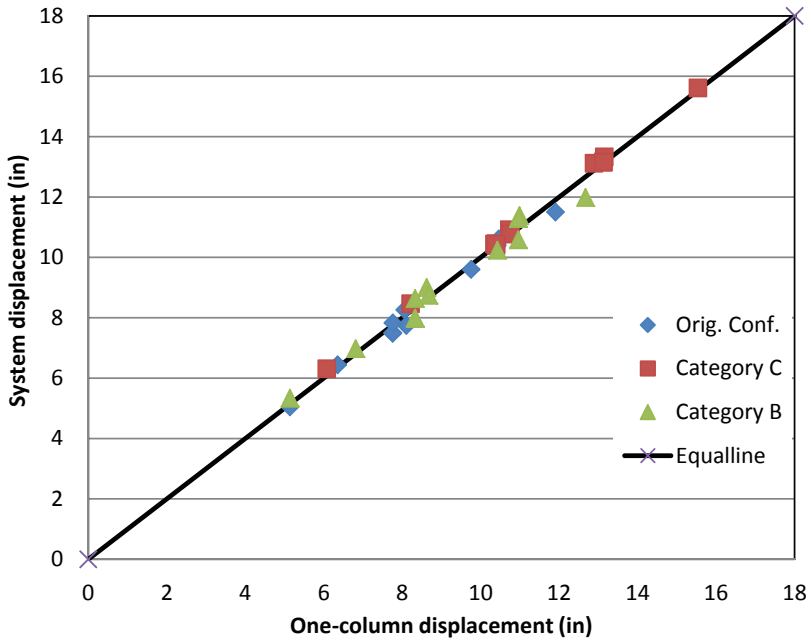

Figure 3.2. System displacement versus one-column displacement for I-girder bridge.

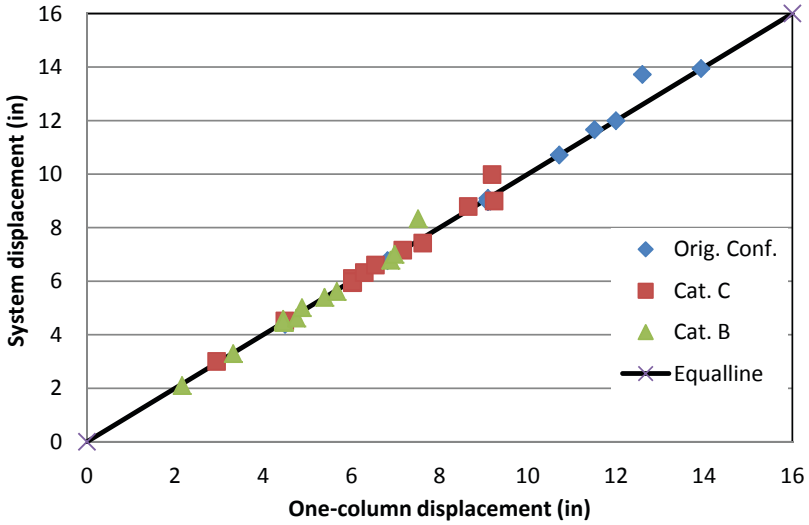

Figure 3.3. System displacement versus one-column displacement for multi-cell box-girder bridge.

columns through bearing supports. Changes in the abutment bearing stiffnesses also are considered, including the case where the bearings have negligible stiffness. Figure 3.3 shows the plot of the displacement capacity of the system versus the displacement obtained when one isolated column is analyzed. Here again, the data points are clearly aligned along the equal displacement line indicating that δ_{uc} is very close to δ_{1c} or $R_{du} = 1.0$ for all the cases analyzed. This also demonstrates that the displacement capacity of one column reflects the displacement capacity of the entire bridge structural system very accurately and the redundancy of the system is directly accounted for when using the displacement-based approach for evaluating bridges under lateral loads.

The results for the two-box-girder bridge are presented in Figure 3.4. The displacements are provided on the last two columns of Table 4.5. The analysis included columns designed with lateral confinement reinforcement ratios $\rho_s = 1\%$, 0.3% (detail category B) and 0.5% (detail category C). The columns' height was varied between 4.6-ft, 8.3-ft, 15-ft, 20-ft, 26.7-ft, and 33.3-ft. Although some of the low column heights may not be

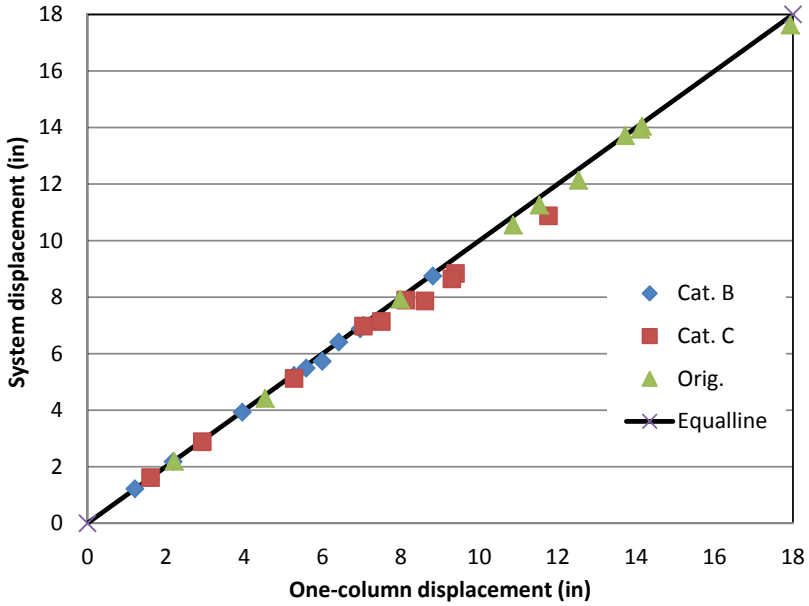

Figure 3.4. System displacement versus one-column displacement for two-box-girder bridge.

typical, they are used in order to study the effect of large changes in bridge configurations. Different longitudinal reinforcement ratios for the 6-ft diameter columns varying between 1.66% (original design with steel area A_s = 67.5 in^2), 1.44%, 1.22%, 0.99%, and 0.83% also are investigated. Here again, the data points are clearly aligned along the equal displacement line indicating that δ_{uc} is very close to δ_{1c} or R_{du} = 1.0 for all the cases analyzed. This confirms that the displacement capacity of one column reflects the displacement capacity of the entire bridge structural system very accurately and the redundancy of the system is directly accounted for when using the displacement-based approach for evaluating bridges under lateral loads. These results are due to the large stiffness of the superstructure, which ensures the compatibility of the lateral displacement of the top of the bridge columns of symmetric bridge configurations.

Comments on Displacement-Based Redundancy

The results shown in Section 3.2 demonstrate very clearly that the displacement capacity of a bridge system is equal to the displacement capacity of its most critical column. This fact has been recognized in the AASHTO Guide Specifications for LRFD Seismic Bridge Design, which provides empirical equations to calculate the displacement capacity of bridge columns with structural detailing categories SDC B and SDC C. The equations are given as

$$\textit{For category B: } \delta_{1c}^{*} = 0.12 \times H_0 \cdot \left(-1.27 \cdot \ln\left(\frac{\Lambda \cdot B_0}{H_0} \right) - 0.32 \right) \geq 0.12 \times H_0 \quad (3.3)$$

$$\textit{For category C: } \delta_{1c}^{*} = 0.12 \times H_0 \cdot \left(-2.32 \cdot \ln\left(\frac{\Lambda \cdot B_0}{H_0} \right) - 1.22 \right) \geq 0.12 \times H_0 \quad (3.4)$$

where δ_{1c}^{*} is the code-specified displacement capacity of the column in inches, Λ = 2 for columns fixed at the top and the bottom, Λ = 1 for fixed-pinned columns, B_0 is the width of the column in feet, and H_0 is the height in feet.

According to the AASHTO LRFD Seismic Design Specifications, column-based Equations 3.3 and 3.4 should be used to determine the seismic displacement capacity of a bridge system. Tables 3.1 and 3.2 compare the displacement capacities obtained from Equations 3.3 and 3.4 to those obtained from the nonlinear analysis of the systems for the I-girder bridges and the multi-cell box-girder bridges analyzed.

The results in Tables 3.1 and 3.2 show the large differences between the displacements obtained from the pushover analysis and those of Equation 3.3 and 3.4. The ratio between the two displacements ranges from 1.01 up to 2.75, demonstrating an inconsistent level of conservatism in the AASHTO equations.

The sources of the AASHTO empirical equations are not known, and it is clear from the sensitivity analysis performed in this study that they generally provide a safe lower bound estimate of the displacement capacity of bridge columns under lateral load. However, the level of safety was found to be inconsistent as the AASHTO equations ignore important parameters that affect the displacement capacity of bridge columns. The most notable omission is that of the longitudinal reinforcement ratio and the material properties. Therefore, it may be worthwhile to direct future research to developing improved models for evaluating the displacement capacity of bridge

Table 3.1. Comparison of code displacement to analysis results for I-girder bridge.

		System Analysis	System Analysis		
	Column Height	Load Capacity	Displacement Capacity	Code Displacement	Ratio of Actual Displacement to Code
Detail Category B	H (inch)	Pult. (kip)	δ_{uc} (in)	δ^{*}_{1c} (in)	
Base Case	331	1077	7.99	5.35	1.49
Height = 32.6 ft	391	1070	10.24	7.15	1.43
Height = 37.6 ft	451	1065	11.99	9.07	1.32
Base Pinned	331	871	11.38	8.27	1.38
Integral Top – Fixed Base	331	1080	7.97	5.35	1.49
Integral Top – Pinned Base	331	839	10.58	8.27	1.28
Pinned Top – Fixed Base	331	870	11.29	8.27	1.37
Detail Category C	H	Pult. (kip)	δ_{uc} (in)	δ^{*}_{1c} (in)	
Base Case	331	1212	10.44	7.68	1.36
Height = 32.6 ft	391	1219	13.12	10.58	1.24
Height = 37.6 ft	451	1246	15.62	13.70	1.14
Base Pinned	331	970	13.33	13.00	1.03
Integral Top – Fixed Base	331	1214	10.40	7.68	1.35
Integral Top – Pinned Base	331	966	13.16	13.00	1.01
Pinned Top – Fixed Base	331	967	13.15	13.00	1.01

Table 3.2. Comparison of code displacement to analysis results for multi-cell box-girder bridge.

		System Analysis	System Analysis		
	Column Height	Load Capacity	Displacement Capacity	Code Displacement	Ratio of Actual Displacement to Code
Detail Category B	H (inch)	Pult. (kip)	δ_{uc} (in)	δ^*_{1c} (in)	
Base Case	240	5527	4.49	2.40	1.87
Spring on Top	240	2704	5.40	2.90	1.86
Height =25 ft	300	4584	5.62	3.00	1.87
Height =30 ft	360	4004	6.78	3.60	1.88
Diameter =7ft	240	8287	4.62	2.40	1.93
Diameter = 8ft	240	11925	5.02	2.40	2.09
Detail Category C	H (inch)	Pult. (kip)	δ_{uc} (in)	δ^*_{1c} (in)	
Base Case	240	5865	5.97	2.40	2.49
Spring on Top	240	2942	7.17	3.78	1.90
Height =25 ft	300	4977	7.43	3.00	2.48
Height =30 ft	360	4332	9.00	3.60	2.50
Diameter =7ft	240	8837	6.33	2.40	2.64
Diameter = 8ft	240	12650	6.61	2.40	2.75

columns that take into consideration the columns' structural properties in addition to their dimensions.

3.3 Calibration of System Factors for Displacement-Based Approach

Procedure

The evaluation of the safety of a bridge under lateral load can be expressed in terms of the probability of failure, which for the displacement-based approach can be presented in terms of the probability that the ultimate system displacement capacity, δ_{uc}, is smaller than the displacement demand δ_d:

$$P_f = \Pr\left[\frac{\delta_{uc}}{\delta_d} \le 1\right] \tag{3.5}$$

It is common in probabilistic seismic hazard analysis (Hazus, 2003) to describe both the seismic demand and capacity by lognormal probability distributions. Accordingly, the probability of failure can be expanded as

$$P_f = \Phi\left[\frac{-\left[\ln\left(\delta^*_{uc}\right) - \ln\left(\delta^*_d\right)\right]}{\sqrt{\xi_c^2 + \xi_d^2}}\right] = \Phi\left[\frac{-\ln\left(\delta^*_{uc} \Big/ \delta^*_d\right)}{\sqrt{\xi_c^2 + \xi_d^2}}\right]$$

$$= \Phi\left[-\frac{\ln\left(\frac{\overline{\delta_{uc}}}{\overline{\delta_d}}\frac{\sqrt{1+V_d^2}}{\sqrt{1+V_c^2}}\right)}{\sqrt{\ln[(1+V_c^2)(1+V_d^2)]}}\right] \tag{3.6}$$

where δ^*_{uc} is the median of the displacement capacity δ_{uc}, $\overline{\delta_{uc}}$ is its mean value, ξ_c is the dispersion of the lognormal distribution of the capacity and V_c is the COV of the capacity. The variables with the subscript "d" are the statistics for the displacement demand. Φ is the cumulative normal distribution function.

Using the lognormal model, the reliability index for the system defined as, β_{system}, can be calculated as

$$\beta_{system} = \frac{\ln\left(\delta^*_{uc} \Big/ \delta^*_d\right)}{\sqrt{\xi_c^2 + \xi_d^2}} = \frac{\ln\left(\frac{\overline{\delta_{uc}}}{\overline{\delta_d}}\frac{\sqrt{1+V_d^2}}{\sqrt{1+V_c^2}}\right)}{\sqrt{\ln[(1+V_c^2)(1+V_d^2)]}} \tag{3.7}$$

The reliability index for one column defined as, β_{column}, can be calculated as

$$\beta_{column} = \frac{\ln\left(\delta^*_{1c} \Big/ \delta^*_d\right)}{\sqrt{\xi_c^2 + \xi_d^2}} = \frac{\ln\left(\frac{\overline{\delta_{1c}}}{\overline{\delta_d}}\frac{\sqrt{1+V_d^2}}{\sqrt{1+V_c^2}}\right)}{\sqrt{\ln[(1+V_c^2)(1+V_d^2)]}} \tag{3.8}$$

In the program Hazus (2003) developed by FEMA for evaluating the seismic risk of structures, the combined dispersion for capacity and demand for typical bridge structures and structural members is set at $\sqrt{\xi_c^2 + \xi_d^2} = 0.60$ for all damage types and all bridge members.

If the demand on the system is set in terms of the basic seismic input, which could be related to the peak ground acceleration and the overall properties of the entire system such as its natural period and soil conditions, and given that as shown in Figures 3.2, 3.3, and 3.4, the system displacement and the one-column displacement capacities are equal, then all the variables in β_{system} and β_{column} have the same values.

As explained in Chapter 2, a probabilistic measure of system redundancy can be expressed in terms of the additional reliability provided by the system compared to that of the member defined by the reliability index margin as

$$\Delta\beta_u = \beta_{system} - \beta_{column} \tag{3.9}$$

Substituting Equations 3.7 and 3.8 into Equation 3.9, the reliability index margin is

$$\Delta\beta_u = \frac{\ln\left(\delta^*_{uc}/\delta^*_d\right)}{\sqrt{\xi_c^2+\xi_d^2}} - \frac{\ln\left(\delta^*_{1c}/\delta^*_d\right)}{\sqrt{\xi_c^2+\xi_d^2}} = \frac{\ln\left(\delta^*_{uc}/\delta^*_{1c}\right)}{\sqrt{\xi_c^2+\xi_d^2}} \tag{3.10}$$

As demonstrated in Figures 3.2, 3.3, and 3.4, the one column displacement capacity is essentially equal to the system displacement capacity such as $\delta_{1c} = \delta_{uc}$ leading to $\Delta\beta_u = 0$. Since the system does not provide any additional reliability compared to that of the most critical member, then bridge systems designed to meet the displacement-based requirements of the AASHTO Guide Specifications for LRFD Seismic Bridge Design are not redundant. Therefore, they must be designed to higher reliability index levels than equivalent redundant systems.

As explained in Chapter 2 and in *NCHRP Report 406*, redundant superstructure systems subjected to vertical loads have been defined as those that meet a target system reliability margin $\Delta\beta_{u\ target} = 0.85$. This target margin was selected to match the average reliability margin of all four-girder bridges assuming that the overall COV for the safety margin is approximately equal to 0.25, which reflects the uncertainties in estimating the superstructure capacity and live load. Bridge systems that do not meet this minimum target reliability margin should be designed to higher standards by applying a system factor ϕ_s. The system factor should be calibrated to offset the difference between the target reliability margin and the reliability margin that the system provides. In *NCHRP Report 458*, the target reliability margin was set at $\Delta\beta_{u\ target} = 0.50$ based on a COV for the safety margin equal to 0.35 reflecting the uncertainty in estimating the substructure capacity and lateral wind load.

For example, assume that the same target margin $\Delta\beta_{u\ target} = 0.85$ set for superstructures under vertical loads also is used for systems subjected to lateral load being evaluated using the displacement-based approach. As shown in this report, the displacement-based approach shows that the provided reliability margin is $\Delta\beta_u = 0$. Therefore, following the same calibration process outlined in Section 2.5, all bridges designed using the displacement-based approach should include a system factor ϕ_s such that

$$\beta^*_{column} = \frac{\ln\left(\delta^*_{1c}/\phi_s\delta^*_d\right)}{\sqrt{\xi_c^2+\xi_d^2}} = \beta_{column} + \left(\Delta\beta_{u\ target} - \Delta\beta_u\right) \tag{3.11}$$

where β_{column} is the reliability index that has been specified based on the member reliability criteria as shown in Equation 3.5, β^*_{column} is the reliability index for the column after applying the system factor, and $\Delta\beta_{u\ deficit} = (\Delta\beta_{u\ target} - \Delta\beta_u)$ is the deficit in the reliability index margin that the new columns' design should offset. Substituting Equation 3.8 into Equation 3.11 and expanding, provides

$$\beta^*_{column} = \frac{\ln\left(\delta^*_{1c}/\delta^*_d\right)}{\sqrt{\xi_c^2+\xi_d^2}} - \frac{\ln(\phi_s)}{\sqrt{\xi_c^2+\xi_d^2}} = \frac{\ln\left(\delta^*_{1c}/\delta^*_d\right)}{\sqrt{\xi_c^2+\xi_d^2}} + \left(\Delta\beta_{u\ target} - \Delta\beta_u\right) \tag{3.12}$$

$$\phi_s = e^{-\sqrt{\xi_c^2+\xi_d^2}\left(\Delta\beta_{u\ target}-\Delta\beta_u\right)} = e^{-\sqrt{\xi_c^2+\xi_d^2}\left(\Delta\beta_{u\ target}\right)} \tag{3.13}$$

Equation 3.13 can be used for any dispersion value and any target reliability index margin. For example, if $(\Delta\beta_{u\ target} - \Delta\beta_u) = (0.85 - 0) = 0.85$ and $\sqrt{\xi_c^2+\xi_d^2} = 0.60$ Equation 3.13 can be solved for the system factor $\phi_s = 0.60$. This means that the calculated capacity should be reduced by a factor of 0.60 to meet the new target reliability level. Alternatively, this indicates that the calculated capacity can only sustain 0.60 times the required demand with a sufficient level of reliability.

This system factor $\phi_s = 0.60$ would be applied to reflect the lack of system redundancy when evaluating the safety of bridges using the displacement-based approach to give an additional reliability index equal to 0.85 on top of the reliability index and safety factors already embedded in the displacement-based design methodologies. Such embedded reliability is included by using the 1,000-year design earthquake, which has about 5% probability of exceedance within 50 years or 7.2% probability of exceedance within 75 years, which is the design life stipulated in the AASHTO LRFD. If no other safety factors are applied, Equation 2.7 shows that a 7.2% probability would lead to a reliability index $\beta = 1.45$.

In actuality, for detail categories B and C, the use of Equations 3.3 and 3.4 proposed in the AASHTO LRFD seismic provisions include some additional safety. As demonstrated in Tables 3.1 and 3.2, the safety factor seems to be in the range of 1.0 to 2.75 for different column dimensions, end conditions, and confinement detailing for bridges in categories C and B. For detail category D, the AASHTO LRFD seismic provisions recommend that the displacement capacity be evaluated using a pushover analysis that would give very good approximations of the member as well as the system capacity. Since no rigorous evaluation of the safety factors implied in the AASHTO LRFD seismic provisions was performed, the reliability index implied in the AASHTO seismic provisions is not exactly known but is higher than $\beta = 1.45$. Applying an additional system factor of 1/0.60 will lead to a lower bound reliability index of $\beta = 2.30$.

Table 3.3. Variation of system factor with target margin and dispersion.

Target Reliability Margin $\Delta\beta_{u\ target}$	Dispersion Coefficient $\sqrt{\xi_c^2+\xi_d^2}$	System Factor ϕ_s
0.30	0.2	0.94
	0.3	0.91
	0.4	0.89
	0.5	0.86
	0.6	0.84
0.40	0.2	0.92
	0.3	0.89
	0.4	0.85
	0.5	0.82
	0.6	0.79
0.50	0.2	0.90
	0.3	0.86
	0.4	0.82
	0.5	0.78
	0.6	0.74
0.60	0.2	0.89
	0.3	0.84
	0.4	0.79
	0.5	0.74
	0.6	0.70
0.70	0.2	0.87
	0.3	0.81
	0.4	0.76
	0.5	0.70
	0.6	0.66
0.80	0.2	0.85
	0.3	0.79
	0.4	0.73
	0.5	0.67
	0.6	0.62
0.90	0.2	0.84
	0.3	0.76
	0.4	0.70
	0.5	0.64
	0.6	0.58
1.00	0.2	0.82
	0.3	0.74
	0.4	0.67
	0.5	0.61
	0.6	0.55

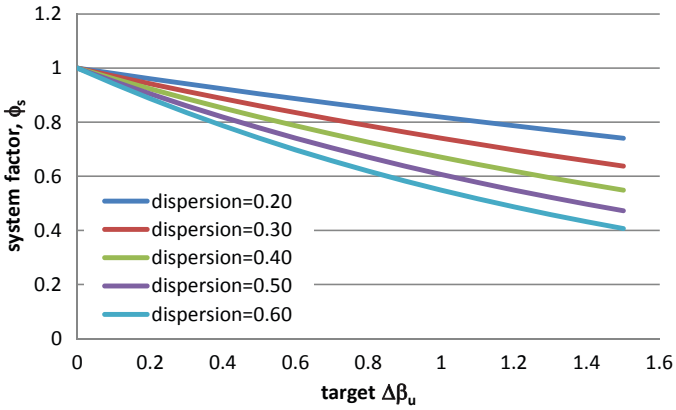

Figure 3.5. System factor for different target reliability and dispersion coefficient.

Sensitivity Analysis and Recommendation

A sensitivity analysis is presented to study the effect of the dispersion coefficient and the target reliability index margin on the system factor for the displacement-based approach as calculated from Equation 3.13. The results are presented in Table 3.3 and in Figure 3.5, which show that the system factor is sensitive to the target reliability index margin and the dispersion coefficient.

Although the target margin for superstructures under vehicular live loads can be established based on configurations known to provide sufficient levels of redundancy, it is much more difficult to decide on the appropriate target reliability margin that a system subjected to seismic displacement demand should be able to achieve. It is suggested that the target reliability index margin should at a minimum be set at $\Delta\beta_{u\ target} = 0.50$. This recommendation is based on the fact that the 1,000-year design earthquake may be providing a system reliability level on the order of $\beta = 1.45$. Providing an additional reliability equal to 0.50 would raise that available system reliability to a value close to 2.0, which is slightly lower than the target reliability set for bridge members being evaluated under vertical load for operating rating. According to Table 3.3, a target reliability margin $\Delta\beta_{u\ target} = 0.50$ when the dispersion coefficient is equal to 0.60 will require a system factor $\phi_s = 0.74$ or an additional safety factor = 1.35 ($=1/\phi_s$). This value is approximately equal to the overstrength factor traditionally used when detailing bridge columns whose capacity was set based on ultimate bending moment criteria.

References

AASHTO (2011) *Guide Specifications for LRFD Seismic Bridge Design*, 2nd ed, Washington, D.C.

Buckle, I., et al. (2006) Seismic Retrofitting Manual for Highway Structures, Part 1 Bridges, FHWA-HRT-06-032, Turner-Fairbank Highway Research Center, McLean, VA.

HAZUS - MH MR4 (2003) Multi-Hazard Loss Estimation Methodology Earthquake Model, Technical Manual, Department of Homeland Security, Emergency Preparedness and Response Directorate, FEMA Mitigation Division, Washington, D.C.

CHAPTER 4

Force-Based System Safety and Redundancy of Bridges

4.1 Redundancy of Bridge Systems under Lateral Load

Traditionally, structural design codes have defined a structure's capacity in terms of the ability of its individual members to sustain the applied loads using a linear-elastic analysis. Given that the failures of individual members do not necessarily lead to the collapse of the system, structural redundancy is defined as the ability of a structural system to continue to carry load after one critical member reaches its load carrying capacity. Based on the system behavior explained in Section 3.1 of this report as described in Figure 3.1 and to remain consistent with the definition of bridge redundancy established for systems under vertical loads as explained in *NCHRP Report 406* and Chapter 2, quantifiable measures of system redundancy for bridges subjected to a distributed lateral load are proposed as follows for force-based designs:

$$R_{fu} = \frac{P_u}{P_{p1}} \tag{4.1}$$

where R_{fu} gives the redundancy ratio or the system reserve ratio expressed in terms of the forces, P_{p1} gives the force capacity of a bridge system under lateral load assuming linear-elastic behavior and assuming that failure takes place when the most critical member reaches its plastic limit as typically done when using a force-based analysis, and P_u gives the ultimate capacity of the system accounting for the entire system's nonlinear behavior.

The analyses of the results of hundreds of bridge systems and substructure bents have demonstrated that a simple empirical model can be used to describe the relationship between the ultimate capacity of a multi-column bridge substructure system represented by P_u and the lateral load carrying capacity of one column represented by P_{p1} as functions of the number of columns in the bent and the ultimate curvature capacity of the bent columns. This relationship is expressed by an equation of the form

$$P_u = P_{p1}\left[F_{mc} + C_\varphi \frac{\varphi_u - \varphi_{tunc}}{\varphi_{tconf} - \varphi_{tunc}}\right] \tag{4.2}$$

where P_{p1} gives the capacity of a bridge system under lateral load assuming that the analysis is performed using linear-elastic behavior and failure is defined when one column reaches its maximum load carrying capacity as typically done when using a force-based analysis, F_{mc} is a multi-column factor, C_φ is a curvature factor, φ_u is the ultimate curvature of the weakest column in the bent, φ_{tunc} is the average curvature for a typical unconfined column, φ_{tconf} is the average curvature for a typical confined column. The typical curvature values for the confined and unconfined columns are extracted from the results of the survey conducted in *NCHRP Report 458.*

For a particular bridge system, P_{p1} is calculated using a linear structural analysis of the system under the effect of the applied lateral load. To find P_{p1}, failure is defined as the load at which one column reaches its ultimate capacity. The value for the ultimate curvature at failure φ_u is calculated from the ultimate plastic analysis of the column's cross section.

Values for F_{mc}, C_φ, φ_{tunc}, and φ_{tconf} have been extracted from the analysis of a large number of bridges with two-column, three-column, and four-column bents. The bents analyzed included a range of column sizes, vertical reinforcement ratios, and confinement ratios. The analyses also considered the effect of different foundation stiffnesses. The recommended values for these parameters are provided in Table 4.1. The values for φ_{tunc} and φ_{tconf} are the average curvatures obtained from the analysis of the column sizes used in *NCHRP Report 458.* The columns analyzed in *NCHRP Report 458* represent typical column sizes and reinforcement ratios collected from a national survey conducted as part of the study. The values for φ_{tunc} and φ_{tconf} are used in Equation 4.2 to compare

Table 4.1. Recommended values for redundancy parameters.

Variable	Applicability	Recommended Value
F_{mc}, multi-column factor	Two-column bents	1.10
	Three-column bents	1.16
	All other multi-column bents	1.18
C_{φ}, curvature factor	All systems	0.24
φ_{tunc}, typical unconfined column ultimate curvature	All systems	3.64×10^{-4} (1/in)
φ_{tconf}, typical confined column ultimate curvature	All systems	1.55×10^{-3} (1/in)

the confinement ratio of the column being evaluated to the average confinement ratios observed in typical confined and unconfined columns.

This chapter summarizes the results of the analyses conducted during this project and those extracted from *NCHRP Report 458.* The results of the analyses of typical bridge system configurations considered different bridge and column dimensions, confinement and reinforcement ratios, foundation stiffnesses, and deficiencies in the columns and their connecting elements. The results are used to calibrate a system factor equation for use during the force-based design and safety evaluation of columns of bridges subjected to distributed lateral load. Specifically, this chapter consists of the following:

- Section 4.2 summarizes the results obtained in this study and in *NCHRP Report 458* from all the analyses of bridge systems subjected to lateral load at the superstructure level. Tables listing all the results are provided for bridges consisting of two-column, three-column, and four-column bents with various column heights and cross-section dimensions, vertical and transverse reinforcement ratios, foundation stiffnesses, as well as different connections between columns and superstructures.
- Section 4.3 summarizes the validation of the proposed model for the cases previously analyzed.
- Section 4.4 contains a few additional analyses to study if the proposed model remains essentially valid when considering P-delta effects. Also, additional analyses are performed to consider different foundation stiffnesses for bridge systems having three-column bents. Additionally, this section describes how the model can be adjusted to account for the effect of inadequate cap beams on substructure redundancy and how to account for columns weak in shear. Examples describing how an engineer can use the proposed model along with the necessary adjustments are also provided.
- Section 4.5 gives the conclusions.

4.2 Summary of Bridge Analyses and Results

This summarizes the bridge models analyzed during the course of this study along with a summary of the results obtained during the course of this study and in *NCHRP Report 458.* The bridges analyzed in this study consist of a continuous three-span I-girder steel bridge with two bents supported by three columns each, a three-span bridge carrying a multi-cell prestressed concrete bridge superstructure where each bent is formed by two columns, and a three-span bridge carrying two prestressed concrete girder boxes where each bent has two columns. The results of the analyses performed in this study are supplemented by the results of the two-column and four-column bents analyzed in *NCHRP Report 458.*

Two-Column Bents Supporting a Prestressed Concrete Twin Box-Girder Bridge

Bridge Description

A three-span (80-ft, 120-ft, 80-ft) continuous bridge with two precast prestressed concrete box sections is selected for analysis. Figure 4.1 gives the frame element model used in this set of analyses.

Prestressed Concrete Box

Figure 4.2 shows the dimensions of the box cross section. The material properties of concrete and steel are listed in Tables 4.2 and 4.3, respectively. The corresponding stress-strain curves for steel and concrete are obtained from the library of the program XTRACT, which are based on the Mander model for concrete, parabolic strain hardening steel model for reinforcing steel and low-relaxation strands model in Collins and Mitchell's book for prestressed strands.

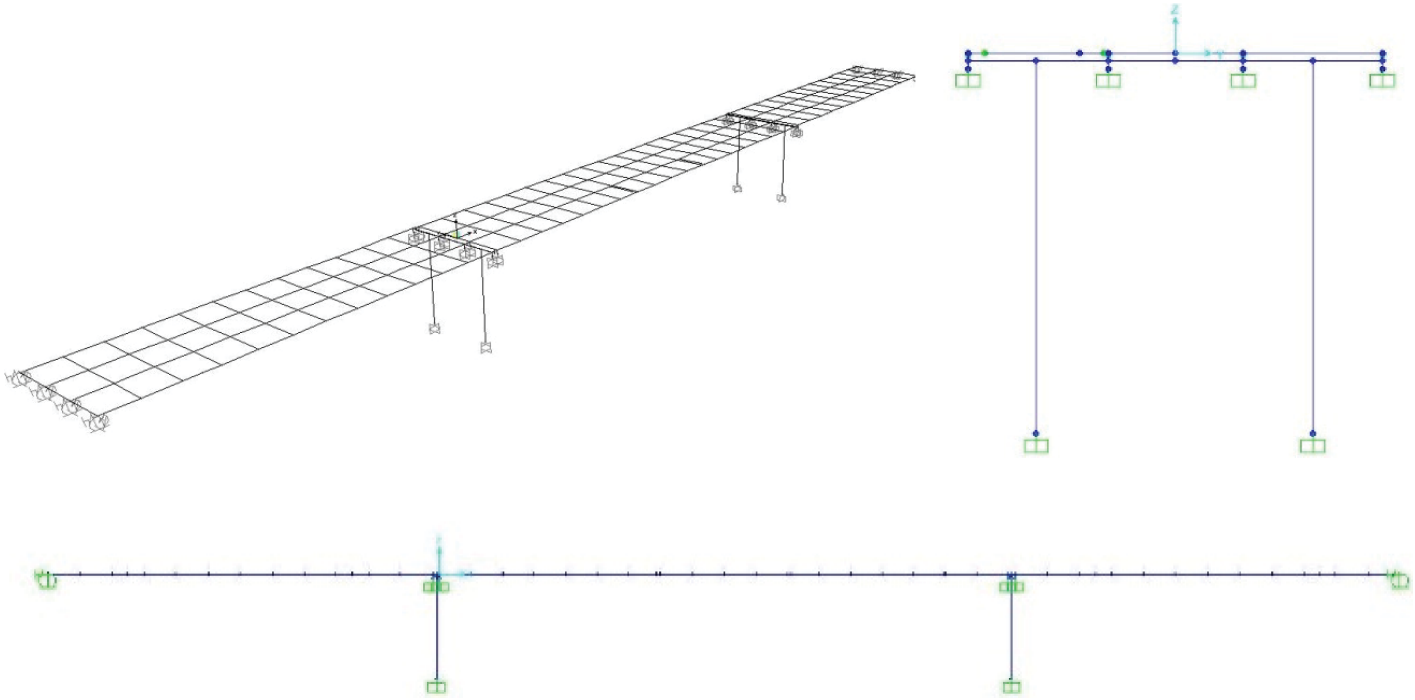

Figure 4.1. The 3-D, profile, and elevation views of the twin box-girder bridge.

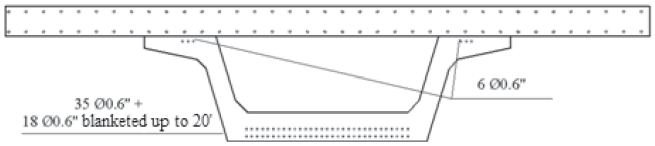

(a) Configuration of prestressing steel

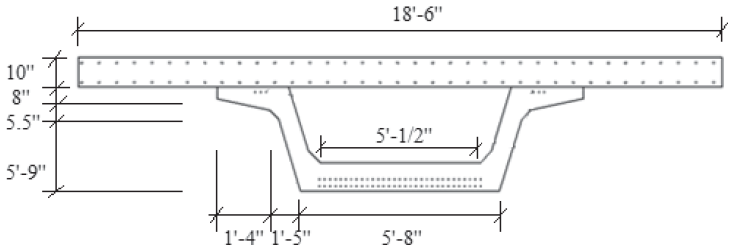

(b) Dimensions of one box

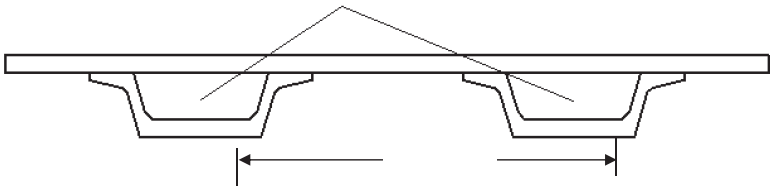

(c) Spacing of two boxes

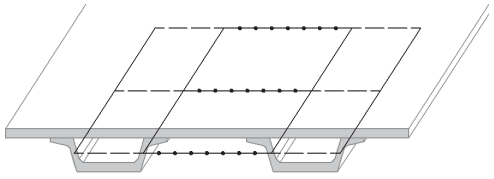

(d) Grillage model for box-girder bridge

Figure 4.2. Detailed dimensions of cross section of the twin box bridge.

Table 4.2. Concrete properties.

Parameters	Box	Slab	Column	
			Unconfined	Confined
28-Day Strength (ksi)	7.250	4.350	4.000	4.000
Crushing Strain	4.000E-3	4.000E-3	4.000E-3	18.740E-3
Elastic Modulus (ksi)	4853	3759	3605	3605

Table 4.3. Steel properties.

Parameters	Rebar	Strand
Yield stress (ksi)	60	--
Fracture stress (ksi)	90	270
Failure strain	90.00E-3	4.20E-2

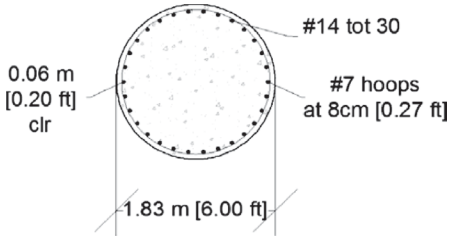

Figure 4.3. Column cross section for base cases.

Bridge Columns

The bridge columns are the most important contributors for the resistance of the bridge to lateral load. The lateral load is applied on the top of the bents, in particular on the middle point of the cap beams. The cross section of the four typical columns used for the substructure is shown in Figure 4.3. The column height used in the base case is 20 feet.

In this study, three cases with different column confinement ratios, ρ_s, are investigated. The original confinement ratio is 0.01. Two other cases are analyzed where the confinement ratios meet the LRFD seismic criteria for bridges of category B and C. In summary, the three confinement ratios are

- $\rho_s = 0.01$ (base case),
- $\rho_s = 0.003$ (category B), and
- $\rho_s = 0.005$ (category C).

The pushover analysis of the frame element model is performed using SAP2000. Moment-curvature relationships are used to model the nonlinear behavior of the columns. This nonlinear behavior is related to the axial load acting on it. In fact, different axial loads lead to different moment-curvature curves. Therefore, an important input for the pushover analysis is the axial force versus moment interaction (P-M) curve. As an example, Figure 4.4 shows the moment interaction diagram for the column in the base case ($\rho_s = 0.01$) that is valid for all bending axes because the section is axisymmetric.

In the base case, the axial load value due to dead load is about P = 512 kip and the axial load value due to dead load plus live load is about P = 523 kip assuming a load combination factor of 0.20. Figure 4.5 gives the different moment-

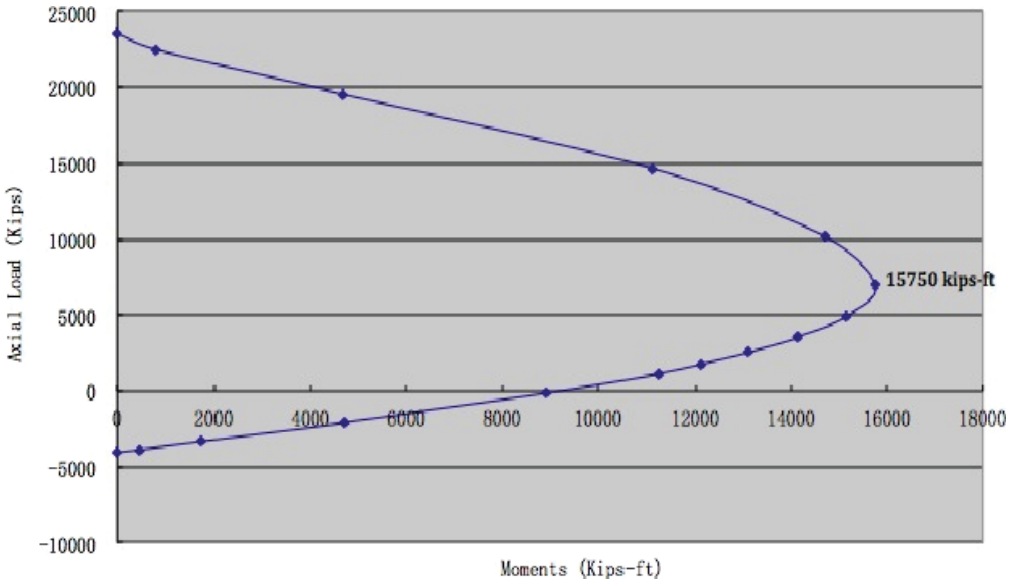

Figure 4.4. Column P-M interaction curve for base case.

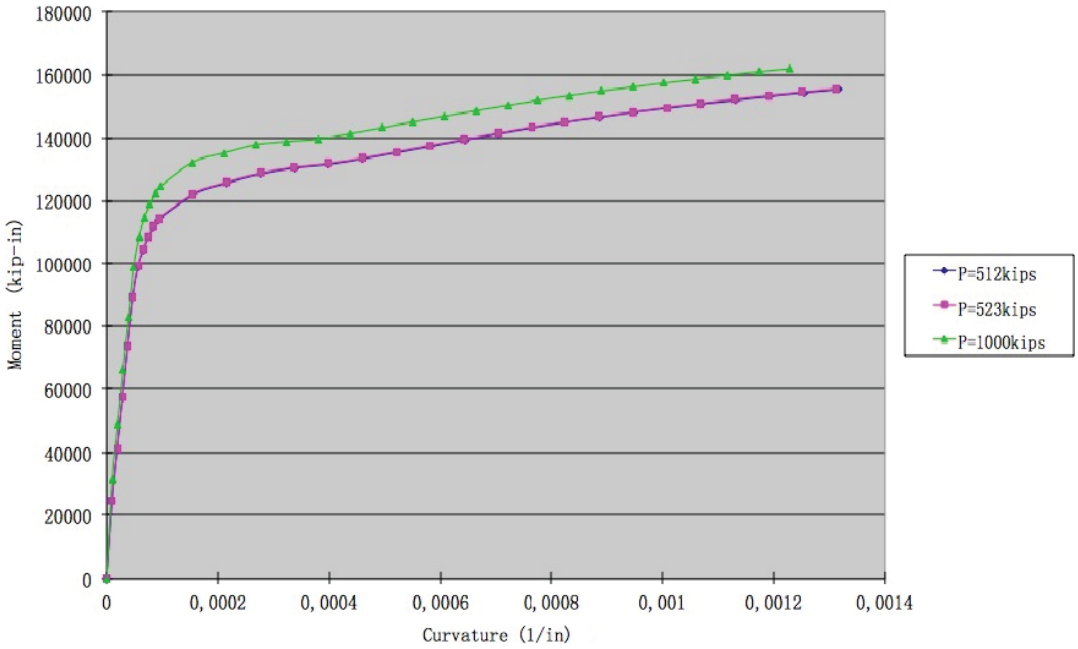

Figure 4.5. Column M-phi curve for different values of axial load.

curvature (M-phi) curves constructed using the software XTRACT to illustrate the differences due to the axial load. SAP2000 updates the M-phi curve based on the axial load calculated at each step of the pushover analysis by updating the ultimate moment and curvature capacities using the P-M curve and the equivalent energy principle.

Figure 4.5 also shows that the difference in the M-phi curve between the two cases when P = 512 kips and P = 523 kips is negligible where the blue line practically coincides with the purple line with a maximum difference smaller than 0.13%. It is observed that even a doubling of the axial load will result in a relatively small change in the M-phi curve. In this particular case, because the loading on the column lies below the balanced point of the P-M interaction curve, the moment capacity of the section increases by about 4% when the axial load is increased to 1000 kips.

Cap Beam

The dimensions of the cap beam are provided in Figure 4.6.

Bearings

The bearings are assumed to be placed at the abutments below each box's web. The bearings at the abutments are modeled as linear-elastic springs. In the base case model, the

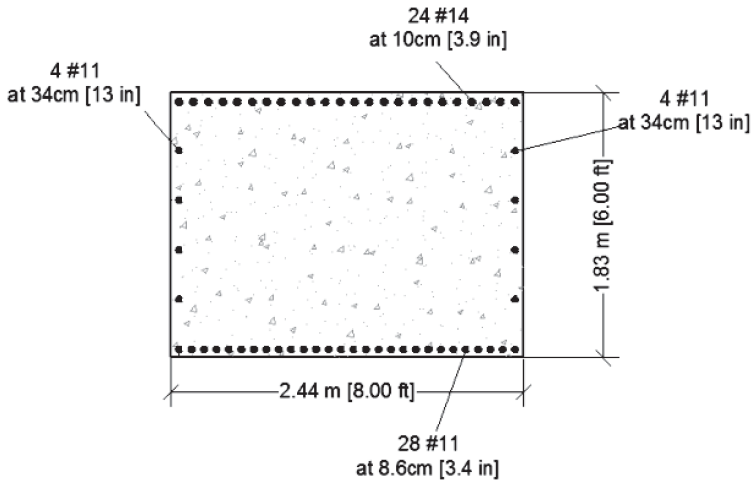

Figure 4.6. Dimensions of cap beam.

Table 4.4. Bearing stiffness values.

	Left Abutment (kip/in.)	Right Abutment (kip/in.)
k_x	4	4
k_y	4	4
k_z	∞	∞

bearings are assumed to allow for longitudinal expansion and for transverse displacement. The same stiffness values are assumed for the bearings in the longitudinal and lateral directions. The displacement in the perpendicular direction to the slab is assumed to be locked. Table 4.4 summarizes the spring values assumed for the base case.

Summary of Results

The three-span box-girder bridge system analyzed in the base case consists of two prestressed concrete boxes supported on two columns at each bent. The columns have integral connections to the cap beam. A sensitivity analysis is performed to study how variations in column dimensions and other parameters affect the results of the pushover analysis. Specifically, the Nonlinear Static Pushover Analysis (NSPA) is used to study the sensitivity of the results to the following parameters: (1) column height, (2) column confinement ratio, and (3) column reinforcement ratio. The numerical results from the analyses are summarized in Table 4.5, which gives the diameter of the column, its height, the longitudinal reinforcement ratio in percent, the force P_{p1} which gives the failure load of the first column assuming elasto-plastic behavior and using the force-based approach, the force P_u, which gives the ultimate curvature for the entire system assuming nonlinear behavior, the ultimate curvature for the columns, the lateral displacement of the system at failure δ_u, and the maximum displacement when one column fails δ_1.

The analysis included columns designed with lateral confinement reinforcement ratios ρ_s = 1%, 0.3% (detail category B) and 0.5% (detail category C). The columns' height was varied between 4.6-ft, 8.3-ft, 15-ft, 20-ft, 26.7-ft, and 33.3-ft. Although some of the low column heights may not be typical, they are used in order to study the effect of large changes in bridge configurations. Different longitudinal reinforcement ratios for the 6-ft diameter columns varying between 1.66% (original design with steel area $A_s = 67.5$ in^2), 1.44%, 1.22%, 0.99%, and 0.83% are also investigated.

The validation of Equation 4.2 for the ultimate capacity of the system is verified in Figure 4.7, which plots P_u from Equation 4.2 versus that obtained from the SAP2000 analysis. Figure 4.7 shows that the data points are clearly aligned along the equal force line indicating that Equation 4.2 is reasonably accurate with a regression coefficient $R^2 = 0.99$. The COV of the ratio between the value from Equation 4.2 and the SAP2000 is less than 4%. The worst cases are those for which the bearing stiffness is assumed to be over 10 times the actual stiffness, which is extremely high for this type of bridge.

Two-Column Bents Supporting a Multi-Cell P/S Concrete Box Bridge

Bridge Description

A multi-cell prestressed concrete bridge system is investigated to understand the behavior of such systems when subjected to lateral loads applied on top of the bents. The configuration of the multi-cell prestressed concrete box-girder bridge system analyzed is a variation on an actual bridge configuration that had been designed to sustain high levels of seismic motions. The superstructure is a three-span continuous prestressed multi-cellular box girder with diaphragms located over the abutments and over the bents. The bridge is assumed to have three spans with a middle span of 150 feet and two end spans 110 feet in length each, as shown in Figure 4.8. Each bent is formed by two columns connected integrally to the diaphragms. For the base case, all the columns are 20 feet high and their diameters are 72 inches. The superstructure is supported on elastomeric bearings at the abutments. Figure 4.9 shows detailed dimensions of the box cross section. The rigid connections of the columns to the diaphragms would allow for the transfer of forces and moments between the two subsystems. This design should provide a higher capacity to sustain lateral loads as compared to traditional bearing on bent bridges. The basic bridge configuration assumes that the foundation is very stiff, approaching fixed conditions.

Summary of Results

The three-span box-girder bridge system analyzed in the base case consists of a multi-cell prestressed concrete box supported on two columns at each bent. Following the analysis of the base case bridge, NSPA is used to study the sensitivity of the structure to (1) different bearing stiffness values at the abutments, (2) different column diameters and reinforcement ratios, (3) changes in the rigidity of the connections between the columns and diaphragm elements, and (4) different foundation stiffness. Numerical results are summarized in Table 4.6, which gives the column diameter and height, with the longitudinal reinforcement ratio and the ultimate bending moment curvature along with the force, P_{p1}, that causes the failure of the first column assuming elastic behavior and the ultimate capacity of the non-

Table 4.5. Results summary of two box-girder bridge with two-column bent.

Original case (column lateral confinement ratio=1.0%)								
	Diameter (in.)	Height (in.)	Long. rebar ratio ρ (%)	P_{p1} (kips)	P_u (kips)	φ_u (in^{-1})	δ_u of system (in.)	δ_1 for column (in.)
50% rebar	72	240	0.83	2364	3624	0.00168	13.94	14.10
60% rebar	72	240	0.99	2708	4072	0.00166	13.39	13.72
73% rebar	72	240	1.22	3126	4552	0.00154	12.14	12.53
87% rebar	72	240	1.44	3526	5052	0.00140	11.26	11.53
100% rebar	72	240	1.66	4150	5535	0.00132	10.55	10.86
H=55 in.	72	55	1.66	14969	22662	0.00132	2.20	2.21
H=100 in.	72	100	1.66	9028	12618	0.00132	4.42	4.53
H=180 in.	72	180	1.66	5386	7188	0.00132	7.93	7.98
H=280 in.	72	280	1.66	3602	4854	0.00132	10.55	10.86
H=320 in.	72	320	1.66	3184	4334	0.00132	14.05	14.15
H=400 in.	72	400	1.66	2585	3679	0.00132	17.63	17.93
H=450 in.	72	450	1.66	2315	3408	0.00132	--	--
H=500 in.	72	500	1.66	2097	3189	0.00132	--	--
Category B (column lateral confinement ratio=0.3%)								
	Diameter (in.)	Height (in.)	Long. rebar ratio ρ (%)	P_{p1} (kips)	P_u (kips)	φ_u (in^{-1})	δ_u of system (in.)	δ_1 for column (in.)
50% rebar	72	240	0.83	2351	2989	0.000847	6.88	6.96
60% rebar	72	240	0.99	2676	3341	0.000783	6.41	6.41
73% rebar	72	240	1.22	3039	3808	0.000735	5.73	5.99
87% rebar	72	240	1.44	3437	4250	0.000688	5.49	5.58
100% rebar	72	240	1.66	3808	4692	0.000652	5.23	5.27
H=55 in.	72	55	1.66	13768	19758	0.000652	1.22	1.21
H=100 in.	72	100	1.66	8297	10939	0.000652	2.18	2.19
H=180 in.	72	180	1.66	4949	6158	0.000652	3.93	3.95
H=280 in.	72	280	1.66	3304	4068	0.000652	5.23	5.27
H=320 in.	72	320	1.66	2920	3602	0.000652	7.00	7.04
H=400 in.	72	400	1.66	2370	2982	0.000652	8.75	8.81
H=450 in.	72	450	1.66	2122	2700	0.000652	--	--
H=500 in.	72	500	1.66	1922	2497	0.000652	--	--
Category C (column lateral confinement ratio=0.5%)								
	Diameter (in.)	Height (in.)	Long. rebar ratio ρ (%)	P_{p1} (kips)	P_u (kips)	φ_u (in^{-1})	δ_u of system (in.)	δ_1 for column (in.)
50% rebar	72	240	0.83	2430	3218	0.00113	8.65	9.30
60% rebar	72	240	0.99	2764	3576	0.00104	7.87	8.61
73% rebar	72	240	1.22	3160	4064	0.000936	7.80	8.12
87% rebar	72	240	1.44	3536	4500	0.000864	7.14	7.50
100% rebar	72	240	1.66	3906	4986	0.000857	6.98	7.04
H=55 in.	72	55	1.66	14088	20811	0.000857	1.62	1.61
H=100 in.	72	100	1.66	8496	11542	0.000857	2.89	2.93
H=180 in.	72	180	1.66	5069	6524	0.000857	5.13	5.27
H=280 in.	72	280	1.66	3390	4338	0.000857	6.98	7.04
H=320 in.	72	320	1.66	2996	3854	0.000857	8.84	9.39
H=400 in.	72	400	1.66	2433	3214	0.000857	10.88	11.76
H=450 in.	72	450	1.66	2179	2928	0.000857	--	--
H=500 in.	72	500	1.66	1973	2730	0.000857	--	--

linear system represented by the force P_u and the maximum displacement at failure δ_u. The displacement δ_1 is the maximum displacement if the pushover analysis is performed on a single column.

The sensitivity analysis assumed column heights equal to 20-ft, 25-ft, and 30-ft with lateral confinement reinforcement ratios $\rho_s = 1\%$, 0.3% (detail category B) and 0.5% (detail category C), in addition to cases where the maximum curvature is reduced by 50% and 75% to account for deficiencies in design. The columns' diameters were varied between 6-ft, 7-ft, and 8-ft. Different foundation stiffnesses are used to represent pile and spread footing foundation as well as rigid foundation. The possibility of integral column/superstructure connections is compared to the cases where the load is transferred between the superstructure and the columns through bearing supports. Changes in the abutment bearing stiffness also are considered, including the case where the bearings have negligible stiffness.

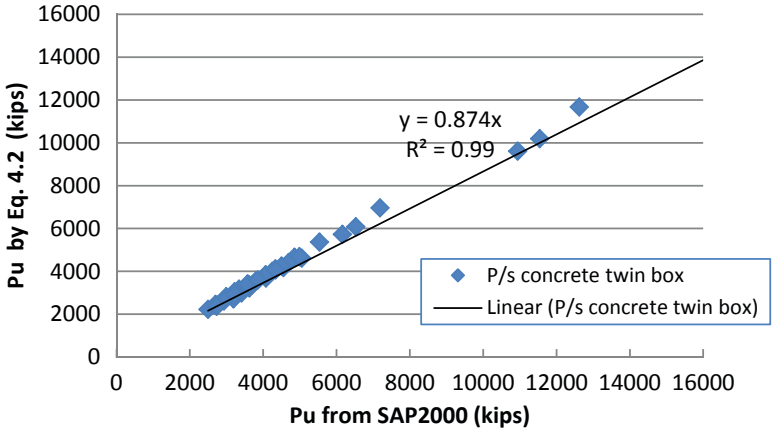

Figure 4.7. Lateral capacity by Equation 4.2 vs. lateral capacity from SAP2000 for two box-girder bridges.

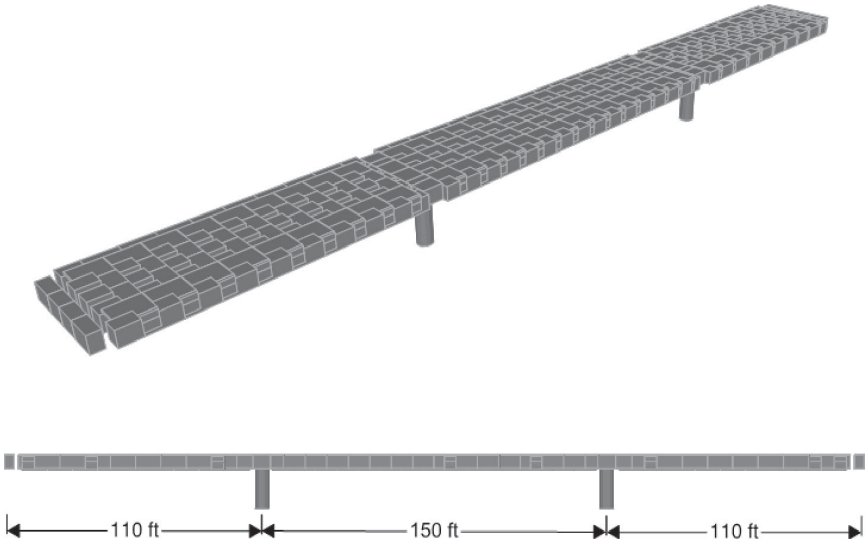

Figure 4.8. The 3-D isometric view and span dimensions.

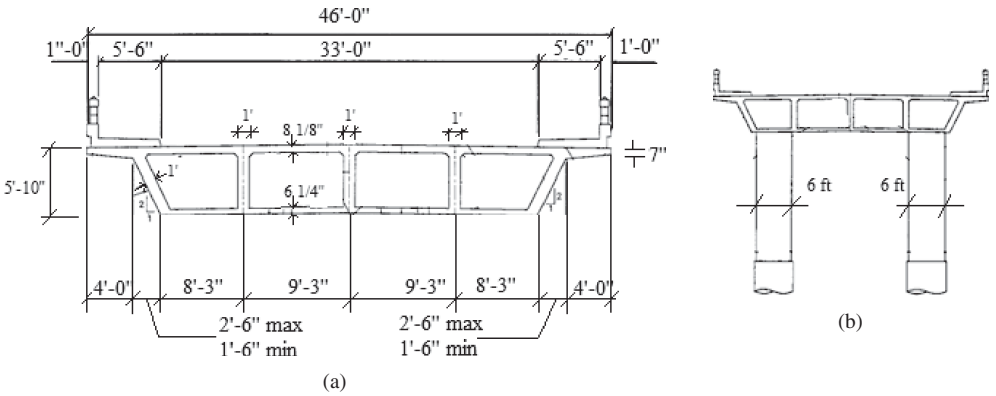

Figure 4.9. Typical cross section of bridge system.

Table 4.6. Results summary of multi-cell box-girder bridge with two-column bent.

Category B (column lateral confinement ratio=0.3%)								
	Diameter (in.)	Height (in.)	Long. rebar ratio ρ (%)	P_{p1} (kips)	P_u (kips)	φ_u (in^{-1})	δ_u of system (in.)	δ_1 for column (in.)
Base Case	72	240	1.66	4907	5527	0.00061	4.48	4.49
50% Phi	72	240	1.66	4907	5018	0.00031	2.16	2.10
75% Phi	72	240	1.66	4907	5312	0.00046	3.32	3.30
Spring Top Column	72	240	1.66	2460	2704	0.00061	5.39	5.40
25 ft	72	300	1.66	4011	4584	0.00061	5.67	5.62
30 ft	72	360	1.66	3406	4004	0.00061	6.89	6.78
Pile Foundation	72	240	1.66	3649	5448	0.00061	6.98	7.01
Spread Foundation	72	240	1.66	5451	5823	0.00061	7.51	8.33
No bearing	72	240	1.66	4561	5152	0.00061	4.45	4.58
2X bearing	72	240	1.66	4940	5844	0.00061	4.47	4.48
4X bearing	72	240	1.66	4982	6317	0.00061	4.47	4.46
10X bearing	72	240	1.66	5053	7160	0.00061	4.45	4.48
Diameter–7 ft	84	240	1.66	7582	8287	0.00053	4.75	4.62
Diameter–8 ft	96	240	1.66	10984	11925	0.00046	4.88	5.02
Category C (column lateral confinement ratio=0.5%)								
	Diameter (in.)	Height (in.)	Long. rebar ratio ρ (%)	P_{p1} (kips)	P_u (kips)	φ_u (in^{-1})	δ_u of system (in.)	δ_1 for column (in.)
Base Case	72	240	1.66	5047	5865	0.00082	6.03	5.97
50% Phi	72	240	1.66	5047	5300	0.00041	2.94	3.01
75% Phi	72	240	1.66	4907	5592	0.00061	4.49	4.52
Spring Top Column	72	240	1.66	2530	2942	0.00082	7.16	7.16
25 ft	72	300	1.66	4125	4977	0.00082	7.61	7.43
30 ft	72	360	1.66	3503	4332	0.00082	9.23	9.00
Pile Foundation	72	240	1.66	3753	5858	0.00082	8.65	8.80
Spread Foundation	72	240	1.66	5604	6128	0.00082	9.19	9.98
No bearing	72	240	1.66	4693	5385	0.00082	6.02	6.10
2X bearing	72	240	1.66	5081	6286	0.00082	6.02	5.95
4X bearing	72	240	1.66	5124	6905	0.00082	6.02	5.97
10X bearing	72	240	1.66	5197	7984	0.00082	6.02	5.98
Diameter–7 ft	84	240	1.66	7806	8837	0.00071	6.29	6.32
Diameter–8 ft	96	240	1.66	11334	12650	0.00062	6.54	6.61

(continued on next page)

Table 4.6. (Continued).

Original Design (column lateral confinement ratio=1.0%)								
	Diameter (in.)	Height (in.)	Long. rebar ratio ρ (%)	P_{p1} (kips)	P_u (kips)	φ_u (in^{-1})	δ_u of system (in.)	δ_1 for column (in.)
Base Case	72	240	1.66	5326	6643	0.00123	9.15	8.99
50% Phi	72	240	1.66	5326	5723	0.00061	4.49	4.39
75% Phi	72	240	1.66	5326	6210	0.00092	6.82	6.77
Spring Top Column	72	240	1.66	2669	3474	0.00123	10.71	10.72
25 ft	72	300	1.66	4353	5702	0.00123	11.51	11.66
30 ft	72	360	1.66	3697	5108	0.00123	13.93	13.94
Pile Foundation	72	240	1.66	3961	6603	0.00123	12.00	12.00
Spread Foundation	72	240	1.66	5912	6947	0.00123	12.60	13.72
No bearing	72	240	1.66	4956	5848	0.00123	9.09	9.10
2X bearing	72	240	1.66	5362	7277	0.00123	9.09	8.97
4X bearing	72	240	1.66	5407	8231	0.00123	9.09	8.98
10X bearing	72	240	1.66	5485	9933	0.00123	9.09	8.98

The validation of Equation 4.2 for the ultimate capacity of the system is verified in Figure 4.10, which plots P_u from Equation 4.2 versus the one obtained from the SAP2000 analysis. Figure 4.10 shows that the data points are almost aligned along the equal force line, indicating that Equation 4.2 is reasonably accurate with a regression coefficient $R^2 = 0.86$. The COV of the ratio between the value from Equation 4.2 and the SAP2000 is less than 10%. The maximum differences are those corresponding to soft foundations and for the cases where the bearing stiffness is extremely high.

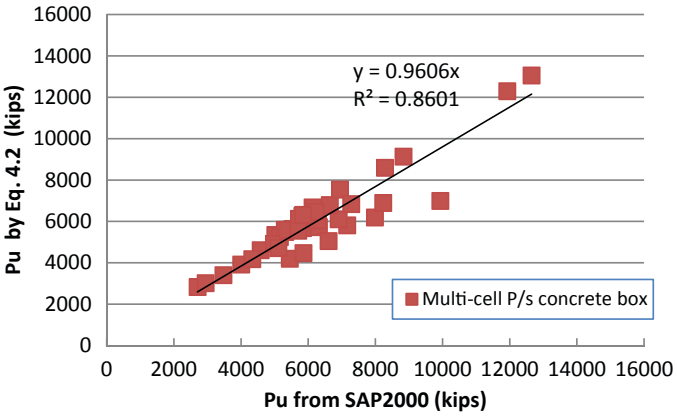

Figure 4.10. Lateral capacity by Equation 4.2 vs. lateral capacity from SAP2000 for multi-cell box bridges.

Three-Column Bents Supporting an I-Girder Bridge

Bridge Description

A combined 3-D space frame model is used to analyze the behavior of a combined superstructure-substructure multi-girder bridge system under lateral loads. Figure 4.11 gives the profile and elevation views of the frame element model used in this set of analyses. The bridge has three spans with a middle span that is 80-ft long and two end spans of 50-ft length each. Each bent is formed by three 27.58-ft columns connected by a cap beam. The six girders are connected to the cap beams through bearing supports. The analysis accounts for material nonlinearity of the columns, cap beams, and superstructure under the effect of lateral loads while a reduced level of traffic load is applied on the bridge.

Figure 4.12 illustrates the 3-D space frame model of the combined superstructure-substructure system. The longitudinal members labeled "A" represent the contribution of the composite I-girders to the longitudinal bending. The transverse elements labeled "B" model the bending of the slabs in the transverse direction. The vertical elements labeled "C" represent the columns. The elements labeled "D" represent the cap beams. The elements labeled E are link elements representing the connection between the superstructure and substructure provided by the bearings. The elements labeled F are rigid links used to connect the centers of the longi-

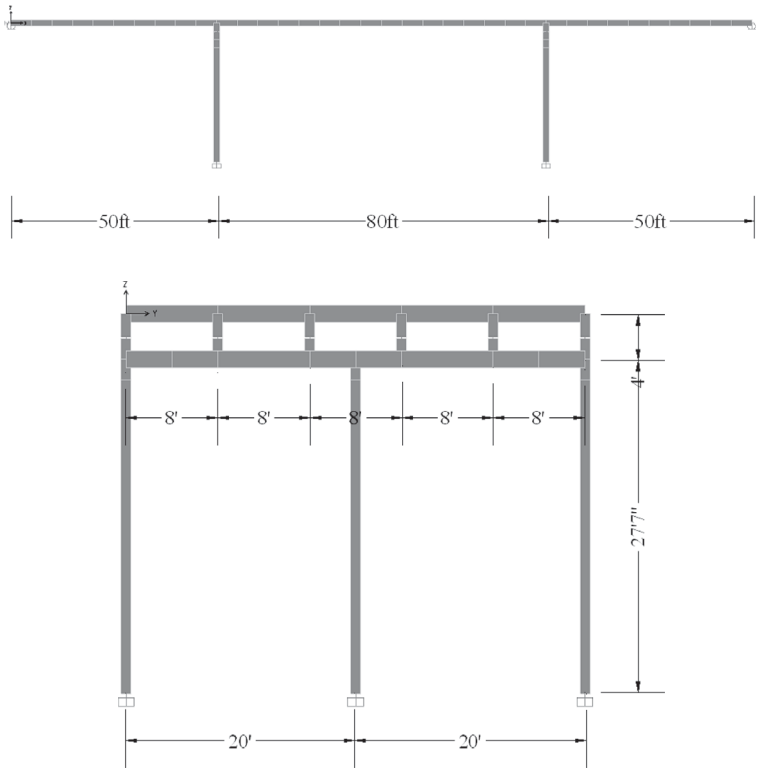

Figure 4.11. Profile and elevation view of the bridge.

tudinal girders to the center of the cap beams through the bearings.

Figure 4.13 shows cross sections of the column, cap beam, and girder. The 20 rebars in the column have 1.25-in. diameters. The 28 rebars in the cap beam have ⅝ in. (0.625-in.) diameters. The reinforcement is assumed to have a yielding stress F_y = 60 ksi. The girders are assumed to be Grade 36. The unconfined concrete strength is assumed to be 4 ksi. A confinement ratio of 2.4×10^{-3} is assumed in the columns.

Summary of Results

An extensive sensitivity analysis is performed to study how variations in the loading condition and the structure's

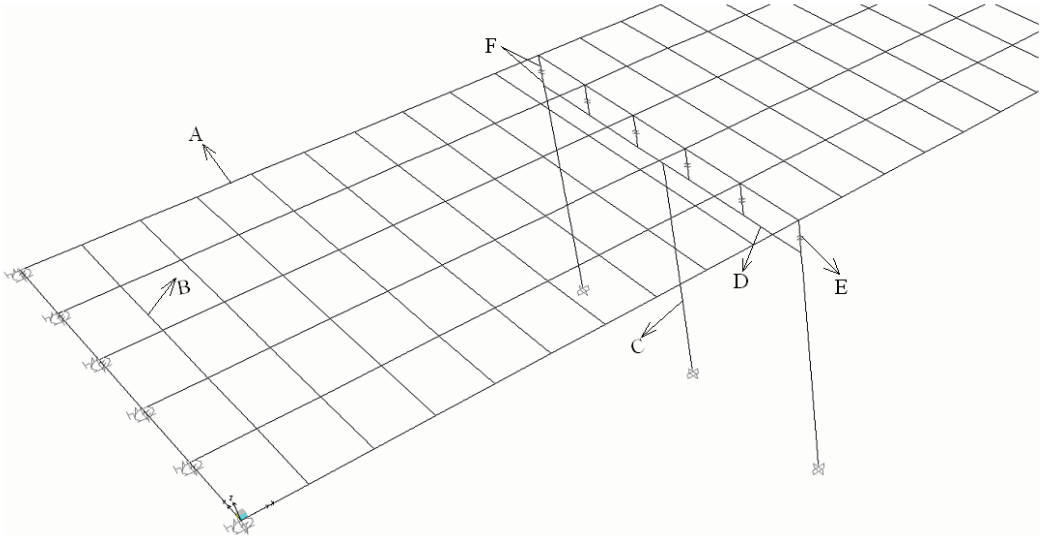

Figure 4.12. The 3-D space frame model of three-span I-girder bridge.

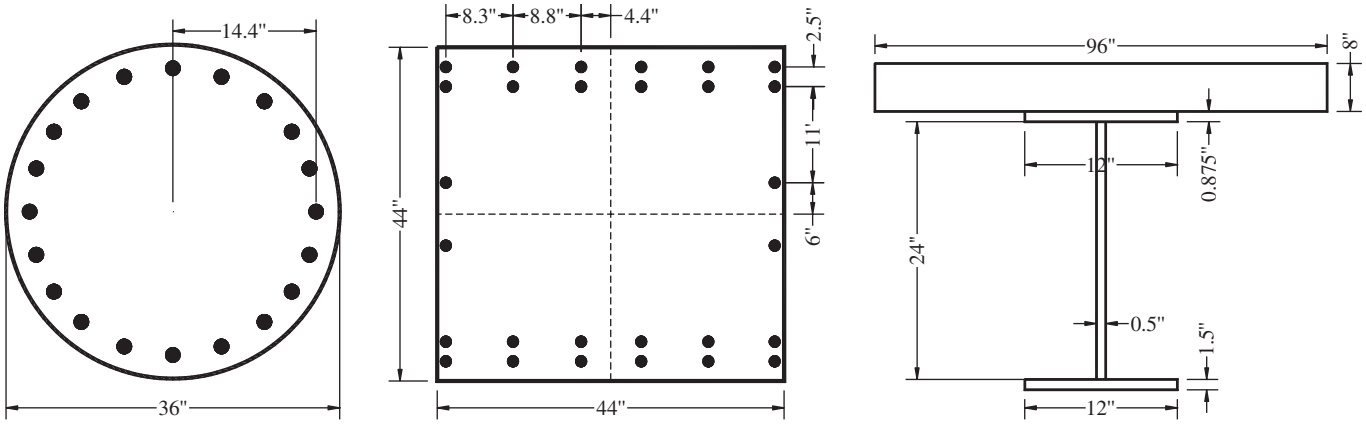

(a) Cross section of bridge columns (b) Cross section of cap beam (c) Cross section of I-girder

Figure 4.13. Cross sections of bridge members.

properties affect the response of the bridge system. Specifically, the sensitivity analysis performed in this section describes the effect of changes in the following parameters: (1) loading condition, (2) column height, (3) foundation flexibility, (4) concrete confinement, and (5) superstructure-substructure connection type. Numerical results of the nonlinear analyses are summarized in Table 4.7.

The analysis included 27.5-ft, 32.5-ft, and 37.5-ft columns designed with lateral confinement reinforcement ratios ρ_s = 0.24%, 0.3% (detail category B) and 0.5% (detail category C) in addition to cases where the maximum curvature is reduced by 50% and 75% to account for deficiencies in design. Different foundation stiffnesses are used to represent pile foundations and spread footing foundation as well as rigid and pinned foundations. The possibility of integral girder/cap-beam/column connections is compared to girder bearings on cap beam designs and to cases where the top of the column is pinned to the cap beam. Also, the analysis compares the behavior when a lateral load is applied to the case when the load is in the longitudinal direction. Table 4.7 gives the results for the ultimate load capacity and the ultimate displacements in comparison to the load at which the first column reaches its capacity, assuming linear analysis and the maximum displacement of one column.

The validation of Equation 4.2 for the ultimate capacity of the system is verified in Figure 4.14, which plots P_u from Equation 4.2 versus that obtained from the SAP2000 analysis.

Table 4.7. Results summary of three-column bent supporting an I-girder bridge.

Category B (column lateral confinement ratio=0.3%)								
	Diameter (in.)	Height (in.)	Long. rebar ratio ρ (%)	P_{p1} (kips)	P_u (kips)	φ_u (in^{-1})	δ_u of system (in.)	δ_1 for column (in.)
Base Case	36	331	2.41	765	1077	0.00106	8.0	8.3
32.5-ft	36	391	2.41	723	1070	0.00106	10.2	10.4
37.5-ft	36	451	2.41	709	1065	0.00106	12.0	12.7
Pile Foundation	36	331	2.41	788	1125	0.00106	9.0	8.6
Spread Foundation	36	331	2.41	798	1113	0.00106	8.7	8.7
Base Pinned	36	331	2.41	572	871	0.00106	11.4	11.0
Longitudinal Load	36	331	2.41	622	962	0.00106	13.5	8.3
Integral Top/Fixed Base	36	331	2.41	772	1080	0.00106	8.0	8.3
Integral Top/Pinned Base	36	331	2.41	567	839	0.00106	10.6	11.0
Integral Longitudinal	36	331	2.41	756	1131	0.00106	8.6	8.3
Column Top Pinned	36	331	2.41	582	870	0.00106	11.3	11.0
50% Phi	36	331	2.41	765	943	0.00053	5.3	5.1
75% Phi	36	331	2.41	765	1032	0.00079	7.0	6.8

Table 4.7. (Continued).

Category C (column lateral confinement ratio=0.5%)								
	Diameter (in.)	Height (in.)	Long. rebar ratio ρ (%)	P_{p1} (kips)	P_u (kips)	φ_u (in^{-1})	δ_u of system (in.)	δ_1 for column (in.)
Base Case	36	331	2.41	773	1212	0.00138	10.4	10.3
32.5-ft	36	391	2.41	730	1219	0.00138	13.1	12.9
37.5-ft	36	451	2.41	717	1246	0.00138	15.6	15.5
Pile Foundation	36	331	2.41	796	1232	0.00138	10.9	10.7
Spread Foundation	36	331	2.41	806	1226	0.00138	10.8	10.8
Base Pinned	36	331	2.41	578	970	0.00138	13.3	13.1
Longitudinal Load	36	331	2.41	628	1080	0.00138	15.7	10.3
Integral Top/Fixed Base	36	331	2.41	780	1214	0.00138	10.4	10.4
Integral Top/Pinned Base	36	331	2.41	573	966	0.00138	13.2	13.1
Integral Longitudinal	36	331	2.41	764	1237	0.00138	10.5	10.4
Column Top Pinned	36	331	2.41	588	967	0.00138	13.2	13.1
50% Phi	36	331	2.41	773	989	0.00069	6.3	6.1
75% Phi	36	331	2.41	773	1107	0.00104	8.5	8.2
Original Design (column lateral confinement ratio=0.24%)								
	Diameter (in.)	Height (in.)	Long. rebar ratio ρ (%)	P_{p1} (kips)	P_u (kips)	φ_u (in^{-1})	δ_u of system (in.)	δ_1 for column (in.)
Base Case	36	331	2.41	761	1060	0.00096	7.5	7.8
32.5-ft	36	391	2.41	719	1044	0.00096	9.6	9.8
37.5-ft	36	451	2.41	706	1047	0.00096	11.5	11.9
Pile Foundation	36	331	2.41	784	1095	0.00096	8.3	8.1
Spread Foundation	36	331	2.41	794	1071	0.00096	7.7	8.1
Base Pinned	36	331	2.41	569	839	0.00096	10.6	10.5
Longitudinal Load	36	331	2.41	619	922	0.00096	12.6	7.8
Integral Top/Fixed Base	36	331	2.41	768	1063	0.00096	7.5	7.8
Integral Top/Pinned Base	36	331	2.41	564	834	0.00096	10.4	10.4
Integral Longitudinal	36	331	2.41	752	1096	0.00096	7.8	7.8
Column Top Pinned	36	331	2.41	579	831	0.00096	10.4	10.4
50% Phi	36	331	2.41	761	929	0.00048	5.0	5.1
75% Phi	36	331	2.41	761	1011	0.00072	6.4	6.4
Category B (column lateral confinement ratio=0.3%) **New data using M-phi curve from multi-girder bridge in Category B, Category B below is different from the above one**								
Category B	Diameter (in.)	Height (in.)	Long. rebar ratio ρ (%)	P_{p1} (kips)	P_u (kips)	φ_u (in^{-1})		
Diameter–20 ft	72	240	1.66	3512.1	3767	0.000717		
Diameter–32.5 ft	72	391	1.66	2359.9	2676.3	0.000717		
Diameter–37.5 ft	72	451	1.66	2252.8	2480.7	0.000717		
Diameter–7 ft	84	391	1.66	5365.9	5865.9	0.000574		
Diameter–7 ft	84	240	1.66	8079.5	9116.3	0.000574		
Diameter–8 ft	96	391	1.66	7733.2	8541.4	0.000516		
Diameter–8 ft	96	240	1.66	11603.3	13508.8	0.000516		
Pile Foundation	96	240	1.66	8870.5	11528.4	0.000516		
Spread Foundation	96	240	1.66	11881.2	13016.1	0.000516		

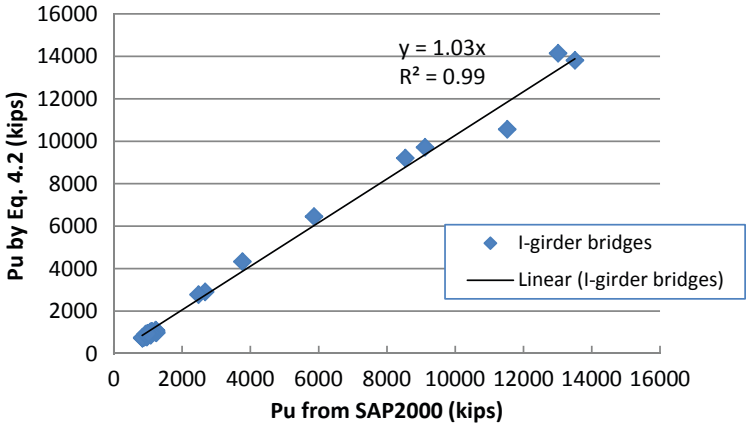

Figure 4.14. Lateral capacity by Equation 4.2 vs. lateral capacity from SAP2000 for I-girder bridges.

Figure 4.14 shows that the data points are clearly aligned along the equal force line indicating that Equation 4.2 is reasonably accurate with a regression coefficient $R^2 = 0.99$. The COV of the ratio between the value from Equation 4.2 and the SAP2000 is less than 9%. The maximum differences are those corresponding to a soft foundation.

Two-Column and Four-Column Bents in *NCHRP Report 458*

Bridge Description

NCHRP Report 458 also analyzed many bridge bents subjected to lateral load, and analyzed individual bents rather than entire bridge systems. However, an overview of the results of analyses performed in this study has shown that the results from single bents are very similar to those of entire bridge systems. Accordingly, the results from *NCHRP Report 458* can be used to supplement the database assembled in this study.

In *NCHRP Report 458*, the gravity loads applied on the substructure include both the dead load and the entire AASHTO HL-93 vehicular live load. The analysis process incremented the lateral load until system failure occurred. In the *NCHRP Report 458* analyses it was assumed that the vertical loads (dead load and vehicular live load) are set at their maximum design values. This approach is conservative as it is generally unlikely that the vehicular live load will be at its expected maximum value when the maximum lateral (wind, seismic, etc.) load is applied on the structure. The pier configurations used in the *NCHRP Report 458* analysis are illustrated in Figures 4.15 and 4.16 for the two-column and four-column bents, respectively.

The material properties (concrete strength, yielding stress of steel) and geometric properties (section size and amount and location of reinforcement) combine to produce the moment curvature and the capacity of the column section. For

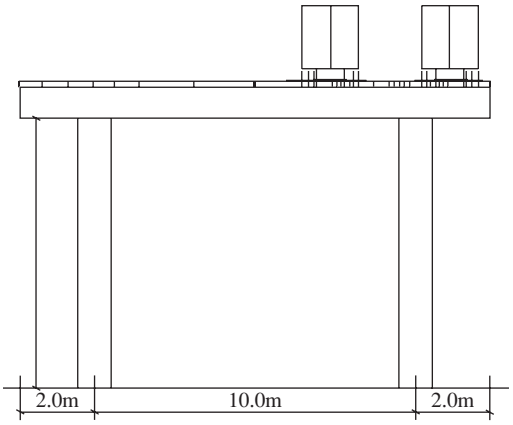

***Figure 4.15. Configuration of two-column bent in* NCHRP Report 458.**

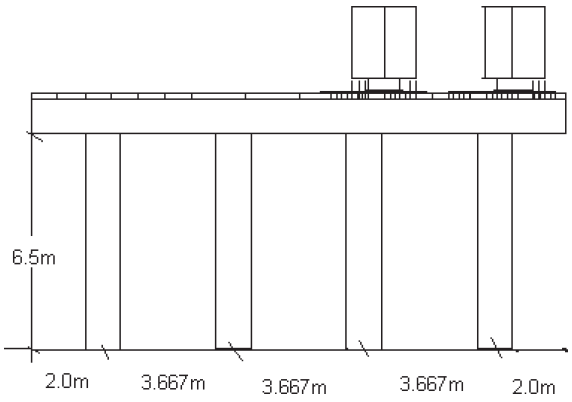

***Figure 4.16. Configuration of four-column bent in* NCHRP Report 458.**

Table 4.8. Parameters for two-column bent.

Variation #	Variation	Low	Average	High
1	Height [m]	4	11	18
2	Width [m]	0.8	1.2	1.6
3	Concrete Strength [MN/m^2]	22	27	32
4	Steel Strength [MN/m^2]	400	450	500
5	ρ_{long} [%]	1.10	2.30	3.50
6	ρ_{trans} [%]	0.18	0.32	0.45

Table 4.9. Parameters for four-column bent.

Variation #	Variation	Low	Average	High
1	Height [m]	3.5	6.5	9.5
2	Width [m]	0.5	1.0	1.5
3	Concrete Strength [MN/m^2]	22	27	32
4	Steel Strength [MN/m^2]	400	450	500
5	ρ_{long} [%]	0.60	1.85	3.10
6	ρ_{trans} [%]	0.18	0.32	0.45

the two-column bent and four-column bent cases, material parameters and column details are summarized in Tables 4.8 and 4.9, respectively. Two limiting values for the strain that produce concrete crushing are given in *NCHRP Report 458*. The first value assumes that the columns are unconfined and the corresponding concrete crushing strain is $\varepsilon_u = 0.004$. The second value is for the confined columns, which are assumed to crush when the concrete strain reaches the value $\varepsilon_c = 0.015$. *NCHRP Report 458* used an in-house program to perform the nonlinear pushover analysis. The model used for the analysis accounts for the P-delta effect produced when large values of lateral displacement interact with gravity loads to increase the moments in the columns.

Foundation stiffness coefficients for the eight categories are summarized in Table 4.10 for the two-column bents and in Table 4.11 for four-column bents. These foundation stiffness coefficients are obtained using the standard procedure developed in a FHWA funded study (Lam and Martin, 1986). Also, different column heights and column dimensions are assumed as listed in the second and third columns of Table 4.12. The longitudinal reinforcement ratio for each column configuration is provided in the fourth column of Table 4.12.

Summary of Results

The numerical results for all the two-column and four-column bents analyzed in *NCHRP Report 458* are summarized in Tables 4.12 and Table 4.13, respectively. For each

Table 4.10. Two-column bent, foundation stiffness.

a. Two-Column Bent—Average Column Width

	$K_{vertical}$ (kN/m)	$K_{transverse}$ (kN/m)	$K_{rotation}$ (kNm)
1 spread\normal\	97200	72900	3650000
2 spread\stiff\	147000	110000	5530000
3 extension\soft\	443077	5226	113726
4 extension\normal\	1107000	17784	220882
5 extension\stiff\	1994000	46628	367348
6 pile\soft\	675400	18870	376700
7 pile\normal\	1689000	85870	941700
8 pile\stiff\	3039000	299000	1695000

b. Two-Column Bent—Low Column Width

	$K_{vertical}$ (kN/m)	$K_{transverse}$ (kN/m)	$K_{rotation}$ (kNm)
1 spread\normal\	61500	46100	999000
2 spread\stiff\	93100	69800	1510000
3 extension\soft\	295358	2283	34614
4 extension\normal\	738462	7474	65038
5 extension\stiff\	1329231	19067	105915
6 pile\soft\	450300	12580	94170
7 pile\normal\	1126000	57240	235400
8 pile\stiff\	2026000	199300	423800

c. Two-Column Bent—High Column Width

	$K_{vertical}$ (kN/m)	$K_{transverse}$ (kN/m)	$K_{rotation}$ (kNm)
1 spread\normal\	120000	89900	7120000
2 spread\stiff\	182000	136000	10800000
3 extension\soft\	590769	9259	260623
4 extension\normal\	1476923	32421	519329
5 extension\stiff\	2658462	86849	879287
6 pile\soft\	1351000	37730	1413000
7 pile\normal\	3377000	171700	3531000
8 pile\stiff\	6079000	598000	6357000

Table 4.11. Four-column bent, foundation stiffness.

a. Four-Column Bent—Average Column Width

	$K_{vertical}$ (kN/m)	$K_{transverse}$ (kN/m)	$K_{rotation}$ (kNm)
1 spread\normal\	77800	58300	1870000
2 spread\stiff\	118000	88300	2830000
3 extension\soft\	369000	8030	54195
4 extension\normal\	923100	36500	109932
5 extension\stiff\	1661000	127200	188483
6 pile\soft\	450000	12580	94170
7 pile\normal\	1126000	57200	235000
8 pile\stiff\	2026000	199000	424000

b. Four-Column Bent—Low Column Width

	$K_{vertical}$ (kN/m)	$K_{transverse}$ (kN/m)	$K_{rotation}$ (kNm)
1 spread\normal\	38900	29200	234000
2 spread\stiff\	58900	44200	354000
3 extension\soft\	184615	2647	7339
4 extension\normal\	461500	12050	14000
5 extension\stiff\	830700	42000	23000
6 pile\soft\	450300	12580	94170
7 pile\normal\	1126000	57240	235400
8 pile\stiff\	2026000	199300	423800

c. Four-Column Bent—High Column Width

	$K_{vertical}$ (kN/m)	$K_{transverse}$ (kN/m)	$K_{rotation}$ (kNm)
1 spread\normal\	117000	87500	6310000
2 spread\stiff\	177000	133000	9560000
3 extension\soft\	553900	15350	168600
4 extension\normal\	1380000	69900	356000
5 extension\stiff\	2490000	243300	628600
6 pile\soft\	1013000	28300	565000
7 pile\normal\	2533000	128800	1413000
8 pile\stiff\	4560000	448500	2543000

Table 4.12. Results summary of two-column bent in *NCHRP Report 458.*

(Column lateral confinement ratio=0.6%) Confined core concrete ultimate strain is 0.015								
				First Member	**Unconfined**	**Confined**	**Unconfined**	**Confined**
Foundation Type	b×d (in.)	Height (in.)	Long. rebar ratio (%)	P_{p1} (kips)	P_u (kips)	P_u (kips)	φ_u (in^{-1})	φ_u (in^{-1})
Spread_Normal	47.2 ×47.2	433	2.3	2481	2821	2973	3.01E-04	1.217E-03
Spread_Stiff	47.2 ×47.2	433	2.3	2479	2857	2986	3.01E-04	1.217E-03
Extension_Soft	47.2 ×47.2	433	2.3	1606	1754	1893	3.01E-04	1.217E-03
Extension_Normal	47.2 ×47.2	433	2.3	1692	1956	2298	3.01E-04	1.217E-03
Extension_Stiff	47.2 ×47.2	433	2.3	1825	2181	2727	3.01E-04	1.217E-03
Piles_Soft	47.2 ×47.2	433	2.3	1902	2228	2772	3.01E-04	1.217E-03
Piles_Normal	47.2 ×47.2	433	2.3	2215	2728	2987	3.01E-04	1.217E-03
Piles_Stiff	47.2 ×47.2	433	2.3	2427	2967	3011	3.01E-04	1.217E-03
Spread_Normal	47.2 ×47.2	157.5	2.3	5072	5877	7595	3.01E-04	1.217E-03
Spread_Stiff	47.2 ×47.2	157.5	2.3	5258	6237	7960	3.01E-04	1.217E-03
Extension_Soft	47.2 ×47.2	157.5	2.3	4667	4745	4966	3.01E-04	1.217E-03
Extension_Normal	47.2 ×47.2	157.5	2.3	4714	4924	5448	3.01E-04	1.217E-03
Extension_Stiff	47.2 ×47.2	157.5	2.3	4834	5186	6077	3.01E-04	1.217E-03
Piles_Soft	47.2 ×47.2	157.5	2.3	5142	5451	6270	3.01E-04	1.217E-03
Piles_Normal	47.2 ×47.2	157.5	2.3	5883	6510	8160	3.01E-04	1.217E-03
Piles_Stiff	47.2 ×47.2	157.5	2.3	6673	7505	8382	3.01E-04	1.217E-03
Spread_Normal	47.2 ×47.2	708.7	2.3	1557	1739	1758	3.01E-04	1.217E-03
Spread_Stiff	47.2 ×47.2	708.7	2.3	1573	1761	1771	3.01E-04	1.217E-03
Extension_Soft	47.2 ×47.2	708.7	2.3	956	1062	1110	3.01E-04	1.217E-03
Extension_Normal	47.2 ×47.2	708.7	2.3	1071	1248	1446	3.01E-04	1.217E-03
Extension_Stiff	47.2 ×47.2	708.7	2.3	1187	1424	1641	3.01E-04	1.217E-03
Piles_Soft	47.2 ×47.2	708.7	2.3	1210	1439	1647	3.01E-04	1.217E-03
Piles_Normal	47.2 ×47.2	708.7	2.3	1423	1752	1768	3.01E-04	1.217E-03
Piles_Stiff	47.2 ×47.2	708.7	2.3	1528	1796	1796	3.01E-04	1.217E-03
Spread_Normal	31.5 ×31.5	433	2.3	753	849	849	3.50E-04	1.543E-03
Spread_Stiff	31.5 ×31.5	433	2.3	747	856	856	3.50E-04	1.543E-03
Extension_Soft	31.5 ×31.5	433	2.3	447	486	481	3.50E-04	1.543E-03
Extension_Normal	31.5 ×31.5	433	2.3	480	560	638	3.50E-04	1.543E-03
Extension_Stiff	31.5 ×31.5	433	2.3	516	630	746	3.50E-04	1.543E-03
Piles_Soft	31.5 ×31.5	433	2.3	511	614	728	3.50E-04	1.543E-03
Piles_Normal	31.5 ×31.5	433	2.3	593	755	824	3.50E-04	1.543E-03

Table 4.12. (Continued).

(Column lateral confinement ratio=0.6%) Confined core concrete ultimate strain is 0.015								
				First Member	Unconfined	Confined	Unconfined	Confined
Foundation Type	b×d (in.)	Height (in.)	Long. rebar ratio (%)	P_{p1} (kips)	P_u (kips)	P_u (kips)	φ_u (in^{-1})	φ_u (in^{-1})
Piles_Stiff	31.5 ×31.5	433	2.3	638	835	852	3.50E-04	1.543E-03
Spread_Normal	63 ×63	433	2.3	4984	5649	7085	2.55E-04	1.013E-03
Spread_Stiff	63 ×63	433	2.3	5135	5826	7116	2.55E-04	1.013E-03
Extension_Soft	63 ×63	433	2.3	4099	4358	4849	2.55E-04	1.013E-03
Extension_Normal	63 ×63	433	2.3	4516	4963	6074	2.55E-04	1.013E-03
Extension_Stiff	63 ×63	433	2.3	5084	5700	7030	2.55E-04	1.013E-03
Piles_Soft	63 ×63	433	2.3	5948	6697	7136	2.55E-04	1.013E-03
Piles_Normal	63 ×63	433	2.3	6279	7020	7176	2.55E-04	1.013E-03
Piles_Stiff	63 ×63	433	2.3	6007	6874	7175	2.55E-04	1.013E-03
Spread_Normal	47.2 ×47.2	433	1.1	1519	1821	1851	3.56E-04	1.585E-03
Spread_Stiff	47.2 ×47.2	433	1.1	1510	1852	1860	3.56E-04	1.585E-03
Extension_Soft	47.2 ×47.2	433	1.1	963	1127	1267	3.56E-04	1.585E-03
Extension_Normal	47.2 ×47.2	433	1.1	966	1293	1625	3.56E-04	1.585E-03
Extension_Stiff	47.2 ×47.2	433	1.1	1018	1469	1789	3.56E-04	1.585E-03
Piles_Soft	47.2 ×47.2	433	1.1	1087	1497	1791	3.56E-04	1.585E-03
Piles_Normal	47.2 ×47.2	433	1.1	1226	1849	1868	3.56E-04	1.585E-03
Piles_Stiff	47.2 ×47.2	433	1.1	1324	1877	1877	3.56E-04	1.585E-03
Spread_Normal	47.2 ×47.2	433	3.5	3420	3756	4075	2.66E-04	1.107E-03
Spread_Stiff	47.2 ×47.2	433	3.5	3422	3823	4092	2.66E-04	1.107E-03
Extension_Soft	47.2 ×47.2	433	3.5	2223	2339	2507	2.66E-04	1.107E-03
Extension_Normal	47.2 ×47.2	433	3.5	2389	2604	2964	2.66E-04	1.107E-03
Extension_Stiff	47.2 ×47.2	433	3.5	2604	2889	3448	2.66E-04	1.107E-03
Piles_Soft	47.2 ×47.2	433	3.5	2678	2944	3496	2.66E-04	1.107E-03
Piles_Normal	47.2 ×47.2	433	3.5	3176	3591	4088	2.66E-04	1.107E-03
Piles_Stiff	47.2 ×47.2	433	3.5	3481	3990	4124	2.66E-04	1.107E-03

bent, the results show the ultimate capacity P_u assuming that the columns are confined and also assuming that the columns are unconfined. These results are compared to those obtained when the first column reaches its limiting capacity, assuming linear behavior.

The validity of Equation 4.2 for the ultimate capacity of the unconfined and confined two-column bent systems analyzed in *NCHRP Report 458* is verified in Figure 4.17 (a) and Figure 4.17 (b), respectively. The figures plot P_u from Equation 4.2 versus that obtained from the *NCHRP Report 458* analysis and show that the data points are clearly aligned along the equal force line, indicating that Equation 4.2 is reasonably accurate with a regression coefficient $R^2 = 0.99$ and $R^2 = 0.97$ for the unconfined and confined two-column bents. The COV of

Table 4.13. Results summary of four-column bent in *NCHRP Report 458.*

(Column lateral confinement ratio=0.6%) Confined core concrete ultimate strain is 0.015								
				First Member	**Unconfined**	**Confined**	**Unconfined**	**Confined**
Foundation Type	b×d (in.)	Height (in.)	Long. rebar ratio (%)	P_{p1} (kips)	P_u (kips)	P_u (kips)	φ_u (in^{-1})	φ_u (in^{-1})
Spread_Normal	39.4 ×39.4	255.9	1.85	3787	4651	4857	3.68E-04	1.494E-03
Spread_Stiff	39.4 ×39.4	255.9	1.85	3923	4707	4876	3.68E-04	1.494E-03
Extension_Soft	39.4 ×39.4	255.9	1.85	2468	2692	3011	3.68E-04	1.494E-03
Extension_Normal	39.4 ×39.4	255.9	1.85	2570	3016	3622	3.68E-04	1.494E-03
Extension_Stiff	39.4 ×39.4	255.9	1.85	2749	3377	4346	3.68E-04	1.494E-03
Piles_Soft	39.4 ×39.4	255.9	1.85	2581	2915	3466	3.68E-04	1.494E-03
Piles_Normal	39.4 ×39.4	255.9	1.85	2884	3550	4679	3.68E-04	1.494E-03
Piles_Stiff	39.4 ×39.4	255.9	1.85	3175	4080	4848	3.68E-04	1.494E-03
Spread_Normal	39.4 ×39.4	137.8	1.85	6388	7520	8841	3.68E-04	1.494E-03
Spread_Stiff	39.4 ×39.4	137.8	1.85	6587	7992	8984	3.68E-04	1.494E-03
Extension_Soft	39.4 ×39.4	137.8	1.85	4494	4731	5210	3.68E-04	1.494E-03
Extension_Normal	39.4 ×39.4	137.8	1.85	4695	5079	5949	3.68E-04	1.494E-03
Extension_Stiff	39.4 ×39.4	137.8	1.85	4775	5457	6802	3.68E-04	1.494E-03
Piles_Soft	39.4 ×39.4	137.8	1.85	4747	5040	5757	3.68E-04	1.494E-03
Piles_Normal	39.4 ×39.4	137.8	1.85	5102	5744	7306	3.68E-04	1.494E-03
Piles_Stiff	39.4 ×39.4	137.8	1.85	5323	6442	8808	3.68E-04	1.494E-03
Spread_Normal	39.4 ×39.4	708.7	1.85	2697	3224	3290	3.68E-04	1.494E-03
Spread_Stiff	39.4 ×39.4	708.7	1.85	2773	3262	3308	3.68E-04	1.494E-03
Extension_Soft	39.4 ×39.4	708.7	1.85	1687	1918	2109	3.68E-04	1.494E-03
Extension_Normal	39.4 ×39.4	708.7	1.85	1825	2180	2664	3.68E-04	1.494E-03
Extension_Stiff	39.4 ×39.4	708.7	1.85	2006	2470	3145	3.68E-04	1.494E-03
Piles_Soft	39.4 ×39.4	708.7	1.85	1798	2116	2523	3.68E-04	1.494E-03
Piles_Normal	39.4 ×39.4	708.7	1.85	2088	2616	3197	3.68E-04	1.494E-03
Piles_Stiff	39.4 ×39.4	708.7	1.85	2349	3018	3280	3.68E-04	1.494E-03
Spread_Normal	19.7 ×19.7	255.9	1.85	500	581	581	3.96E-04	1.692E-03
Spread_Stiff	19.7 ×19.7	255.9	1.85	514	586	586	3.96E-04	1.692E-03
Extension_Soft	19.7 ×19.7	255.9	1.85	292	318	295	3.96E-04	1.692E-03
Extension_Normal	19.7 ×19.7	255.9	1.85	326	366	403	3.96E-04	1.692E-03
Extension_Stiff	19.7 ×19.7	255.9	1.85	360	414	481	3.96E-04	1.692E-03
Piles_Soft	19.7 ×19.7	255.9	1.85	468	567	573	3.96E-04	1.692E-03
Piles_Normal	19.7 ×19.7	255.9	1.85	514	592	592	3.96E-04	1.692E-03

Table 4.13. (Continued).

(Column lateral confinement ratio=0.6%) Confined core concrete ultimate strain is 0.015								
				First Member	Unconfined	Confined	Unconfined	Confined
Foundation Type	b×d (in.)	Height (in.)	Long. rebar ratio (%)	P_{p1} (kips)	P_u (kips)	P_u (kips)	φ_u (in^{-1})	φ_u (in^{-1})
Piles_Stiff	19.7 ×19.7	255.9	1.85	535	597	597	3.96E-04	1.692E-03
Spread_Normal	59 ×59	255.9	1.85	10340	12261	15674	2.86E-04	1.211E-03
Spread_Stiff	59 ×59	255.9	1.85	10710	13034	15850	2.86E-04	1.211E-03
Extension_Soft	59 ×59	255.9	1.85	8166	8735	10110	2.86E-04	1.211E-03
Extension_Normal	59 ×59	255.9	1.85	8307	9452	12110	2.86E-04	1.211E-03
Extension_Stiff	59 ×59	255.9	1.85	8813	10505	14496	2.86E-04	1.211E-03
Piles_Soft	59 ×59	255.9	1.85	9402	10662	14219	2.86E-04	1.211E-03
Piles_Normal	59 ×59	255.9	1.85	10793	13248	16508	2.86E-04	1.211E-03
Piles_Stiff	59 ×59	255.9	1.85	12242	15286	16541	2.86E-04	1.211E-03
Spread_Normal	39.4 ×39.4	255.9	0.60	1739	2484	2529	4.46E-04	1.981E-03
Spread_Stiff	39.4 ×39.4	255.9	0.60	1795	2541	2542	4.46E-04	1.981E-03
Extension_Soft	39.4 ×39.4	255.9	0.60	1189	1527	1846	4.46E-04	1.981E-03
Extension_Normal	39.4 ×39.4	255.9	0.60	1305	1797	2347	4.46E-04	1.981E-03
Extension_Stiff	39.4 ×39.4	255.9	0.60	1417	2118	2463	4.46E-04	1.981E-03
Piles_Soft	39.4 ×39.4	255.9	0.60	1277	1727	2285	4.46E-04	1.981E-03
Piles_Normal	39.4 ×39.4	255.9	0.60	1476	2280	2488	4.46E-04	1.981E-03
Piles_Stiff	39.4 ×39.4	255.9	0.60	1628	2527	2536	4.46E-04	1.981E-03
Spread_Normal	39.4 ×39.4	255.9	3.10	5791	6595	7107	3.19E-04	1.344E-03
Spread_Stiff	39.4 ×39.4	255.9	3.10	5988	6749	7131	3.19E-04	1.344E-03
Extension_Soft	39.4 ×39.4	255.9	3.10	3652	3864	4190	3.19E-04	1.344E-03
Extension_Normal	39.4 ×39.4	255.9	3.10	3792	4206	4827	3.19E-04	1.344E-03
Extension_Stiff	39.4 ×39.4	255.9	3.10	4023	4600	5575	3.19E-04	1.344E-03
Piles_Soft	39.4 ×39.4	255.9	3.10	3809	4126	4667	3.19E-04	1.344E-03
Piles_Normal	39.4 ×39.4	255.9	3.10	4241	4837	5980	3.19E-04	1.344E-03
Piles_Stiff	39.4 ×39.4	255.9	3.10	4650	5459	7042	3.19E-04	1.344E-03

the ratio between the value from Equation 4.2 and *NCHRP Report 458* is less than 7% and 11% for the unconfined and confined two-column bents, respectively. The maximum differences are those corresponding to a soft foundation.

Figure 4.18 (a) and (b) plot P_u from Equation 4.2 versus that obtained from the *NCHRP Report 458* analysis for the unconfined and confined four-column bent systems, respectively. The figures show that the data points are clearly aligned along the equal force line indicating that Equation 4.2 is reasonably accurate with a regression coefficient $R^2 = 0.99$ and $R^2 = 0.97$ for the unconfined and confined four-column systems. The COV of the ratio between the value from Equation 4.2 and *NCHRP Report 458* is less than 8% and 14% for the unconfined and confined four-column system, respectively. The maximum differences are those corresponding to a soft foundation.

The larger differences and wider spread of data points around the equal force line observed in Figures 4.17 and 4.18 for the confined cases are due to the larger P-delta effects in *NCHRP Report 458* related to the high applied vertical live load. When the columns are highly confined and the vertical load is very high, the P-delta effects produce a softening in the

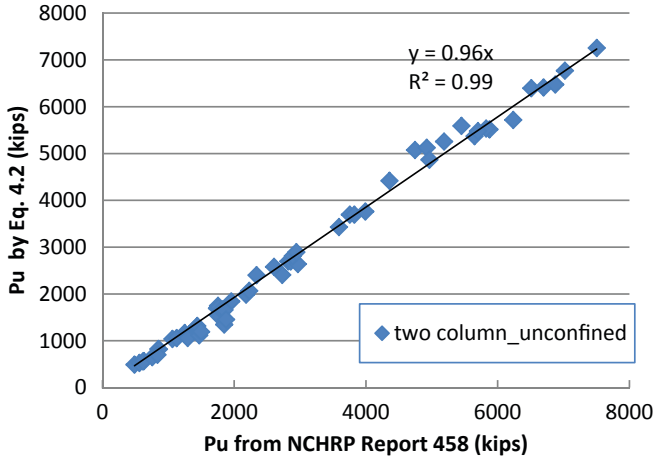

(a) Unconfined

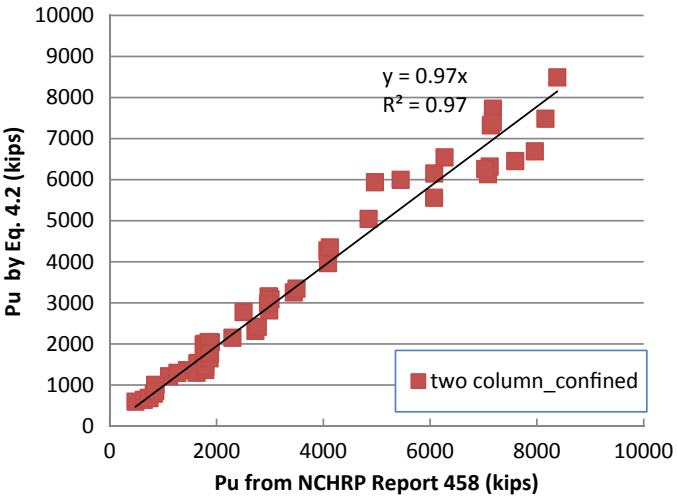

(b) Confined

Figure 4.17. Lateral capacity by Equation 4.2 vs. lateral capacity from* NCHRP Report 458 *for two-column bents.

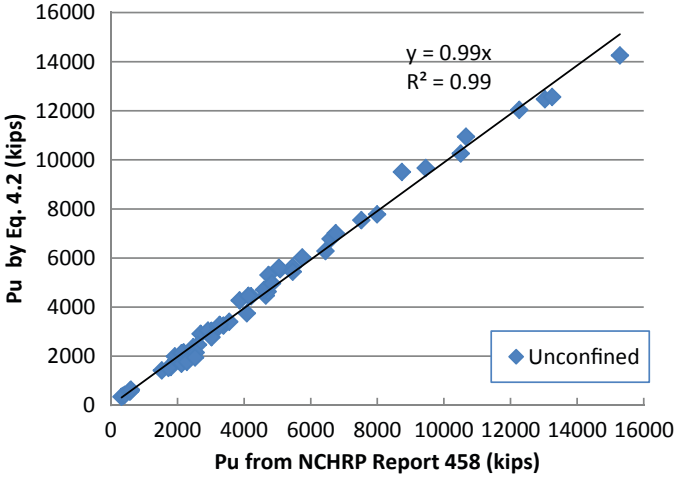

(a) Unconfined

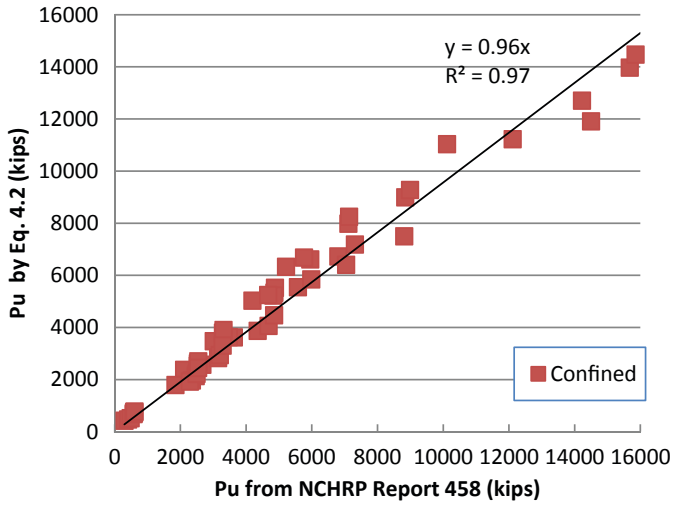

(b) Confined

Figure 4.18. Lateral capacity by Equation 4.2 vs. lateral capacity from* NCHRP Report 458 *for four-column bents.

force versus lateral deformation curve. This has caused some difficulty in defining the exact failure point in the *NCHRP Report 458* model.

Model Verification

The empirical model proposed in this study to establish the relationship between the ultimate capacity of a multi-column bridge substructure system and the lateral load carrying capacity of one column in the system is a function of the number of columns in the bent and the ultimate curvature capacity of the bent columns. This relationship is expressed by an equation of the form:

$$P_u = P_{p1}\left[F_{mc} + C_\varphi \frac{\varphi_u - \varphi_{tunc}}{\varphi_{tconf} - \varphi_{tunc}}\right] \quad (4.2)$$

where P_{p1} gives the capacity of a bridge system under lateral load assuming that the analysis is performed using linear-elastic behavior and failure is defined when one column reaches its maximum load carrying capacity as typically done when using a force-based analysis, F_{mc} is a multi-column factor, C_φ is a curvature factor, φ_u is the ultimate curvature of the weakest column in the bent, φ_{tunc} is the average curvature for a typical unconfined column, φ_{tconf} is the average curvature for a typical confined column. The typical curvature values for the confined and unconfined columns are extracted from the results of the survey conducted in *NCHRP Report 458*.

For a particular bridge system, P_{p1} is calculated using a linear structural analysis of the system under the effect of the applied lateral load. To find P_{p1}, failure is defined as the load at which one column reaches its ultimate capacity. The value for the ultimate curvature at failure φ_u is

calculated from the ultimate plastic analysis of the column's cross section.

Values for F_{mc}, C_{φ}, φ_{tunc}, and φ_{tconf} have been extracted from the analysis of a large number of bridges with two-column, three-column and four-column bents. The bents analyzed included a range of column sizes, vertical reinforcement ratios, and confinement ratios. The analyses also considered the effect of different foundation stiffnesses. The recommended values for these parameters are provided in Table 4.1, shown previously. The values for φ_{tunc} and φ_{tconf} are the average curvatures obtained from the analysis of the column sizes used in *NCHRP Report 458*. The columns analyzed in *NCHRP Report 458* represent typical column sizes and reinforcement ratios collected from a national survey conducted as part of the study. The values for φ_{tunc} and φ_{tconf} are used in Equation 4.2 to compare the confinement ratio of the column being evaluated to the average confinement ratios observed in typical confined and unconfined columns.

Figures 4.19, 4.20, and 4.21 summarize the results presented in the previous section. These figures are provided to visualize how well the proposed model of Equation 4.2 matches the results obtained from the nonlinear pushover analysis of hundreds of bridge systems subjected to lateral load applied at the top of the bent. The plots show the values of the system capacity P_u obtained from Equation 4.2 versus the values obtained from the pushover analysis.

Figure 4.19 is for systems with two-column bents analyzed during the course of this study in green as well as those analyzed during *NCHRP Report 458* in blue for unconfined columns and in red for confined columns. Different levels of confinement ratios were considered during the analyses performed in *NCHRP Report 458*. The green data points labeled NCHRP 12-86 were obtained during the course of this study using a large range of sensitivity analyses. The green data points also represent a combination of different confinement ratios. The solid lines give the trend lines obtained from a regression analysis of the data. The equations in the figure give the equations of the trend lines that describe the relationship between the estimated P_u obtained from Equation 4.2 and the calculated P_u obtained from the nonlinear pushover analysis of actual bridge systems. A perfect match would lead to a trend line having an equation of the form $y = 1.0x$ with a coefficient of regression $R^2 = 1.0$. The results in Figure 4.20 are for the bridge systems with three-column bents analyzed in this study including all the sensitivity analyses. Figure 4.21 shows the results of the four-column bents analyzed in *NCHRP Report 458* including those with confined columns (in red) and unconfined columns (in blue). All the trend lines in Figures 4.19, 4.20, and 4.21 have slopes close to 1.0 and coefficients of regression R^2 also close to 1.0. This serves to confirm that Equation 4.2 provides a good model for estimating the ultimate capacity of bridge systems

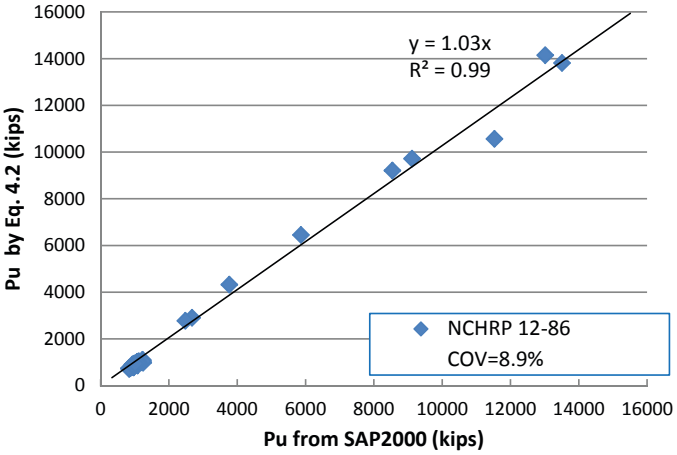

Figure 4.20. Three-column model verification.

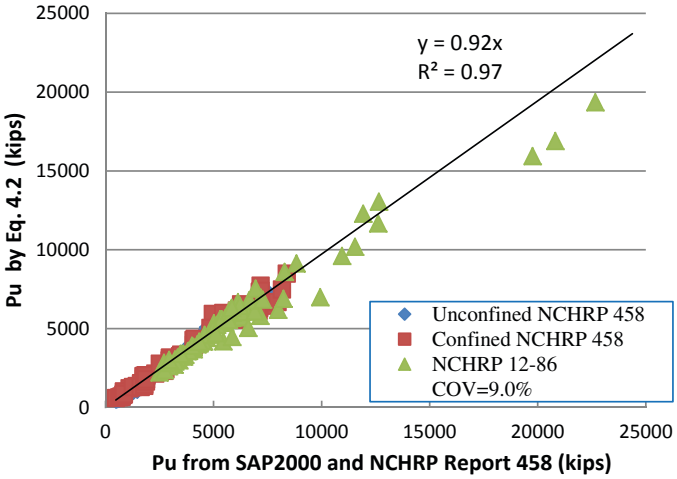

Figure 4.19. Two-column model verification.

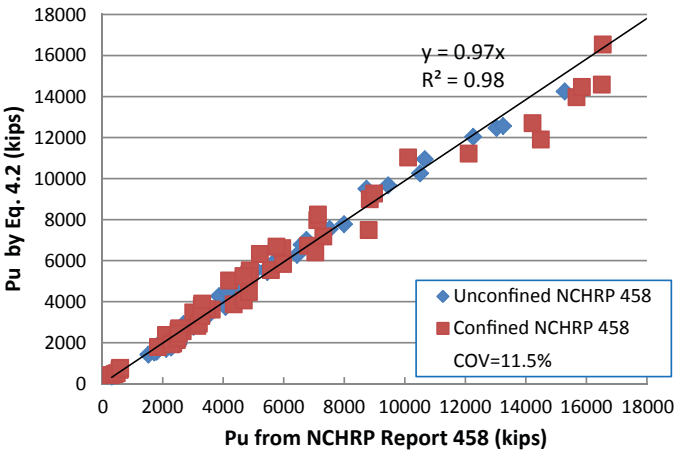

Figure 4.21. Four-column model verification.

subjected to lateral load. Another parameter that identifies the variation between Equation 4.2 and the analysis results is the COV of the ratio between the equation and the analysis results. It is observed that the COV is about 9% for the two- and three-column systems and about 11.5% for the four-column system. The higher COV in the latter case is primarily due to the difficulty of determining the failure point when P-delta effects are considered for soft foundations as observed in the *NCHRP Report 458* data set.

The analyses performed in this study and in *NCHRP Report 458* assumed that the hinges form in the columns and that any weakness in the cap beams, shear capacity, member detailing, and connections is represented by reduction in the ultimate curvatures of the columns. Chapter 5 of this report describes how the weaknesses change the ultimate curvature that should be used in Equation 3.1, which is also given above as Equation 1.3.

4.3 Calibration of System Factors

Calibration Approach

The calibration of system factors for the force-based approach can be executed following the procedure outlined in Chapter 2. The process is based on Figure 3.1 that describes the behavior of bridges under lateral load assuming that the performance is being evaluated using the force levels on the vertical axis. The procedure as presented in this chapter assumes that the lognormal reliability model is valid for the force-based analysis process. Accordingly, the evaluation of the safety of a bridge under lateral load also can be expressed in terms of the probability of failure, which for the force-based approach represents the probability that the load carrying capacity, P, is smaller than the applied extreme load, LE.

$$P_f = \Pr\left[\frac{P}{LE} \le 1\right] \tag{4.3}$$

Assuming that both the capacity and the load can be expressed by lognormal probability distributions, the probability of failure can be expanded as

$$P_f = \Phi\left[\frac{-[\ln(P^*) - \ln(LE^*)]}{\sqrt{\xi_P^2 + \xi_{LE}^2}}\right] = \Phi\left[\frac{-\ln\left(P^*/LE^*\right)}{\sqrt{\xi_P^2 + \xi_{LE}^2}}\right] \tag{4.4}$$

where P^* is the median of the capacity P, ξ_P is the dispersion of the lognormal distribution of the capacity. The variables with the subscript "LE" are the statistics for the load. Φ is the cumulative normal distribution function.

In this case, the reliability index for the system defined as, β_{system}, can be calculated as

$$\beta_{system} = \frac{\ln\left(P_u^*/LE^*\right)}{\sqrt{\xi_P^2 + \xi_{LE}^2}} \tag{4.5}$$

The reliability index for the failure of the first column defined as, β_{column}, can be calculated as

$$\beta_{column} = \frac{\ln\left(P_{p1}^*/LE^*\right)}{\sqrt{\xi_P^2 + \xi_{LE}^2}} \tag{4.6}$$

In the program Hazus (2003) developed by FEMA for evaluating the seismic risk of structures, the combined dispersion for capacity and demand for typical bridge structures and structural members is set at $\sqrt{\xi_P^2 + \xi_{LE}^2} = 0.60$ for all damage types and all bridge members.

As explained in Chapter 2, a probabilistic measure of system redundancy can be expressed in terms of the additional reliability provided by the system compared to that of the member and can be defined as the reliability index margin

$$\Delta\beta_u = \beta_{system} - \beta_{column} \tag{4.7}$$

Substituting Equations 4.5 and 4.6 into Equation 4.7, the reliability index margin is obtained as

$$\Delta\beta_u = \frac{\ln\left(P_u^*/LE^*\right)}{\sqrt{\xi_P^2 + \xi_{LE}^2}} - \frac{\ln\left(P_{p1}^*/LE^*\right)}{\sqrt{\xi_P^2 + \xi_{LE}^2}} \tag{4.8}$$

Or

$$\Delta\beta_u = \frac{\ln\left(P_u^*/P_{p1}^*\right)}{\sqrt{\xi_P^2 + \xi_{LE}^2}} \tag{4.9}$$

This reliability margin can be used as a probabilistic measure of redundancy. Bridges that meet a reliability margin criterion can be defined as being sufficiently redundant. Those that do not meet the criterion are non-redundant. For example, *NCHRP Report 406* observed that redundant superstructure systems subjected to vertical loads have been traditionally associated with bridges that meet or exceed a target system reliability margin $\Delta\beta_{u\,target} = 0.85$. The 0.85 target margin was selected to match the average reliability margin of all four-girder bridges because four-girder bridges have been widely accepted as being redundant.

Following the approach of *NCHRP Report 406*, bridge systems that do not meet the minimum target reliability margin should be designed to higher standards by applying a system factor ϕ_s. The system factor should be calibrated to offset the

difference between the target reliability margin and the reliability margin that a system designed using current methods provides.

Following the same rationale, it can be assumed that bridges under lateral loads should produce a target reliability margin $\Delta\beta_{\text{u target}}$ to be classified as sufficiently redundant. Those that do not meet the target reliability margin must be designed to meet higher system reliability levels. The higher reliability levels should offset the difference between the calculated $\Delta\beta_u$ and the target value $\Delta\beta_{\text{u target}}$. This can be formulated by first evaluating the deficit between the reliability index margin provided by a particular bridge system, $\Delta\beta_u$, and the target reliability index margin $\Delta\beta_{\text{u target}}$.

$$\Delta\beta_{u\,\text{deficit}} = \Delta\beta_{u\,\text{target}} - \Delta\beta_u \tag{4.10}$$

A negative $\Delta\beta_{\text{u deficit}}$ means that the system provides a higher level of redundancy than the minimum required. A positive deficit indicates that the bridge system configuration does not provide a sufficient level of redundancy. To compensate for the lack of redundancy, the members of the bridge should be designed to higher standards to ensure that the system provides a reliability index higher than the one obtained according to current standards to offset the reliability deficit. This can be formulated as

$$\beta^{N}_{system} = \beta_{system} + \Delta\beta_{\text{u deficit}} = \beta_{system} + (\Delta\beta_{\text{u target}} - \Delta\beta_u) \tag{4.11}$$

where β^{N}_{system} is the reliability index that a more conservatively designed system should achieve to compensate for the lack of adequate levels of redundancy while β_{system} is the reliability index obtained for the current design. β^{N}_{system} can be expressed as

$$\beta^{N}_{system} = \frac{\ln\left(LP^{\star\text{N}}_u \big/ LE^{\star}\right)}{\sqrt{\xi^2_P + \xi^2_{LE}}} \tag{4.12}$$

where $P^{\star\text{N}}_u$ is the required ultimate load capacity needed to reach the system reliability β^{N}_{system}.

Substituting Equations 4.5, 4.9, and 4.12 into Equation 4.11 leads to

$$\frac{\ln\left(P^{\star\text{N}}_u \big/ LE^{\star}\right)}{\sqrt{\xi^2_P + \xi^2_{LE}}} = \frac{\ln\left(P^{\star}_u \big/ LE^{\star}\right)}{\sqrt{\xi^2_P + \xi^2_{LE}}} + \left(\Delta\beta_{\text{u target}} - \frac{\ln\left(P^{\star}_u \big/ P^{\star}_{p1}\right)}{\sqrt{\xi^2_P + \xi^2_{LE}}}\right) \tag{4.13}$$

The above expression is simplified to give

$$\frac{\ln\left(P^{\star\text{N}}_u \big/ P^{\star}_{p1}\right)}{\sqrt{\xi^2_P + \xi^2_{LE}}} = \Delta\beta_{\text{u target}} \tag{4.14}$$

which can be written as

$$\frac{\ln\left(\dfrac{P^{\star\text{N}}_u}{P^{\star\text{N}}_{p1}}\dfrac{P^{\star\text{N}}_{p1}}{P^{\star}_{p1}}\right)}{\sqrt{\xi^2_P + \xi^2_{LE}}} = \Delta\beta_{\text{u target}} \tag{4.15}$$

where $P^{\star\text{N}}_{p1}$ is the required column capacity obtained by adjusting the currently required member capacity $P^{\star}_{p1}$ by a system factor ϕ_s such that $P^{\star\text{N}}_{p1} = \dfrac{P^{\star}_{p1}}{\phi_s}$ so that

$$\frac{\ln\left(\dfrac{P^{\star\text{N}}_u}{LF^{\star\text{N}}_{p1}}\dfrac{1}{\phi_s}\right)}{\sqrt{\xi^2_P + \xi^2_{LE}}} = \Delta\beta_{\text{u target}} \tag{4.16}$$

Or

$$\ln\left(\frac{1}{\phi_s}\frac{P^{\star\text{N}}_u}{P^{\star\text{N}}_{p1}}\right) = \sqrt{\xi^2_P + \xi^2_{LE}}\,\Delta\beta_{\text{u target}} \tag{4.17}$$

Finally

$$\phi_s = \left(P^{\star\text{N}}_u \big/ P^{\star\text{N}}_{p1}\right)\exp^{-\left(\sqrt{\xi^2_P+\xi^2_{LE}}\right)\Delta\beta_{\text{u target}}} \tag{4.18}$$

The evaluation of the system factor can then be executed if the target margin reliability $\Delta\beta_{\text{u target}}$ is set, and if the dispersion coefficient $\sqrt{\xi^2_P + \xi^2_{LE}}$ as well as the redundancy ratio $\dfrac{P^{\star\text{N}}_u}{P^{\star\text{N}}_{p1}}$ are known.

In *NCHRP Report 458*, it was assumed that the ratio $\dfrac{P^{\star\text{N}}_u}{P^{\star\text{N}}_{p1}}$ remains constant, independent of the value of $P^{\star\text{N}}_{1p}$ such that $R_u = \dfrac{P^{\star\text{N}}_u}{P^{\star\text{N}}_{p1}} = \dfrac{P^{\star}_u}{P^{\star}_{p1}}$. This is a reasonable assumption as long as the redundancy ratio R_u is evaluated for bridges having similar configurations including the same number of columns, similar column cross sections and column heights. This led to the development of very complex tables of system factors that attempt to cover a large array of substructure systems with different combinations of properties and dimensions.

Instead, a review of the *NCHRP Report 458* data, complemented with the results of the analyses performed during the course of this study, have shown that the relationship between the ultimate capacity of a multi-column bridge substructure system and the lateral load carrying capacity of one column can be reasonably well represented as a function of the number of columns in the bent and the ultimate curvature capacity of the bent columns as demonstrated in Section 4.2 of this chapter. A system's ultimate

capacity under lateral load can be represented by an equation of the form:

$$P_u = P_{p1}\left[F_{mc} + C_{\phi}\frac{\varphi_u - \varphi_{tunc}}{\varphi_{tconf} - \varphi_{tunc}} \right] \quad (4.2)$$

where P_{p1} gives the capacity of a bridge system under lateral load assuming linear-elastic behavior as typically done when using a force-based analysis, F_{mc} is a multi-column factor, C_{φ} is a curvature factor, φ_u is the ultimate curvature of the weakest column in the bent, φ_{tunc} is the average curvature for a typical unconfined column, φ_{tconf} is the average curvature for a typical confined column.

For a particular bridge system, P_{p1} is calculated using a linear structural analysis of the system under the effect of the applied lateral load. To find P_{p1}, failure is defined as the load at which one column reaches its ultimate capacity assuming elasto-plastic behavior. The value for the ultimate curvature at failure φ_u is calculated from the ultimate plastic analysis of the column's cross section.

Values for F_{mc}, C_{φ}, φ_{tunc}, and φ_{tconf} have been extracted from the analysis of a large number of two-column, three-column, and four-column bents. The bents analyzed included a range of column sizes, vertical reinforcement ratios, and confinement ratios. The analyses also considered the effect of different foundation stiffnesses. The recommended values for these parameters are provided in Table 4.1. The values for φ_{tunc} and φ_{tconf} are the average curvatures obtained from the analysis of the column sizes used in *NCHRP Report 458*. The columns analyzed in *NCHRP Report 458* represent typical column sizes and reinforcement ratios collected from a national survey conducted as part of the study. The values for φ_{tunc} and φ_{tconf} are used in Equation 4.2 to compare the confinement ratio of the column being evaluated to the average confinement ratios observed in typical confined and unconfined columns.

The implementation of Equation 4.2 in combination with the recommended factors provided in Table 4.1 into Equation 4.18 will lead to the system factors to be used when evaluating the force capacity of bridge systems subjected to lateral loads. Specifically, the system factor is a function of the target reliability level as well as the combined dispersion coefficient. Substituting Equation 4.2 into Equation 4.18, the system factor is

$$\phi_s = \exp^{-\left(\sqrt{\xi_{LF}^2+\xi_{LE}^2}\right)\Delta\beta_{u\ target}}\left[F_{mc} + C_{\varphi}\frac{\varphi_u - \varphi_{tunc}}{\varphi_{tconf} - \varphi_{tunc}} \right] \quad (4.19)$$

The target reliability index margin, $\Delta\beta_{u\ target}$, must be set by the code writing authorities to match those of acceptable values obtained from systems recognized as being adequately redundant. The dispersion coefficient $\sqrt{\xi_P^2 + \xi_{LE}^2}$ must reflect the uncertainties associated with estimating the strength and the applied loads. As an example, a dispersion coefficient equal to 0.60 is used in the program Hazus (2003) prepared by FEMA for the analysis of seismic damage risk.

The exponential term in Equation 4.18 is defined as the system risk factor as it reflects the acceptable level of risk for bridge collapse that can be tolerated such that

$$\Re_s = \exp^{-\left(\sqrt{\xi_{LF}^2+\xi_{LE}^2}\right)\Delta\beta_{u\ target}} \quad (4.20)$$

Table 4.14 gives the risk coefficient, $\Re_s$ for different values of $\Delta\beta_{u\ target}$ and dispersion coefficients.

As an example, Figure 4.22 shows how the system factor, ϕ_s, varies as a function of the curvature of the bridge column. The figure shows the system factor for different numbers of columns in a bent. The system factors in Figure 4.22 are calculated assuming a target reliability margin $\Delta\beta_{u\ target} = 0.50$ and a dispersion coefficient $\sqrt{\xi_P^2 + \xi_{LE}^2} = 0.60$ such that the risk factor is $\Re_s = 074$.

The results in Figure 4.22 show a moderate increase in the system factor as the number of columns in the bent increases from two to four columns by 0.06. However, the more significant increase in the system factor is due to the increase in the confinement ratio, which is reflected by the increase in the ultimate curvature of the column. In fact, from Equation 4.19, it is observed that an increase in the ultimate curvature of the section from 3.0×10^{-4} (1/in) to 2.0×10^{-3} (1/in) results in an increase in the system factor by about 0.25. A curvature of 3.0×10^{-4} (1/in) is obtained for this column when the column is unconfined. A confinement ratio of 0.003, which according to the AASHTO LRFD Seismic Design Guide corresponds to a structural detail category B, produces an ultimate curvature equal to 0.974×10^{-3} (1/in). A confinement ratio of 0.005, which corresponds to structural detail category C, produces a curvature equal to 1.30×10^{-3} (1/in). A confinement ratio of 0.008 produces a curvature equal to 1.76×10^{-3} (1/in). A confinement ratio of 0.01 produces a curvature equal to 2.05×10^{-3} (1/in).

Implementation Example

A simple example is presented to illustrate the procedure that an engineer would follow to include redundancy during the safety evaluation of a bridge system subjected to lateral load. In this example, the researchers assume that the seismic design of a bridge system with two-column bents in a low seismic region calls for each column to have a moment capacity $M_p = 3.85 \times 10^4$ kip-in. To meet the preliminary design requirements, the engineer selects a section that has a diameter D = 3.6-ft. The column is reinforced by vertical steel bars such that the vertical reinforcement ratio is 1.85%. Furthermore, the engineer uses a confinement ratio

Table 4.14. Risk coefficient for different target reliability margins.

Target reliability margin $\Delta\beta_{u\ target}$	Dispersion coefficient $\sqrt{\xi_P^2 + \xi_{LE}^2}$	Risk factor $\Re_s$
0.3	0.2	0.94
	0.3	0.91
	0.4	0.89
	0.5	0.86
	0.6	0.84
0.4	0.2	0.92
	0.3	0.89
	0.4	0.85
	0.5	0.82
	0.6	0.79
0.5	0.2	0.90
	0.3	0.86
	0.4	0.82
	0.5	0.78
	0.6	0.74
0.6	0.2	0.89
	0.3	0.84
	0.4	0.79
	0.5	0.74
	0.6	0.70
0.7	0.2	0.87
	0.3	0.81
	0.4	0.76
	0.5	0.70
	0.6	0.66
0.8	0.2	0.85
	0.3	0.79
	0.4	0.73
	0.5	0.67
	0.6	0.62
0.9	0.2	0.84
	0.3	0.76
	0.4	0.70
	0.5	0.64
	0.6	0.58
1.0	0.2	0.82
	0.3	0.74
	0.4	0.67
	0.5	0.61
	0.6	0.55

$\rho_s = 0.003$. The analysis of the section determines that the moment capacity of the column meets the requirement and is equal to $M_p = 3.85 \times 10^{-4}$ kip-in. and the ultimate curvature is $\varphi_u = 0.974 \times 10^{-3}$ (1/in).

A linear-elastic analysis of the system under lateral load indicates that one column reaches its moment capacity $M_p = 3.85 \times 10^{-4}$ kip-in. when a lateral force $P_{1p} = 714$ kips is applied on the two-column bent.

To reduce the risk of collapse under an extreme event, the engineer would like to verify that the system will have significantly additional capacity in case one of the columns reaches its design moment capacity. Using Equation 4.2,

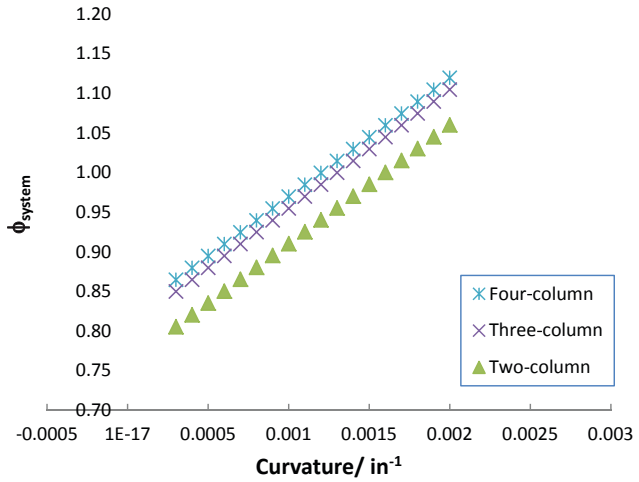

Figure 4.22. System factor vs. ultimate curvature for example column with risk factor $\Re_s = 0.74$.

the engineer calculates the ultimate load capacity of the system to be

$$P_u = P_{p1}\left[F_{mc} + C_\phi \frac{\varphi_u - \varphi_{tunc}}{\varphi_{tconf} - \varphi_{tunc}}\right]$$

$$= 714\left[1.10 + 0.24\frac{0.974\times10^{-3} - 3.64\times10^{-4}}{1.55\times10^{-3} - 3.64\times10^{-4}}\right]$$

$$= 874\ kips$$

The redundancy ratio is obtained as $R_u = {P_u}/{P_{p1}} = {874}/{714} = 1.22$. This indicates that this bridge with two-column bents does provide some level of redundancy. However, this level must be checked against the specified requirements. It is assumed that the specifications applicable to the jurisdiction where the bridge is to be built require a risk factor $\Re_s = 0.74$ corresponding to a reliability margin $\Delta\beta_{u\ target} = 0.50$. To verify whether the bridge columns meet this requirement, a system factor is calculated from Equation 4.19 as

$$\phi_s = \Re_s\left[F_{mc} + C_\varphi \frac{\varphi_u - \varphi_{tunc}}{\varphi_{tconf} - \varphi_{tunc}}\right] = 0.74\times1.22 = 0.90$$

Because the system factor is less than 1.0, the bridge is not sufficiently redundant to meet the risk requirements. Thus, the bridge columns must be designed to a higher moment capacity such that $\phi_s M_p = 3.85 \times 10^4$ kip-in. That is, the moment capacity must be increased by (1/0.90) so that $M_p = 4.28 \times 10^4$ kip-in.

A higher moment capacity will not turn a non-redundant system into a redundant one but it will help compensate for the relatively low level of system reliability by increasing the reliability of the columns to compensate for the low level of redundancy.

Alternatively, the engineer may decide to improve the overall reliability of the system by increasing the confinement ratio from the original $\rho_s = 0.003$ to a higher ratio $\rho_s = 0.008$. In this case, the new system factor is calculated from Equation 4.19 to be $\phi_s = 1.02$ which is higher than 1.0. Thus, the moment capacity $M_p = 3.85 \times 10^4$ kip-in will be acceptable as it will produce the required redundancy level as long as the lateral reinforcement is improved to produce a confinement ratio equal to $\rho_s = 0.008$.

Reliability Check

Using Equation 4.9 with $P_u/P_{p1} = 1.22$, it is found that the original reliability index margin is $\Delta\beta_u = 0.33$, which is lower than the target value $\Delta\beta_{u\ target} = 0.50$. The deficit in the reliability index margin is $\Delta\beta_{u\ deficit} = \Delta\beta_{u\ target} - \Delta\beta_u = 0.17$. Increasing the moment capacity of the column by a factor 1/0.9 will increase the overall reliability of the system to compensate for the low level of redundancy.

4.4 Additional Verifications of Model

P-Delta Effect

P-delta effect, also known as geometric nonlinearity, involves the equilibrium and compatibility relationships of a structural system loaded about its deflected configuration. Of particular concern is the application of gravity load on bridge columns with large lateral deformations. If the deformations become sufficiently large as to break from linear compatibility relationships, then using SAP2000's large-displacement and large-deformation analyses becomes necessary. This condition magnifies the bending moment in the column and reduces the deformation capacity. As explained in the SAP2000 manual, the two sources of P-delta effect are illustrated in Figure 4.23, and described as follows:

- **P-δ effect**, or P-"small-delta," is associated with local deformation relative to the element chord between end nodes.

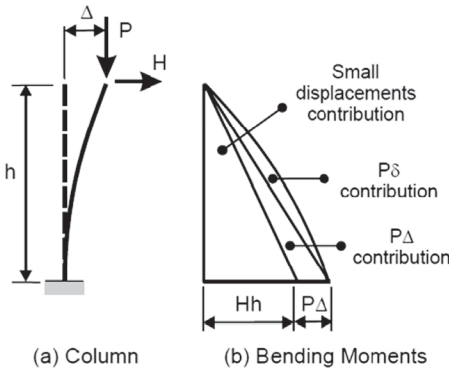

Figure 4.23. P-delta about column.

Typically, P-δ only becomes significant at unreasonably large displacement values, or in especially slender columns.

- **P-Δ effect**, or P-"big-delta," is associated with displacements relative to member ends. Unlike P-δ, this type of P-delta effect *is critical* to nonlinear modeling and analysis. Gravity loading *will* influence structural response under significant lateral displacement.

To verify that Equation 4.2 is still valid for predicting bridge system capacity when P-delta effect is taken into account, the analysis of the three-column multi-girder bridge described in Section 4.2 is performed for the following three cases: (1) without geometric nonlinearity, (2) with P-δ effect, and (3) P-delta including large displacement effects. Twenty-four bridge-bent models with various diameters ranging from 6-ft to 8-ft and different column heights ranging from 20-ft to 40-ft are investigated. The results of the analysis for first column failure P_{p1} are compared to the system's ultimate capacity P_u obtained from the SAP2000 analysis and the predicted P_u by Equation 4.2 are listed in Table 4.15. The results with P-delta effect (in red) and those without the effect (in blue) also are compared in Figure 4.24.

The last column in Table 4.15 shows that the errors remain within the same range whether P-delta effects are considered or not, with the largest differences observed for the very slender long columns when the error in Equation 4.2 may increase by less than 4%. The trend lines in Figure 4.24 show that R^2 remains essentially similar whether the P-delta effects are considered or not.

Effect of Foundation Stiffness on Bridge Systems with Three-Column Bents

The analyses performed in *NCHRP Report 458* considered different foundation types and soil conditions to reflect

Table 4.15. Comparison of results with and without P-delta effect.

Category B		Diameter	Column Height	System Capacity	Plastic Capacity	Ultimate Column Curvature	System Capacity by Eq. 4.2	Error
		D (in.)	H (in.)	P_u (kips)	P_{p1} (kips)	φ_u (in^{-1})	P_u (kips)	
None	451-inch	72	451	2480.7	2252.8	0.000717	2774.22	11.83%
P-δ	451-inch	72	451	2279.5	2121.2	0.000717	2612.16	14.59%
P-Δ	451-inch	72	451	2259.5	2119.9	0.000717	2610.56	15.54%
None	Diameter–7 ft	84	240	9116.3	8079.5	0.000574	9715.24	6.57%
P-δ	Diameter–7 ft	84	240	9074.1	8076.9	0.000574	9712.11	7.03%
P-Δ	Diameter–7 ft	84	240	9018.6	8074.5	0.000574	9709.23	7.66%
None	Pile	96	240	11528.4	8870.5	0.000516	10562.1	-8.38%
P-δ	Pile	96	240	11464	8863.1	0.000516	10553.3	-7.94%
P-Δ	Pile	96	240	11347.6	8863.9	0.000516	10554.2	-6.99%
None	Pile	96	360	8087.1	6210.4	0.000516	7394.71	-8.56%
P-δ	Pile	96	360	8002.6	6201.6	0.000516	7384.23	-7.73%
P-Δ	Pile	96	360	7972.3	6202.5	0.000516	7385.31	-7.36%
None	Pile	96	480	6401	4936.2	0.000516	5877.52	-8.18%
P-δ	Pile	96	480	6290.4	4926.1	0.000516	5865.5	-6.75%
P-Δ	Pile	96	480	6252.1	4927	0.000516	5866.57	-6.17%
None	Spread	96	240	13016.1	11881.2	0.000516	14146.9	8.69%
P-δ	Spread	96	240	13010	11820.5	0.000516	14074.6	8.18%
P-Δ	Spread	96	240	12866.1	11796.6	0.000516	14046.2	9.17%
None	Spread	96	360	9169.2	8459.6	0.000516	10072.8	9.86%
P-δ	Spread	96	360	9125.3	8405.8	0.000516	10008.8	9.68%
P-Δ	Spread	96	360	9089.3	8383.6	0.000516	9982.34	9.83%
None	Spread	96	480	7225.7	6696	0.000516	7972.91	10.34%
P-δ	Spread	96	480	7157.2	6651.4	0.000516	7919.81	10.66%
P-Δ	Spread	96	480	7091.9	6671.4	0.000516	7943.62	12.01%

NOTES: "P-δ" (i.e., P-"small-delta") is associated with local deformation relative to the element chord between end nodes. The equilibrium equations take into partial account the deformed configuration of the structure.
"P-Δ" includes P-"small-delta" plus large displacement.
"None" means neither P-"small-delta" nor P-"large-delta" effect is considered.

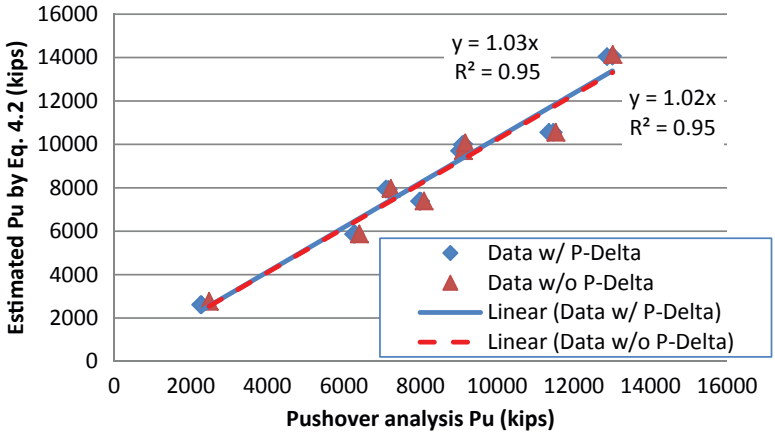

Figure 4.24. Comparison of results with and without P-delta effect.

typical substructure design cases. To investigate situations where the foundations may be overdesigned or underdesigned, this section analyzes the multi-girder bridge with three-column bents assuming different foundation stiffnesses. The analysis is then performed for the different foundation stiffness values shown in Table 4.16, which has been extracted from *NCHRP Report 458*, where foundations and supporting soils were grouped into eight categories.

In this section, 40 bridge system models with eight types of foundations are studied. The analysis results are summarized in Table 4.17. The results also are presented in Figure 4.25, which plots the estimated ultimate system capacity P_u obtained from Equation 4.2 versus the value of P_u obtained from the pushover analysis for the different column dimensions and foundations analyzed. The analysis included 3-ft diameter columns designed with lateral confinement reinforcement ratios ρ_s = 0.24% (original detail), 0.3% (detail category B) and 0.5% (detail category C), in addition to cases where the diameter is increased up to 8-ft with lateral confinement reinforcement ratios ρ_s = 0.3% to obtain a much larger range of the ultimate system capacity. Although the errors in Table 4.17 are found to vary between −14.68% and +12.78%, the trend line in Figure 4.25 shows a regression slope of 1.02 with a regression coefficient R^2 of 0.99. This demonstrates that, generally speaking, the ultimate system capacity estimated by Equation 4.2 gives a good approximation to the actual ultimate capacity of the bridge system and the bridge foundation stiffness has no overall effect on the proposed equation.

Table 4.16. Foundation types and stiffness.

Foundation types	K_vertical (kN/m)	K_transverse (kN/m)	K_rotation (kN-m)
1 spread\normal\	97200	72900	3650000
2 spread\stiff\	147000	110000	5530000
3 extension\soft\	443077	5226	113726
4 extension\normal\	1107000	17784	220882
5 extension\stiff\	1994000	46628	367348
6 pile\soft\	675400	18870	376700
7 pile\normal\	1689000	85870	941700
8 pile\stiff\	3039000	299000	1695000

Reduction in Column Curvature

The analyses performed in the previous sections of this report and in *NCHRP Report 458* assumed that hinges form in the columns. Accounting for weaknesses in the cap beams, shear capacity, member detailing, and connections can be accommodated by reducing the ultimate curvature of the columns. FHWA's Seismic Retrofitting Manual for Highway Structures: Part 1—Bridges provides a set of models that can be used to estimate the system's ductility for different types of inadequacies in the design of the bridge system. This section describes how the models in the FHWA report can be adopted during the application of Equation 4.2. For that purpose, it is proposed to use a ductility reduction factor that can be applied on the ultimate curvature φ_u in Equation 4.2 to account for the reduction in ductility due to weaknesses in the system design. Also, in some cases, a modification of the force P_{p1} may need to be applied when the capacity of the first member to fail is significantly reduced. The proposed approach is specifically described for the cases when the cap beam is weaker than the bridge columns and when the column shear capacity leads to shearing failures before the ultimate moment capacity of a section is reached. Weaknesses in lap splicing and other connection details can follow the same approach using the models described in the FHWA report.

Table 4.17. Summary of results for three-column bridge bents with various foundations.

	Diameter	Column Height	System Capacity	Plastic Capacity	Ultimate Column Curvature	System Capacity by Eq.4.2	Error
Category B 72" Column	**D (in.)**	**H (in.)**	**P_u (kips)**	**P_{p1} (kips)**	**φ_u (in^{-1})**	**P_u (kips)**	
1 spread\normal\	96	240	13016.1	11881.2	0.000516	14146.9	8.69%
2 spread\stiff\	96	240	13206.3	11846	0.000516	14105	6.81%
2 spread\stiff\	96	180	17012.6	15037.2	0.000516	17904.8	5.24%
2 spread\stiff\	96	150	19847.4	17460.4	0.000516	20790.1	4.75%
2 spread\stiff\	96	480	7195.2	6636.9	0.000516	7902.54	9.83%
3 extension\soft\	96	700	4115.9	3858.4	0.000516	4594.19	11.62%
4 extension\normal\	96	400	5518.6	5200.4	0.000516	6192.11	12.20%
5 extension\stiff\	96	400	5869	5099	0.000516	6071.37	3.45%
6 pile\soft\	96	240	7198.4	6818.1	0.000516	8118.3	12.78%
7 pile\normal\	96	700	4922.4	3828.4	0.000516	4558.47	-7.39%
7 pile\normal\	96	240	11528.4	8870.5	0.000516	10562.1	-8.38%
8 pile\stiff\	96	240	12904.5	9419.7	0.000516	11216	-13.08%
8 pile\stiff\	96	480	6955.3	5349.7	0.000516	6369.88	-8.42%
Category B 36" Column	**D (in.)**	**H (in.)**	**P_u (kips)**	**P_{p1} (kips)**	**φ_u (in^{-1})**	**P_u (kips)**	**Error**
1 spread\normal\	36	331	1113	798.349	0.00106	1038.53	-6.69%
2 spread\stiff\	36	331	1112.4	784.9	0.00106	1021.03	-8.21%
2 spread\stiff\	36	451	922.8	727.1	0.00106	945.843	2.50%
2 spread\stiff\	36	150	1752.2	1385.4	0.00106	1802.19	2.85%
3 extension\soft\	36	150	1650.8	1386.4	0.00106	1803.49	9.25%
4 extension\normal\	36	451	883.6	759.7	0.00106	988.251	11.84%
4 extension\normal\	36	150	1866.1	1290.4	0.00106	1678.61	-10.05%
5 extension\stiff\	36	451	912.2	738.7	0.00106	960.933	5.34%
6 pile\soft\	36	331	1122.2	809.8	0.00106	1053.42	-6.13%
7 pile\normal\	36	331	870	581.638	0.00106	756.62	-13.03%
8 pile\stiff\	36	331	1126.6	785.6	0.00106	1021.94	-9.29%
Category C 36" Column	**D (in.)**	**H (in.)**	**P_u (kips)**	**P_{p1} (kips)**	**φ_u (in^{-1})**	**P_u (kips)**	**Error**
1 spread\normal\	36	331	1226	806.364	0.00138	1101.17	-10.18%
2 spread\stiff\	36	331	1235.9	792.7	0.00138	1082.51	-12.41%
3 extension\soft\	36	331	1388.6	867.6	0.00138	1184.79	-14.68%
4 extension\normal\	36	331	1268.4	794.2	0.00138	1084.56	-14.49%
5 extension\stiff\	36	331	1237.8	781.7	0.00138	1067.49	-13.76%
6 pile\soft\	36	331	1270.4	818	0.00138	1117.06	-12.07%
7 pile\normal\	36	331	1232	796.269	0.00138	1087.38	-11.74%
8 pile\stiff\	36	331	1225.8	793.5	0.00138	1083.6	-11.60%
Original 36" Column	**D (in.)**	**H (in.)**	**P_u (kips)**	**P_{p1} (kips)**	**φ_u (in^{-1})**	**P_u (kips)**	**Error**
1 spread\normal\	36	331	1071.186	794.341	0.00096	1017.24	-5.04%
2 spread\stiff\	36	180	1509.2	1178.8	0.00096	1509.58	0.03%
3 extension\soft\	36	180	1722.9	1200.7	0.00096	1537.62	-10.75%
4 extension\normal\	36	180	1609.8	1107	0.00096	1417.63	-11.94%
5 extension\stiff\	36	180	1554.3	1111.7	0.00096	1423.65	-8.41%
6 pile\soft\	36	180	1610.2	1197.6	0.00096	1533.66	-4.75%
7 pile\normal\	36	331	1095.164	784.356	0.00096	1004.45	-8.28%
8 pile\stiff\	36	180	1512	1183.8	0.00096	1515.98	0.26%

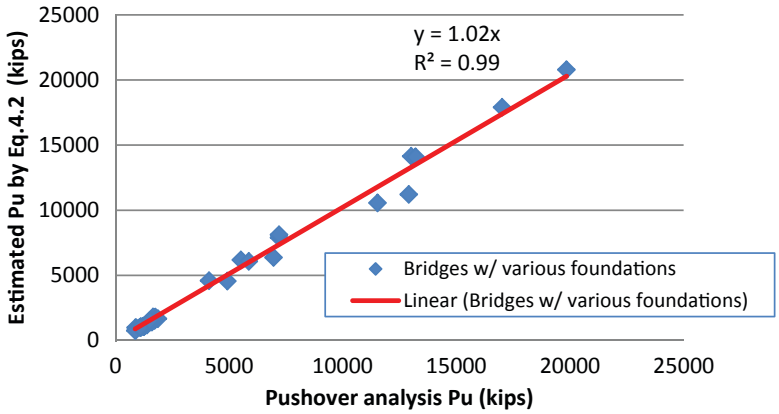

Figure 4.25. Effect of foundation on Equation 4.2.

Effect of Inadequate Cap Beams

In a properly designed bridge system, the cap beam should be at least as strong as the columns. Thus, no plastic hinges are expected to form in the cap beam during a pushover analysis. However, reinforced or prestressed concrete cap beams may yield and form plastic hinges due to inadequacies in their design or to reductions in their capacities due to deterioration or other phenomena. Plastic hinges form at locations of peak bending moment and are therefore likely to occur in the end regions of the columns or cap beams. The interaction between columns and cap beams and their strengths will determine the likely mode of failure.

Equation 4.2 gives the relationship between the ultimate capacity of a multi-column bridge system and the lateral load carrying capacity of one column as a function of the number of columns in the bent and the ultimate curvature capacity of the bent columns. The equation has been developed based on the assumption of having strong cap beams. FHWA's Seismic Retrofitting Manual for Highway Structures: Part 1—Bridges uses a capacity/demand (C/D) ratio to account for the effect of weak cap beams of bridge bents. The same concept can be used to reflect the weakness of the cap beam when using Equation 4.2. However, in the context of this study, the definition of demand is not the "demand of the design earthquake" as defined in the FHWA report, but the minimum demand on the cap beam strength to make it at least as strong as the column.

Two parameters need to be checked to verify that the cap beam is at least as strong as the column: the moment capacity of the beam and the ultimate curvature of the cap beam. The moment capacity of the cap beam divided by the moment capacity of the column is defined as the moment capacity of demand ratio C/D_{moment}. The ultimate curvature of the cap beam divided by the ultimate curvature of the column is defined as curvature capacity over demand ratio $C/D_{curvature}$. In a properly designed system, capacity over demand ratios, C/D, for both the moment and the curvature should always be greater than or equal to 1.0. If C/D is less than 1.0, the system's ability to carry lateral load is reduced. Three cases can be considered, as shown in Figure 4.26. For Case A, the moment capacity of the cap beam is larger than that of the column, but the ultimate curvature of the beam is lower than that of the column. For Case B, the moment capacity of the beam is

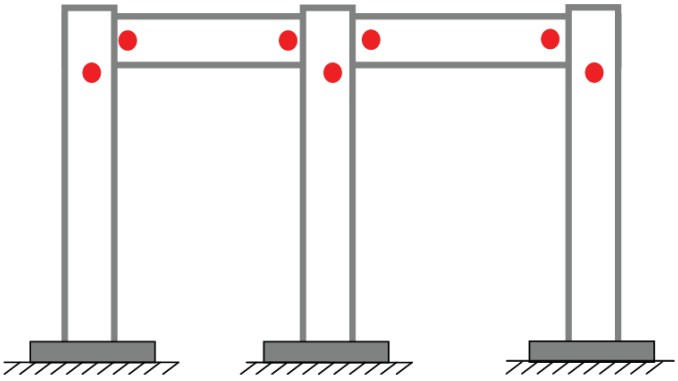

(a) Beam-column connection for a three-column bent showing potential top bent hinge locations

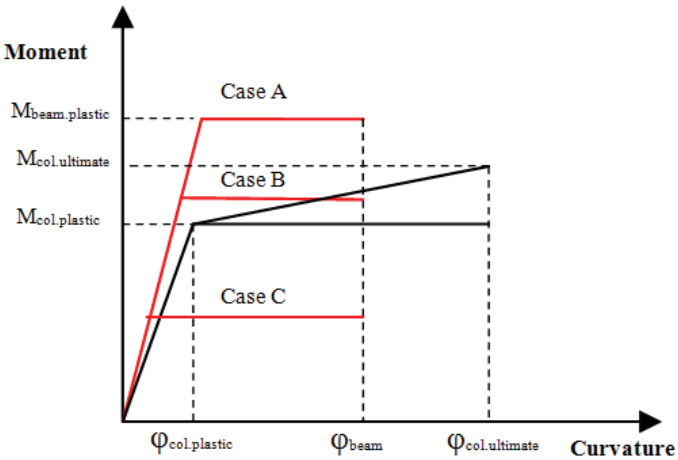

(b) Idealized moment-curvature relationships for cap beam (in red) and column (in black)

Figure 4.26. Model for cap beam-column capacities.

lower than that of the column but higher than the column's plastic moment. In Case C, the cap beam's moment capacity is lower than the column's plastic moment. The adjustments to be made for Equation 4.2 in each of these cases are studied in this section.

Cap Beam Capacity Higher Than Column Capacity

Case A: This is the situation when $C/D_{curvature}$ of the cap beam leads to a reduction in the curvature capacity of the beam-column connection, which can be modeled by an equivalent reduction in the column's curvature. The reduction can be represented by a factor $\gamma_{\varphi c} = C/D_{curvature}$ if less than 1.0, otherwise no reduction is needed and one can use $\gamma_{\varphi c} = 1.0$. The modified Equation 4.2 is then presented as

$$\gamma_{\varphi c} = \frac{\varphi_{beam}}{\varphi_{column}} \tag{4.21}$$

$$P_u = P_{p1}\left[F_{mc} + C_{\varphi}\frac{\gamma_{\varphi c}\varphi_u - \varphi_{tunc}}{\varphi_{tconf} - \varphi_{tunc}}\right] \tag{4.22}$$

Cap Beam Capacity Lower Than Column Capacity

When the cap beam strength is weaker than the column strength and C/D_{moment} is less than 1.0, then two cases can be considered. Case B considers the situation where the cap beam moment capacity is higher than the plastic moment capacity of the column but lower than the ultimate capacity of the column. In this case, the ultimate curvature φ_u in Equation 4.2 needs to be reduced to reflect the lower moment capacity of the system as well as the lower ultimate curvature. Case C considers the situation where the cap beam moment capacity is even lower than the plastic moment capacity of the column. In this case, both the load at failure assuming linear-elastic behavior, P_{p1}, as well as the ultimate curvature would need to be reduced. Changing the force P_{p1} reflects the insufficient moment capacity of the connection between the cap beam and the bridge columns. In this case, P_{p1} is calculated as the load at which the cap beam reaches its moment capacity.

Case B: If the cap beam strength is higher than the plastic moment of the column, but less than the ultimate moment capacity of the column, $[M_{col.ultimate} > M_{beam.plastic} > M_{col.plastic}]$, then $\gamma_{\varphi c}$ for the beam-column connection will depend on the cap beam capacity including moment and curvature capacity, which will cause a weak beam-column connection. The column curvature reduction factor $\gamma_{\varphi c}$ is used to reduce φ_u using the following equations:

$$\gamma_{\varphi c} = \gamma_M \gamma_{\varphi} = \frac{M_{beam.plastic} - M_{col.plastic}}{M_{col.ultimate} - M_{col.plastic}} \times \frac{\varphi_{beam}}{\varphi_{column}} \tag{4.23}$$

$$P_u = P_{p1}\left[F_{mc} + C_{\phi}\frac{\gamma_{\varphi c}\varphi_u - \varphi_{tunc}}{\varphi_{tconf} - \varphi_{tunc}}\right] \tag{4.24}$$

Such that $\gamma_{\varphi c}\varphi_u \approx$ effective curvature for beam-column connection.

Case C: If the cap beam strength is weaker than the plastic moment of the column, $[M_{beam.plastic} < M_{col.plastic}]$, then P_{p1} is the load at which a plastic hinge forms in the cap beam assuming linear-elastic analysis and $\gamma_{\varphi c}$ is used to reduce the column curvature.

$$\gamma_{\varphi c} = \frac{\varphi_{beam}}{\varphi_{column}} \tag{4.25}$$

$$P_u = P_{p1}\left[F_{mc} + C_{\varphi}\frac{\gamma_{\varphi c}\varphi_u - \varphi_{tunc}}{\varphi_{tconf} - \varphi_{tunc}}\right] \tag{4.26}$$

Forty bridge-bent models are analyzed using SAP2000 and compared to Equations 4.21 through 4.26 as appropriate for Cases A, B, and C to demonstrate the validity of the proposed approach for treating bridges with weak cap beams. For simplicity, Equations 4.21 through 4.26 will be referred to as modified Equation 4.2.

Weak Cap Beam Model Verification

To verify if Equations 4.21 through 4.26 are valid, 40 bridge models with 7-ft diameter columns having different column heights in the range of 16.7-ft up to 32.6-ft are investigated. All column sections have a transverse confinement ratio of 0.3%. The result of the linear-elastic analysis at which the first member reaches its plastic capacity is defined as P_{p1}. The values for P_{p1}, as well as those of the system ultimate capacity P_u obtained from the nonlinear SAP2000 pushover analysis, are presented in Table 4.18. The table also gives the column curvatures and the capacity over demand ratios $C/D_{curvature}$ column curvature and C/D_{moment}. The SAP2000 results for Case A are compared to P_u predicted by Equation 4.22 showing a maximum difference on the order of 7.64%. The maximum differences for Case B and Case C are 8.26% and 8.64%, respectively.

Figure 4.27 plots all the data of the predicted P_u from the modified empirical model versus the pushover analysis values. All the trend lines in Figure 4.27 have slopes close to 1.0 and the coefficients of regression are $R^2 = 0.97$, $R^2 = 0.95$, and $R^2 = 0.94$ for Cases A, B, and C, respectively. These results show that the proposed equations can be used in engineering practice to estimate the ultimate capacity of bridge systems subjected to lateral load for cases involving weaknesses in the moment and curvature capacities of the cap beams. Several examples are presented to illustrate how an engineer can use

Table 4.18. Comparison of system capacities from SAP2000 and Equations 4.22, 4.24, and 4.26.

Case A								
Diameter	**Column Height**	**System Capacity**	**Plastic Capacity**	**Ultimate Column Curvature**	**C/D Ratio Moment**	**C/D Ratio Curvature**	**System Capacity by Eq.4.22**	**Error**
D (in.)	H (in.)	P_u (kips)	P_{pl} (kips)	Phi_ult. (in^{-1})	γ_M*	γ_φ*	P_u (kips)	ε
84	391	5859	5244.8	0.000574	1.26	1.00	6306.6	7.64%
84	391	5859	5244.8	0.000574	1.26	0.90	6245.7	6.60%
84	391	5811.6	5244.8	0.000574	1.26	0.80	6184.8	6.42%
84	391	5811.6	5244.8	0.000574	1.26	0.70	6123.9	5.37%
84	391	5785.2	5244.8	0.000574	1.26	0.60	6063.0	4.80%
84	391	5766	5244.8	0.000574	1.26	0.50	6002.1	4.10%
84	391	5742.4	5244.8	0.000574	1.26	0.40	5941.2	3.46%
84	391	5714.4	5244.8	0.000574	1.26	0.30	5880.3	2.90%
84	360	6291.4	5609.4	0.000574	1.26	0.80	6614.8	5.14%
84	330	6775.4	6018.3	0.000574	1.26	0.80	7097.0	4.75%
84	300	7384.1	6495.5	0.000574	1.26	0.80	7659.7	3.73%
84	270	8205.3	7058.2	0.000574	1.26	0.80	8323.3	1.44%
84	240	9103.1	7729.2	0.000574	1.26	0.80	9114.5	0.13%
84	200	10801.7	8848.9	0.000574	1.26	0.80	10434.9	-3.40%
Case B								
Diameter	**Column Height**	**System Capacity**	**Plastic Capacity**	**Ultimate Column Curvature**	**C/D Ratio Moment**	**C/D Ratio Curvature**	**System Capacity by Eq.4.24**	**Error**
D (in.)	H (in.)	P_u (kips)	P_{pl} (kips)	Phi_ult. (in^{-1})	γ_M*	γ_φ*	P_u (kips)	ε
84	391	5713.3	5244.8	0.000574	0.00	1.25	5697.6	-0.27%
84	391	5725.8	5244.8	0.000574	0.21	1.25	5827.1	1.77%
84	391	5740.8	5244.8	0.000574	0.30	1.25	5880.3	2.43%
84	391	5740.2	5244.8	0.000574	0.40	1.25	5941.2	3.50%
84	391	5746.6	5244.8	0.000574	0.50	1.25	6002.1	4.45%
84	391	5747.6	5244.8	0.000574	0.60	1.25	6063.0	5.49%
84	391	5762.6	5244.8	0.000574	0.74	1.25	6150.6	6.73%
84	391	5769	5244.8	0.000574	0.90	1.25	6245.7	8.26%
84	360	6161.1	5609.4	0.000574	0.21	1.25	6232.1	1.15%
84	330	6619.7	6018.3	0.000574	0.21	1.25	6686.4	1.01%
84	300	7214.6	6495.5	0.000574	0.21	1.25	7216.6	0.03%
84	270	7932.9	7058.2	0.000574	0.21	1.25	7841.8	-1.15%
84	240	8782.4	7729.2	0.000574	0.21	1.25	8587.3	-2.22%
84	200	10424.4	8848.9	0.000574	0.21	1.25	9831.3	-5.69%

Table 4.18. (Continued).

Case C								
Diameter	**Column Height**	**System Capacity**	**Plastic Capacity**	**Ultimate Column Curvature**	**C/D Ratio Moment**	**C/D Ratio Curvature**	**System Capacity by Eq.4.26**	**Error**
D (in.)	H (in.)	P_u (kips)	P_{p1} (kips)	Phi_ult. (in^{-1})	γ_M *	γ_φ *	P_u (kips)	ε
84	391	5084.7	4314.3	0.000574	N/A	1.00	5187.8	2.03%
84	391	4896	4314.3	0.000574	N/A	0.50	4937.3	0.84%
84	391	4535.2	4314.3	0.000574	N/A	0.20	4787.0	5.55%
84	391	3730.1	3294.0	0.000574	N/A	0.05	3597.5	-3.55%
84	391	3955.1	3294.5	0.000574	N/A	0.09	3613.4	-8.64%
84	391	3191	3020.4	0.000574	N/A	0.05	3298.7	3.38%
84	391	3199.7	3020.6	0.000574	N/A	0.09	3313.0	3.54%
84	391	3180.6	3020.6	0.000574	N/A	0.05	3298.9	3.72%
84	391	3180.6	3020.6	0.000574	N/A	0.09	3313.0	4.16%
84	360	3359.5	3233.4	0.000574	N/A	0.09	3546.4	5.56%
84	330	3548.1	3480.7	0.000574	N/A	0.09	3817.7	7.60%
84	300	3768.8	3600.7	0.000574	N/A	0.09	3949.3	4.79%

NOTES: * When γ_M or γ_φ is larger than 1.0, the maximum value of 1.0 is used to calculate the reduction factor $\gamma_{\varphi c} = \gamma_M \gamma_\varphi$ which is applied for the ultimate curvature of column, otherwise use the actual values. γ_M is not applicable (N/A) for Case C.

the proposed approach when evaluating the ultimate load carrying capacity of a bridge system subjected to distributed lateral load.

Implementation Example: Weak Cap Beam Case A

Case A is the situation when $C/D_{curvature}$ of the cap beam leads to a reduction in the curvature capacity of the beam-column connection, which can be modeled by an equivalent reduction in the column's curvature. The reduction can be represented by a factor $\gamma_{\varphi c}$ and the modified Equation 4.22 is then presented as

$$\gamma_{\varphi c} = \frac{\varphi_{beam}}{\varphi_{column}} P_u = P_{p1}\left[F_{mc} + C_\varphi \frac{\gamma_{\varphi c}\varphi_u - \varphi_{tunc}}{\varphi_{tconf} - \varphi_{tunc}} \right]$$

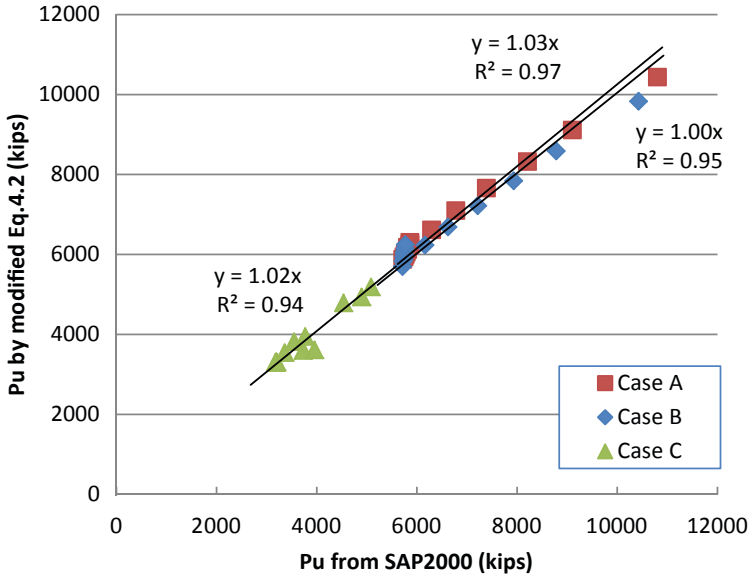

Figure 4.27. Predicted P_u vs. P_u from SAP2000 for weak cap beams.

This example is for a three-span continuous bridge with two three-column bents where the lateral confinement reinforcement ratio of each column is $\rho_s = 0.3\%$ (detail category B). Each column's height is 32.6-ft with a 7-ft diameter. The columns of the bridge system are based on stiff foundations that are assumed to be fixed. A cross-section analysis shows that the plastic moment capacity M_p for the cap beam without axial loads is 250,000 kip-in. The ultimate curvatures for the cap beam and column without axial load are 3.6×10^{-4} in^{-1} and 7.2×10^{-4} in^{-1}. The ultimate curvature of the middle column subjected to the axial load of 214 kips including dead load and 20% of live load is 5.74×10^{-4} in^{-1}. The pushover analysis shows that the first column reaches its plastic capacity when the lateral force is $P_{p1} = 5{,}244.8$ kip.

The steps necessary to obtain the maximum ultimate capacity of the system and the system factor ϕ_s are as follows:

1. Determine the curvature capacity/demand ($C/D_{curvature}$) ratio $\gamma_{\varphi c}$

$$\gamma_{\varphi c} = \frac{\varphi_{beam}}{\varphi_{column}} = \frac{3.60 \times 10^{-4}}{7.20 \times 10^{-4}} = 0.50 \le 1.0$$

2. Estimate the ultimate system capacity. According to Equation 4.22, the lateral load capacity of the entire bridge system is

$$P_u = P_{p1}\left[F_{mc} + C_\varphi \frac{\gamma_{\varphi c}\varphi_u - \varphi_{tunc}}{\varphi_{tconf} - \varphi_{tunc}}\right]$$

$$= 5244.8\left[1.16 + 0.24\frac{0.50(5.74 \times 10^{-4}) - 3.64 \times 10^{-4}}{1.55 \times 10^{-3} - 3.64 \times 10^{-4}}\right]$$

$$= 6{,}002 \; kips$$

The pushover analysis would give $P_u = 5{,}766$ kips. The error in P_u observed when Equation 4.22 is used as compared to the pushover analysis is

$$\varepsilon = \frac{6002 - 5766}{5766} \times 100\% = 4\%$$

3. Find the system factor. The bridge columns with the weak cap beam in Case A should be evaluated using a system factor equal to

$$\phi_s = \exp^{-\xi \times \Delta\beta_{u\,target}}\left[F_{mc} + C_\varphi \frac{\gamma_{\varphi c}\varphi_u - \varphi_{tunc}}{\varphi_{tconf} - \varphi_{tunc}}\right]$$

$$= \exp^{-0.6 \times 0.5}\left(\frac{6{,}002}{5{,}244.8}\right) = 0.85$$

Implementation Example: Weak Cap Beam Case B

If the cap beam strength is higher than the plastic moment of the column, but less than the ultimate moment capacity of the column, [$M_{col.ultimate} > M_{beam.plastic} > M_{col.plastic}$], then $\gamma_{\varphi c}$ for the beam-column connection will depend on the cap beam capacity accounting for both the moment and curvature capacities, which will cause a weak beam-column connection. The column curvature reduction factor $\gamma_{\varphi c}$ is used to reduce φ_u using the following equations:

$$\gamma_{\varphi c} = \gamma_M \gamma_\varphi = \frac{M_{beam.plastic} - M_{col.plastic}}{M_{col.ultimate} - M_{col.plastic}} \times \frac{\varphi_{beam}}{\varphi_{column}}$$

$$P_u = P_{p1}\left[F_{mc} + C_\phi \frac{\gamma_{\varphi c}\varphi_u - \varphi_{tunc}}{\varphi_{tconf} - \varphi_{tunc}}\right]$$

such that $\gamma_{\varphi c}\,\varphi_u \approx$ effective curvature for beam-column connection.

In this example, the same multi-girder three-span bridge with two three-column bents is used where the lateral confinement reinforcement ratio is $\rho_s = 0.3\%$ (detail category B). The column height is 32.6-ft with a 7-ft diameter. The columns are fixed to the stiff foundation. A cross-section analysis shows that the plastic moment capacity M_p for cap beam without axial loads is 202,000 kip-in. The ultimate curvatures for the cap beam and column without axial load are 9.03×10^{-4} in^{-1} and 7.2×10^{-4} in^{-1}. The ultimate moment, plastic moment and ultimate curvature of the middle column subjected to the axial load of 214 kips including dead load and 20% of live load is 214,600 kip-in., 198,600 kip-in., and 5.74×10^{-4} in.$^{-1}$, respectively. The pushover analysis shows that the first column reaches its plastic capacity when the lateral force is $P_{p1} = 5{,}244.8$ kip.

The steps necessary to obtain the maximum ultimate capacity of the system and the system factor ϕ_s are as follows:

1. Determine the moment capacity/demand (C/D_{moment}) ratio γ_M

$$\gamma_M = \frac{M_{beam.plastic} - M_{col.plastic}}{M_{col.ultimate} - M_{col.plastic}} = \frac{202{,}000 - 198{,}600}{214{,}600 - 198{,}600} = 0.21$$

2. Determine the curvature capacity/demand ($C/D_{curvature}$) ratio γ_φ

$$\gamma_\varphi = \frac{\varphi_{beam}}{\varphi_{column}} = \frac{9.03 \times 10^{-4}}{7.20 \times 10^{-4}} = 1.25 \ge 1.0$$

therefore use $\gamma_\varphi = 1.0$

3. Determine the reduction factor $\gamma_{\varphi c}$

$$\gamma_{\varphi c} = \gamma_M \gamma_\varphi = 0.21 \times 1.0 = 0.21$$

4. Estimate the ultimate system capacity. According to Equation 4.24, the lateral load capacity of the entire bridge system is

$$P_u = P_{p1}\left[F_{mc} + C_\varphi \frac{\gamma_{\varphi c}\varphi_u - \varphi_{tunc}}{\varphi_{tconf} - \varphi_{tunc}}\right]$$
$$= 5,244.8\left[1.16 + 0.24\frac{0.21(5.74\times10^{-4}) - 3.64\times10^{-4}}{1.55\times10^{-3} - 3.64\times10^{-4}}\right]$$
$$= 5,827.1\ kips$$

The pushover analysis would give P_u = 5,725.8 kips. The error in P_u observed when Equation 4.24 is used as compared to the pushover analysis is $\varepsilon = \frac{5827.1 - 5725.8}{5725.8} \times 100\% = 1.77\%$

5. System factor. The bridge columns with the weak cap beam in Case B should be evaluated using a system factor equal to

$$\phi_s = \exp^{-\xi\times\Delta\beta_{u\ target}}\left[F_{mc} + C_\varphi \frac{\gamma_{\varphi c}\varphi_u - \varphi_{tunc}}{\varphi_{tconf} - \varphi_{tunc}}\right]$$
$$= \exp^{-0.6\times0.5}\left(\frac{5,827.1}{5,244.8}\right) = 0.82$$

Implementation Example: Weak Cap Beam Case C

If the cap beam strength is weaker than the plastic moment of the column [$M_{beam.plastic} < M_{col.plastic}$], then $\gamma_{\varphi c}$ is used to reduce column curvature using the following equation:

$$\gamma_{\varphi c} = \frac{\varphi_{beam}}{\varphi_{column}} P_u = P_{p1}\left[F_{mc} + C_\varphi \frac{\gamma_{\varphi c}\varphi_u - \varphi_{tunc}}{\varphi_{tconf} - \varphi_{tunc}}\right]$$

Note: In the linear-elastic analysis used in Case C, P_{p1} is the load at which the moment in the cap beam reaches its plastic moment capacity.

The same multi-girder three-span bridge with two three-column bents where the lateral confinement reinforcement ratio is $\rho_s = 0.3\%$ (detail category B) is used in this example. Each column's height is 30.0-ft with a 7-ft diameter. The columns are fixed to the stiff foundation. A cross-section analysis shows that the plastic moment capacity M_p for the cap beam without axial loads is 30,000 kip-in. The ultimate curvatures for the cap beam and column without axial load are 6.49×10^{-5} in^{-1} and 7.2×10^{-4} in^{-1}. The ultimate curvature of the middle column subjected to the axial load of 214 kips including dead load and 20% of live load is 5.74×10^{-4} in^{-1}. The pushover analysis shows that the cap beam reaches its plastic capacity when the lateral force is P_{p1} = 3,233.4 kips.

The steps necessary to obtain the maximum ultimate capacity of the system and the system factor ϕ_s are as follows:

1. Determine the curvature capacity/demand ($C/D_{curvature}$) ratio $\gamma_{\varphi c}$

$$\gamma_{\varphi c} = \frac{\varphi_{beam}}{\varphi_{column}} = \frac{6.49\times10^{-5}}{7.20\times10^{-4}} = 0.09 \le 1.0$$

2. Estimate ultimate system capacity. According to Equation 4.26, the lateral load capacity of the entire bridge system is

$$P_u = P_{p1}\left[F_{mc} + C_\varphi \frac{\gamma_{\varphi c}\varphi_u - \varphi_{tunc}}{\varphi_{tconf} - \varphi_{tunc}}\right]$$
$$= 3233.4\left[1.16 + 0.24\frac{0.09(5.74\times10^{-4}) - 3.64\times10^{-4}}{1.55\times10^{-3} - 3.64\times10^{-4}}\right]$$
$$= 3,546.4\ kips$$

The pushover analysis would give P_u = 3,359.5 kips. The error in P_u observed when Equation 4.26 is used as compared to the pushover analysis is

$$\varepsilon = \frac{3546.4 - 3359.5}{3359.5} \times 100\% = 5.56\%$$

3. System factor. The bridge columns with the weak cap beam in Case C should be evaluated using a system factor equal to

$$\phi_s = \exp^{-\xi\times\Delta\beta_{u\ target}}\left[F_{mc} + C_\varphi \frac{\gamma_{\varphi c}\varphi_u - \varphi_{tunc}}{\varphi_{tconf} - \varphi_{tunc}}\right]$$
$$= \exp^{-0.6\times0.5}\left(\frac{3546.4}{3233.4}\right) = 0.81$$

Effect of Column Shear

Weak shear model: Equation 4.2 and the modified versions in Equations 4.22, 4.24, and 4.26 are derived based on the assumption that the shear strength of a column is sufficiently large so that no column shear failure occurs when the bridge system is subjected to incremental lateral loads. However, in inadequately designed bridges or deteriorated bridges, column shear failure may occur prior to flexural yielding or after flexural yielding but before bending failures. Using the same approach followed by the FHWA Seismic Retrofitting Manual (2006), a weakness in the shear capacity can be expressed in terms of the ratio of shear capacity over shear demand where in this context shear demand is the shear capacity corresponding to the load at which the column

reaches its bending moment capacity. This ratio will be represented by the term C/D_{shear}.

Figure 4.28 describes the model for the shear capacity evaluation process where $V_u(d)$ is defined as the maximum column shear force observed in the column during the pushover analysis assuming that the column will fail in bending moment. As an example, in idealistic elasto-plastic conditions, $V_u(d)$ is the shear resulting from plastic hinging at both the top and bottom of the column if both ends are fixed or the maximum shear force in the column when the fixed end reaches its maximum moment capacity if the other end is pinned. The shear demand in idealistic conditions can be calculated as $V_u(d) = M_u/L_{ceff}$ where L_{ceff} is the effective column length, which depends on boundary conditions at the two ends of the column. For fixed-fixed columns L_{ceff} = Height of column/2. For pinned-fixed columns L_{ceff} = Height of column. The actual boundary conditions of the columns are usually neither fixed-fixed nor pinned-fixed because the actual stiffnesses of the cap beam and foundations are not infinitely stiff, which may cause difficulties in determining the effective length. Therefore, it is recommended that $V_u(d)$ be obtained from the pushover analysis.

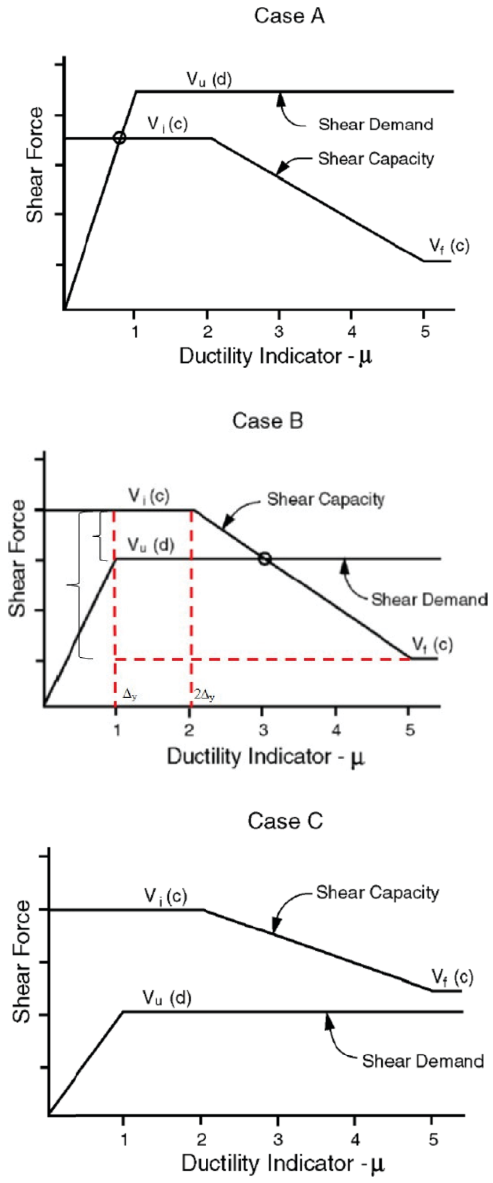

Figure 4.28. Resolution of shear demand and shear capacity.

Following the FHWA Seismic Retrofitting Manual (2006) and Figure 4.28, $V_i(c)$ is defined as the initial shear resistance of the undamaged column, which includes the resistance of the gross concrete section and the transverse steel. Also, $V_f(c)$ is defined as the final shear resistance of the damaged column, which considers only the transverse steel that is effectively anchored. The overall shear capacity of the column can then be modeled by a trilinear curve as shown in Figure 4.28.

Three possible cases mentioned in the FHWA manual are considered for evaluating the capacity over demand, C/D_{shear}, ratio for column shear. Case A represents the situation where the initial shear capacity $V_i(c)$ is lower than the shear demand $V_u(d)$. Case B reflects the situation where the shear demand is lower than $V_i(c)$ but higher than $V_f(c)$. Case C is when the shear demand is lower than $V_i(c)$ and $V_f(c)$. The three cases are treated as described next.

Case A: If the initial shear resistance of the undamaged column is insufficient to withstand the maximum shear force due to plastic hinging, $[V_i(c) < V_u(d)]$, a brittle shear failure may occur prior to the formation of a plastic hinge. In this case, the ultimate system capacity P_u is estimated by multiplying P_{p1}, which is the capacity of the system when one column reaches its moment capacity by C/D_{shear} ratio, which is defined as $C/D_{shear} = V_i(c)/V_u(d)$:

$$P_u = P_{p1}\frac{V_i(c)}{V_u(d)} \tag{4.27}$$

Case B: If the initial shear resistance of the column is sufficient to withstand the maximum shear force due to plastic hinging, but the final shear resistance of the column is not, $[V_i(c) > V_u(d) > V_f(c)]$, then $\gamma_v = C/D_{shear}$ ratio for column shear will depend on the amount of flexural yielding, which will cause a degradation in shear capacity from $V_i(c)$ to $V_u(d)$. The shear reduction factor γ_v is used to reduce φ_u using the following equations:

$$\gamma_V = \frac{V_i(c) - V_u(d)}{V_i(c) - V_f(c)} \tag{4.28}$$

$$P_u = P_{p1}\left[F_{mc} + C_\phi \frac{\gamma_V \varphi_u - \varphi_{tunc}}{\varphi_{tconf} - \varphi_{tunc}}\right] \tag{4.29}$$

such that $\gamma_V \varphi_u \approx$ effective curvature for columns weak in shear.

Case C: If the final shear resistance of the column is sufficient to withstand the maximum shear force due to plastic hinging, $[V_f(c) > V_u(d)]$, then no modification shall be made to Equation 4.2.

As described in the FHWA manual, the method proposed for evaluating the effect of column shear failure on bridge system redundancy is based on engineering judgment and assumes an idealized model of shear column behavior. This method may be visualized by examining the assumed relationships between shear capacity and shear demand as shown in Figure 4.28. Case A occurs when the column cannot achieve flexural yielding because of a low initial shear capacity. In this case, the column's C/D_{shear} ratio is calculated by dividing the initial shear capacity of the column by the shear demand. Case B will result when a shear failure is expected to occur due to shear capacity degradation resulting from plastic hinging of the column. Case C is assumed when the degradation in column shear capacity is not expected to result in a shear failure.

Weak shear model verification: The implementation of Equation 4.27 for Case A for brittle shear failures is straightforward. For Case C, shear failure will not take place because the shear capacity of the columns is sufficient to withstand the maximum shear force due to plastic hinging. Therefore, Equation 4.2 is valid without any modification. On the other hand, Equations 4.28 and 4.29 need to be validated for columns that meet the Case B criteria.

Following the FHWA manual's model of Figure 4.28, the shear capacity of a Case B column starts to decrease when the ductility is larger than 2.0 as the concrete damages during the pushover analysis. As shown in Figure 4.28, the reduction in the shear capacity will not allow the curvature of the column section to reach its ultimate value and failure takes place at a lower ductility. Based on Figure 4.28, a measure of the ductility reduction can be calculated as

$$\gamma_V = \frac{V_i(c) - V_u(d)}{V_i(c) - V_f(c)}$$

where $V_i(c)$ = initial shear resistance of the undamaged column including the resistance of the gross concrete section and the transverse steel, $V_f(c)$ = final shear resistance of the damaged column accounting for the transverse steel that is effectively anchored, and $V_u(d)$ = demand shear force.

When $V_u(d) = V_f(c)$ the shear reduction factor is $\gamma_v = 1.0$. This means that the shear resistance of the column is sufficient to withstand the maximum shear force due to plastic hinging and no reduction in the column's ductility capacity is observed. When $V_u(d) = V_i(c)$ the shear reduction is $\gamma_v = 0$, which means that the initial shear resistance is only capable of withstanding the linear-elastic loading stage after which point the column fails in shear with very little ductility. In this case, we assume that the column will fail at or close to the initiation of plastic hinging.

Based on the logic described above and assuming a linear relationship between the moment and the shear, as well as a linear relationship between the moment and the curvature, the shear reduction factor can be approximately used to express the reduction in the curvature capacity of the column using the schematic of Figure 4.29. Therefore, the shear reduction factor γ_v can be applied in Equation 4.29 to obtain the ultimate capacity of a multi-column bridge system whose column may be weak in shear. In the following parts of this section, the validity of the model is verified by comparing the results obtained using Equation 4.29 and those obtained from SAP2000 for columns with different levels of shear capacity.

To demonstrate the validity of the proposed approach for treating bridges with potential weaknesses in shear strength, several bridge systems with different levels of shear capacity are analyzed. The three-span multi-girder steel bridge with three columns per bent is used as the base case for the analyses described in this section. Two analyses are performed: the first analysis is performed assuming that the M-phi curve is elasto-plastic in order to find P_{p1} and the results are used to find an approximation to the shear demand force $V_u(d)$, which is assumed to be the shear force when one column reaches its plastic moment capacity M_p. The second analysis accounts for the nonlinear M-phi curve as well as the ductile shear hinge to find P_u. As shown in Figure 4.28, the shear hinge model requires as input the initial shear capacity $V_i(c)$ and the displacement Δ_y, which is the displacement at which M_p is reached and that can be taken from the first linear-elastic analysis. The model assumes that the shear force capacity begins to degrade when the displacement is $2\Delta_y$. Also, the shear hinge model requires the final shear capacity $V_f(c)$,

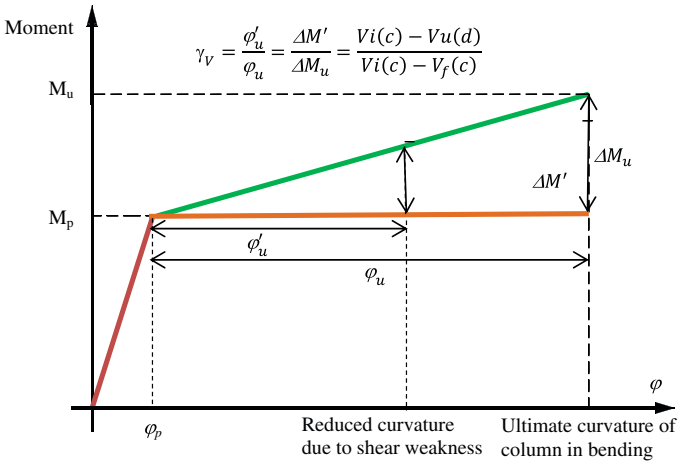

Figure 4.29. Relationship between insufficient shear capacity, moment, and curvature.

which is assumed to be reached when the displacement is at 5 Δ_y. A linear interpolation is used to find the shear capacity when the displacement is between 2 Δ_y and 5 Δ_y.

Following the shear-strength models of Ang et al. (1989) and Wong et al. (1993) that have been used in the FHWA manual, the initial shear force capacity is defined by

$$V_i(c) = V_{si} + V_{ci} \tag{4.30}$$

where V_{si} is the shear strength due to the reinforcing steel and V_{ci} is the shear strength due to the concrete. The steel's contribution to the shear capacity is

$$V_{si} = \frac{\pi}{2}\frac{A_{sh} f_{yh} D'}{s} \tag{4.31}$$

and the concrete shearing strength is

$$V_{ci} = 0.37\alpha\left(1 + \frac{3P}{f_c' A_g}\right)\sqrt{f_c'}A_e \qquad \text{(in megapascals)} \tag{4.32a}$$

$$V_{ci} = 4.45\alpha\left(1 + \frac{3P}{f_c' A_g}\right)\sqrt{f_c'}A_e$$

(in pounds per square inch) (4.32b)

where the column aspect ratio α is equal to 1.0, and D and D′ = column diameter and core diameter measured to the centerline of the transverse hoop or spiral, which has a cross-sectional area A_{sh} and yield strength f_{yh}. The effective shear area is $A_e = 0.8A_g$.

According to the FHWA manual, the final shearing force $V_f(c)$ is shear capacity of the transverse steel that is effectively anchored represented by V_{si} and residual concrete capacity is not considered.

To verify the validity of Equation 4.29, 16 bridge models with columns having various diameters ranging from 3-ft to 8-ft and different column heights in the range of 16.7-ft up to 40-ft are investigated. All column sections have a transverse confinement ratio of 0.3%. The results of shear capacities, shear demand, shear reduction factors, first column yielding displacement, plastic capacity P_{p1}, and system ultimate capacity P_u obtained from the SAP2000 analysis are listed in Table 4.19. The SAP2000 results are compared to P_u predicted by Equation 4.29 showing a maximum difference on the order of 13%.

Figure 4.30 plots all the data of the predicted P_u versus the pushover analysis values. The trend line in Figure 4.30 shows a trend line with a slope equal to 1.02 and regression coefficient $R^2 = 0.99$. A perfect model would produce a slope equal to 1.00 and $R^2 = 1.0$. The results in Figure 4.30 demonstrate that the proposed shear reduction factor approach can be used to estimate the reduction in the column's curvature due to weaknesses in the shear capacity of bridge columns.

Implementation Example: Shear Example for Case A—If the initial shear resistance of the undamaged column is insufficient to withstand the maximum shear force due to plastic

Table 4.19. Results summary for Case B.

Dia. In.	Col. Length In.	V_u(d) Kips	$V_i(c)=V_{ci}+V_f$ Kips	V_{ci} kips	V_f(c) kips	γ_V	Δy In.	P_u by SAP kips	P_{p1} kips	φ_u $in^{-1}x10^{-3}$	Esti. P_u kips	Error
36	391	101	343	251	92	0.96	3.79	1078	723	1.06	934	-13%
36	300	131	343	251	92	0.84	2.28	1125	802	1.06	1017	-10%
36	200	193	343	251	92	0.60	1.07	1392	1042	1.06	1265	-9%
72	480	436	1305	939	366	0.93	3.57	3152	2314	0.717	2825	-10%
72	400	507	1305	939	366	0.85	2.61	3563	2621	0.717	3171	-11%
72	300	639	1305	939	366	0.71	1.62	4447	3234	0.717	3847	-13%
84	480	783	1768	1270	499	0.78	2.52	4956	4518	0.574	5315	7%
84	440	850	1768	1270	499	0.72	2.15	5299	4858	0.574	5686	7%
84	400	930	1768	1270	499	0.66	1.81	5753	5264	0.574	6122	6%
84	360	1026	1768	1270	499	0.58	1.50	6284	5754	0.574	6641	6%
84	320	1145	1768	1270	499	0.49	1.22	7004	6355	0.574	7266	4%
84	280	1294	1768	1270	499	0.37	0.97	7914	7109	0.574	8031	1%
84	240	1487	1768	1270	499	0.22	0.75	9095	8080	0.574	8985	-1%
84	200	1749	1768	1270	499	0.02	0.57	9887	9375	0.574	10201	3%
96	280	1836	2303	1652	651	0.28	0.92	11483	10228	0.516	11413	-1%
96	240	2101	2303	1652	651	0.12	0.72	12186	11603	0.516	12753	5%

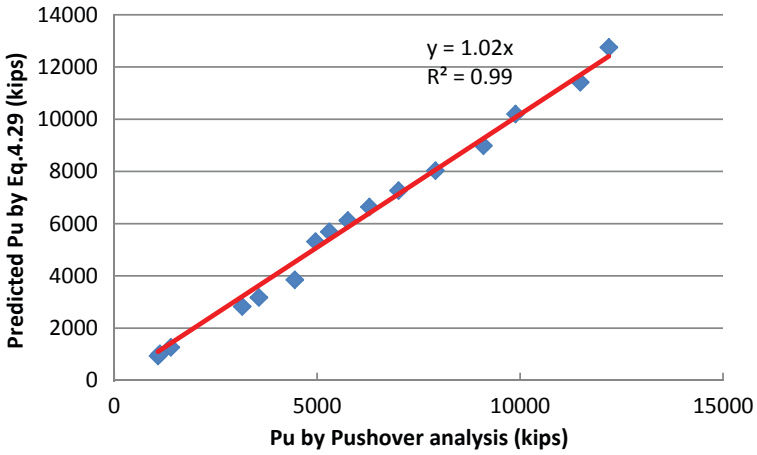

Figure 4.30. Estimated Pu by Equation 4.29 vs. Pu from SAP2000.

hinging, $[V_i(c) < V_u(d)]$, a brittle shear failure may occur prior to the formation of a plastic hinge and the C/D_{shear} ratio may be calculated and multiplied by the capacity when one column reaches the plastic moment of the weakest column in the bent, such that

$$P_u = P_{p1}\frac{V_i(c)}{V_u(d)}$$

This example assumes that the bridge has three-column bents where the lateral confinement reinforcement ratio in the columns is $\rho_s = 0.3\%$ (detail category B) and the longitudinal reinforcement ratio is $\rho = 1.66\%$. Each column's height is 16.67-ft with a 7-ft diameter. The columns are based on stiff foundations that are assumed to be fixed and the cap beam is also assumed to be very rigid. The reinforcement is assumed to have a yielding stress $F_y = 60$ ksi. The unconfined concrete strength is assumed to be 4 ksi. The axial force on a single column is equal to 130 kip. A cross-section analysis shows that the plastic moment capacity M_p is 197,400 kip-in. The pushover analysis shows that the first column reaches its plastic capacity when the lateral force is $P_{p1} = 6{,}355$ kip.

The steps necessary to obtain the maximum ultimate capacity of the system and the system factor ϕ_s are as follows:

1. Determine the shear capacity contributed by concrete V_{ci}.

$$V_{ci} = 4.45\alpha\left(1+\frac{3P}{f_c'A_g}\right)\sqrt{f_c'}A_e$$

$$= 4.45(1.0)\left(1+\frac{3\times 130{,}000}{4000\times\pi\times 84^2/4}\right)$$

$$\sqrt{4000}\,(0.8)(\pi)(84^2)/4/1000$$

$$= 1270\ kips$$

2. Determine the shear capacity contributed by reinforcement V_{si}. For a circular column with hoop reinforcement, the lateral confinement ratio is expressed as

$$\rho_s = \frac{V_s}{V_c} = \frac{\pi D' A_{sh}}{s\pi D'^2/4} = \frac{4A_{sh}}{sD'}$$

Where, D' = column core diameter measured to the centerline of the transverse hoop, which has a cross-sectional area A_{sh} and yield strength f_{yh}. S is spacing of hoops. The effective shear area is $A_e = 0.8A_g$.

The shear capacity due to the steel is

$$V_{si} = \frac{\pi}{2}\frac{A_{sh}f_{yh}D'}{s} \qquad \text{where } s = \frac{4A_{sh}}{\rho_s D'}$$

which leads to

$$V_{si} = \frac{\pi}{2}A_{sh}f_{yh}D'\frac{\rho_s D'}{4A_{sh}} = \frac{\pi f_{yh}\rho_s D'^2}{8}$$

$$= \frac{3.1416(60)(0.003)(84)^2}{8} = 499\ kips$$

3. Determine initial shear resistance of the undamaged column $V_i(c)$.

$$V_i(c) = V_{ci} + V_{si} = 1{,}270 + 499 = 1{,}769\ kips$$

4. Determine the maximum column shear force resulting from plastic hinging $V_u(d)$. For this simple example, an approximation to the shear demand can be obtained as $V_u(d) = M_u/L_{ceff}$. For the fixed-fixed column $V_u(d) = M_u/L_{ceff} = 2M_u/L = 2 \times 197{,}400/200 = 1{,}974$ kips.
5. Estimate the ultimate system capacity.

Since $V_i(c) = 1{,}769$ kips $< V_u(d) = 1{,}974$ kips, a brittle shear failure will occur prior to the formation of a plastic

hinge during the pushover analysis. Therefore, according to Equation 4.27, the lateral load capacity of the entire bridge system is

$$P_u = P_{p1}\frac{V_i(c)}{V_d(d)} = 6{,}355 \times \frac{1{,}769}{1{,}974} = 5{,}695\ kip$$

6. Find the system factor. This bridge system will fail in brittle shear and is non-redundant. Therefore, the bridge columns should be evaluated using a system factor equal to

$$\phi_s = \exp^{-\xi \times \Delta\beta_{u\,target}}\left[F_{mc} + C_\varphi \frac{\varphi_u - \varphi_{tunc}}{\varphi_{tconf} - \varphi_{tunc}}\right]$$

$$= \exp^{-0.6\times 0.5}\left(\frac{5{,}695}{6355}\right) = 0.66$$

Implementation Example: Shear Example for Case B

If the initial shear resistance of the column is sufficient to withstand the maximum shear force due to plastic hinging, but the final shear resistance of the column is not, [$V_i(c) > V_u(d) > V_f(c)$], then the C/D_{shear} ratio for the column will depend on the extent of flexural yielding, which will cause a degradation in the shear capacity from $V_i(c)$ to $V_u(d)$. The ultimate curvature capacity of the column φ_u obtained from the ultimate bending capacity is multiplied by the shear reduction factor γ_v to obtain the actual curvature at failure and the system capacity is calculated from

$$P_u = P_{p1}\left[F_{mc} + C_\varphi \frac{\gamma_v\varphi_u - \varphi_{tunc}}{\varphi_{tconf} - \varphi_{tunc}}\right]$$

where $\gamma_V = \dfrac{V_i(c) - V_u(d)}{V_i(c) - V_f(c)}$

$\gamma_V\varphi_u \approx$ effective curvature

This example assumes the same multi-girder three-span bridge with two three-column bents where the lateral confinement reinforcement ratio is $\rho_s = 0.3\%$ (detail category B) and the longitudinal reinforcement ratio is $\rho = 1.66\%$. The column height is 26.7-ft with a 7-ft diameter. The columns are fixed to the stiff foundation and the rigid cap beam. The reinforcement is assumed to have a yielding stress $F_y = 60$ ksi. The unconfined concrete strength is assumed to be 4 ksi. The axial load is 130 kips and the plastic moment capacity of the column M_p is 197,400 kip-in. The pushover analysis assuming elastic behavior indicates that the first column reaches its plastic moment capacity at $P_{p1} = 6{,}355$ kip. The nonlinear pushover analysis shows that the ultimate lateral load capacity is P_u is 7003.8 kip.

The steps necessary to obtain the maximum ultimate capacity of the system and the system factor ϕ_s are as follows:

1. Determine the shear capacity contributed by concrete, V_{ci}.

$$V_{ci} = 4.45\alpha\left(1 + \frac{3P}{f_c'A_g}\right)\sqrt{f_c'}A_e$$

$$= 4.45(1.0)\left(1 + \frac{3\times 130{,}000}{4000\times\pi\times 84^2/4}\right)$$

$$\sqrt{4000}\,(0.8)(\pi)(84^2)/4/1000$$

$$= 1270\ kip$$

2. Determine the shear capacity contributed by the reinforcement V_{si}. For a circular column with hoop reinforcement, the lateral confinement ratio is expressed as

$$\rho_s = \frac{V_s}{V_c} = \frac{\pi D' A_{sh}}{s\pi D'^2/4} = \frac{4A_{sh}}{sD'}$$

where, D' = column core diameter measured to the centerline of the transverse hoop, which has a cross-sectional area A_{sh} and yield strength f_{yh}. S is spacing of hoops. The effective shear area is $A_e = 0.8A_g$.

The steel shear capacity is

$$V_{si} = \frac{\pi}{2}\frac{A_{sh}f_{yh}D'}{s} \text{ where } s = \frac{4A_{sh}}{\rho_s D'}$$

By combining the two equations, the contribution of the steel reinforcement to the shear capacity is

$$V_{si} = \frac{\pi}{2}A_{sh}f_{yh}D'\frac{\rho_s D'}{4A_{sh}} = \frac{\pi f_{yh}\rho_s D'^2}{8}$$

$$= \frac{3.1416(60)(0.003)(84)^2}{8} = 449\ kips$$

The final shear resistance of the damaged column, $V_f(c)$, includes only that transverse steel which is effectively anchored, giving $V_f(c) = V_{si} = 499\ kip$.

3. Determine the initial shear resistance of the undamaged column $V_i(c)$.

$$V_i(c) = V_{ci} + V_{si} = 1{,}270 + 499 = 1{,}769\ kip$$

4. Determine the maximum column shear force resulting from plastic hinging $V_u(d)$.

Assuming elastic behavior, the pushover analysis indicates that the first column reaches its plastic moment

capacity when the load is P_p = 6355 kip. At that load, the shear force in the column is assumed to be equal to the demand shear force $V_u(d)$, which is equal to 1,145 kip.

Another way to estimate this lateral force $V_u(d)$ is to use the equation $V_u(d) = M_u/L_{ceff}$. For a fixed-fixed column, $V_u(d) = M_u/L_{ceff} = 2M_u/L = 2 \times 197{,}400/320 =$ 1,234 kips. The 8% difference between the two approaches is partially due to the flexibility of the cap beam but also due to the axial forces that are obtained in the column when the pushover analysis is performed as compared to the M_u/L_{ceff} approach that ignores the axial forces.

5. Determine the shear reduction factor and find load factor P_u. According to Equation 4.28, the reduction factor for the ultimate curvature is found from

$$\gamma_V = \frac{V_i(c) - V_u(d)}{V_i(c) - V_f(c)} = \frac{1769 - 1145}{1769 - 449} = 0.49$$

and the ultimate system capacity for the bridge is

$$P_u = P_{p1}\left[F_{mc} + C_\varphi \frac{\gamma_V \varphi_u - \varphi_{tunc}}{\varphi_{tconf} - \varphi_{tunc}}\right]$$
$$= 6{,}355\left[1.16 + 0.24\frac{0.49(5.74\times10^{-4}) - 3.64\times10^{-4}}{1.55\times10^{-3} - 3.64\times10^{-4}}\right]$$
$$= 7{,}266\ kip$$

The pushover analysis would give P_u = 7003.8 kip. The error in P_u observed when Equation 4.29 is used as compared to the pushover analysis is

$$\varepsilon = \frac{7266 - 7003.8}{7003.8} \times 100\% = 4\%$$

Using the more approximate $V_u(d) = M_u/L_{ceff}$, the shear reduction factor is calculated as

$$\gamma_V = \frac{V_i(c) - V_u(d)}{V_i(c) - V_f(c)} = \frac{1769 - 1234}{1769 - 449} = 0.405$$

and the ultimate system capacity is

$$P_u = P_{p1}\left[F_{mc} + C_\varphi \frac{\gamma_V \varphi_u - \varphi_{tunc}}{\varphi_{tconf} - \varphi_{tunc}}\right]$$
$$= 6{,}355\left[1.16 + 0.24\frac{0.405(5.74\times10^{-4}) - 3.64\times10^{-4}}{1.55\times10^{-3} - 3.64\times10^{-4}}\right]$$
$$= 7{,}203\ kip$$

The error in P_u is $\varepsilon = \frac{7203 - 7003.8}{7003.8} \times 100\% = 3\%$

6. System factor.

This bridge system will fail in shear due to shear capacity degradation resulting from plastic hinging of the column and is non-redundant. Therefore, the bridge columns should be evaluated using a system factor equal to

$$\phi_s = \exp^{-\xi \times \Delta\beta_{u\ target}}\left[F_{mc} + C_\varphi \frac{\gamma_V \varphi_u - \varphi_{tunc}}{\varphi_{tconf} - \varphi_{tunc}}\right]$$
$$= \exp^{-0.6\times0.5}\left(\frac{7{,}203}{6{,}355}\right) = 0.84$$

The system factor is calculated to be, $\phi_s = 0.84$.

Implementation Example: Shear Example for Case C

If the final shear resistance of the column is sufficient to withstand the maximum shear force due to plastic hinging, $[V_f(c) > V_u(d)]$, then no modification shall be made to Equation 4.2.

In this example, the researchers assume that the bridge system and column properties are the same as those given in the previous example for Case B except for the column height, which is taken to be 33.33-ft, and the boundary condition, which is assumed to be pinned at the bottom, and the column is assumed to be fixed to the cap beam. The pushover analysis performed assuming elastic behavior shows that the lateral force P_{p1} at which the first column reaches its plastic moment capacity is P_{p1} = 5,263.8 kip. The nonlinear pushover analysis gives an ultimate capacity P_u = 6,122 kip.

Following the same steps outlined in the Case B example, the researchers find $V_f(c) = V_{si}$ = 499 kip. Also, for a fixed-pinned column, $V_u(d) = M_u/L_{ceff} = M_u/L$ = 197,400/400 = 493.5 kips < 499 kips = $V_f(c)$.

Therefore, no modification shall be made to Equation 4.2, and the ultimate system capacity is

$$P_u = P_{p1}\left[F_{mc} + C_\varphi \frac{\varphi_u - \varphi_{tunc}}{\varphi_{tconf} - \varphi_{tunc}}\right]$$
$$= 5{,}263.8\left[1.16 + 0.24\frac{5.74\times10^{-4} - 3.64\times10^{-4}}{1.55\times10^{-3} - 3.64\times10^{-4}}\right] = 6{,}330\ kip$$

If comparing results of the pushover analysis, the researchers find that the error in P_u is $\varepsilon = \frac{6{,}330 - 6{,}122}{6{,}122} \times 100\% = 3.4\%$

This bridge system will fail in ductile bending and the columns should be evaluated using a system factor equal to

$$\phi_s = \exp^{-\xi \times \Delta\beta_{u\ target}} \left[F_{mc} + C_{\varphi} \frac{\varphi_u - \varphi_{tunc}}{\varphi_{tconf} - \varphi_{tunc}} \right]$$

$$= \exp^{-0.6 \times 0.5} \left(\frac{6,330}{5,263.8} \right) = 0.89$$

The system factor is calculated to be, $\phi_s = 0.89$ which is higher than that needed when the failure is due to shear.

4.5 Conclusions

This chapter presents the proposed model for estimating the system capacity of bridge systems subjected to uniform lateral load at the superstructure level and how the model can be used to define system factors that can be applied during the safety evaluation of new and existing bridge systems. A summary of the results of the analyses conducted during the course of the project and those assembled from *NCHRP Report 458* to validate the proposed model is given. A method to adjust the model to account for weaknesses in the pier cap beams and weaknesses in the shear capacity of the columns also is described. Several examples of how the equation can be used for particular types of bridges are provided.

References

Ang, B. G., Priestley, M. J. N., and Paulay, T. (1989) "Seismic Shear Strength of Circular Reinforced Concrete Columns," *ACI Structural Journal* 86(1) 45–59.

Buckle, I., et al. (2006) *Seismic Retrofitting Manual for Highway Structures: Part 1—Bridges* (No. FHWA-HRT-06-032).

Collins, M. P. and D. Mitchell (1991) *Prestressed Concrete Structures.* Prentice-Hall, Englewood Cliffs, NJ.

Liu, D., et al. (2001) *NCHRP Report 458: Redundancy in Highway Bridge Substructures.* Transportation Research Board, National Research Council, Washington, D.C.

Mander, J. B. and Priestly, M. J. N. (1988) "Observed Stress-Strain Behavior of Confined Concrete," *Journal of Structural Engineering*, ASCE, 114(8) Aug, 1827–1849.

Wong, Y. L., Paulay, T., and Priestley, M. N. (1993) "Response of Circular Reinforced Concrete Columns to Multi-Directional Seismic Attack," *ACI Structural Journal* 90(2) 180–191.

CHAPTER 5

Calibration of System Factors for Bridges under Vertical Load

5.1 Measures of System Safety and Redundancy

Figure 5.1 gives a conceptual representation of the performance of a structure under increasing loads and the different levels that should be considered when evaluating member safety, system safety, and system redundancy. For example, the green line labeled "Intact system" may represent the applied load versus maximum vertical displacement of a ductile multi-girder bridge superstructure. In this case, the load is incremented to study the behavior of an intact system that was not previously subjected to any damaging load or event when the system is subjected to increasing live loads. The bilinear brown line represents the behavior assumed using traditional linear-elastic analysis methods. The blue line labeled "Damaged bridge" represents the response of a bridge system that has been previously damaged by deterioration, overloading, or an extreme event.

To obtain the response of the originally intact system, it is assumed that the vertical live load applied on the structure has the configuration of the AASHTO HS-20 vehicle. The bridge is first loaded by the dead load and then the HS-20 load is applied. Usually, due to the presence of safety factors, no failure occurs after the application of the dead load plus the HS-20 load. Using traditional safety evaluation procedures, the first structural member is assumed to fail when the HS-20 truck weight is multiplied by a factor LF_1. LF_1 would then be related to member safety. Note that if the bridge is under designed, or has major structural deficiencies, it is possible to have LF_1 less than 1.0. Although the analysis can be performed using any basic truck model, the HS-20 truck configuration is used because it is the standard truck in the AASHTO specifications.

Generally, the actual behavior follows the green curve and the ultimate capacity of the entire bridge system is not reached until the HS-20 truck weight is multiplied by a factor LF_u. LF_u would give an evaluation of system safety. Large vertical deformations rendering the bridge unfit for use are reached when the HS-20 truck weight is multiplied by a factor LF_f. LF_f gives a measure of system functionality. A bridge that has been loaded up to this point is said to have lost its functionality.

If the bridge has sustained major damage due to the failure of one or more of its members, its behavior is represented by the curve labeled "Damaged bridge." Examples of damaged bridges include structures that may have lost or suffered reduced member capacities in one or several members due to an extreme event such as collisions, fire, blast, fatigue fracture, or major degradation of member capacity caused by corrosion or deterioration. In these cases, the ultimate capacity of the damaged bridge is reached when the weight of the HS-20 truck is multiplied by a factor LF_d. LF_d would give a measure of the remaining safety of a damaged system.

The load multipliers, LF_1, LF_f, LF_u, and LF_d provide deterministic estimates of critical limit states that describe the safety of a structural system in its original intact state and its damaged state. These load multipliers are usually obtained by performing an incremental nonlinear finite element analysis of the structure. Because of the presence of large uncertainties in estimating the parameters that control member properties, the bridge response, and the applied loads, the safety of the bridge members or system may be represented by the probability of failure, P_f, or the reliability index, β.

Both P_f and β can be evaluated for each of the four critical limit states identified in Figure 5.1. Assuming that the load carrying capacity and the load follow lognormal distributions, the relationship between the reliability index and the load multipliers, LF, for a bridge superstructure subjected to multiples of the HS-20 truck loading can be approximated as

$$\beta = \frac{\ln\left(\frac{\overline{R}-\overline{D}}{\overline{P}}\right)}{\sqrt{V_{R-D}^2+V_P^2}} = \frac{\ln\left(\frac{\overline{R'}}{\overline{P}}\right)}{\sqrt{V_{R'}^2+V_P^2}} = \frac{\ln\left(\frac{\overline{LF}\times HS20}{\overline{LL}\times HS20}\right)}{\sqrt{V_{LF}^2+V_{LL}^2}} = \frac{\ln\left(\frac{\overline{LF}}{\overline{LL}}\right)}{\sqrt{V_{LF}^2+V_{LL}^2}} \quad (5.1)$$

where $R' = R - D$ in this case represents the ability of the system to carry live load or the strength in the system beyond the dead load. R' is related to the load multiplier obtained from

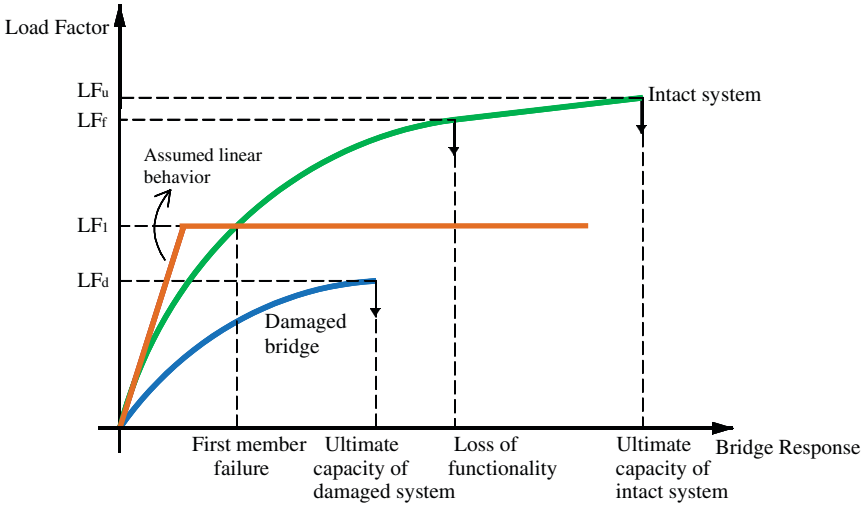

Figure 5.1. Representation of typical behavior of bridge systems.

the incremental analysis by $R' = LF \times HS20$. The applied live load $P = LL \times HS20$ is the expected maximum live load that will be applied on the superstructure within the appropriate service period. *HS20* is the load effect of the nominal HS-20 design truck. V_{LF} is the COV of the bridge resistance defined as the standard deviation divided by the mean value. V_{LL} is the COV of the applied live load. Equation 5.1 gives a good approximation to the actual reliability index β as long as the COV V_{LF} and V_{LL} remain below 20%, which is generally the case for bridge superstructures subjected to vertical live loads. Several sensitivity analyses have indicated that the lognormal model provides a reasonable model for system reliability index calculations in bridge engineering (Ghosn et al., 2010, 2012).

In Equation 5.1, both the resistance and the applied live load are expressed as a function of the HS-20 truck load effect, which can then be factored out. The same formulation can be executed if the analysis is performed using a different nominal load such as the HL-93 design load or the AASHTO legal trucks.

If redundancy is defined as the capability of a structure to continue to carry loads after the failure of the most critical member, then comparisons between the load multipliers LF_u, LF_f, LF_d, and LF_1 would provide non-subjective and quantifiable measures of system redundancy. Thus, the following three deterministic measures of system redundancy may be defined in terms of the ratio of the system's capacity as compared to the most critical member's capacity:

$$R_u = \frac{LF_u}{LF_1}$$

$$R_f = \frac{LF_f}{LF_1} \qquad (5.2)$$

$$R_d = \frac{LF_d}{LF_1}$$

where R_u = system reserve ratio for the ultimate limit state, R_f = system reserve ratio for the functionality limit state, R_d = system reserve ratio for the damage condition. R_u, R_f, and R_d can thus be used as measures of system redundancy as they represent the ability of a system to carry load beyond the failure of the most critical member.

The system reserve ratios of Equation 5.2, as defined in *NCHRP Report 406* and *NCHRP Report 458*, provide nominal deterministic measures of bridge redundancy. For example, when the ratio R_u is equal to 1.0 ($LF_u = LF_1$), the ultimate capacity of the system is equal to the capacity of the bridge to resist failure of its most critical member. Such a bridge is non-redundant. As R_u increases, the level of bridge redundancy increases.

A redundant bridge also should be able to function without leading to high levels of deformations as its members undergo large nonlinear deformations. Thus, R_f provides another measure of redundancy.

Similarly, a robust bridge structure should be able to carry some load after damage to one or more of its members, and R_d would provide another quantifiable non-subjective measure of structural redundancy.

During the course of this study and upon the review of *NCHRP Report 406* results, it was established that a strong correlation exists between LF_f and LF_u obviating the need to use both of these measures. The strong correlation between LF_f and LF_u has been discussed in Chapter 2 and presented in Figures 2.3 and 2.4. This strong correlation led the calculations in *NCHRP Report 406* to produce similar system factors for the ultimate capacity and functionality limit states. For this reason, the analyses performed in this chapter are based on the ultimate capacity LF_u, and the analysis of system redundancy will be represented by R_u for the originally intact system and R_d for a damaged system.

The load multipliers, LF_i, and the system reserve ratios in Equation 5.2 provide deterministic estimates of system safety and redundancy while Equation 5.1 can be used to determine the reliability index, β, for any member or system limit state. The reliability indices corresponding to the load multipliers LF_1, LF_u, or LF_d of Figure 5.1 may be expressed respectively as β_{member}, $\beta_{ultimate}$, and $\beta_{damaged}$. The relationship between these three reliability indices can be investigated by studying the differences between them. This is achieved by defining $\Delta\beta_u$ and $\Delta\beta_d$ to be respectively the reliability index margins for the system's ultimate and damaged limit states as

$$\Delta\beta_u = \beta_{ultimate} - \beta_{member}$$
$$\Delta\beta_d = \beta_{damaged} - \beta_{member} \tag{5.3}$$

The reliability index margins of Equation 5.3 give probabilistic measures of redundancy as they represent the additional safety provided by the system as compared to the safety of the most critical bridge member. These reliability measures are directly related to the deterministic measures defined in Equation 5.2. As an example, using the simplified lognormal reliability model of Equation 5.1 for a bridge system under the effect of vertical live loading and assuming that the COV of LF_u, LF_d, and LF_1 are all equal to the same value, V_{LF}, the relation between the probabilistic and deterministic measures of redundancy are obtained from

$$\Delta\beta_u = \beta_{ultimate} - \beta_{member} = \frac{\ln\left(\frac{\overline{LF_u}}{\overline{LL_{75}}}\right) - \ln\left(\frac{\overline{LF_1}}{\overline{LL_{75}}}\right)}{\sqrt{V_{LF}^2 + V_{LL}^2}}$$
$$= \frac{\ln\left(\frac{\overline{LF_u}}{\overline{LF_1}}\right)}{\sqrt{V_{LF}^2 + V_{LL}^2}} = \frac{\ln(R_u)}{\sqrt{V_{LF}^2 + V_{LL}^2}}$$
$$\Delta\beta_d = \beta_{damaged} - \beta_{member} = \frac{\ln\left(\frac{\overline{LF_d}}{\overline{LL_2}}\right) - \ln\left(\frac{\overline{LF_1}}{\overline{LL_{75}}}\right)}{\sqrt{V_{LF}^2 + V_{LL}^2}} \tag{5.4}$$
$$= \frac{\ln\left(\frac{\overline{LF_f}}{\overline{LF_1}}\frac{\overline{LL_{75}}}{\overline{LL_2}}\right)}{\sqrt{V_{LF}^2 + V_{LL}^2}} = \frac{\ln\left(R_d\frac{\overline{LL_{75}}}{\overline{LL_2}}\right)}{\sqrt{V_{LF}^2 + V_{LL}^2}}$$

In Equation 5.4, the live load for the ultimate and first member failure limit states is taken as the 75-year maximum live load to remain consistent with the AASHTO LRFD specifications that assume that a bridge structure should have a design life equal to 75 years. However, for damaged bridges under the effect of live load, the calculation of the reliability index for the damaged system is executed using the 2-year maximum load represented by the load multiplier, LL_2, rather than the maximum load for the 75-year design life. The use of the 2-year load is based on the assumption that any major damage to a bridge should, in a worst case scenario, be detected during the mandatory biennial inspection cycle and thus no bridge is expected to remain damaged for more than 2 years.

Because bridge engineers are not expected to perform incremental load analyses or reliability analyses and use the reliability index margins to ascertain the level of redundancy of typical bridge configurations, *NCHRP Report 406* proposed to calibrate system factors that can be directly used in the design-check equation to account for the redundancy of typical bridge structural systems. The process followed to establish the system factors is described in Chapter 2 and is expanded in Section 5.3 for bridge systems under vertical loads. The calibration of the system factors requires the results of the analyses of typical bridge configurations that have been designed to meet current design standards, those that do not meet the standards, as well as those that may be overdesigned. The analysis compares the ultimate system capacity of originally intact systems as well as the capacity of damaged systems. Section 5.2 summarizes the results for the originally intact systems analyzed in this study and in *NCHRP Report 406.* Section 5.4 calibrates the system factors for the originally intact systems. Section 5.5 summarizes the results of the analysis for the damaged systems. Section 5.6 calibrates the system factors for the damaged bridges.

5.2 Summary of Bridge Analysis and Results for Originally Intact Systems

The bridges analyzed in this study consist of continuous three-span composite steel I-girder bridges with two bents supported by three columns each, simple-span and continuous three-span composite steel tub girders, and simple-span and continuous span prestressed concrete spread box girders. The results of these analyses are supplemented by the results of simple-span and two-span continuous composite steel I-girder bridges and simple-span and two-span continuous prestressed concrete I-girder bridges performed in *NCHRP Report 406.* Validation of the results of the nonlinear analyses was made by comparing analytical results of representative bridges using the simplified space frame models adopted in this study and the results of more advanced finite element models and experimental test results. These comparisons have demonstrated that the 3-D space frame models were reasonably accurate and can be used for the purposes of this study.

Prestressed Concrete I-Girder Bridges

Many simple-span and continuous-span prestressed I-girder bridges were analyzed in *NCHRP Report 406.* The results of these analyses were extracted for this project to study how the redundancy of these bridges varies with the number of beams, beam spacing, and span length. Specifically, over 100 simple-span

bridges varying in length between 45-ft and 150-ft with a composite concrete deck supported by 4, 6, 8, and 10 beams spaced at 4-ft, 6-ft, 8-ft, 10-ft, and 12-ft are analyzed. Also, over 50 prestressed concrete I-girder bridges with two continuous spans varying in length between 100-ft and 150-ft supported by 4, 6, 8 and 10 beams spaced at 4-ft, 6-ft, 8-ft, 10-ft, and 12-ft are investigated. The bridges' concrete slabs varied in depth between 7.5-in. and 8.5-in. depending on the beam spacing. The beams are assumed to have a compressive concrete strength $f'_c = 5$ ksi while the deck's strength is equal to $f'_c = 3.5$ ksi. The prestressing tendons are assumed to be 270-ksi steel. The bridges were designed to exactly satisfy the strength requirements of the AASHTO LRFD design specifications. This was done even though normally it is the serviceability criteria that govern the design of prestressed members because bridge redundancy is related to member strength and ultimate system capacity. Sensitivity analyses also were performed to investigate the effect of changes in member strength, slab strength, and dead weight, as well as other parameters. The material data were used to obtain the moment-curvature relationships for the steel beams using analytical methods. The moment-curvature relationships were then used to perform the nonlinear analysis of the bridge. For the prestressed concrete bridges, the material data were used to obtain the moment-curvature relationships for the beams using analytical methods. The moment-curvature relationships were then used to perform the nonlinear analysis of the bridge.

The results of the analysis of the prestressed concrete I-girder bridges are separated into two groups: narrow bridges are defined as those that have four beams at 4-ft spacing, four beams at 6-ft spacing, and six beams at 4-ft spacing; all the other bridges are defined as wide bridges. The results of the wide bridges are used to compare the ultimate capacity of the originally intact bridge represented by LF_u to the capacity to resist first member failure represented by LF_1. The comparison showed that LF_u is highly dependent on LF_1 with a relationship that can be well represented by an equation of the form

$$LF_u = 1.16LF_1 + 0.75\gamma \tag{5.5}$$

where LF_u is the ultimate capacity of the originally intact system expressed in terms of the number of side-by-side HS-20 trucks that the bridge can carry when the ultimate capacity is reached. LF_1 is the load capacity at first member failure expressed in terms of the number of side-by-side HS-20 trucks that the system can carry before the first member reaches its load carrying capacity. γ is a normalized stiffness ratio that represents the stiffness of the non-composite beam member compared to the stiffness of the deck. For I-girder bridges, $\gamma = 1$.

The validity of Equation 5.5 for the response of simple-span and continuous prestressed concrete I-girder bridges is verified in Figure 5.2, which plots the results obtained from Equation 5.5 versus the results obtained from the nonlinear analysis in blue for simple-span and in red for continuous span bridges. These results are for bridges loaded by two side-by-side trucks in the middle of one span. These data exclude the results for narrow bridges consisting of four beams at 4-ft and 6-ft spacing and for six beams at 4-ft spacing. The plots show how the results follow a consistent trend that, for the wide bridges, is largely independent of span length, number of beams, or beam spacing. Also, the trend is largely independent of the beam

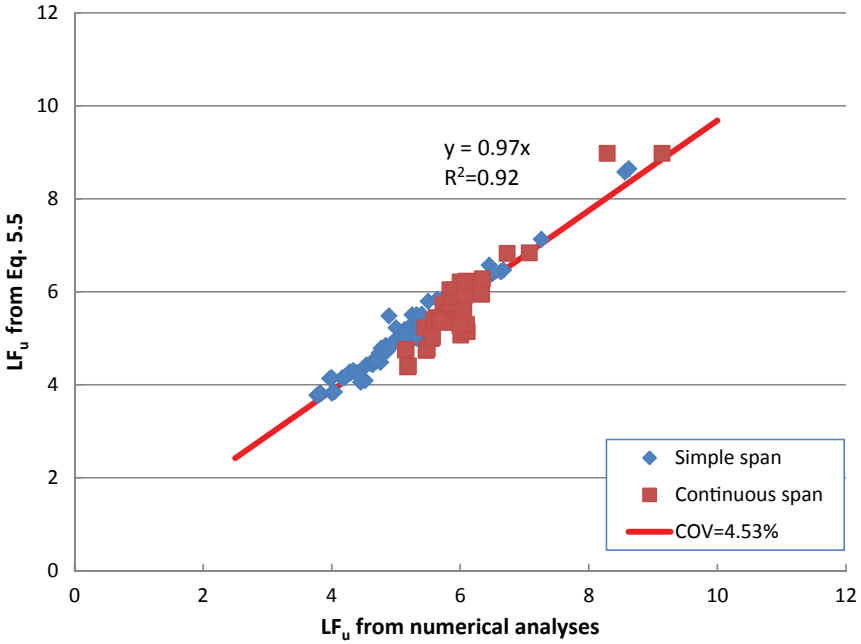

Figure 5.2. Verification of Equation 5.5 for prestressed concrete I-girder bridges.

strength and the dead load. The plot shows that the points lie close to a 45° line. The equation in the figure gives the equation of the trend line, which describes the relationship between the predicted LF_u obtained from Equation 5.5 and the calculated LF_u obtained from the nonlinear pushdown analysis of actual bridge systems. The trend line shows a slope equal to 0.97 and a coefficient of regression $R^2 = 0.92$. A perfect match would lead to a trend line having an equation of the form $y = 1.0\ x$ with a coefficient of regression $R^2 = 1.0$. The COV of the error between the predicted values and the analytical results is 4.53%.

Composite Steel I-Girder Bridges

Numerous simple-span and continuous-span composite-steel I-girder bridges were analyzed in *NCHRP Report 406*. The results of these analyses were extracted for this project to study how the redundancy of these bridges varies with the number of beams, beam spacing, and span length. Specifically, over 100 simple-span bridges varying in length between 45-ft and 150-ft with a composite concrete deck supported by 4, 6, 8, and 10 beams spaced at 4-ft, 6-ft, 8-ft, 10-ft, and 12-ft are analyzed. Also, over 30 composite steel I-girder bridges with two 120-ft continuous spans supported by 4, 6, 8, and 10 beams spaced at 4-ft, 6-ft, 8-ft, 10-ft, and 12-ft are investigated. The bridges' concrete slabs varied in depth between 7.5-in. and 8.5-in. depending on the beam spacing. The beams are assumed to be A-36 steel while the deck's strength is equal to $f'_c = 3.5$ ksi. The bridges were designed to exactly satisfy the strength requirements of the AASHTO LRFD design specifications. Sensitivity analyses also were performed to investigate the effect of changes in member strength, slab strength, and dead weight, as well as other parameters. The moment-rotation relationships for the bridges analyzed in *NCHRP Report 406* were obtained using existing empirical models based on test results as described in the appendices of *NCHRP Report 406*. The moment-rotation relationships were then used to perform the nonlinear analysis of the bridge. The analyses were performed assuming that the sections in negative bending are compact and the results are compared to the cases where the sections in negative bending are noncompact.

The results in *NCHRP Report 406* were supplemented by the results of the analysis of three-span continuous bridges with span lengths 50-ft, 80-ft, and 50-ft. The bridges were assumed to have 4, 5, or 6 beams at 8-ft spacing. The bridges were analyzed for different strengths and beam stiffness by assuming that they have different values for ultimate moment capacities and moments of inertia.

The results of the analysis of the wide composite steel I-girder bridges that compare the ultimate capacity of the originally intact bridge system represented by LF_u to the capacity to resist first member failure represented by LF_1 also were found to be well represented by Equation 5.5. The validity of Equation 5.5 with $\gamma = 1$ for the response of simple-span and continuous composite steel I-girder bridges is verified in Figure 5.3, which plots the results obtained from Equation 5.5 versus the results obtained from the nonlinear analysis in blue for simple-span

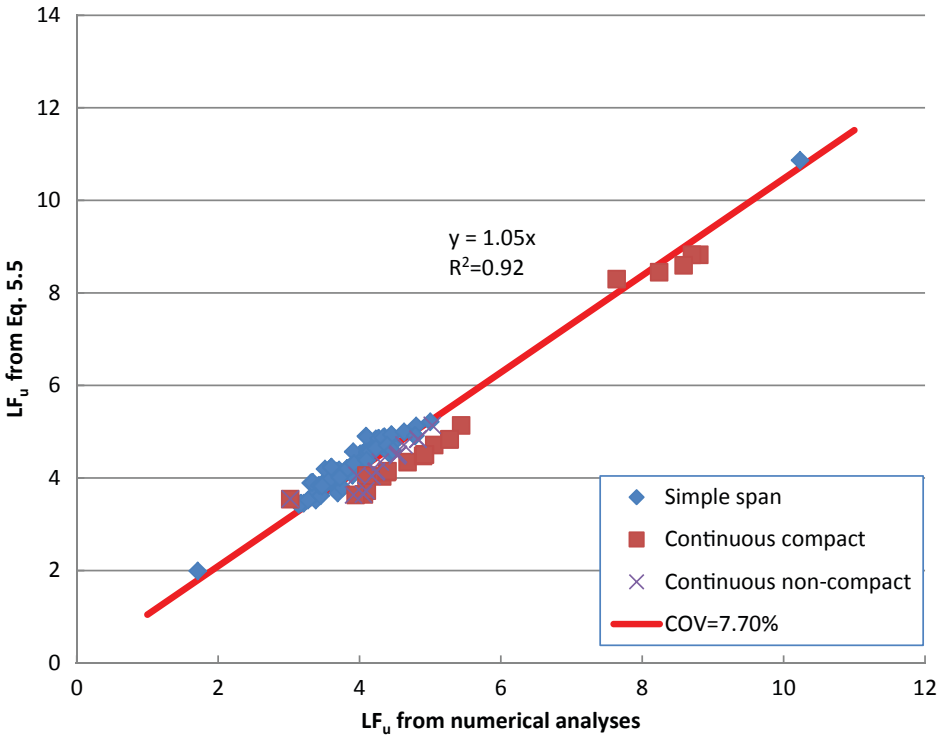

Figure 5.3. Verification of Equation 5.5 for composite steel I-girder bridges.

and in red for continuous span bridges. These results are for bridges loaded by two side-by-side trucks in the middle of one span. These data exclude the results for narrow bridges consisting of four beams at 4-ft and 6-ft spacing and for six beams at 4-ft spacing. The plots show how the results follow a consistent trend that, for the wide bridges, is largely independent of span length, number of beams, or beam spacing. Also, the trend is largely independent of the beam strength and the dead load. The plot shows that the points lie along a 45° line. The equation in the figure gives the equation of the trend line, which describes the relationship between the estimated LF_u obtained from Equation 5.5 and the calculated LF_u obtained from the nonlinear pushdown analysis of actual bridge systems. The trend line shows a slope equal to 1.05 and a coefficient of regression $R^2 = 0.92$. A perfect match would lead to a trend line having an equation of the form y = 1.0 x with a coefficient of regression $R^2 = 1.0$. The plot shows that Equation 5.5 under predicts the ultimate capacity of continuous bridges with noncompact sections by a very slight amount and those of continuous bridges with compact sections by a little more. However, the differences in the behavior of simple-span, continuous noncompact and continuous compact bridges are very small and can be ignored for the sake of keeping the prediction model as simple as possible. The COV of the error between the predicted values and the analytical results is 7.70%, which is quite reasonable given the large variations in the bridge geometries.

Prestressed Concrete Box-Girder Bridges

A 120-ft simply supported bridge consisting of twin prestressed concrete box girders was analyzed during this course of study. The spacing between the two boxes from center to center is 14′9″. The bridge width is 37′ with 10″ depth concrete slab and the box's depth is 6′10.5″. The boxes are assumed to have a compressive concrete strength $f'_c = 7.35$ ksi while the deck's strength is equal to $f'_c = 4.35$ ksi. Mander's model (Mander, 1984) was adopted for the stress-strain curve for concrete. The prestressing tendons are assumed to be 270-ksi steel.

Sensitivity analyses also were performed to investigate the effect of changes in member strength, dead load, and span continuity. The baseline continuous bridge has three spans at 80-ft, 120-ft, 80-ft. The analysis was performed for the narrow bridge configuration with one lane loaded. The results of the analysis of the prestressed concrete box-girder bridges that compare the ultimate capacity of the originally intact bridge represented by LF_u to the capacity to resist first member failure represented by LF_1 also were found to be well represented by Equation 5.5. However, for continuous box-girder bridges, the value of γ was found to depend on the stiffness of the box near the support as described in Equation 5.6. The modification to γ reflects the ability of continuous bridges with very high box stiffness to slab ratio to transfer the load longitudinally to the adjacent spans when the loaded span experiences nonlinear deformations as opposed to simple-span bridges and bridges with relatively low beam stiffness which would tend to transfer the load laterally to the other beams within the loaded span. The modified γ is expressed as

$$\gamma = \frac{\left[EI_{box} \Big/ \left(E_{slab} \frac{120 t_s^3}{12} \right) \right]}{38} \quad \text{for continuous box-girder bridges}$$

$$\gamma = 1 \quad \text{for other bridges} \qquad (5.6)$$

where EI_{box} is the stiffness of the non-composite main longitudinal girder equal to the modulus of elasticity E_{girder} in lb/in^2 times the moment of inertia I_{box} in in^4, $\left(E_{slab} \frac{120 t_s^3}{12} \right)$ is the stiffness of a 120-in. segment of the slab with a modulus of elasticity E_{slab} in lb/in^2 and a slab thickness t_s in inches. The value in the denominator is a typical stiffness ratio for I-girder bridges used as a baseline. The moment of inertia I_{box} is for the cracked section that ignores the portion of the concrete in tension.

The validity of Equation 5.5 with the modified γ of Equation 5.6 for the response of simple-span and continuous prestressed concrete box-girder bridges is verified in Figure 5.4, which plots the results obtained from Equation 5.5 versus the results obtained from the nonlinear analysis in blue for simple-span and in red for continuous span bridges. These results are for bridges loaded by one HS-20 truck in the middle of one span. The plots show how the results follow a consistent trend that is largely independent of the beam strength and the dead load. The plot shows that the points lie along a 45° line. The equation in the figure gives the equation of the trend line, which describes the relationship between the estimated LF_u obtained from Equation 5.5 and the calculated LF_u obtained from the nonlinear pushdown analysis of actual bridge systems. The trend line shows a slope equal to 1.01 and a coefficient of regression $R^2 = 0.98$. A perfect match would lead to a trend line having an equation of the form y = 1.0 x with a coefficient of regression $R^2 = 1.0$. The COV of the error between the predicted values and the analytical results is 6.27%.

In the final recommendation it is suggested that a $\gamma = 2$ be used as a conservative value to keep the approach simple.

Composite Steel Box-Girder Bridges

A twin steel tub girder bridge with sections having a box with 9″ plate thickness supporting a three-span continuous bridge was also analyzed as a baseline for studying the behavior of steel box-girder bridges. The bridge span configuration is 100-ft, 120-ft, 100-ft. The analyses also were performed on variations of the bridge assuming different member strengths. The results were supplemented with those of simple-span steel box bridges with different member strengths, span lengths, dimension of

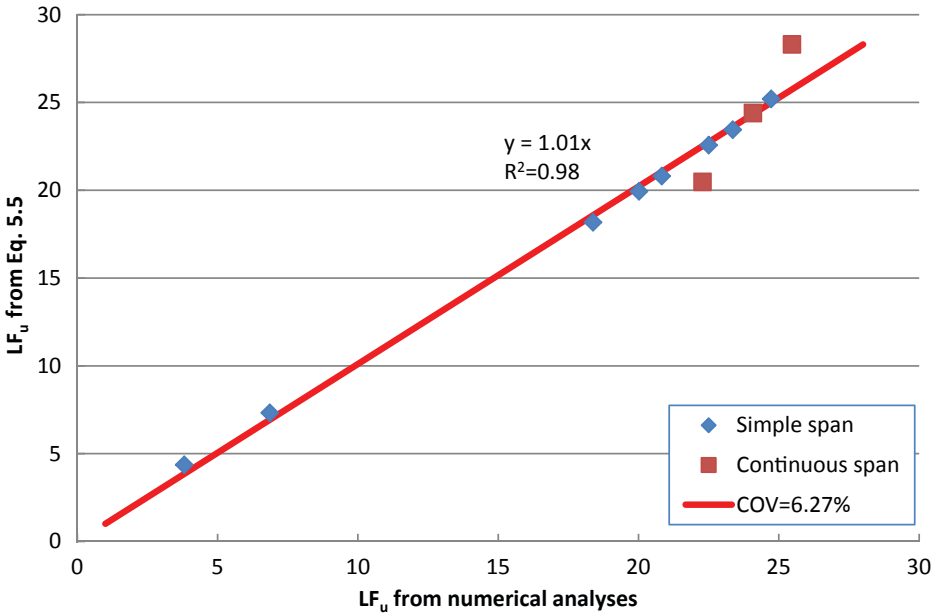

Figure 5.4. Verification of Equation 5.5 for P/S concrete box bridges.

box sections, number of boxes, and box spacing. During the analyses of the bridges, wide bridges were loaded by two side-by-side trucks; narrow bridges were loaded by only one truck.

The results of the analysis of the steel box-girder bridges, which compare the ultimate capacity of the originally intact bridge represented by LF_u to the capacity to resist first member failure represented by LF_1, also were found to be well represented by Equation 5.5 with the modified γ of Equation 5.6. The validity of Equation 5.5 for the response of simple-span and continuous steel box-girder bridges is verified in Figure 5.5, which plots the results obtained from Equation 5.5 versus the results obtained from the nonlinear analysis in blue for simple-span and in red for continuous span bridges. These results are for wide bridges loaded by two side-by-side trucks and narrow bridges loaded by only one truck. The plot shows that the points lie along a 45° line. The equation in the figure gives the equation of the trend line that describes the relationship between the estimated LF_u obtained from Equation 5.5 and the calculated LF_u obtained from the nonlinear pushdown analysis of actual bridge systems. The trend line shows a slope equal to 1.02 and a coefficient of regression $R^2 = 0.99$. A perfect match would lead to a trend

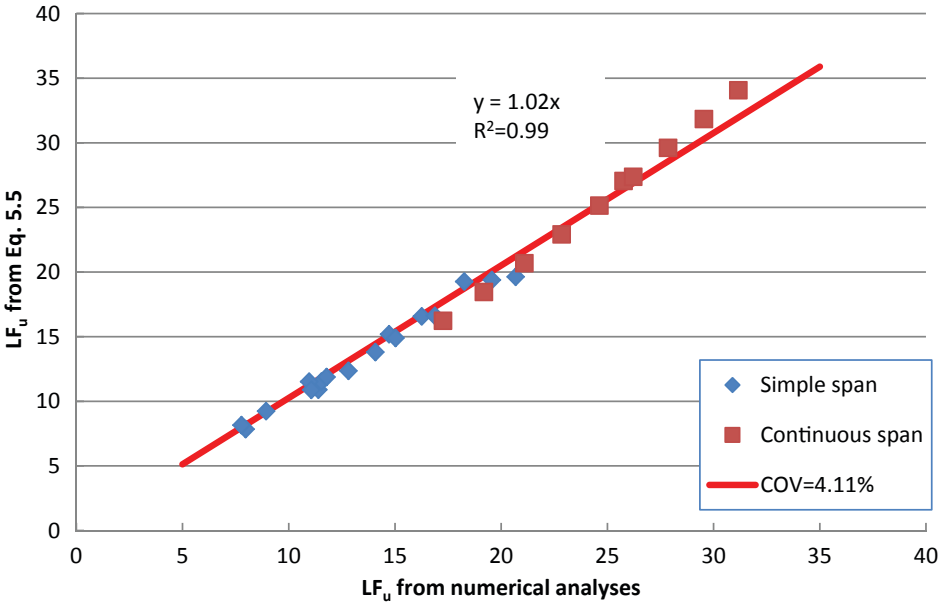

Figure 5.5. Verification for steel box-girder bridges.

line having an equation of the form y = 1.0 x with a coefficient of regression $R^2 = 1.0$. The COV of the error between the predicted values and the analytical results is 4.11%.

Model Modification for Continuous Box-Girder Bridges

Modified Model

The sensitivity analyses described in this report demonstrated that continuous box-girder bridges provide significantly higher redundancy levels than other types of bridges. This was attributed to the high stiffness of the boxes near the interior supports, which improved their ability to transfer the load to the adjacent spans as represented by the term γ in Equation 5.5. Additional observations indicated that the moment capacity of the box girder in the negative bending region also plays an important role in allowing for the transfer of the load to the other spans. To account for this effect, a large number of three-span and two-span composite steel box-girder bridges, as well as three-span prestressed concrete box-girder bridges, were analyzed for different stiffness and strength values. In particular, the additional sensitivity analysis studied the effect of the stiffness of the boxes, the moment capacity of the boxes in the negative bending region, the moment capacity in the positive bending region, dead load magnitude, thickness of the slab, and the moment capacity of the slab.

The results of the additional analyses performed indicated that the originally proposed Equations 5.5 and 5.6 can be further modified to account for the effect of the negative bending capacity and the stiffness of the box girders. An updated unified equation that would estimate the load factor LF_u for the ultimate limit state of originally intact bridges in function of the load factor LF_1 corresponding to the first member failure taking account the span continuity for box girders is presented as

$$LF_u = 1.16LF_1 + 0.75\gamma \tag{5.7}$$

where

$$LF_1 = LF_1^+ = \frac{R^+ - D^+}{L_1^+} \quad \text{when} \quad \frac{LF_1^-}{LF_1^+} \geq 1.0$$
$$LF_1 = LF_1^- = \frac{R^- - D^-}{L_1^-} \quad \text{when} \quad \frac{LF_1^-}{LF_1^+} < 1.0 \tag{5.8}$$

That is, LF_1 in Equation 5.7 represents the ability of the weakest section of the beam, which can be either the positive bending section or the negative bending section depending on the moment capacity in each region (R), the dead load moment in each region (D), and the effect of the applied live load moment on the most critical beam (L_1) where the live load represents two side-by-side HS-20 trucks applied at the middle of the span. The positive superscript in Equation 5.8 is for the positive bending region; the negative superscript is for the negative bending region.

Furthermore, the value of γ in Equation 5.7 should be modified as shown in Equation 5.9.

$$\gamma = \begin{cases} \dfrac{EI_{box} \Big/ \left(E_{\text{transverse slab}} \dfrac{b_s t_s^3}{12} \right)}{38} & \text{for continuous boxes with } \dfrac{LF_1^-}{LF_1^+} \geq 1.75 \\ \dfrac{1}{1.75} \left(\dfrac{EI_{box} \Big/ \left(E_{\text{transverse slab}} \dfrac{b_s t_s^3}{12} \right)}{38} - 1 \right) \dfrac{LF_1^-}{LF_1^+} + 1 & \text{for continuous boxes with } \dfrac{LF_1^-}{LF_1^+} < 1.75 \\ 1.0 & \text{for other bridges.} \end{cases} \leq 8.0$$

$$Use\ b_s = 120\ in \tag{5.9}$$

The modification factor γ is thus adjusted to take into account the stiffness of continuous box-girder bridges relative to slab stiffness as well as the negative bending strength capacity of the box. EI_{box} is the stiffness for the cracked section of the box girder in negative bending that ignores the portion of the concrete in tension. $E_{\text{transverse slab}}$ is the modulus of elasticity for the slab between the boxes, $b_s = 120$ in gives the width of the slab assuming the stiffness is calculated based on a 120-in. wide slab section having a depth t_s, $LF_1^+ = \dfrac{R^+ - D^+}{L_1^+}$ is the load factor in the positive bending region due to two side-by-side HS-20 trucks applied in the middle of the span and R^+, D^+, and L_1^+ are the moment resistance, dead load, and maximum live load effect of the most critical beam in the positive bending region. LF_1^- is the load factor in the most critical member in negative bending where $LF_1^- = \dfrac{R^- - D^-}{L_1^-}$ obtained for the two side-by-side HS-20 trucks applied at the middle of the span and R^-, D^-, and L_1^- are the moment capacity, dead load moment, and live load moment in the most critical negative bending section. The value of 38 is used to normalize the equation and is based on the stiffness of typical steel I-girder bridges designed to exactly satisfy the specifications' strength criteria.

Verification of Modified Model

To verify the validity of the proposed modified model, a sensitivity analysis is performed by analyzing several three-span and two-span steel box-girder bridges, three-span prestressed concrete box-girder bridges, as well as three-span steel I-girder bridges.

Figures 5.6, 5.7, 5.8, and 5.9 plot the predicted load factor LF_u obtained from Equations 5.7, 5.8, and 5.9 versus the

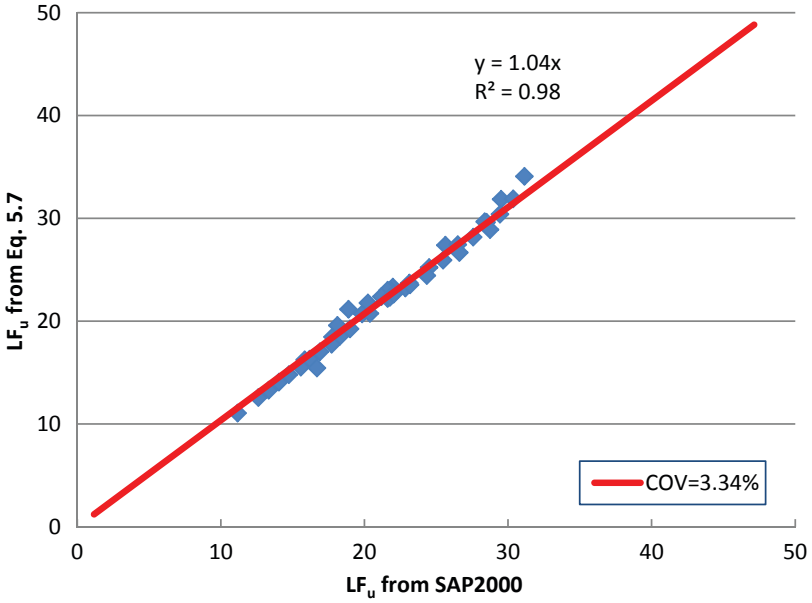

Figure 5.6. Verification of model for three-span continuous steel box-girder bridges.

LF_u value obtained from the nonlinear analysis performed using SAP2000. The plots are for three-span continuous steel box-girder bridges (Figure 5.6), two-span continuous steel box-girder bridges (Figure 5.7), three-span continuous prestressed concrete box-girder bridges (Figure 5.8) and three-span continuous I-girder bridges (Figure 5.9). All the trend lines in the figures have slopes close to 1.0 and coefficients of regression R^2 also close to 1.0. This serves to confirm that Equation 5.7 provides a good model for estimating the ultimate capacity of bridge systems subjected to vertical live load. The maximum COV for the error between the predicted and the SAP2000 values is on the order of 5.5%.

Narrow Simple-Span I-Girder Bridges

The load factors for simple-span prestressed concrete and steel I-girder bridges having 4 beams at 4-ft spacing and four beams at 6-ft spacing or six beams at 4-ft spacing are plotted in Figures 5.10 and 5.11. These bridges are considered to be narrow bridges. The figures show a different trend in the behavior

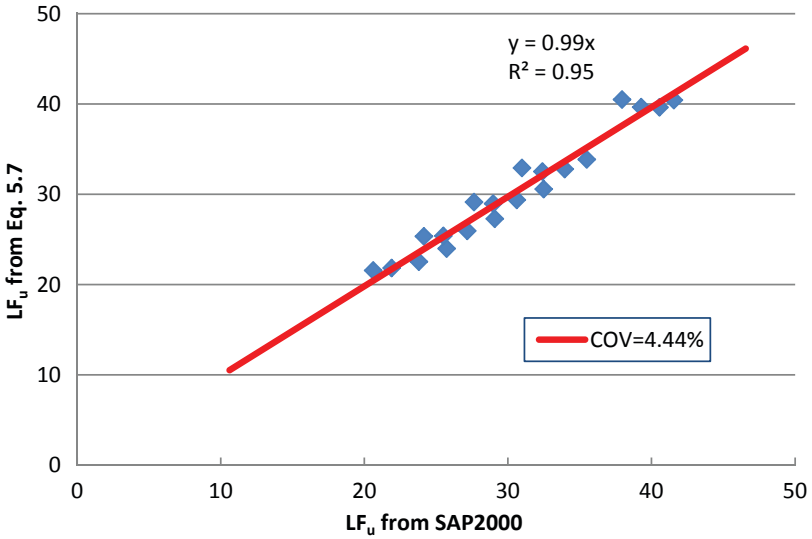

Figure 5.7. Verification of model for two-span continuous steel box-girder bridges.

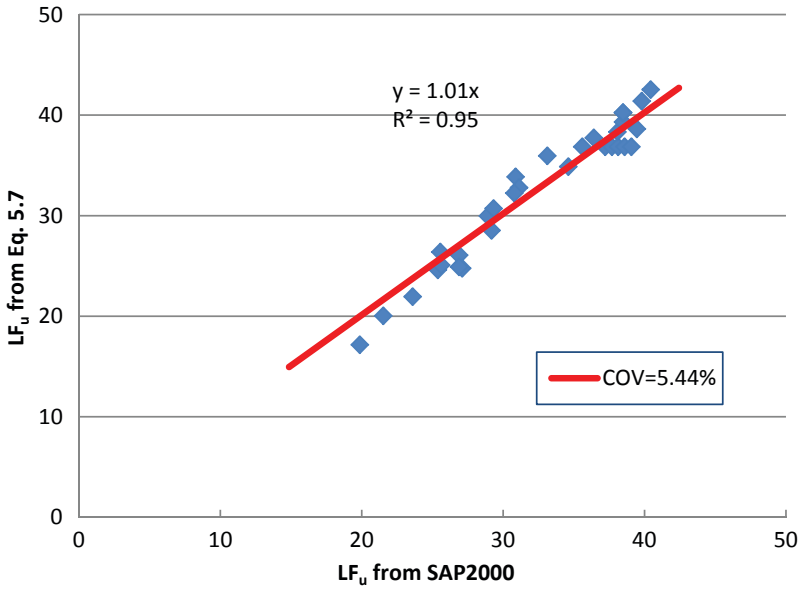

Figure 5.8. Verification of model for three-span continuous prestressed concrete box-girder bridges.

of simple-span narrow bridges where the ultimate capacity of the originally intact systems is considerably lower than that of wide bridges. No discernible difference is observed between steel I-girder and prestressed concrete I-girder bridges.

Simple-span bridges with four beams at 4-ft spacing are not redundant for the ultimate limit state with $LF_u = LF_1$. The actual slope of the trend line for these cases obtained in Figure 5.10 is 1.01. That is, when one beam fails, the entire bridge will collapse. Bridges with four beams at 6-ft spacing are slightly more redundant showing that LF_u is approximately equal to $1.11xLF_1$. The relationship between LF_u and LF_1 for bridges with six beams at 4-ft spacing is $LF_u = 1.18xLF_1$.

Narrow Continuous Span I-Girder Bridges

The load factors for narrow continuous span prestressed concrete bridges having 4 beams at 4-ft spacing and four beams at 6-ft spacing or six beams at 4-ft spacing are plotted in Figure 5.11. These bridges are considered to be narrow bridges. The plot shows LF_u versus LF_1 obtained of the narrow continuous bridges and compares them to those of wide continuous span bridges. The figure demonstrates that bridge continuity helps improve bridge redundancy for the four beams at 6-ft and the six beams at 4-ft bridges placing them within the same range as the continuous wide bridges. However, the continuity

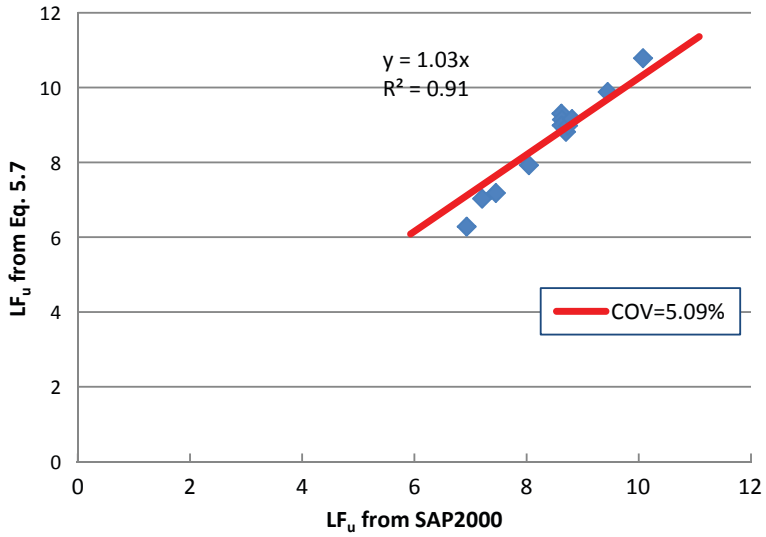

Figure 5.9. Verification of model for three-span continuous I-girder bridges.

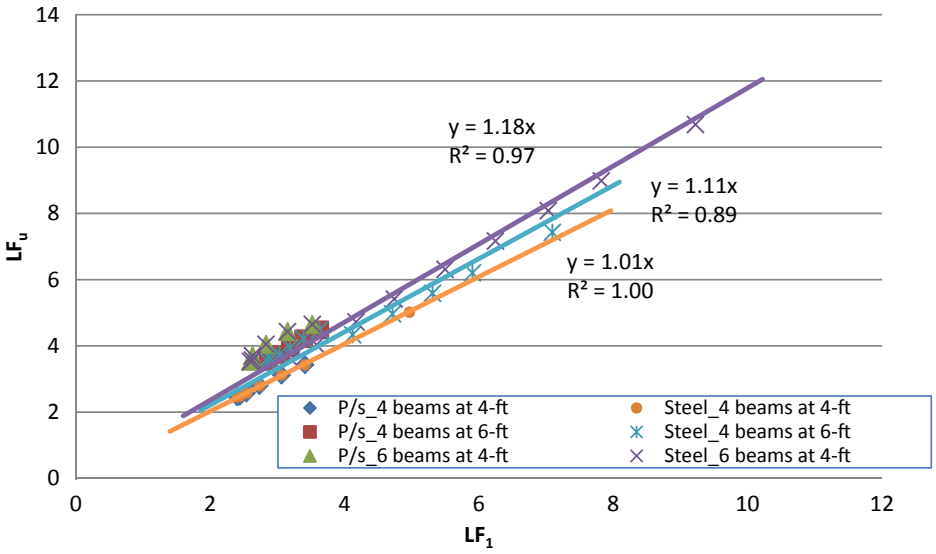

Figure 5.10. Plot of LF_u vs. LF_1 for narrow simple-span I-girder bridges.

did not sufficiently improve the redundancy of four beams at 4-ft which remained at a lower level of redundancy. Only four narrow continuous steel I-girder bridges were analyzed having 4 beams at 60-ft and six beams at 4-ft spacing with compact and noncompact sections in negative bending. These data points were also plotted in Figure 5.11 but no discernible difference is observed between the narrow steel I-girder and prestressed concrete I-girder bridges. These observations are made when the bridge is loaded by two side-by-side trucks in the same span.

The results of the analysis as plotted in Figure 5.11 demonstrate that for narrow continuous bridges, Equation 5.7 is applicable with $\gamma = 0$ for 4 beams at 4-ft spacing and $\gamma = 1.0$ for all other number of beams and beam spacing.

Narrow Box-Girder Bridges

The load factors for narrow continuous box-girder bridges having two boxes each 6-ft wide spaced at 12-ft center on center for a bridge width of 24-ft are plotted in Figure 5.12. These bridges are considered to be narrow bridges. Three plots are given. Two plots are for simple-span concrete and steel bridges loaded by a single lane of traffic. The third plot shows the results when the bridge is loaded by two side-by-side HS-20 trucks. The plots show LF_u versus LF_1 obtained of the narrow simple-span bridges loaded in two lanes and compare them to those loaded in a single lane. The figure demonstrates that narrow box-girder bridges loaded by a single lane behave like

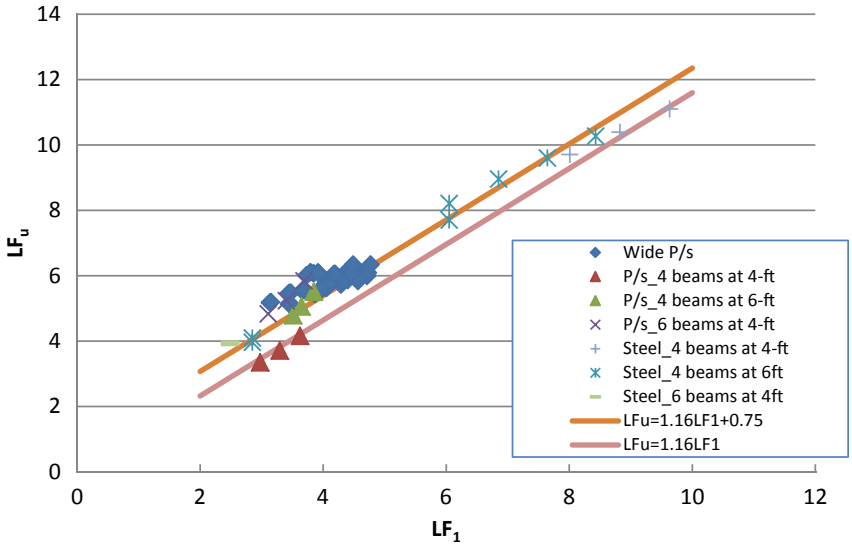

Figure 5.11. Plot of LF_u vs. LF_1 for narrow continuous span I-girder bridges.

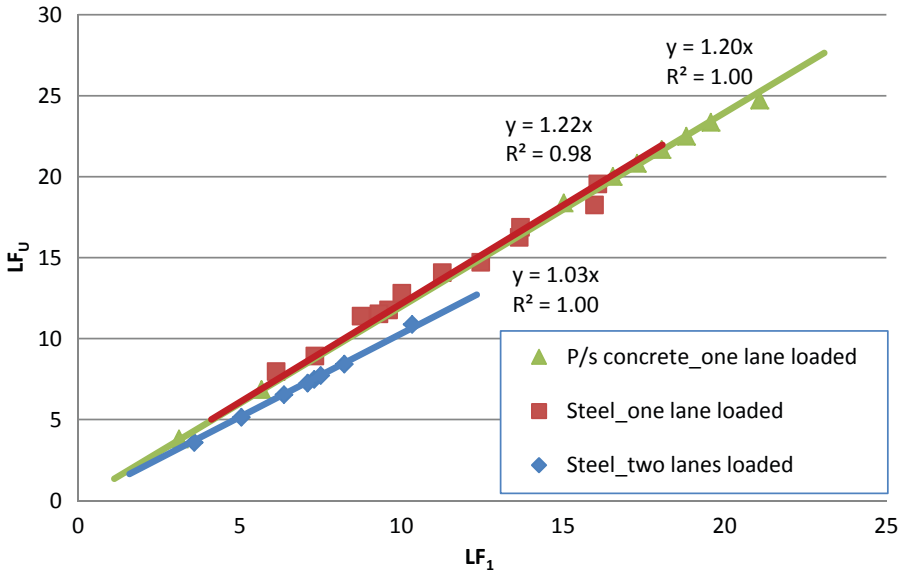

Figure 5.12. Plot of LF_u vs. LF_1 for narrow box-girder bridges.

wide bridges while those loaded in two lanes show practically no redundancy with $LF_u = 1.03\ LF_1$.

Continuous Span I-Girder Bridges with Noncompact Sections

When the section in negative bending is noncompact, the dominant failure mechanism may be due to trucks in different contiguous spans of the bridge rather than the two side-by-side trucks in the same span. The analysis of noncompact bridges loaded by a single HS-20 truck in each of two contiguous spans was performed in *NCHRP Report 406* and augmented by additional analyses performed during the course of this study. These analyses are used to supplement the analysis of the bridges loaded by two side-by-side trucks in one span. The minimum value of LF_u from both loading scenarios is then compared to the minimum of LF_I^+ and LF_I^- as defined in Equation 5.8. The results of the analysis show that, generally speaking, when first member failure takes place in negative bending with LF_I^- less than LF_I^+, the loading of the two spans governs the ultimate capacity of the system and the bridge reaches its ultimate capacity soon after the noncompact member in negative bending reaches its limiting capacity. These bridges show essentially no redundancy and $LF_u = LF_I^-$. Generally, when LF_I^+ is lower than LF_I^-, failure is controlled by the system loaded by two side-by-side trucks in a single span and Equation 5.7 is valid. Figure 5.13 shows the results obtained from noncompact bridges for the two failure modes governed by Equation 5.7 and $LF_u = LF_I^-$. Figure 5.14 serves to verify that the proposed approach for predicting the ultimate load capacity of continuous I-girder bridges with noncompact sections in the negative bending region is reasonably accurate.

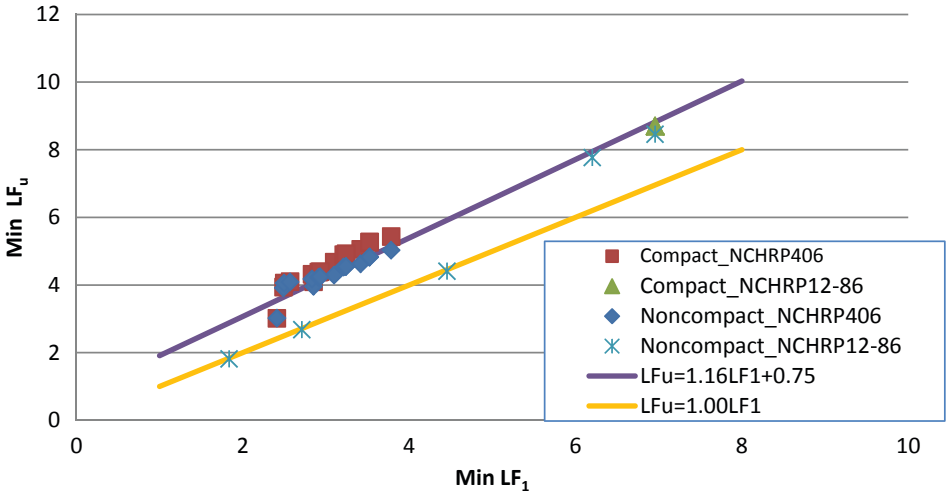

Figure 5.13. Plot of LF_u vs. LF_1 for continuous span I-girder bridges with compact and noncompact sections in negative bending.

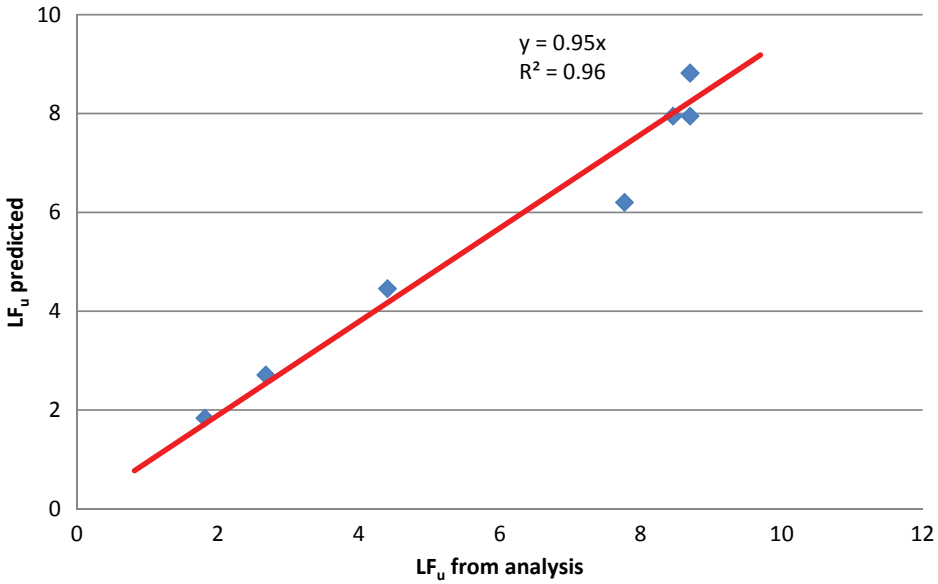

Figure 5.14. Verification of model for continuous I-girder bridges with noncompact sections in negative bending.

Continuous-Span Steel Box-Girder Bridges with Noncompact Negative Sections

The AASHTO LRFD Bridge Design Specifications indicate that steel box-girder sections in negative bending should be considered to be noncompact. For this reason, several analyses were performed assuming that the boxes in the negative bending regions have no ductility and that they will fail as soon as their moment capacity is first reached. The bridges are analyzed under the effect of two trucks placed in different contiguous spans of the bridge, and the results are compared to those obtained when two side-by-side trucks are placed in the same span. The minimum value of LF_u from both loading scenarios is then compared to the minimum of LF_I^+ and LF_I^- as defined in Equation 5.8. The results of the analysis show that, generally speaking, first member failure takes place in negative bending when LF_I^- is considerably lower than LF_I^+ and the loading of the two spans governs the ultimate capacity of the system. For these cases, the bridge reaches its ultimate capacity soon after the noncompact member in negative bending reaches its limiting capacity. These bridges show some level of redundancy and $LF_u = 1.16LF_I^-$. Generally, when LF_I^+ is lower than LF_I^-, failure is controlled by the system loaded by two side-by-side trucks in a single span and Equation 5.7 is valid. Figure 5.15 shows the results obtained from noncompact bridges for the two failure modes governed by Equation 5.7 and $LF_u = 1.16LF_I^-$. A sensitivity analysis shows that the transition between the two curves takes places when

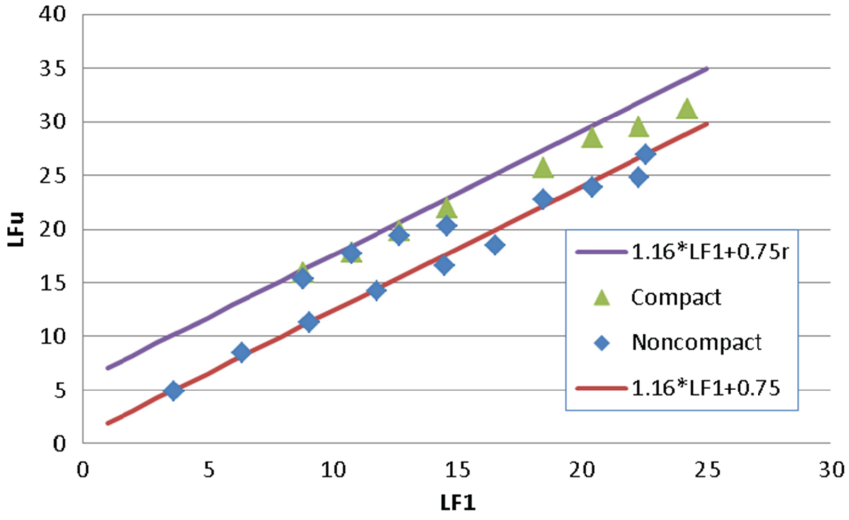

Figure 5.15. LF_u versus LF_1 for continuous box-girder bridges with noncompact sections in negative bending.

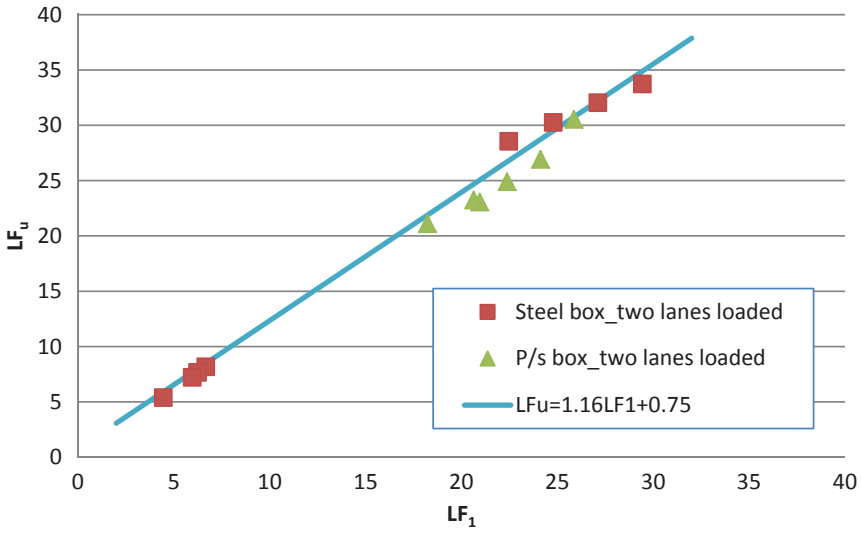

Figure 5.16. LF_u vs. LF_1 for narrow continuous box-girder bridges.

$LF_I^- < 1.75LF_I^+$. The transition between the two curves describing the two failure modes is not sudden and can be expressed using the parameter γ defined in Equation 5.9.

Continuous-Span Narrow Box-Girder Bridges

To investigate the behavior of originally intact narrow continuous bridges under overload, several analyses were performed for prestressed concrete and steel bridges covering bridges with compact and noncompact sections in negative bending. Narrow box-girder bridges are defined as those having two boxes with a total travel width equal to 24-ft. The analyses are performed for bridges composed of two boxes each 6-ft wide, spaced at 12-ft center to center. The bridges are analyzed under the effect of two trucks placed in different contiguous spans of the bridge and the results are compared to those obtained when two side-by-side trucks are placed in the same span. The minimum value of LF_u from both loading scenarios is then compared to the minimum of LF_I^+ and LF_I^- as defined in Equation 5.8. The analysis was performed for bridges with compact sections in negative bending and also sections that are noncompact in negative bending. It is observed that the results closely follow the model established in Equation 5.7 as demonstrated in Figures 5.16 and 5.17.

Summary

The analyses performed during the course of this project and *NCHRP Report 406* have produced results on the ulti-

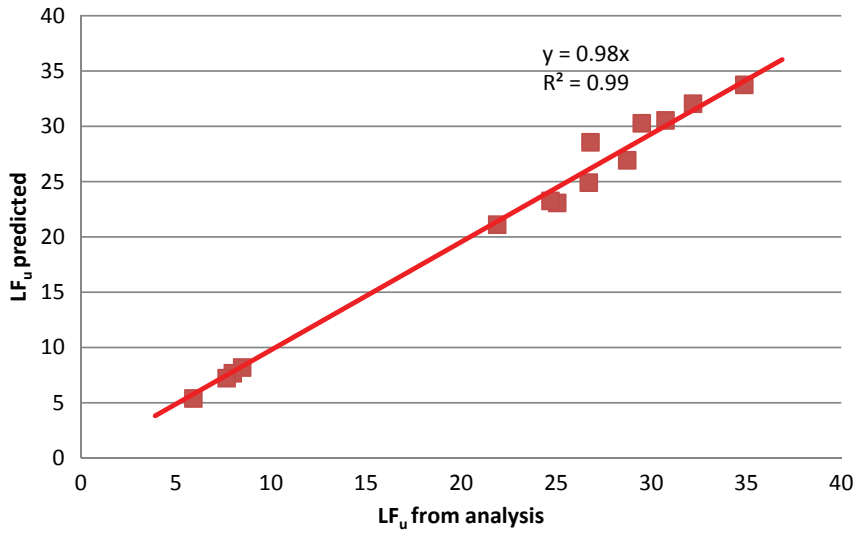

Figure 5.17. Verification of model for narrow continuous box-girder bridges.

mate load carrying capacities of originally intact typical bridge configurations and compared these to the load capacity of critical members. Consistent patterns for the relationship between these parameters describing the performance of bridges are possible for evaluating the redundancy of bridge superstructures using a few characteristic parameters that, as described in Equations 5.7, 5.8, and 5.9, consist of the member moment resistance in positive and negative bending regions, the applied dead load moment, the moment from live load applied on the most critical member and, for continuous bridges, the parameter γ which gives the relative stiffness of the beam near the support to the stiffness of the slab. The parameter γ reflects the ability of continuous bridges with stiff sections near the support to spread the load to the adjacent spans as the loaded span undergoes nonlinear deformations. The results of the relationship between the ultimate capacity of originally intact systems under vertical load and the load carrying capacity of the most critical member are summarized in Table 5.1. The analyses performed in this section addressed the ultimate capacities of originally intact bridges. Section 5.5 addresses damaged bridge systems that may have lost the load carrying capacity of a critical member due to various possible deterioration or extreme events.

That is, LF_1 in Equation 5.7 represents the load carrying capacity of the weakest section of the beam, which can be either the positive bending section or the negative bending section depending on the moment capacity in each region (R), the dead load moment in each region (D), and the effect of the applied live load moment on the most critical beam (L_1) where the live load represents two side-by-side HS-20 trucks applied at the middle of the span or two trucks in one lane applied in each of two contiguous spans. The positive superscript in R, D, and L_1 is for the positive bending region, the negative superscript is for the negative bending region.

Furthermore, the value of γ for the box-girder bridges in Table 5.1 is obtained from

$$\gamma = \begin{cases} \dfrac{EI_{box} \Big/ \left(E_{\text{transverse slab}} \dfrac{b_s t_s^3}{12} \right)}{38} & \text{for continuous boxes with } \dfrac{LF_1^-}{LF_1^+} \geq 1.75 \\ \dfrac{1}{1.75} \left(\dfrac{EI_{box} \Big/ \left(E_{\text{transverse slab}} \dfrac{b_s t_s^3}{12} \right)}{38} - 1 \right) \dfrac{LF_1^-}{LF_1^+} + 1 & \text{for continuous boxes with } \dfrac{LF_1^-}{LF_1^+} < 1.75 \\ 1.0 & \text{for other bridges.} \end{cases} \leq 8.0$$

Use $b_s = 120$ *in*

Table 5.1. Summary of LF_u vs. LF_1 for originally intact systems under vertical loads.

Bridge Cross-Section Type	
Simple-span 4 I-beams at 4-ft	LF_u=1.01 LF_1
Simple-span 4 I-beams at 6-ft	LF_u=1.11 LF_1
Simple-span 6 I-beams at 4-ft	LF_u=1.18 LF_1
Continuous span 4 I-beams at 4-ft with compact members	LF_u=1.16 LF_1
Continuous steel I-girder bridges with noncompact negative bending sections and $LF_1^- \leq 1.16 LF_1^+ + 0.75$	$LF_u = 1.00 LF_1^-$
All other simple-span and continuous I-beam bridges	LF_u=1.16 LF_1+0.75
Narrow simple-span box-girder bridges less than 24-ft wide	LF_u=1.03 LF_1
All other simple-span box-girder bridges	LF_u=1.16 LF_1+0.75
Narrow continuous box-girder bridges less than 24-ft wide	LFu=1.16 LF1+0.75
Continuous steel box-girder bridges with noncompact negative bending sections and $\dfrac{LF_1^-}{LF_1^+} \leq 1.75$	LF_u=1.16 LF_1+0.75
All other continuous box-girder bridges	LF_u=1.16 LF_1+0.75γ

where

$$LF_1 = LF_1^+ = \frac{R^+ - D^+}{L_1^+} \quad \text{when} \quad \frac{LF_1^-}{LF_1^+} \geq 1.0$$

$$LF_1 = LF_1^- = \frac{R^- - D^-}{L_1^-} \quad \text{when} \quad \frac{LF_1^-}{LF_1^+} < 1.0$$

The modification factor γ takes into account the stiffness of continuous box-girder bridges relative to slab stiffness as well as the negative bending strength capacity of the box. EI_{box} is the stiffness for the cracked section of the box girder in negative bending, which ignores the portion of the concrete in tension. $E_{\text{transverse slab}}$ is the modulus of elasticity for the slab between the boxes, $b_s = 120$ in. gives the width of the slab assuming the stiffness is calculated based on a 120-in. wide slab section having a depth t_s, $LF_1^+ = \dfrac{R^+ - D^+}{L_1^+}$ is the load factor in the positive bending region due to two side-by-side HS-20 trucks applied in the middle of the span or two trucks in one lane applied in each of two contiguous spans; and R^+, D^+, and L_1^+ are the moment resistance, dead load, and maximum live load effect of the most critical beam in the positive bending region. LF_1^- is the load factor in the most critical member in negative bending where $LF_1^- = \dfrac{R^- - D^-}{L_1^-}$ obtained for the two side-by-side HS-20 trucks applied at the middle of the span or two trucks in one lane applied in each of two contiguous spans and R^-, D^-, and L_1^- are the moment capacity, dead load moment, and live load moment in the most critical negative bending section. The value of 38 is used to normalize the equation and is based on the stiffness of typical steel I-girder bridges designed to exactly satisfy the specifications' strength criteria.

5.3 Calibration of System Factors for Bridges under Vertical Loads

Concept of System Factors

Following the procedures proposed in the AASHTO LRFD Bridge Design Specifications and the Canadian bridge code, it is recommended that different member design criteria be established for bridges based on their levels of redundancy. This can be achieved by applying a system factor in the safety-check equation such that bridges with low levels of redundancy be required to have higher member resistances than those of bridges with high levels of redundancy. The system factor can be implemented in the member safety-check equation that takes the form

$$\phi_s \phi R_n^N = \gamma_d D_n + \gamma_l L_n (1 + I) \tag{5.10}$$

where ϕ_s is the system factor that is defined as a statistically based multiplier relating to the safety and redundancy of the complete system. The system factor is applied to the factored nominal member resistance R_n^N that would be needed to meet the required factored loads accounting for the system's redundancy. The proposed system factor replaces the load modifier η used in Section 1.3.2 of the LRFD specifications. The system factor is placed on the left side of the equation because the system factor is related to the capacity of the system and should be used as a resistance multiplier as is the norm in reliability-based LRFD codes. ϕ is the member resistance factor, γ_d is the dead load factor, D_n is the dead load effect, γ_l is the live load factor, L_n is the live load effect on an individual member, and I is the dynamic amplification factor.

When ϕ_s is equal to 1.0, Equation 5.10 becomes the same as the current design equation. If ϕ_s is greater than 1.0, this indicates that the system's configuration provides a sufficient level of redundancy and thus the members of the bridge can be designed to have lower strengths than those of bridges with low levels of redundancy. When it is less than 1.0, then the level of redundancy is not sufficient and the bridge members must be designed to have higher strengths than members of bridges with high levels of redundancy.

The system factors should be calibrated using a reliability model such that a system factor equal to 1.0 indicates that the reliability index of the system is higher than that of the member by an amount equal to a target value. Specifically, the reliability index for the ultimate limit state of the originally intact system, β_{ultimate}, is higher than the reliability index of the member, β_{member} by a margin reliability index $\Delta\beta_u$ equal to the target reliability margin $\Delta\beta_{u\,\text{target}}$. For bridges susceptible to local damage, the reliability index for the ultimate limit state of the damaged system, β_{damaged}, is higher than the reliability index of the member of the originally intact bridge, β_{member} by a margin reliability index $\Delta\beta_d$ equal to the target reliability margin $\Delta\beta_{d\,\text{target}}$.

Based on the analysis of typical four-girder steel and prestressed concrete bridges, *NCHRP Report 406* recommended that the target reliability index margins be set at $\Delta\beta_u$ equal to 0.85 and $\Delta\beta_d$ equal to −2.70. These targets were selected to match the average reliability index margins of typical four-girder bridges because these bridges have been traditionally accepted as providing sufficient levels of redundancy. In this chapter, system factors are calibrated so that bridge configurations that produce reliability index margins equal to the target values are assigned a system factor $\phi_s = 1.0$. If the margin is less than the target value, then the system factor will serve to increase the reliability of the system by an amount equal to the difference. Thus, a system factor less than 1.0 is assigned. If the reliability index margin is higher than the target, then a system factor greater than 1.0 may be used to lower the reliability index of the system by an amount equal to the difference between the available margin and the target value.

Calibration Approach

The calibration of the system factor ϕ_s can be executed using Equations 5.1 through 5.4 so that the reliability index for the intact system β_{ultimate} and that of the damaged system β_{damage} are increased when the available $\Delta\beta_u$ and $\Delta\beta_d$ are lower than the target values set at $\Delta\beta_{u\,\text{target}} = 0.85$ and $\Delta\beta_{d\,\text{target}} = -2.70$. On the

other hand, ϕ_s should serve to lower the reliability index for the system when the available $\Delta\beta_u$ and $\Delta\beta_d$ are higher than the target values. The amount by which $\beta_{ultimate}$ and β_{damage} should be increased should be equal to the deficit in the available $\Delta\beta_u$ and $\Delta\beta_d$ when compared to the target values while the amount by which $\beta_{ultimate}$ and β_{damage} should be decreased should be equal to the surplus in the available $\Delta\beta_u$ and $\Delta\beta_d$ when compared to the target values. The formulation can be summarized as described next for the ultimate limit state of originally intact systems. The same exact procedure also is valid for finding the system factor for the damaged condition limit state.

The reliability index for a bridge member is calculated using the lognormal model as

$$\beta_{member} = \frac{\ln\left(\frac{\overline{LF_1}}{\overline{LL_{75}}}\right)}{\sqrt{V_{LF}^2 + V_{LL}^2}} \tag{5.11}$$

where $\overline{LF_1}$ is the mean value of LF_1, which is calculated from the linear structural analysis of the bridge up until the first member fails. LF_1 gives the number of HS-20 trucks that the bridge member can carry in addition to the dead load. It can be expressed as

$$LF_1 = \frac{R - D}{L_1} \tag{5.12}$$

where R is the bridge member capacity, D is the dead load effect, and L_1 is the effect on that member due to the application of one set of HS-20 trucks on the bridge.

If LF_1 is found based on the nominal values of R and D, then the mean $\overline{LF_1}$ is related to the nominal value of LF_1 through a bias b_{LF} such that

$$b_{LF} = \frac{\overline{LF_1}}{LF_1} \tag{5.13}$$

The results of the nonlinear analysis of the entire system will serve to find the load factor LF_u, which also is used to find the reliability index for the ultimate limit state

$$\beta_{ultimate} = \frac{\ln\left(\frac{\overline{LF_u}}{\overline{LL_{75}}}\right)}{\sqrt{V_{LF}^2 + V_{LL}^2}} \tag{5.14}$$

The reliability index margin is found from

$$\Delta\beta_u = \beta_{ultimate} - \beta_{member} \tag{5.15}$$

The calculated reliability index margin is compared to the target value and the deficit is found as

$$\Delta\beta_{u\,deficit} = \Delta\beta_{u\,target} - \Delta\beta_u = \Delta\beta_{u\,target} - (\beta_{ultimate} - \beta_{member}) \tag{5.16}$$

A negative $\Delta\beta_{u\,deficit}$ indicates that the redundancy level of the system is more than adequate, while a positive $\Delta\beta_{u\,deficit}$ indicates that the redundancy of the system is not sufficient.

The system factor should serve to change the resistances of the bridge members so that a system that is adequately redundant could be allowed to have lower member resistances while the member resistances of a system that is not adequately redundant should be increased. The change in the member resistance should be sufficient to offset the deficit in the reliability index margin defined as $\Delta\beta_{u\,deficit}$, so that the modified bridge will produce a modified system reliability index $\beta^N_{ultimate}$. A bridge that is non-redundant should have a higher system reliability $\beta^N_{ultimate}$ value than a system designed using current methods. The higher system reliability index should serve to compensate for the deficit in the reliability margin so that

$$\begin{aligned}\beta^N_{ultimate} &= \beta_{ultimate} + \Delta\beta_{u\,deficit} \\ &= \beta_{ultimate} + \Delta\beta_{u\,target} - (\beta_{ultimate} - \beta_{member}) \\ &= \Delta\beta_{u\,target} + \beta_{member}\end{aligned} \tag{5.17}$$

The new ultimate system capacity is related to the higher reliability index by

$$\beta^N_{ultimate} = \frac{\ln\left(\frac{\overline{LF_u^N}}{\overline{LL_{75}}}\right)}{\sqrt{V_{LF}^2 + V_{LL}^2}} \tag{5.18}$$

where $\overline{LF_u^N}$ is the mean value that the new system ultimate capacity should reach. Substituting Equation 5.18 into Equation 5.17 gives

$$\frac{\ln\left(\frac{\overline{LF_u^N}}{\overline{LL_{75}}}\right)}{\sqrt{V_{LF}^2 + V_{LL}^2}} = \Delta\beta_{u\,target} + \beta_{member} \tag{5.19}$$

Equation 5.19 can be used to solve for the mean value of the required new system capacity using

$$\overline{LF_u^N} = \overline{LL_{75}} e^{(\Delta\beta_{u\,target} + \beta_{member})\sqrt{V_{LF}^2 + V_{LL}^2}} \tag{5.20}$$

Given the mean value $\overline{LF_u^N}$, the nominal required system capacity is obtained from

$$LF_u^N = \frac{\overline{LF_u^N}}{b_{LF}} \tag{5.21}$$

The required member capacity associated with a system having an ultimate capacity LF_u^N can be inferred from the relationship established between LF_u and LF_1 for typical bridge configurations. For example, in *NCHRP Report 406* it was observed that the ratio $R_u = LF_u/LF_1$ is approximately constant. This assumption was found valid when LF_1 remained

within the range of typical new designs. Further review of the *NCHRP Report 406* data augmented by the results of the analyses performed as part of this project show that a better approximation for the relationship between LF_u and LF_1 for all simple-span and continuous I-girder bridges is obtained from an equation of the form

$$LF_u = 1.16 \times LF_1 + 0.75 \tag{5.22}$$

Therefore, the required load factor for first member failure can be obtained from

$$LF_1^N = \frac{LF_u^N - 0.75}{1.16} \tag{5.23}$$

Using Equation 5.8, the load factor for first member failure is related to the nominal member capacity by $LF_1^N = \frac{R^N - D}{L_1}$. Thus, the required member resistance is

$$R^N = LF_1^N \times L_1 + D \tag{5.24}$$

The system factor associated with this bridge system configuration should serve to increase R to a new value R^N. Thus, the system factor, ϕ_s can be obtained from

$$\phi_s = \frac{R}{R^N} \tag{5.25}$$

If the traditional design gives a value for the resistance $R_n = \frac{[\gamma_d D_n + \gamma_l L_n (1+I)]}{\phi}$, then the modified member design equation becomes the same as that in Equation 5.10, repeated below.

$$\phi_s \phi R_n^N = \gamma_d D_n + \gamma_l L_n (1+I)$$

The process described above also can be used to derive an algebraic expression that gives the system factor directly as a function of the coefficient in Equation 5.7 and the dead load to member resistance ratio. The closed-form expression is given as

$$\eta = e^{\xi \Delta\beta_T}\left[\frac{1 - D/R}{C_{red1}}\right] + D\Big/R - \frac{C_{red2}}{C_{red1} LF_1}[1 - D/R]$$

$$\phi_s = \frac{1}{\eta} \tag{5.26}$$

where C_{red1} and C_{red2} are respectively the slopes and intercepts of the redundancy equations in Table 5.1. As an example, in Equation 5.7 $C_{red1} = 1.16$ and $C_{red2} = 0.75\gamma$. D/R in Equation 5.26 is the dead load to resistance ratio, LF_1 is the live load capacity of the most critical member as defined in Equation 5.8, $\Delta\beta_T$ is the target reliability index margin set at $\Delta\beta_T = 0.85$, and $\xi = \sqrt{V_{LF}^2 + V_{LL}^2}$ is the dispersion coefficient defined as the square root of the sum of the square of the COV for the live load carrying capacity LF and the maximum applied live load LL.

Calibration Example

A numerical example is presented to illustrate the calibration of system factors. The example uses a three-span continuous composite steel I-girder bridge having span lengths of 50-ft, 80-ft, 50-ft. The bridge is composed of six parallel members at 8-ft spacing. The ultimate moment capacity in the positive bending region was found to be R = 49,730 kip-in. The dead load effect at the midpoint of the center span is found to be D = 4,860 kip-in. The moment at the midpoint of the external girder of the center span due to the two side-by-side HS-20 AASHTO trucks is L_1 = 6,450 kip-in.

The nonlinear push down analysis showed that the ultimate capacity is reached when the weights of the HS-20 trucks are multiplied by a factor $LF_u = 8.70$.

A traditional check of member safety assuming no resistance or load factors gives the load factor for first member failure as shown in Equation 5.8 by

$$LF_1 = \frac{R - D}{L_1} = \frac{49{,}730 - 4{,}860}{6{,}450} = 6.96$$

Using the data provided by Nowak (1999), the bias in the estimated value of LF_1 is obtained as $b_{LF} = 1.13$. The COV for the live load and the load factors are estimated as $V_{LL} = 19\%$, $V_{LF} = 13.5\%$. It is assumed that an adequately redundant system should have a reliability index margin $\Delta\beta_{target} = 0.85$.

a. Calculation of β_{member}

Table 5.2 gives the mean value for the applied load as extracted from Nowak (1999) for simple-span bridges; because no such data is available for continuous bridges in positive bending the same values are used in this analysis. Accordingly mean maximum applied live load for the

Table 5.2. Mean of applied loads as function of the effect of AASHTO HS-20 trucks.

	Two-Lane Loading		One-Lane Loading	
Span	LL_{75}	LL_2	LL_{75}	LL_2
45 ft	1.67	1.53	1.97	1.81
60 ft	1.72	1.60	2.02	1.86
80 ft	1.81	1.67	2.14	1.98
100 ft	1.89	1.75	2.26	2.08
120 ft	1.98	1.84	2.35	2.17
150 ft	2.01	1.87	2.37	2.19

design life of the structure $\overline{LL_{75}}$ for the 80-ft span loaded in two lanes is 1.81.

Assuming a lognormal model, the reliability index β_{member} for the failure of the first member can be expressed as

$$\beta_{member} = \frac{\ln \frac{\overline{LF_1}}{\overline{LL_{75}}}}{\sqrt{V_{LL}^2 + V_{LF}^2}} = \frac{\ln \frac{1.13 \times 6.96}{1.81}}{\sqrt{0.19^2 + 0.135^2}} = 6.31$$

b. Calculation of $\beta_{ultimate}$

Assuming that the load factor LF_u and the live load factor LL_{75} follow lognormal distributions, the reliability index of the system for the ultimate limit state can be found as

$$\beta_{ultimate} = \frac{\ln \frac{\overline{LF_u}}{\overline{LL_{75}}}}{\sqrt{V_{LL}^2 + V_{LF}^2}} = \frac{\ln \frac{1.13 \times 8.70}{1.81}}{\sqrt{0.19^2 + 0.135^2}} = 7.26$$

Thus, the reliability index margin for this bridge configuration is found to be larger than the target value.

$$\Delta\beta_u = \beta_{ultimate} - \beta_{member} = 7.26 - 6.31 = 0.95 > \Delta\beta_{u\,target} = 0.85$$

c. Calculating LF_1^N

Because the reliability index margin is greater than the target value, it would be allowed to lower the required member capacities of the main bridge members, so that the system reliability is reduced. The target system reliability index for the ultimate limit state can then be reduced by the difference between the existing

$$\beta_{ultimate}^N = \frac{\ln\left(\frac{\overline{LF_u^N}}{\overline{LL_{75}}}\right)}{\sqrt{V_{LF}^2 + V_{LL}^2}} = \beta_{ultimate} - (\Delta\beta_u - \Delta\beta_{u\,target})$$

$$= 7.26 - (0.95 - 0.85) = 7.16$$

$$\text{Thus, } \overline{LF_u^N} = e^{7.16 \times \sqrt{V_{LL}^2 + V_{LF}^2}} \times \overline{LL_{75}} = e^{7.16 \times \sqrt{0.19^2 + 0.135^2}} \times 1.81 = 9.60$$

$$LF_u^N = \frac{\overline{LF_u^N}}{b_{LF}} = \frac{9.60}{1.13} = 8.50$$

The analysis of a large number of I-girder bridges has established an empirical relationship between LF_u and LF_1 given as

$$LF_u = 1.16 \times LF_1 + 0.75\gamma$$

Thus, for $\gamma = 1$, $LF_1^N = (LF_u^N - 0.75)/1.16 = (8.50 - 0.75)/1.16 = 6.68$ which would provide the required nominal member capacity from $LF_1^N = \frac{R^N - D}{L_1}$ or $R^N = LF_1^N \times L_1 + D = 6.68 \times 6{,}450 + 4{,}860 = 47{,}946$ *kip–in*

d. Calculating System Factor ϕ_{system}

The system factor for this bridge configuration is obtained as

$$\phi_{system} = \frac{R}{R^N} = \frac{49{,}730}{47{,}946} = 1.04$$

e. Alternate Calculation of System Factor ϕ_{system} from Equation 5.26

Given the redundancy coefficients $C_{red1} = 1.16$ and $C_{red2} = 0.75$, a dead load to resistance ratio D/R = 4860/49730 = 0.098, $LF_1 = 6.96$, $\Delta\beta_T = 0.85$ and $\xi = \sqrt{V_{LF}^2 + V_{LL}^2} = \sqrt{0.19^2 + 0.135^2} = 0.233$, the load modifier is obtained as

$$\eta = e^{\xi\Delta\beta_T}\left[\frac{1 - D/R}{C_{red1}}\right] + D/R - \frac{C_{red2}}{C_{red1}LF_1}\left[1 - D/R\right]$$

$$= e^{0.85 \times 0.233}\left[\frac{1 - 0.098}{1.16}\right] + 0.098 - \frac{0.75}{1.16 \times 6.96}[1 - 0.098]$$

$$= 0.962$$

The system factor for this bridge configuration is obtained as

$$\phi_{system} = \frac{1}{\eta} = \frac{1}{0.962} = 1.04$$

which is the same value obtained going through the process (a) through (d).

This result indicates that this bridge configuration is redundant providing a sufficient margin of safety against collapse should the most critical girder of the bridge reach its ultimate capacity. Therefore, it would be possible to reduce the member capacity by a factor of 1.04 and have a bridge system capacity sufficiently high to safely carry the maximum expected live load during the service life of the bridge.

The results of the implementation of the calibration process for the ultimate limit state of originally intact typical bridge configurations analyzed in *NCHRP Report 406* and during the course of this project are summarized in Section 5.4.

5.4 System Factors for Ultimate Limit State of Originally Intact Bridges

Implementation of System Factors in Bridge Specifications

Table 5.1 presented a set of equations that were calibrated to describe the relationship between member load carrying capacity and the ultimate load carrying capacity of bridge

systems under vertical load. The relationships in Table 5.1 can be presented by equations of the form

$$LF_u = C_{red1} LF_1 + C_{red2} \tag{5.27}$$

The relationships in Table 5.1 can be used to calibrate the system factors to be incorporated into the member design equation to account for bridge system redundancy as presented in Equation 5.10 and repeated below.

$$\phi_s \phi R_n^N = \gamma_d D_n + \gamma_l L_n (1+I)$$

As derived in Section 5.3, the calibration of the system factor would lead to an expression that gives the system factor directly as a function of the coefficients of Equation 5.27 as listed in Table 5.1, and the dead load to member resistance ratio. The closed-form expression for the system factors, ϕ_s, is given in terms of a load modifier, η, as was shown

$$\eta = e^{\xi \Delta\beta_T}\left[\frac{1-D/R}{C_{red1}}\right] + D/R - \frac{C_{red2}}{C_{red1} LF_1}[1-D/R]$$

$$\phi_s = \frac{1}{\eta} \tag{5.26}$$

where C_{red1} and C_{red2} are respectively the slopes and intercepts of the redundancy equations in Table 5.1. As an example, Equation 5.7 would give $C_{red1} = 1.16$ and $C_{red2} = 0.75\gamma$. D/R in Equation 5.26 is the dead load to resistance ratio, LF_1 is the live load capacity of the most critical member as defined in Equation 5.8, $\Delta\beta_T$ is the target reliability index margin set at $\Delta\beta_T = 0.85$ and $\xi = \sqrt{V_{LF}^2 + V_{LL}^2}$ is the dispersion coefficient defined as the square root of the sum of the square of the COV for the live load carrying capacity LF and the maximum applied live load LL. An investigation of the COV for LF shows that V_{LF} is about 15% and $V_{LL} = 20\%$ so that $\xi = \sqrt{15\%^2 + 20\%^2} = 25\%$.

The implementation of Equation 5.26 for different values of LF_1 and D/R for bridges that satisfy the relationship $LF_u = 1.16LF_1 + 0.75\gamma$ where $C_{red1} = 1.16$ and $C_{red2} = 0.75\gamma$ leads to plots similar to those presented in Figures 5.18 and 5.19. Although Equation 5.26 should be relatively easy to apply, the data points were found to be well represented by the red curves, which follow an equation of the form

$$\phi_s = 1 + \frac{1 - 1.5(D/R)^2}{1 + LF_1^2}\gamma^2 \tag{5.28}$$

The range of error in ϕ_s from Equations 5.26 and 5.28 was found to be −0.03 and 0.01 when $\gamma = 1.0$ and from −0.03 to 0.05 when $\gamma = 4$. This range of error is deemed acceptable.

When C_{red2} in Equation 5.26 is equal to zero, the system factor equation reduces to

$$\begin{aligned}
\phi_s &= \frac{1}{\frac{e^{\Delta\beta\times\xi}}{C_{red1}} - \left[\frac{e^{\Delta\beta\times\xi}}{C_{red1}} - 1\right]\times D/R} \\
&= \frac{\frac{e^{\Delta\beta\times\xi}}{C_{red1}} + \left[\frac{e^{\Delta\beta\times\xi}}{C_{red1}} - 1\right]\times D/R}{\left[\frac{e^{\Delta\beta\times\xi}}{C_{red1}}\right]^2 - \left[\frac{e^{\Delta\beta\times\xi}}{C_{red1}} - 1\right]^2 \times (D/R)^2} \\
&= \frac{\frac{C_{red1}}{e^{\Delta\beta\times\xi}} + \frac{C_{red1}}{e^{\Delta\beta\times\xi}}\left[1 - \frac{C_{red1}}{e^{\Delta\beta\times\xi}}\right]\times D/R}{1 - \left[1 - \frac{C_{red1}}{e^{\Delta\beta\times\xi}}\right]^2 \times (D/R)^2} \\
&\approx \frac{C_{red1}}{e^{\Delta\beta\times\xi}} + \frac{C_{red1}}{e^{\Delta\beta\times\xi}}\left[1 - \frac{C_{red1}}{e^{\Delta\beta\times\xi}}\right]\times D/R
\end{aligned} \tag{5.29}$$

which can be implemented to find the system factors for the cases where $LF_u = C_{red1} x LF_1$.

The implementation of Equations 5.28 and 5.29 into the bridge categories of Table 5.1 leads to the set of system factors listed in Table 5.3.

That is, LF_1 in Table 5.3 represents the load carrying capacity of the weakest section of the beam, which either can be the positive bending section or the negative bending section

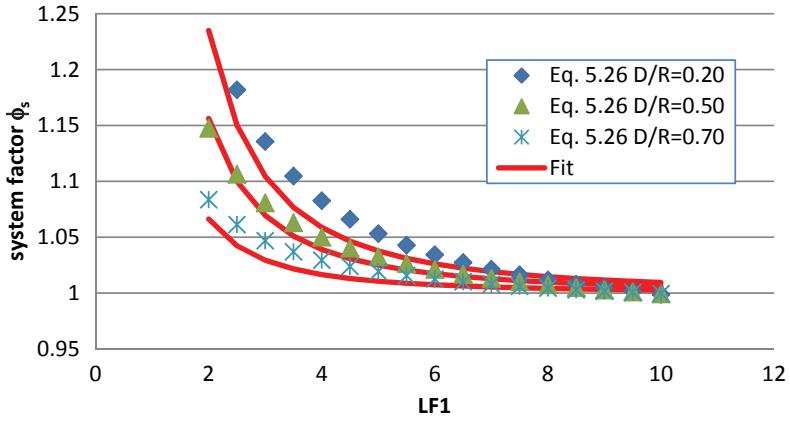

Figure 5.18. Plot of system factor vs. LF_1 for Equations 5.26 and 5.28 with $\gamma = 1$.

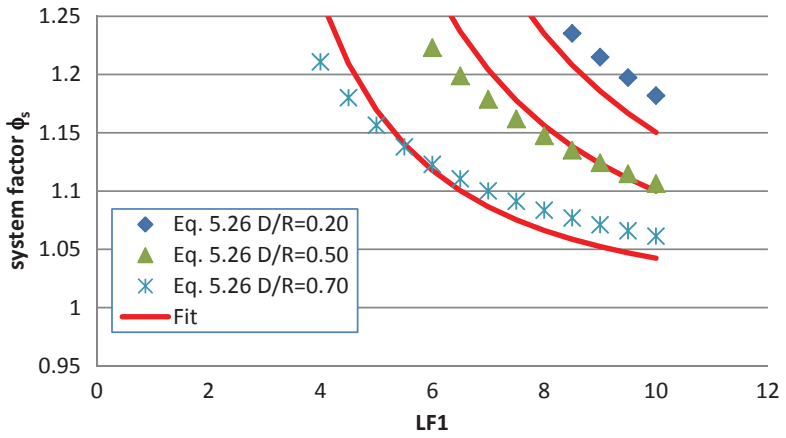

Figure 5.19. Plot of system factor vs. LF_1 for Equations 5.26 and 5.28 with $\gamma = 4$.

Table 5.3. System factors for originally intact systems under vertical loads.

Bridge Cross-Section Type	System Factor
Simple-span 4 I-beams at 4-ft	$\phi_s = 0.80 + 0.16\,D/R$
Simple-span 4 I-beams at 6-ft	$\phi_s = 0.90 + 0.09\,D/R$
Simple-span 6 I-beams at 4-ft	$\phi_s = 0.95 + 0.05\,D/R$
Continuous span 4 I-beams at 4-ft with compact members	$\phi_s = 0.93 + 0.07\,D/R$
Continuous steel I-girder bridges with noncompact negative bending sections and $LF_1^- \le 1.16LF_1^+ + 0.75$	$\phi_s = 0.80 + 0.16\,D/R$
All other simple-span and continuous I-beam bridges	$\phi_s = 1 + \frac{1 - 1.5(D/R)^2}{1 + LF_1^2}$
Narrow simple-span box-girder bridges less than 24-ft wide	$\phi_s = 0.83 + 0.14\,D/R$
All other simple-span box-girder bridges	$\phi_s = 1 + \frac{1 - 1.5(D/R)^2}{1 + LF_1^2}$
Narrow continuous box-girder bridges less than 24-ft wide	$\phi_s = 1 + \frac{1 - 1.5(D/R)^2}{1 + LF_1^2}$
Continuous steel box-girder bridges with noncompact negative bending sections and $LF_1^- \le 1.75LF_1^+$	$\phi_s = 1 + \frac{1 - 1.5(D/R)^2}{1 + LF_1^2}$
All other continuous box-girder bridges	$\phi_s = 1 + \frac{1 - 1.5(D/R)^2}{1 + LF_1^2}\gamma^2$

where

$LF_1 = LF_1^+ = \frac{R^+ - D^+}{L_1^+}$ when $\frac{LF_1^-}{LF_1^+} \ge 1.0$

$LF_1 = LF_1^- = \frac{R^- - D^-}{L_1^-}$ when $\frac{LF_1^-}{LF_1^+} < 1.0$

depending on the moment capacity in each region (R), the dead load moment in each region (D), and the effect of the applied live load moment on the most critical beam (L_1) where the live load represents two side-by-side HS-20 trucks applied at the middle of the span or two trucks in one lane applied in each of two contiguous spans. The positive superscript in R, D, and L_1 is for the positive bending region, the negative superscript is for the negative bending region.

The parameter L_1 gives the live load applied on the most critical member, which is defined as the member that fails first. It can be calculated as

$$L_1 = D.F._{actual} \times LL = \frac{D.F._{AASHTO\ LRFD\ Table}}{1.10} \times LL$$

where D.F. is the distribution factor and LL is the effect of the HL-93 truck load with no impact factor and no lane load. Because the distribution factors in the AASHTO LRFD specifications are conservative, a correction factor = 1.10 is applied when D.F. is taken from the AASHTO table. The bias = 1.10 was applied during the development of the AASHTO LRFD load distribution tables for conservative designs. In the case of estimating the redundancy of a bridge system, keeping the bias would lead to unconservative estimates of the system factor. For the analysis of a single lane of traffic load, the multiple presence factor M.P. = 1.2 should also be removed from the tabulated D.F. values.

Furthermore, it is proposed to use a factor equal to $\gamma = 2$ as a conservative value. In actuality, the value of γ for the continuous box-girder bridges in Table 5.2 is obtained as

$$\gamma = \begin{cases} \dfrac{EI_{box} \Big/ \left(E_{\text{transverse slab}} \dfrac{b_s t_s^3}{12} \right)}{38} & \text{for continuous boxes with } \dfrac{LF_1^-}{LF_1^+} \geq 1.75 \\ \dfrac{1}{1.75} \left(\dfrac{EI_{box} \Big/ \left(E_{\text{transverse slab}} \dfrac{b_s t_s^3}{12} \right)}{38} - 1 \right) \dfrac{LF_1^-}{LF_1^+} + 1 & \text{for continuous boxes with } \dfrac{LF_1^-}{LF_1^+} < 1.75 \\ 1.0 & \text{for other bridges.} \end{cases} \leq 8.0$$

Use $b_s = 120$ *in*

The modification factor γ takes into account the stiffness of continuous box-girder bridges relative to slab stiffness as well as the negative bending strength capacity of the box. EI_{box} is the stiffness for the cracked section of the box girder in negative bending, which ignores the portion of the concrete in tension. $E_{\text{transverse slab}}$ is the modulus of elasticity for the slab between the boxes, b_s = 120 in. gives the width of the slab assuming the stiffness is calculated based on a 120-in.-wide slab section having a depth t_s, $LF_1^+ = \dfrac{R^+ - D^+}{L_1^+}$ is the load factor in the positive bending region due to two side-by-side HS-20 trucks applied in the middle of the span or two trucks in one lane applied in each of two contiguous spans, and R^+, D^+, and L_1^+ are the moment resistance, dead load, and maximum live load effect of the most critical beam in the positive bending region. LF_1^- is the load factor in the most critical member in negative bending where $LF_1^- = \dfrac{R^- - D^-}{L_1^-}$ obtained for the two side-by-side HS-20 trucks applied in the middle of the span or due to two trucks in one lane applied in each of two contiguous spans, and R^-, D^-, and L_1^- are the moment capacity, dead load moment, and live load moment in the most critical negative bending section. The value of 38 is used to normalize the equation and is based on the stiffness of typical steel I-girder bridges designed to exactly satisfy the specifications' strength criteria.

The implementation of the system factors for I-girder bridges presented in this chapter is straightforward so that engineers could apply the concept in a routine manner. For example, during the rating process, the engineer can calculate the resistance R, the dead load effect D, and the AASHTO LRFD load distribution factor D.F., and find M_{truck}, which is the moment of the design truck load of the HL-93 (which is the same as the HS-20 truck). The effect on one beam is calculated as $L_1 = D.F. x M_{truck}$ where D.F. is the distribution factor. Next, the engineer finds the load factor that causes the first member to fail LF_1 from the equation

$$LF_1 = \frac{R - D}{L_1}$$

Although L_1 is calculated in this study using a structural model of the entire bridge, an approximation for L_1 can be obtained using the distribution factors of the LRFD specifications. Because of their lack of accuracy, using the simplified AASHTO distribution factors given in the standard specifications is not recommended. The equation to find LF_1 is the rating factor equation without safety factors or impact. Given LF_1, the engineer can find the system factor from Equation 5.26 as illustrated in the following example.

Numerical Example for Implementation

A numerical example is provided to illustrate the procedure for using the system factor during the rating of an existing bridge.

In this example the researchers assume a hypothetical case where the bending moment capacity of a 120-ft prestressed concrete bridge with six beams at 8-ft spacing was found

to be R = 7200 kip-ft. The dead load effect is found to be 3500 kip-ft. The moment due to the AASHTO truck load alone is 1880 kip-ft. The moment for the AASHTO 3S-2 legal load is 1682 kip-ft. The distribution factor from the AASHTO LRFD is 0.75 and the impact factor is 1.33.

The LRFR Operating Rating for a site where the average daily truck traffic is ADTT>5,000 is obtained as

$$R.F. = \frac{\phi R_n - \gamma_D D_n}{\gamma_L L_n} = \frac{1.0 \times 7200 - 1.25 \times 3500}{1.80 \times 1682 \times 0.75 \times 1.33} = 0.94$$

This rating factor value based on individual member capacity implies that the bridge should be closed, posted, immediately rehabilitated, or replaced. Given the redundant configuration of the bridge, the bridge owners may choose to delay such actions if the bridge system capacity is found to be sufficiently high so that the bridge would be able to withstand the potential overloading of a main girder.

To assess the entire system's load carrying capacity, the system factor is calculated based on Equation 5.26. A first step would require the calculation of LF_1 according to Equation 5.8

$$LF_1 = \frac{R - D}{D.F. \times LL_{HS20}} = \frac{7200 - 3500}{\frac{0.75 \times 1880}{1.10}} = 2.89$$

where the 1.10 bias is applied because the D.F. is taken from the AASHTO LRFD tables. If the bridge's six beams are spaced at more than 4-ft then Equation 5.26 is used to find the system factor with $D/R = 3500/7200 = 0.49$.

$$\eta = e^{\xi \Delta \beta_T}\left[\frac{1 - D/R}{1.16}\right] + D/R - \frac{0.75\gamma}{1.16 LF_1}\left[1 - D/R\right]$$

$$= e^{0.25*0.85}\left[\frac{1 - 0.49}{1.16}\right] + 0.49 - \frac{0.75}{1.16 \times 2.89}[1 - 0.49] = 0.92$$

$$\phi_s = \frac{1}{\eta} = 1.09$$

The adjusted system rating of the bridge is then executed using

$$R.F. = \frac{\phi_s \phi R_n - \gamma_D D_n}{\gamma_L L_n} = \frac{1.09 \times 1.0 \times 7200 - 1.25 \times 3500}{1.80 \times 1682 \times 0.75 \times 1.33} = 1.15$$

where the system factor ϕ_s is 1.09 and the other factors and variables are those that are normally used during the usual rating process.

The adjusted rating factor R.F. = 1.15, which is higher than 1.0, implies that the bridge system will still be able to support the applied loads should one member reach its limiting capacity because of the bridge's redundant configuration. The bridge's redundancy is making the system's capacity significantly higher than the capacities of the individual members. Thus, even if one member reaches its limiting capacity, the bridge system will not collapse.

In calculating LF_1, the researchers have assumed in this exercise that the distribution factors in the AASHTO LRFD are on the average conservative by a factor of about 1.10 for I-girder bridges. Accounting for this difference leads to a system factor lower than estimated from the use of the AASHTO LRFD distribution factors and a lower rating than would have been obtained if the AASHTO table is used without the correction. If, for the sake of simplicity, it is assumed that the load distribution factor in the AASHTO tables is accurate, then calculated value for LF_1 is approximated as

$$LF_1 = \frac{R - D}{D.F. \times LL_{HS20}} = \frac{7200 - 3500}{0.75 \times 1880} = 3.18$$

leading to a system factor ϕ_s

$$\eta = e^{\xi \Delta \beta_T}\left[\frac{1 - D/R}{1.16}\right] + D/R - \frac{0.75\gamma}{1.16 LF_1}\left[1 - D/R\right]$$

$$= e^{0.25*0.85}\left[\frac{1 - 0.49}{1.16}\right] + 0.49 - \frac{0.75}{1.16 \times 3.18}[1 - 0.49] = 0.93$$

$$\phi_s = \frac{1}{\eta} = 1.075$$

The adjusted system rating of the bridge is then executed leading to a slightly more conservative rating factor.

$$R.F. = \frac{\phi_s \phi R_n - \gamma_D D_n}{\gamma_L L_n} = \frac{1.075 \times 1.0 \times 7200 - 1.25 \times 3500}{1.80 \times 1682 \times 0.75 \times 1.33} = 1.11$$

The proposed approach is believed to be superior to those of the current AASHTO LRFD specifications and the Canadian bridge code because the proposed approach eliminates the subjectivity in deciding which load modifier or reliability index the engineer should use. The proposed approach is based on non-subjective parameters and criteria that are available to the engineer from the bridge cross section (number of beams and beam spacing) and the resistance and applied loads that are calculated during traditional bridge design and rating processes.

5.5 Summary of Bridge Analysis and Results for Damaged Bridges

This section summarizes the results of the analyses of damaged I-girder and box-girder bridges. The damage scenario consisted of removing an entire I-beam from the multi-girder

bridges. For the box-girder bridges, the main damage scenario also consisted of removing an entire web. In addition, the analyses considered an alternate damage scenario consisting of removing a 6-in. segment of both webs and the bottom flange of one steel box girder.

Prestressed Concrete and Composite Steel I-Girder Bridges

Numerous simple-span and continuous-span composite-steel I-girder bridges and prestressed concrete I-girder bridges were analyzed in *NCHRP Report 406*. The results of these analyses are extracted for the purposes of this project to study how the redundancy of these bridges varies with the number of beams, beam spacing, and span length. The simple-span bridges varied in length between 45-ft and 150-ft with a composite concrete deck supported by 4, 6, 8, and 10 beams spaced at 4-ft, 6-ft, 8-ft, 10-ft, and 12-ft. Also, the *NCHRP Report 406* sample included composite steel I-girder bridges with two 120-ft continuous spans supported by 4, 6, 8, and 10 beams spaced at 4-ft, 6-ft, 8-ft, 10-ft, and 12-ft. The bridges' concrete slabs varied in depth between 7.5-in. and 8.5-in. depending on the beam spacing. The beams are assumed to be A-36 steel while the deck's strength is equal to $f'_c = 3.5$ ksi. Also, over 50 prestressed concrete I-girder bridges with two continuous spans varying in length between 100-ft and 150-ft supported by 4, 6, 8, and 10 beams spaced at 4-ft, 6-ft, 8-ft, 10-ft, and 12-ft were investigated. The bridges' concrete slabs varied in depth between 7.5-in. and 8.5-in. depending on the beam spacing. The beams are assumed to have a compressive concrete strength $f'_c = 5$ ksi while the deck's strength is equal to $f'_c = 3.5$ ksi. The prestressing tendons are assumed to be 270-ksi steel.

The *NCHRP Report 406* bridges were designed to exactly satisfy the strength requirements of the AASHTO LRFD design specifications. Sensitivity analyses also were performed to investigate the effect of changes in member strength, slab strength, dead weight, as well as other parameters. The moment-rotation relationships for the steel bridges analyzed in *NCHRP Report 406* were obtained using existing empirical models based on test results as described in the appendices of *NCHRP Report 406*. The moment-rotation relationships were then used to perform the nonlinear analysis of the bridge. The analyses were performed assuming that the sections in negative bending are compact and the results are compared to the cases where the sections in negative bending are noncompact.

The results provided in *NCHRP Report 406* were supplemented by the results of the analysis of three-span continuous bridges with span lengths 50-ft, 80-ft, and 50-ft. The bridges were assumed to have 4, 5, or 6 beams at 8-ft spacing. The bridges were analyzed for different strengths and beam stiffness by assuming that they have different values for ultimate moment capacities and moments of inertia.

The results of the analysis of the wide composite steel I-girder bridges that compare the damaged system capacity of the bridge system represented by LF_d to the capacity to resist first member failure represented by LF_1 were found to be highly dependent on the beam spacing while the number of beams had generally little influence on the results except for the case where the bridge had only four beams at 4-ft center to center. The results are plotted in Figure 5.20 for the results averaged over their span lengths. The figure shows a clear dependence on beam spacing while the number of beams are only important for the bridge with four beams at 4-ft. The LF_d/LF_1 ratio was not related to the span length as illustrated in Figure 5.21.

The prestressed concrete bridges showed similar trends for the effect of beam spacing as shown in Figure 5.22. However, LF_d/LF_1 generally dropped as the span length increased as shown in Figure 5.23.

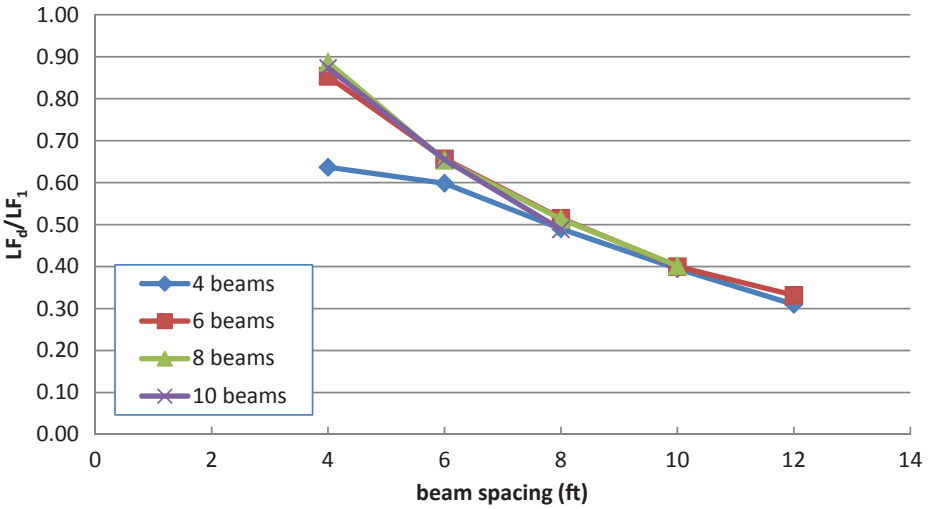

Figure 5.20. Plot of LF_d/LF_1 vs. beam spacing for steel I-girder bridges.

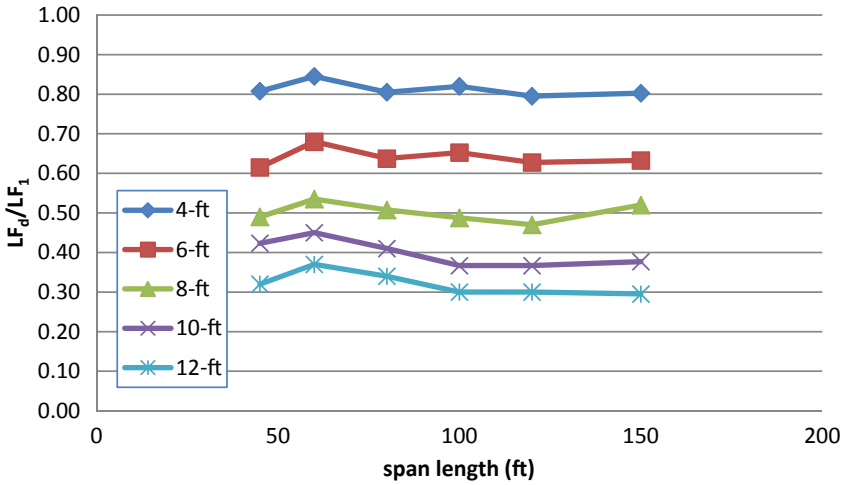

Figure 5.21. Effect of span length on LF_d/LF_1 for steel I-girder bridges.

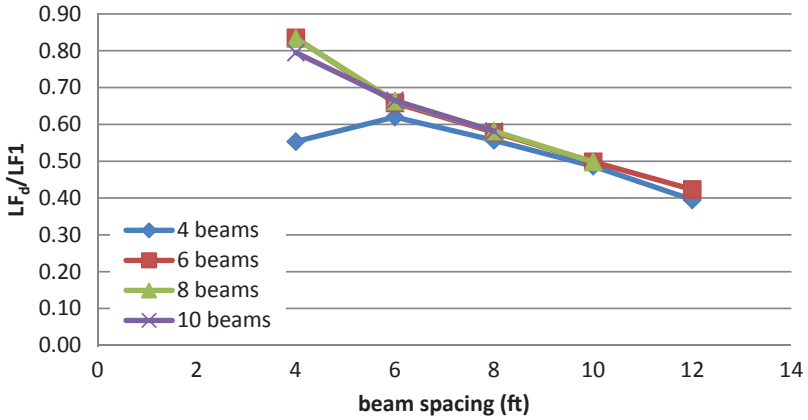

Figure 5.22. Plot of LF_d/LF_1 vs. beam spacing for damaged prestressed concrete I-girder bridges.

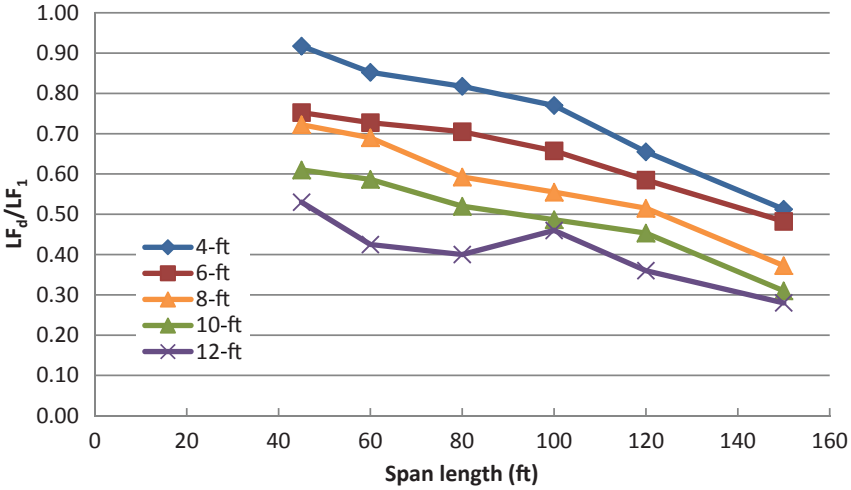

Figure 5.23. Effect of span length on LF_d/LF_1 for damaged prestressed concrete I-girder bridges.

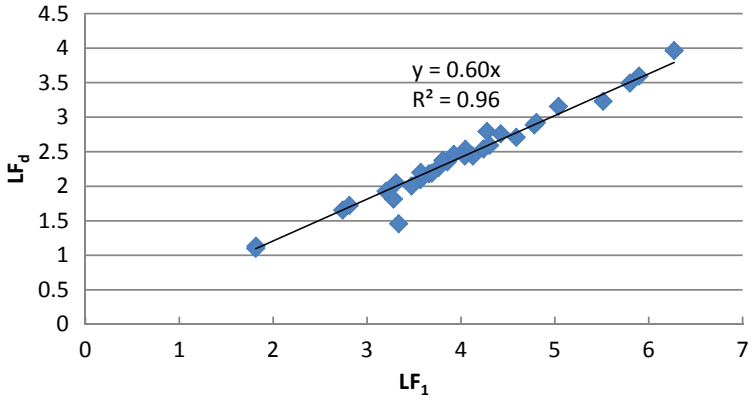

Figure 5.24. Relation between LF_d and LF_1 for simple-span steel I-girder bridges.

The plot of LF_d versus LF_1 for a set of simple-span bridges is presented in Figure 5.24. The results show a strong linear relationship between LF_d and LF_1 with an equation of the form

$$LF_d = 0.60LF_1 \tag{5.30}$$

The same analysis was performed on a set of continuous steel girder bridges. The analysis compared the results of compact and noncompact sections for the case when the damaged bridge was loaded with two lanes in the middle of the span to the case when two trucks are in one lane, one truck placed in each of two consecutive spans. The results are plotted in Figure 5.25 by taking the minimum value of LF_d from the two loading cases and comparing it to the minimum value of LF_1. The plot shows that a lower bound for the results that would cover compact and noncompact sections can be established using a linear relationship of the form

$$LF_d = 0.59LF_1 \tag{5.31}$$

This linear relationship is obtained from the regression analysis of the results of bridges with noncompact sections in negative bending. The analyses in Figures 5.24 and 5.25 were for bridges with four beams at 8-ft spacing and six beams at 8-ft spacing, respectively. As noted, the relationship between LF_d and LF_1 is also affected by the beam spacing. Additional analyses also investigated the effect of the deck slab strength and the weight of the damaged beam.

Box-Girder Bridges with Severe Damage to One Web

Numerous steel and concrete box-girder bridges were analyzed assuming two damage scenarios. The first damage scenario assumes severe damage to an external web representing the consequences of collisions or severe corrosion to the prestressing tendons of prestressed concrete or the corrosion of steel box-girder bridges. In these models, it is assumed that the

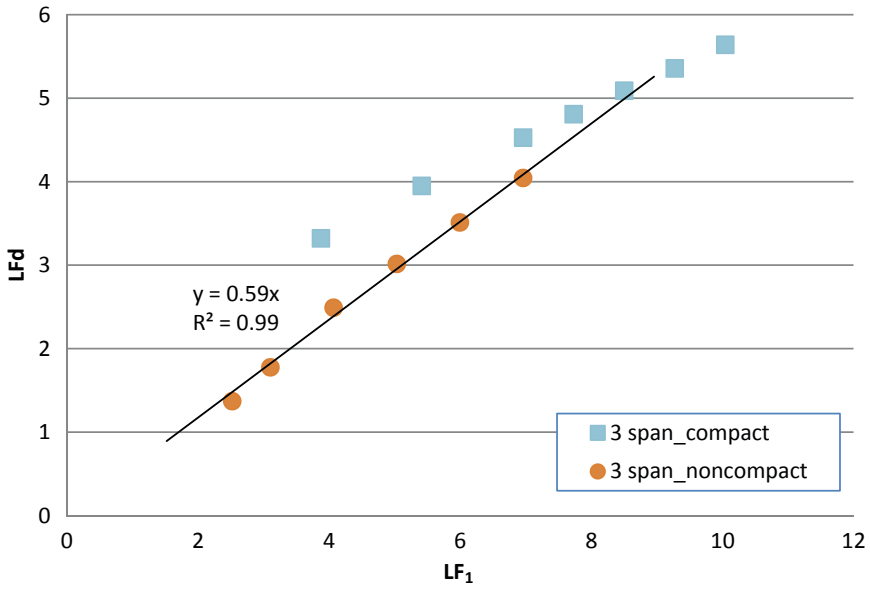

Figure 5.25. Relationship between LF_d and LF_1 for continuous steel I-girder bridges.

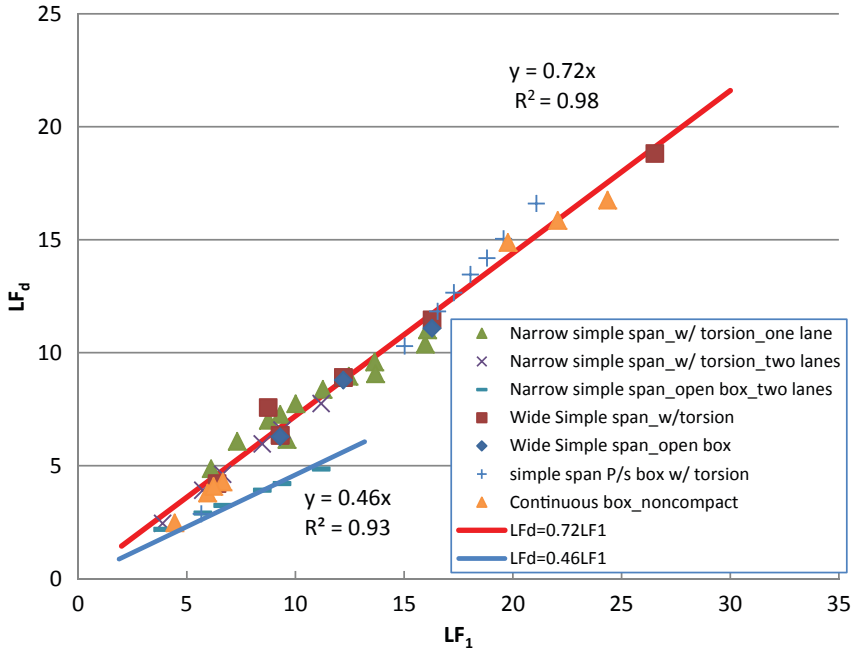

Figure 5.26. Summary of the results for damaged box-girder bridges.

torsional rigidity of the box is not affected by the damage. The results of these analyses are summarized in Figure 5.26. The figure shows that the load carrying capacity of damaged systems is related to the ability of the system to resist first member failure with a relationship of the form

$$LF_d = 0.72LF_1 \tag{5.32}$$

The relationship, which is somewhat similar to that of continuous I-girder bridges, holds for narrow simple-span box-girder bridges, wide simple-span box-girder bridges, as well as three-span and two-span continuous box-girder bridges as long as the damaged box maintains a sufficient level of torsional rigidity. However, if the damaged box of a narrow simple-span bridge loses its torsional capacity altogether, the capacity of the system degrades to close to half its load carrying capacity. This is because the torsional capacity of a damaged narrow box will help redistribute the load to the remaining three box webs and this ability is lost if the torsional capacity is lost. However, the same is not necessarily true for wide boxes that have a much larger web spacing and spacing between the boxes. In this case, the torsional capacity of the box will not add a significant ability to redistribute the load to the undamaged box. This is because the torsional capacity may help redistribute the load locally but, globally, the contribution of the torsion is offset by the longer distance to the undamaged portions of the bridge. The load carrying capacity of damaged narrow simple box-girder bridges that lose one box's torsional capacity along with one web will follow an equation of the form

$$LF_d = 0.46LF_1 \tag{5.33}$$

Although the AASHTO specifications assume that all steel box girders in negative bending should be considered to have noncompact sections, in this project, several continuous steel boxes with compact sections in negative bending were analyzed to study how box ductility would affect the damaged bridge system's capacity assuming severe damage to an external web. Continuous prestressed concrete boxes also are investigated. The results of these analyses are summarized in Figure 5.27. The figure shows that the load carrying capacity of damaged systems is related to the ability of the system to resist first member failure with a relationship of the form

$$LF_d = 0.59LF_1 + 4.50 \tag{5.34}$$

The relationship is different from that of three-span and two-span continuous box-girder bridges with noncompact sections over the supports. The data in Figure 5.27 include wide and narrow prestressed concrete boxes loaded by two lanes of traffic or separately by one lane loaded by one truck, one in each span. The wide steel boxes also were loaded by two trucks side by side or separately by one truck in each span. Two cases are considered for the effect of torsional rigidity for the damaged continuous steel boxes. One case assumes that the torsional rigidity is not affected by the damage, and in another case the damage is assumed to also eliminate the torsional rigidity. Equation 5.34 is found to give a lower bound to all the cases considered.

Steel Box-Girder Bridges with Fractured Box

Several steel simple-span and continuous box-girder bridges were analyzed assuming that one box was damaged due to

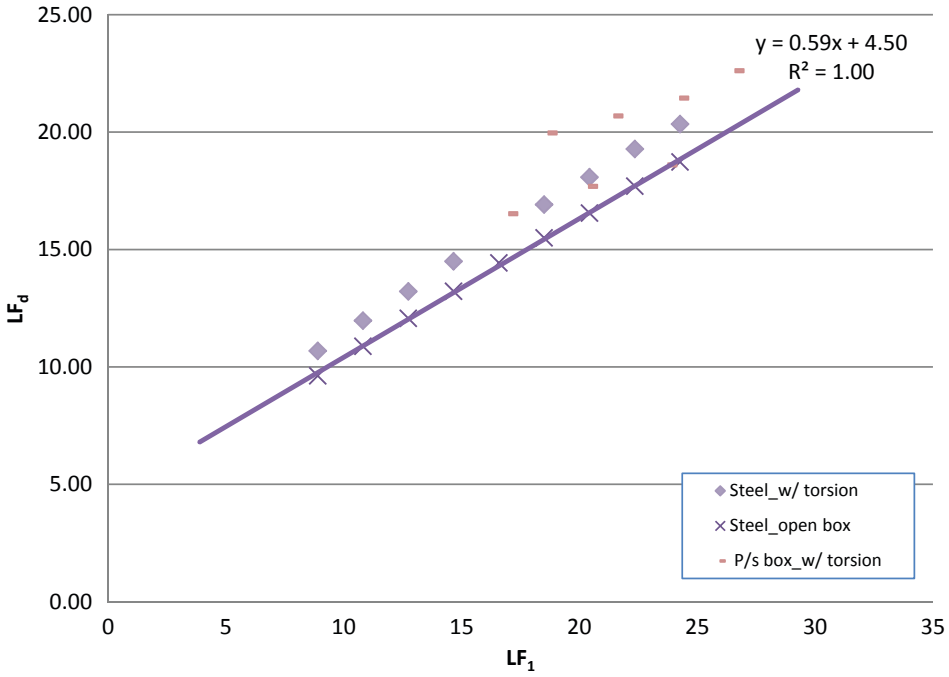

Figure 5.27. Summary of the results for damaged continuous box-girder bridges with compact section at supports.

fatigue fracture. This is done by removing about a 1-ft segment in each of the webs and the bottom flange at the midpoint along the length of one box. In these models, it is assumed that the torsional rigidity of the remaining portions of the box is not affected by the damage. The results of these analyses are summarized in Figure 5.28. The figure shows that the load carrying capacity of simple-span damaged systems also is related to the ability of the system to resist first member failure with a relationship of the form

$$LF_d = 0.82LF_1 - 4.14 \quad (5.35)$$

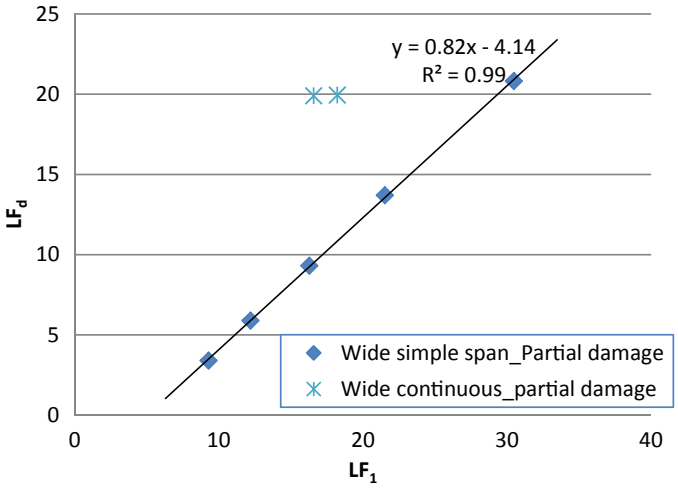

Figure 5.28. Plot of LF_d vs. LF_1 for fractured box-girder bridges.

However, continuous bridges show remarkably strong ability to continue to carry significant loads after damage. This is due to the cantilevering effect that continuous bridges provide allowing for the effect of the damage to be reasonably low.

Effect of Beam Spacing

The results of simple-span bridges provided in *NCHRP Report 406* demonstrate a clear dependence on beam spacing, as shown in Figure 5.20. However, the load factor LF_1 for the bridges analyzed during *NCHRP Report 406* had a very limited range with LF_1 varying between 2.2 and 4.7. This made it difficult to understand how the damaged bridge load factor LF_d varies as the first member failure load factor LF_1 changes. Therefore, additional bridge models having load factors LF_1 ranging between 3.0 and 8.0 were analyzed. In the analysis, the dead load applied along the length of each beam is assumed to be 0.97 kip/ft and the deck's capacity to carry moment in the transverse direction 13.5 kip-ft/ft (or 1615 kip-in. for each 10-ft-wide slab segment). This value for moment capacity of the deck is similar to the one used in *NCHRP Report 406*. Figure 5.29 plots the damaged system capacity of the bridge system represented by LF_d versus the capacity to resist first member failure represented by LF_1. The results show a consistent trend of increasing damaged bridge capacity as the capacity of the first member represented by LF_1 increases. The relationship between LF_d and LF_1 is depicted in Figure 5.30. The figure also shows

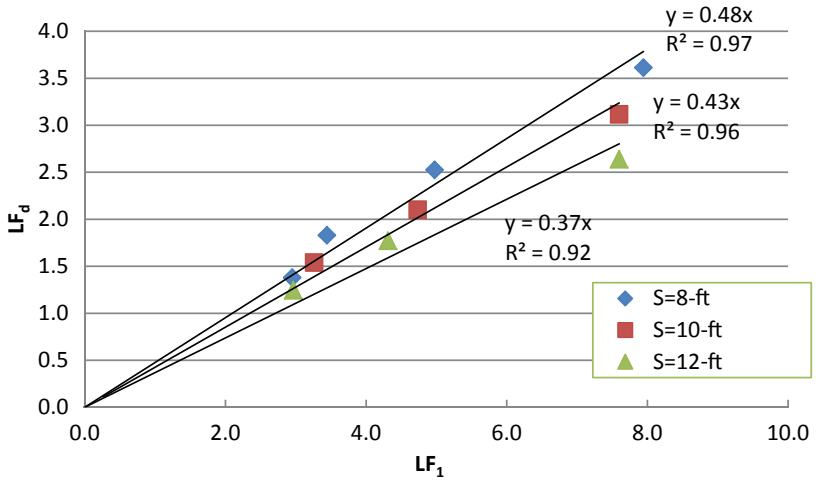

Figure 5.29. Effect of beam spacing on simple-span damaged bridges.

how LF_d decreases for the same LF_1 as the beam spacing increases. The trend with beam spacing is similar to that depicted in Figure 5.20 with $LF_d = 0.48\ LF_1$ for the systems analyzed in this case with beams at 8-ft, $LF_d = 0.43\ LF_1$ for bridges with beams at 6-ft, and $LF_d = 0.37\ LF_1$ for bridges with beams at 12-ft.

As depicted in Figure 5.30, which includes the data from *NCHRP Report 406* and additional data obtained during the course of this project, the relationship that, on average, describes the ratio of LF_d/LF_1 as a function of the beam spacing is found to be

$$\frac{LF_d}{LF_1} = (1 - 0.056\,S) \tag{5.36}$$

where S is the beam spacing in feet.

The relationship is for the average beam with a distributed weight along the length of the bridge of 1.0 kip/ft per beam. The equation gives the general trend with some variation around the trend based on the properties of the girders and the span length.

For continuous two-span steel bridges, *NCHRP Report 406* considered two negative bending section types: those that are compact and those with noncompact sections. Also, two load cases are considered. The first load case consisted of two trucks side-by-side in one span. The second load case placed one truck in each span. The load factor that causes the first failure of a member assuming linear-elastic behavior was used to determine LF_1. LF_d was the lowest load carrying capacity of the damaged system after removing one entire girder from one span. The results for the steel I-girder bridges are presented in Figure 5.31. The results for continuous prestressed concrete I-girder bridges are given in Figure 5.32. The plot shows that the trend line is very similar to that of the compact steel bridges. Therefore, the same equation would be applicable for both the continuous prestressed concrete and compact steel bridges.

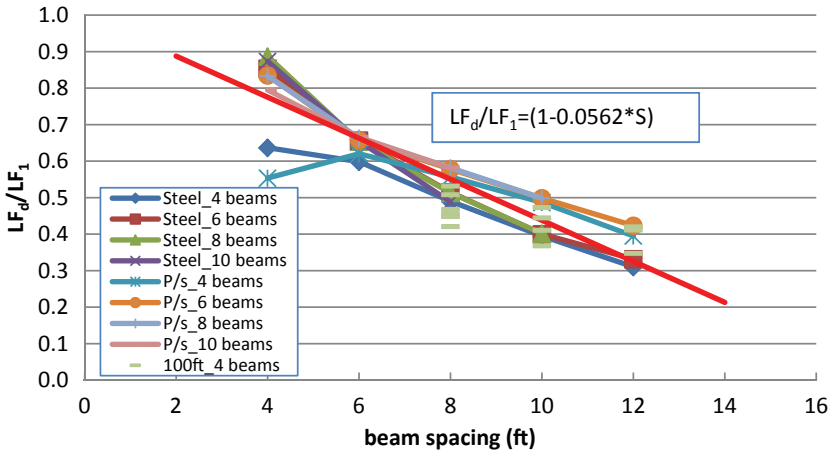

Figure 5.30. Effect of beam spacing on damaged bridges.

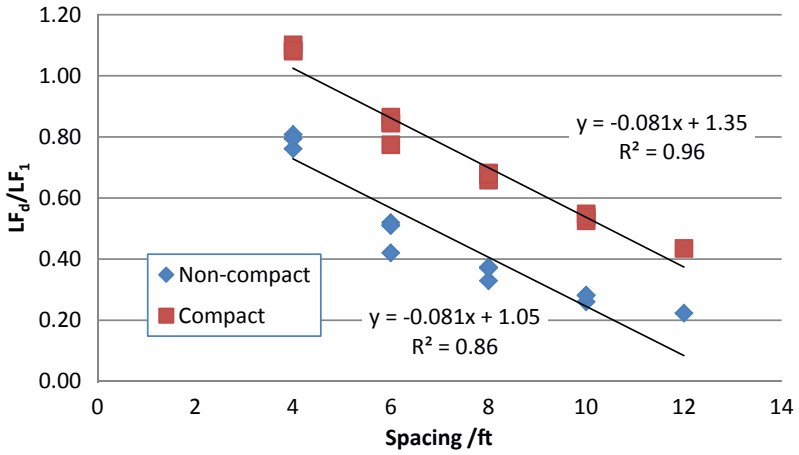

Figure 5.31. Effect of beam spacing on damaged continuous steel I-girder bridges.

Effect of Dead Weight of Damaged Beam

The results of simple-span bridges provided in *NCHRP Report 406* also demonstrate that bridge redundancy for the damaged limit state depends on the weight of the damaged beam that must be transferred to the adjacent undamaged beams as the bridge is loaded. To better establish this relationship, additional bridge models having a load factor LF_1 ranging from 3.0 and up to 8.0 were analyzed. In the analysis, the spacing for each beam was fixed at 8-ft and the deck capacity is kept at 13.5 kip-ft/ft of slab. Figure 5.33 plots the damaged system capacity of the bridge systems analyzed in this case represented by LF_d versus the capacity to resist first member failure represented by LF_1.The results show that a doubling of the beam weight will reduce the slope of LF_d versus LF_1 by 23%.

As depicted in Figure 5.33, the relationship that, on average, describes the ratio of LF_d/LF_1 as a function of the beam spacing is found to be

$$\frac{LF_d}{LF_1} = (0.60 - 0.12\omega) \tag{5.37}$$

where ω is the weight of the beam per unit length expressed in kip/ft.

The relationship is for the average beam with a distributed weight along the length of the bridge of 1.0 kip/ft per beam. The equation gives the general trend with some variation around the trend based on the properties of the girders and the span length.

Alternatively, a correction factor can be used on the original Equations 5.30 through 5.36 to reflect the reduction in

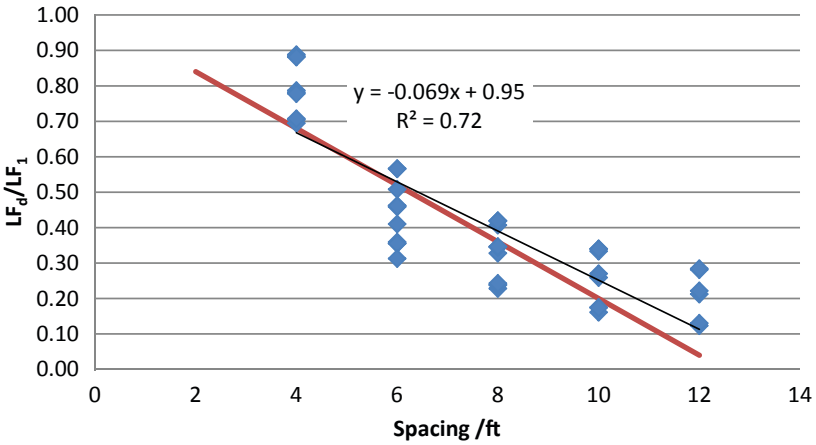

Figure 5.32. Effect of beam spacing on damaged continuous prestressed concrete I-girder bridges.

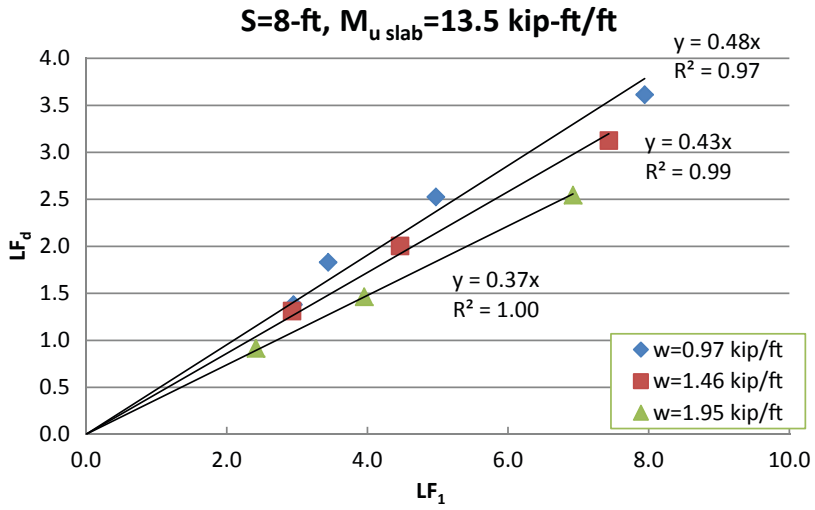

Figure 5.33. Effect of dead weight of damaged beam.

the redundancy ratio. The weight correction factor is defined as γ_{weight}

$$\gamma_{weight} = \frac{LF_{\text{d modified}}}{LF_d} = 1.23 - 0.23\omega_{beam}\,(kip/ft) \qquad (5.38)$$

where ω_{beam} is the total dead weight applied on each beam expressed in kip per unit length.

Effect of Deck Capacity

The effect of the deck's bending moment capacity also is investigated to study how bridge redundancy varies when the deck's bending moment capacity is reduced. In the analysis performed in this section, the spacing between the beams is set at 8-ft or 10-ft, and the dead load on each beam is 0.97 kip/ft. Figure 5.34 plots the damaged system capacity of bridge systems represented by LF_d versus the capacity to resist first member failure represented by LF_1 for systems analyzed in this sensitivity analysis. The results show that damaged bridges will carry less live load as the deck's moment capacity decreases. The trend in Figure 5.34 also demonstrates that the increase in LF_d as the deck capacity increases will be smaller if the bridge member capacity represented by LF_1 itself is small. As LF_1 increases, the deck's contribution to increasing the overall damaged bridge's capacity increases.

The improvement due to deck capacity for damaged bridges can be depicted as shown in Figure 5.35. Furthermore, a

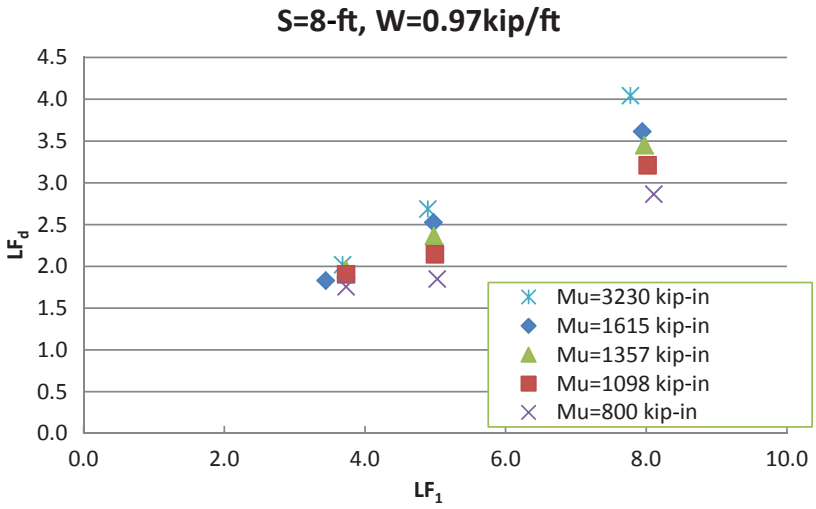

Figure 5.34. Effect of deck capacity Mu deck on capacity of damaged bridges.

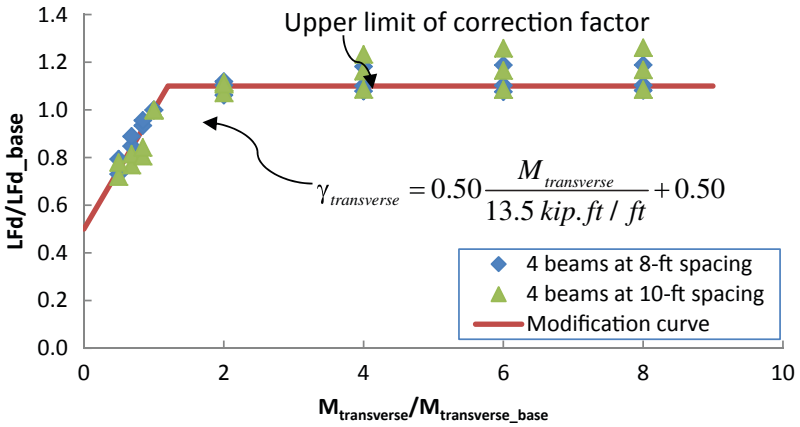

Figure 5.35. Modification curve for deck capacity $M_{transverse}$.

verification of the effect of diaphragm capacity with different spacing is shown in Figure 5.36. The base line is the deck with a transverse bending moment capacity equal to $M_{transverse}$ = 13.5 kip-ft/ft (or 1615 kip-in. for each 10-ft-wide slab segment). The load capacity of the bridge system varies almost linearly as a function of $M_{transverse}$ reaching an upper limit for improvement at about 1.10 to 1.20. The presence of diaphragms and cross beams can be considered in terms of the contribution they make to improve the transverse bending capacity of the system. Of course, this assumes that the cross beams are distributed along the length of the bridge and especially near the middle of the span. It also assumes that they are firmly attached to the longitudinal beams to resist the large bending moments that will develop as the damaged system is overloaded as shown in Figure 5.35. The equation that describes the effect of the transverse bending capacity is given in terms of a slab effect correction factor, $\gamma_{transverse}$, as

$$\gamma_{transverse} = \frac{LF_{d\ \text{modified}}}{LF_d} = 0.50 \frac{M_{transverse}}{13.5\ kip.ft\ /\ ft} + 0.50 \le 1.10 \quad (5.39)$$

$$M_{transverse} = M_{slab} + M_{br/L} \quad (5.40)$$

where $M_{transverse}$ = combined moment capacity for lateral load transverse expressed in kip-ft per unit slab width, M_{slab} = moment capacity of slab per unit width, and $M_{br/L}$ = contribution of the bracing and diaphragms to transverse moment capacity calculated using Equation 5.41 or 5.42.

Equivalent transverse moment capacity for cross bracing as defined in the FHWA Steel Bridge Design Handbook: Bracing System Design (2012)

$$M_{br/L} = \frac{F_{br} h_b}{L_b} \quad (5.41)$$

Equivalent transverse moment capacity for diaphragm

$$M_{br/L} = \frac{M_{br}}{L_b} \quad (5.42)$$

where M_{br} = moment capacity of diaphragms contributing to lateral transverse distribution of vertical load between

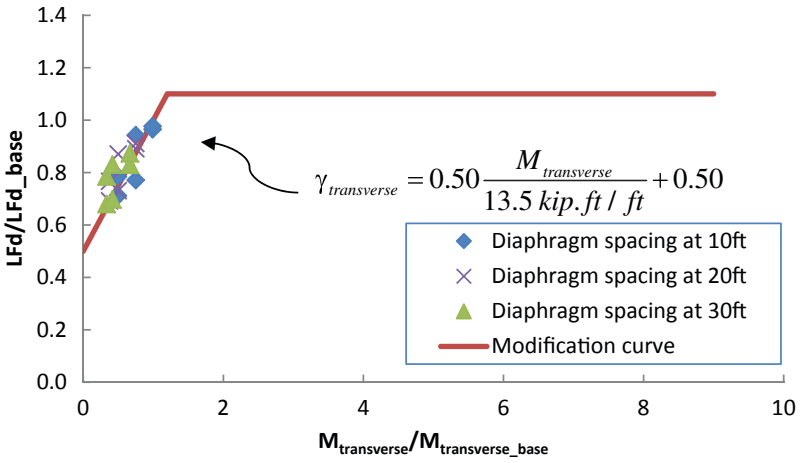

Figure 5.36. Verification for diaphragm and deck capacity $M_{transverse}$.

Table 5.4. Summary of LF_d vs. LF_1 for damaged systems under vertical loads.

Bridge Cross-Section Type	Equation for Redundancy Ratio $R_d = \frac{LF_d}{LF_1}$
Simple-span and continuous prestressed concrete I-beam bridges with four beams at 4-ft	$R_d = 0.56\gamma_{transverse}\gamma_{weight}$
Simple-span and continuous compact steel I-girder bridges with four beams at 4-ft	$R_d = 0.64\gamma_{transverse}\gamma_{weight}$
Continuous noncompact steel I-girder bridges with four beams at 4-ft	$R_d = 0.58\gamma_{transverse}\gamma_{weight}$
Wide simple-span I-girder bridges	$R_d = (1 - 0.056\,S)\gamma_{transverse}\gamma_{weight}$
Wide continuous compact steel and prestressed concrete I-girder bridges	$R_d = (1.35 - 0.08\,S)\gamma_{transverse}$
Wide continuous noncompact steel I-girder bridges	$R_d = (1.00 - 0.08\,S)\gamma_{transverse}$
Narrow simple-span steel box-girder bridges less than 24-ft, open box no torsional rigidity	$R_d = 0.46\gamma_{transverse}$
Fractured simple-span steel box-girder bridges less than 24-ft wide	$R_d = \left(0.82 - \frac{4.14}{LF_1}\right)\gamma_{transverse}$
All other simple-span box-girder bridges	$R_d = 0.72\gamma_{transverse}$
Continuous steel box-girder bridges with noncompact negative bending sections and $\frac{LF_1^-}{LF_1^+} \le 1.75$	$R_d = 0.72\gamma_{transverse}$
All other continuous box-girder bridges	$R_d = \left(0.59 + \frac{4.50}{LF_1}\right)\gamma_{transverse}$

where S = beam spacing in feet.

$$\gamma_{weight} = \frac{LF_{\text{d modified}}}{LF_d} = 1.23 - 0.23\omega_{beam}\,(kip/ft)$$

$$\gamma_{transverse} = \frac{LF_{d\,\text{modified}}}{LF_d} = 0.50\frac{M_{transverse}}{13.5\ kip.ft/ft} + 0.50 \le 1.10$$

and ω_{beam} is the total dead weight applied on each beam expressed in kip per unit length. $M_{transverse}$ is the combined moment capacity of the slab and transverse members including diaphragms expressed in kip-ft per unit slab width.

adjacent main bridge girders; F_{br} = bracing chord force determined from the applicable limit state for the bolts (see AISC Steel Construction Manual, 2011, Part 7), welds (see AISC, 2011, Part 8), and connecting elements (see AISC, 2011, Part 9); L_b = spacing of the cross frames or diaphragms; and h_b = distance between the bracing top and bottom chords.

Summary

The redundancy of damaged bridge systems that may have lost the load carrying capacity of a critical member due to various possible deterioration mechanisms or extreme events is a function of the beam spacing, the slab strength, and the dead load that the damaged beam needs to release to the remaining intact members. The results of damaged bridges show a clear correlation between LF_d and LF_1 represented by the redundancy ratio defined as $R_d = \frac{LF_d}{LF_1}$. Table 5.4 lists the relationship obtained for R_d as a function of span length and the load carrying capacity of the most critical member LF_1 accounting for the variation in R_d with slab strength and dead weight applied on the damaged member for the bridge types analyzed in this study.

5.6 System Factors for Damaged Bridges

The calibration of the system factor for bridges susceptible to major damage to main load carrying members was performed using the same procedure outlined for the ultimate limit state, and the target reliability margin was set at $\Delta\beta_{d\,target} = -2.70$. This target value was selected because it corresponds to the average margin obtained for typical 4-beam I-girder bridges, which have traditionally been accepted as providing acceptable levels of redundancy.

The calibration of the system factor can be performed easily using the expression in Equation 5.26. In most of the cases

listed in Table 5.3, the redundancy equation can be represented in the form

$$LF_d = C_{red1} LF_1 \tag{5.43}$$

where the parameter C_{red1} is equal to the redundancy ratio R_d.

The algebraic manipulation of Equation 5.26 is given as

$$\eta = e^{\xi \Delta \beta_T} \left[\frac{1 - D/R}{C_{red1}} \right] + D/R - \frac{C_{red2}}{C_{red1} LF_1} \left[1 - D/R \right]$$

$$\phi_s = \frac{1}{\eta}$$

with $C_{red1} = R_d$ and $C_{red2} = 0$ leads to an expression for the system factor given as

$$\phi_s = \frac{R_d}{0.47 - (0.47 - R_d)\dfrac{D}{R}} \tag{5.44}$$

where 0.47 is obtained from $0.93e^{(\xi \Delta \beta_T)}$ where the COV for the evaluation of the capacity of the bridge system is assumed to be $\xi = 25\%$ and 0.93 is the live load bias $= \dfrac{\overline{LL_2}}{LL_{75}}$ in Equation 2.16 that accounts for the maximum 2-year live load as compared to the 75-year live load. *NCHRP Report 406* recommends that the calibration of the system factor for the damaged bridge limit state be based on a 2-year live load, which coincides with the normal bridge inspection period at which point in time the damage to the bridge will certainly be detected and appropriate actions taken to close, post, or rehabilitate it.

The process of determining the system factor for the damaged bridge limit state can then be executed using Equation 5.44, where appropriate values for R_d are obtained for the particular bridge configuration from Table 5.4. A summary of the proposed system factors for damaged I-girder and box-girder bridges is provided in Tables 5.5 and 5.6 as a function of the redundancy ratio $R_d = \dfrac{LF_d}{LF_1}$, which gives the capacity of a damaged bridge system that has previously lost the load carrying capacity of a main member given as LF_d and the ability of the originally intact bridge to resist first member failure, which is represented by the variable, LF_1, defined in Equation 5.8. For the box-girder bridges, three different damage scenarios are considered. In the first scenario, one box is assumed to have been exposed to a fatigue type fracture that sliced through the entire bottom flange and two webs. The second scenario assumed major damage to one web while maintaining the torsional capacity of the box. The third scenario considered that the failure of the web also led to the loss of the torsional rigidity of the box.

Tables 5.5 and 5.6 list the expressions for R_d as a function of beam spacing, slab strength, and the dead weight applied on the damaged member for the bridge types analyzed in this study.

5.7 Conclusions

This chapter summarized the results of the redundancy analysis of simple-span and continuous steel and prestressed concrete I-girder and box-girder bridges. The redundancy was evaluated for the ultimate limit state of the originally intact

Table 5.5. System factors for damaged I-girder bridges under vertical loads.

Bridge Cross-Section Type	Redundancy Ratio $R_d = \dfrac{LF_d}{LF_1}$	System Factor
Simple-span and continuous prestressed concrete I-girder bridges with four beams at 4-ft	$R_d = 0.56\gamma_{transverse}\gamma_{weight}$	$\phi_s = \dfrac{R_d}{0.47 - (0.47 - R_d)\dfrac{D}{R}}$
Simple-span and continuous compact steel I-girder bridges with four beams at 4-ft	$R_d = 0.64\gamma_{transverse}\gamma_{weight}$	
All other simple-span I-girder bridges	$R_d = (1 - 0.056\,S)\gamma_{transverse}\gamma_{weight}$	
Continuous noncompact steel I-girder bridges with four beams at 4-ft	$R_d = 0.58\gamma_{transverse}$	
All other continuous noncompact steel I-girder bridges	$R_d = (1.00 - 0.08\,S)\gamma_{transverse}$	
All other continuous compact steel and prestressed concrete I-girder bridges	$R_d = (1.35 - 0.08\,S)\gamma_{transverse}$	

Table 5.6. System factors for damaged box-girder bridges under vertical loads.

Bridge Cross-Section Type	Redundancy Ratio $R_d = \frac{LF_d}{LF_1}$	System Factor
Fractured simple-span steel box-girder bridges less than 24-ft wide	Non-redundant	ϕ_s=0.80
Narrow simple-span steel box-girder bridges less than 24-ft with no torsional rigidity	$R_d = 0.46\gamma_{transverse}$	$\phi_s = \frac{R_d}{0.47 - (0.47 - R_d)\frac{D}{R}}$
All other simple-span box-girder bridges	$R_d = 0.72\gamma_{transverse}$	
Continuous steel box-girder bridges with noncompact negative bending sections and $LF_1^- \le 1.75LF_1^+$	$R_d = 0.72\gamma_{transverse}$	
All other continuous box-girder bridges	$R_d = \left(0.59 + \frac{4.50}{LF_1}\right)\gamma_{transverse}$	

where S = beam spacing in feet.

$\gamma_{weight} = 1.23 - 0.23\omega_{beam}(kip/ft)$

ω_{beam} = total dead weight on the damaged beam in kip per unit length.

$\gamma_{transverse} = 0.50\frac{M_{transverse}}{13.5\ kip.ft/ft} + 0.50$

$M_{transverse}$ = combined moment capacity of the slab and transverse members including diaphragms expressed in kip-ft per unit slab width.

The range of applicability of $\gamma_{transverse}$ has been verified for I-girder bridges for up to a range of $\gamma_{transverse}$ =1.10.

bridges, as well as bridges that have suffered major damage to the most critical bridge member. The results were fitted into equations that best described the redundancy based on a set of simple parameters that describe the bridge geometry and main load carrying characteristics. These parameters include the number of beams and beam spacing; the load carrying capacity of the main members; the dead over live load ratio; and, in the case of damaged bridges, the dead weight that was carried by the damaged beam prior to damage; and the transverse load carrying capacity of the bridge expressed in terms of the maximum moment that the slab and diaphragms can carry.

The analyses performed as part of this study and *NCHRP Report 406* highlight the difficulty of analyzing the behavior and load carrying capacities of damaged bridges. The results for damaged bridges are highly sensitive to many parameters, especially the modeling of the damage scenario and the sharp discontinuities that these create in the structural model, the torsional capacity of the remaining members of the damaged system, and the contributions of the slab and secondary members, including diaphragm and bracings. A large number of sensitivity analyses were performed to understand the interaction between these parameters. However, more sensitivity analyses are needed to better evaluate the range of variations and the upper limits for the proposed models.

References

Ghosn, M., Sivakumar, B., and Miao, F. (2012) "Development of State-Specific Load and Resistance Factor Rating Method," in press, ASCE *Journal of Bridge Engineering*, posted ahead of print February 1, 2012. doi:10.1061/(ASCE)BE.1943-5592.0000382.

Ghosn, M., Sivakumar, B., and Miao, F. (2010) "Calibration of Load and Resistance Factor Rating Methodology in New York State," *Bridge Engineering 2010*, Volume 1, Monograph Accession #:01321766, 81–89 *Transportation Research Record 2200*, Journal of the Transportation Research Board, Transportation Research Board, ISSN: 0361-1981.

Hunley, T. C. and Harik, I. E. (2012) "Structural Redundancy Evaluation of Steel Tub Girder Bridges," *Journal of Bridge Engineering* 17(3) May 1.

FHWA Steel Bridge Design Handbook: Bracing System Design (2012) Publication No. FHWA-IF-12-052, Vol. 13, U.S. Department of Transportation, FHWA, Washington D.C.

AISC Steel Construction Manual, 14th ed (2011) American Institute of Steel Construction, Chicago, IL.

CHAPTER 6

Conclusions

This report calibrated system factors that can be used to account for the presence (or the lack of) redundancy in common-type bridge configurations subjected to distributed lateral loads and vertical live load. The system factors can be used during the design and safety assessment of bridges subjected to lateral loads being evaluated using the displacement-based approach specified in the LRFD Seismic Design provisions or the traditional force-based approach. Also, the report presented system factors calibrated for application with originally intact as well as damaged bridge systems subjected to vertical vehicular overloads.

The proposed system factors are consolidated into equations and fewer tables than those presented in *NCHRP Report 406* and *NCHRP Report 458.* This was achieved by establishing simple relationships between the system factors and relevant geometric properties of the systems or material properties of the primary bridge members. The consolidation of the system factors into fewer tables is meant to simplify the process of applying the system factors in actual bridge engineering practice. The equations and tables proposed in this study are developed following extensive sensitivity analyses to account for bridges with members that may be overdesigned compared to the minimum design requirements of current and previous specifications and for bridges with deficient member strengths. This makes the proposed system factors applicable for the design of new bridges and the safety evaluation of existing bridges.

The proposed equations are necessarily designed to provide an approximate evaluation of the redundancy of bridges as they are meant to cover a wide range of bridge parameters. The proposed sets of system factor equations are presented in a format suitable for inclusion in the AASHTO LRFD Bridge Design Specifications and the manual for bridge evaluation in Appendix A.1 and Appendix A.2 of the contractor's final report (available on the TRB website). Appendix A.3 (also available on the TRB website) gives three examples illustrating how the system factor equations can be used during the design or the rating of I-girder and spread box-girder bridges under vertical loads and the design of a multi-column bridge system under lateral load. These examples complement other examples provided in the body of the report.

For more accurate evaluations of the redundancy of specific bridges, a direct redundancy evaluation involving the nonlinear analysis of bridge systems is required. Appendices B.1, B.2, and B.3 of the contractor's final report (available on the TRB website) describe the analysis process through three examples. These examples consist of the analysis of a multicell prestressed concrete box-girder bridge under vertical and lateral load, a steel truss bridge and a continuous steel two-box-girder bridge under vertical load.

Abbreviations and acronyms used without definitions in TRB publications:

A4A	Airlines for America
AAAE	American Association of Airport Executives
AASHO	American Association of State Highway Officials
AASHTO	American Association of State Highway and Transportation Officials
ACI–NA	Airports Council International–North America
ACRP	Airport Cooperative Research Program
ADA	Americans with Disabilities Act
APTA	American Public Transportation Association
ASCE	American Society of Civil Engineers
ASME	American Society of Mechanical Engineers
ASTM	American Society for Testing and Materials
ATA	American Trucking Associations
CTAA	Community Transportation Association of America
CTBSSP	Commercial Truck and Bus Safety Synthesis Program
DHS	Department of Homeland Security
DOE	Department of Energy
EPA	Environmental Protection Agency
FAA	Federal Aviation Administration
FHWA	Federal Highway Administration
FMCSA	Federal Motor Carrier Safety Administration
FRA	Federal Railroad Administration
FTA	Federal Transit Administration
HMCRP	Hazardous Materials Cooperative Research Program
IEEE	Institute of Electrical and Electronics Engineers
ISTEA	Intermodal Surface Transportation Efficiency Act of 1991
ITE	Institute of Transportation Engineers
MAP-21	Moving Ahead for Progress in the 21st Century Act (2012)
NASA	National Aeronautics and Space Administration
NASAO	National Association of State Aviation Officials
NCFRP	National Cooperative Freight Research Program
NCHRP	National Cooperative Highway Research Program
NHTSA	National Highway Traffic Safety Administration
NTSB	National Transportation Safety Board
PHMSA	Pipeline and Hazardous Materials Safety Administration
RITA	Research and Innovative Technology Administration
SAE	Society of Automotive Engineers
SAFETEA-LU	Safe, Accountable, Flexible, Efficient Transportation Equity Act: A Legacy for Users (2005)
TCRP	Transit Cooperative Research Program
TEA-21	Transportation Equity Act for the 21st Century (1998)
TRB	Transportation Research Board
TSA	Transportation Security Administration
U.S.DOT	United States Department of Transportation